

AMERICAN UNIVERSITY OF BEIRUT

DIABETES-INDUCED VASCULAR COMPLICATIONS: CROSS-TALK BETWEEN KALLIKREIN-KININ SYSTEM AND LEPTIN RECEPTOR THROUGH SPHK/S1P PATHWAY.

by
MOUSTAFA ABED AL SALAM AL HARIRI

A Dissertation
submitted in partial fulfillment of the requirements
for the degree of Doctor of Philosophy
to the Department of Biochemistry and Molecular Genetics
of the Faculty of Medicine
at the American University of Beirut

Beirut, Lebanon
September 2017

AMERICAN UNIVERSITY OF BEIRUT

DIABETES-INDUCED VASCULAR COMPLICATIONS: CROSS-TALK BETWEEN KALLIKREIN-KININ SYSTEM AND LEPTIN RECEPTOR THROUGH SPHK/S1P PATHWAY.

by

MOUSTAFA ABED AL SALAM AL HARIRI

Approved by:

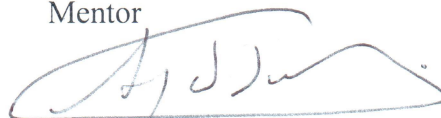
Dr. Fuad Ziyadeh, Professor
Internal Medicine
American University of Beirut

Head of Committee



Dr. Ayad Jaffa, Professor
Biochemistry and Molecular Genetics
American University of Beirut

Mentor



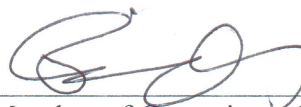
Dr. Aida Habib, Professor
Biochemistry and Molecular Genetics
American University of Beirut

Member of Committee



Dr. Firas Kobeissy, Associate Professor
Biochemistry and Molecular Genetics
American University of Beirut

Member of Committee



Dr. Maria Trojanowska, Professor
Medicine
Boston University School of Medicine

Member of Committee, External



Dr. Eva Hamade, Professor
Biochemistry
Lebanese University

Member of Committee, External



Date of dissertation defense:

September 06, 2017

AMERICAN UNIVERSITY OF BEIRUT

THESIS, DISSERTATION, PROJECT RELEASE FORM

Student Name:

Al Hariri

Moustafa

Abed Al Salam

Last

First

Middle

Master's Thesis

Master's Project

Doctoral Dissertation

I authorize the American University of Beirut to: (a) reproduce hard or electronic copies of my thesis, dissertation, or project; (b) include such copies in the archives and digital repositories of the University; and (c) make freely available such copies to third parties for research or educational purposes.

I authorize the American University of Beirut, to: (a) reproduce hard or electronic copies of it; (b) include such copies in the archives and digital repositories of the University; and (c) make freely available such copies to third parties for research or educational purposes after:

One ---- year from the date of submission of my thesis, dissertation, or project.

Two ---- years from the date of submission of my thesis, dissertation, or project.

Three -X- years from the date of submission of my thesis, dissertation, or project.



September, 14, 2017

Signature

Date

ACKNOWLEDGMENTS

This work would have not been accomplished without the blessing of Allah the almighty who consecrated me with the curiosity-to-know and persistence in the pursuit of truth and evidence.

I would like to acknowledge Dr. Ayad Jaffa as a great mentor and role model. I stand speechless and cannot find the proper words to thank him for all the opportunities he offered me and for his constant and continuous support. He trained me to be sound researcher and made working with him an interesting and memorable experience. I will always be grateful to him for his support, guidance, encouragement, and stimulation. I am sincerely grateful for his precious time he dedicated to fulfilling my dissertation work.

I would like to extend my sincerest gratitude to my Ph.D. committee members: Dr. Fuad Ziyadeh, Dr. Aida Habib, Dr. Firas Kobeissy, Dr. Eva Hamade, and Dr. Maria Trojanowska for their support, feedback, direction, and assistance in improving my dissertation and whenever I needed it.

I would like to express my thanks for Dr. Yehia mechref and his laboratory members, Rui Zhu and Jingfu Zhao, from Texas Tech University for the generation and analysis of the proteomic results of this study. I would also like to thank Dr. Louis Luttrell and Dr. Hesham Al Shewy from Medical University of South Carolina for their great support.

I would like to extend my gratitude and appreciation to the laboratory members: Fatima Al Hajj, Fatima Ghamloush, Oula Dagher, and Richard Saoud. In addition, I cannot express my gratitude to Dr. Hussein Shalhoub, a life time friend. Moreover, Lamis Saad and Mohammad Medawar thanks a lot for being part of my success. Furthermore, I would like thank Abeer Ayoub, Nahed Mogharbel, Rana Ghali, and Ruwayda Khattab for their friendship.

A special recognition goes to Dr. Miran Jaffa for her statistical support across all my research work. I would like also to thank Dr. Nadine Darwiche for all her support and assistance as a Ph.D. coordinator of the Biomedical Sciences program. In addition, a special thanks for Mrs. Samira Al Kadi for her assistance and friendship.

Finally, I would like to immensely thank my two families. My in laws, Hajj Moustafa Dalibalta and Salma Saoudi, and their family, Abed, Mohammad and Aya Dalibalta, thanks a lot for your support and accepting me as a son- and brother-in-law. To my parents and siblings. For all you do, for who you are, I will be forever grateful you are in my life. Dad and Mom, you are the source of inspiration and motivation, all my success is because of your sacrifices and your believing in me. Dr. Lara Al Hariri, my role model and hero, I love you to the stars. Million thanks won't be enough to appreciate your unconditional support and help. Mazen, Safaa, Mohammad, and Aunty Mona thanks a lot for being always by my side, what would I do without all of you in my life.

Finally, to my friend, soulmate, and love. Thanks a lot Nawal Dalibalta Al Hariri for believing in me, supporting me, and motivating me. You stood strong beside me when my whole world was getting darker. You encouraged me with your words. You did not allow me to give up and inspired me to start a new venture that flags success today. All the credit goes to you my darling wife. Thanks for being there in my life. In addition, I would love to dedicate this work to my lovely daughter, Clara Moustafa Al Hariri, who is the reason for all the hard work.

AN ABSTRACT OF THE DISSERTATION OF

Moustafa Abed Al Salam AL Hariri for Doctor of Philosophy
Major: Biomedical Sciences

Title: Diabetes-Induced Vascular Complications: Cross-Talk between Kallikrein-Kinin System and Leptin Receptor through SphK/S1P Pathway.

Diabetes mellitus is among the leading causes of deaths worldwide with a huge healthcare cost due to its high morbidity and associated complications. Since the discovery of kallikrein-kinin system (KKS) as a potent vasodilator, many studies focused on understanding the pathophysiological roles of this system. There is a strong evidence associating KKS components with different pathological conditions related to diabetes. In this study, we aimed at studying the involvement of KKS in diabetes-induced vascular diseases. We studied our aim through four sub-objectives. We employed global protein profiling to study the effect of diabetes on the aorta and kidney, and the effect of BK and leptin on vascular smooth muscle cells (VSMC). Additionally, we used western blot, qPCR analyses and confocal microscopy to examine the signaling of BK, S1p, and leptin in VSMC from rats and mouse models. Our findings showed that diabetes directly induces the expression of kininogen, the precursor of Bradykinin (BK), in the VSMC of the aorta eliminating the vasodilatory possible effect of BK on endothelia cells. The upregulation of BK-producing proteins in the VSMC proposes a mechanism by which BK exerts paradoxical deleterious effects on the physiology of VSMC and subsequently the vessels through promoting inflammation and fibrotic disease. On the other hand, BK induces the expression of two fibrotic proteins, Connective tissue growth factor (Ctgf) and Fibronectin (Fn1), through modulating the activity of reactive oxygen species (ROS)/ERK/SphK1/S1p axis. Moreover, BK induces the expression of leptin pathway, which is responsible for relaying the signal transduction of BK on fibrotic proteins. The regulation of leptin downstream of BK proposes a novel role of the KKS in actin remodeling induced vascular hypertrophy in VSMC. Taken together, the study outcomes show a possible mechanism by which BK could contribute in the development of diabetes-induced vascular disease.

Keywords: KKS, BK, Leptin, SphK1, Ctgf, Fn1, CVD, aorta, vascular fibrosis

CONTENTS

ACKNOWLEDGMENTS	v
AN ABSTRACT OF THE DISSERTATION OF	vii
ILLUSTRATIONS	xiii
TABLES	xv
CHAPTER	
I. INTRODUCTION	1
A. Diabetes Mellitus	1
1. Diabetes Mellitus (DM) Epidemiology:	1
2. DM Types:	2
a. Type 1 Diabetes Mellitus (T1DM):	3
b. Type 2 Diabetes Mellitus (T2DM):	4
c. Gestational Diabetes Mellitus (GDM):	5
3. DM complications:.....	5
a. DM-Related Complications:.....	6
i. DM-induced inflammation:	6
ii. DM-induced Cardiovascular Diseases:	8
iii. DM-induced renal disease:	11
b. Mediators of DM-induced complications:.....	13
B. The Kallikrein-Kinin System (KKS):.....	14
1. Kininogens/Kinins:	15
2. Plasma Kallikrein/Kinin System:.....	19
a. Activation mechanisms of PK:.....	20

i.	Contact Activation mechanism:	20
ii.	Constitutive Activation mechanism:	21
3.	Tissue Kallikrein/Kinin System:	22
4.	Involvement of KKS in different pathologies:.....	24
a.	Involvement of KKS in inflammatory process:.....	25
b.	Involvement of KKS in CVD:.....	25
c.	Involvement of KKS in renal diseases:	27
C.	Sphingosine Kinase/Sphingosine 1 phosphate pathway:.....	30
1.	Properties of SphK:.....	32
2.	Mechanism of activation of SphK:	32
3.	Mechanisms of S1P signaling:.....	34
4.	Involvement of SphK/S1P signaling in diabetes:	34
a.	The role of SphK signaling in hepatic insulin resistance:	34
b.	The role of SphK signaling in pancreatic β -cell death:	35
5.	The role of SphKs in the progression of diabetes complications:	36
a.	The role of the SphK/S1P in vascular complications:.....	36
b.	The role of SphK/S1P in diabetic nephropathy (DN):.....	37
D.	Leptin in CVD:	38
1.	Leptin receptor signaling:	41
2.	The role of Leptin in atherosclerosis development:.....	42
a.	The role of leptin in hypertension:	42
b.	The role of leptin in inflammation:	43
c.	The role of leptin in oxidative stress:	43
E.	Fibrotic proteins in CVD:	43
1.	Risk factors for vascular fibrosis:	44
a.	Effect of hypertension on vascular fibrosis:.....	44
b.	Effect of hyperglycemia on vascular fibrosis:.....	45
c.	Effect of dyslipidemia on vascular fibrosis	47
2.	Pathogenesis of vascular fibrosis:.....	47
a.	CTGF and vascular fibrosis:.....	47
b.	Fibronectin and vascular fibrosis:	49

II. HYPOTHESIS AND OBJECTIVES	51
III. RESULTS	53
A. Proteome Profiling in the Aorta and Kidney of Type 1 Diabetic Rats. ...	53
1. Abstract	54
2. Introduction:.....	55
3. Methods:	56
a. Induction of Diabetes:	56
b. Extraction and Tryptic Digestion of Proteins:.....	57
c. LC-MS/MS Analysis:.....	58
d. Post-Translation Modification Analysis:.....	59
e. Systems Biology Assessment:.....	60
f. Statistical Analysis and LC-MS/MS Data Analysis:.....	61
4. Results:.....	63
a. Characteristics of the Diabetic State:	63
b. Aorta and Kidney Proteomic Analysis:	65
c. Effect of diabetes on proteome profile in the aorta and kidney:	66
d. Effect of diabetes on the expression of oxidative stress enzymes:....	67
e. Effect of diabetes on matrix proteins in the aorta:	68
f. Effect of insulin treatment on proteome profile in aorta and kidney:68	
g. Effect of diabetes and insulin on kininogen and ACE:	69
h. Principal component analysis (PCA):	69
i. Effect of Diabetes on PTMs:	70
j. Pathway and network analysis of proteomic profiles:.....	72
5. Discussion:.....	81
Supplementary data for chapter Four.....	85
B. Role of Sphingosine Kinase 1 in Bradykinin Regulation.....	118
1. Abstract:.....	119
2. Introduction:.....	121
3. Methods:	123

a.	Animals:	123
b.	Primary cell extraction:	124
c.	RNA extraction and Real-Time PCR:	124
d.	Protein extraction and western blots:	126
e.	siRNA down-regulation of SphK1 expression:	127
f.	Confocal fluorescence microscopy:	128
g.	Statistical Analysis:	129
4.	Results:.....	129
a.	BK induces the expression of Fn1, Ctgf, and SphK1 in RASMC:..	129
b.	The role of ERK1/2 in BK-induced SphK1 phosphorylation:	130
c.	The role of SphK1 in the BK-induced of Ctgf and Fn1:	133
d.	Effect of BK on S1P receptors Regulation and internalization:	137
e.	Involvement of S1pr1 in the BK-induced fibrotic markers:.....	139
5.	Discussion:.....	141
C.	Proteome Profiling in the VSMC in response to BK and leptin.....	145
1.	Abstract:.....	146
2.	Introduction:.....	148
3.	Methods:	149
a.	Animals:	149
b.	Primary cell extraction:	150
c.	Extraction and Tryptic Digestion of Proteins:	150
d.	LC MS/MS Analysis:	151
e.	Systems Biology Assessment:.....	152
f.	Statistical Analysis and LC-MS/MS Data Analysis:.....	153
g.	Primary cell extraction:	154
h.	Treatment of RASMC:	154
i.	Protein extraction:	154
j.	Western Blot:.....	155
k.	RNA extraction and RT-qPCR:.....	155
l.	siRNA transfection:	157
m.	Ctgf release from RASMC:	157
4.	Results:.....	157

a. RASMC Proteomic Analysis:.....	157
b. Effect of BK stimulation on proteome profile in RASMC:	158
c. Effect of leptin stimulation on proteome profile in RASMC:	158
d. Principal component analysis (PCA):	159
e. Pathway and network analysis of proteomic profiles:.....	159
f. BK induced leptin and leptin receptor expression in RASMC:	168
g. Leptin induced CTGF, Fn1, and NOX1 expression in RASMC:....	170
5. Discussion:	171
Supplementary data for chapter Four.....	176
IV. DISCUSSION.....	198
A. Significance of the study:	204
B. Limitation of the study:	204
1. Global proteomic profiling of T1DM mouse model:.....	205
2. Assessing the cross-talk between BK and S1P pathways:.....	205
3. Assessing the cross-talk between BK and leptin:	206
C. Future perspectives:	206
D. Possible therapeutic interventions:	207
References:.....	209

ILLUSTRATIONS

Figure	Page
1. Schematic depiction demonstrating the total number of the diabetic patients.....	2
2. Schematic depiction describing the three most occurring types of diabetes	6
3. Hyperglycemia-related mechanisms for the development of CVD.....	9
4. KKS activation pathway.....	15
5. A schematic diagram of the domains of kininogens.....	19
6. A schematic diagram of the components of the SphK1/S1P pathway	31
7. A schematic diagram of the signaling pathway of Leptin receptor (ObRb).....	42
8. Plasma glucose level and body weigh measurements of the rats.....	65
9. Hierarchical clustering (heat maps) of protein expression profiles.....	67
10.Principal Component Analysis (PCA) of the aorta (A) and kidney (B) samples.....	70
11.Scatter plot of the mean intensities of the three PTMs	72
12.Canonical Pathways of the comparative groups in the aorta and the kidney samples	73
13.IPA network analysis of the modified proteins in the aorta of diabetic relative to control rats.....	75
14.IPA network analysis of the modified proteins in the aorta of insulin-treated diabetic relative to diabetic rats.	76
15.IPA network analysis of the modified proteins in the kidney of diabetic relative to control rats.....	78
16.IPA network analysis of the modified proteins in the kidney of insulin-treated diabetic relative to diabetic rats	80
17.BK induces the expression of Fn1, Ctgf, and SphK1 in RASMC.....	130
18.Role of ERK activation in the BK-induced phosphorylation of SphK1 and the protein expression of Ctgf and Fn1 in RASMC.....	132

19. Role of SphK1 in the BK-induced protein expression of Ctgf and Fn1 in RASMC and mouse VSMC	135
20. Effect of BK on the expression of S1P receptors and the internalization of S1pr1	138
21. Role of S1pr1 in the BK-induced protein expression of Ctgf and Fn1 in RASMC....	140
22. Schematic depiction of the proposed pathway for the BK-induced regulation of Ctgf and Fn1 protein expression	144
23. Hierarchical clustering (heat maps) of protein expression profiles in RASMC	160
24. Principal Component Analysis (PCA) of the BK (A) and Leptin (B) RASMC samples	161
25. Canonical Pathways of the comparative groups	162
26. Pathway studio network analysis of the modified proteins in response to BK 24h treatment relative to control in RASMC	164
27. Pathway studio network analysis of the modified proteins in response to BK 48h treatment relative to control in RASMC	165
28. Pathway studio network analysis of the modified proteins in response to leptin 24h treatment relative to control in RASMC	166
29. Pathway studio network analysis of the modified proteins in response to leptin 24h treatment relative to control in RASMC	167
30. <i>BK induced leptin and leptin receptor expression in RASMC</i>	169
31. Leptin receptor signaling is a mediator of BK-induced Ctgf expression	170

TABLES

Table	Page
1. Comparative list of proteins in the aorta of diabetic rats compared to controls.	85
2. Comparative list of proteins in the kidney of diabetic rats compared to controls.	92
3. Common proteins between aorta and kidney in diabetic vs. control.	101
4. Comparative list of proteins in the aorta of insulin-treated diabetic rats compared to diabetic rats.	103
5. Comparative list of proteins in the kidney of the insulin-treated diabetic rats compared to diabetic rats.	110
6. Comparative list of proteins in the BK-stimulated for 24h compared to controls.	176
7. Comparative list of proteins in the BK-stimulated for 48h compared to controls.	179
8. Comparative list of proteins in the leptin-stimulated for 24h compared to controls.	184
9. Comparative list of proteins in the leptin-stimulated for 48h compared to controls.	192

CHAPTER ONE

INTRODUCTION

A. Diabetes Mellitus

1. Diabetes Mellitus (DM) Epidemiology:

Diabetes Mellitus (DM) is a chronic disease that poses a huge healthcare cost worldwide. It affects more than 420 million patients worldwide, as estimated by the World Health Organization (WHO) in 2016, accounting for about nine percent of the total human population [1]. These numbers are projected to increase by 55% by the year 2040 [2,3]. In addition, DM has a high morbidity and mortality rate accounting for about 3 million deaths in 2012 [1]. Centers for Disease Control and Prevention in 2014 estimated that more than 9% of the U.S. population is diabetic, and the direct and indirect healthcare cost for these patients is more than \$240 billion in 2012 [4]. On the other hand, the number of the diabetic patients in the Middle East and North Africa region is drastically more than those of the U.S. reaching more than 10% of the total region's population with a huge healthcare expense (Figure 1) [5].

Therefore, DM is a serious life changing condition that requires blood glucose control by medications or insulin supplementation, accompanied by lifestyle modifications. DM is manifested with hyperglycemia, or increase in blood glucose, accompanied by insulin deficiency or insulin resistance [6]. Insulin is the glucose-lowering hormone in the body, and it is produced by the β -cells of the pancreas [6]. Controlling blood glucose is

crucial for the health of the patients, however, if glycemia was not controlled, many diabetes-related complications would occur leading to high medical cost, less productivity in the work, restrictive lifestyle, disability, and subsequently death [7-9].

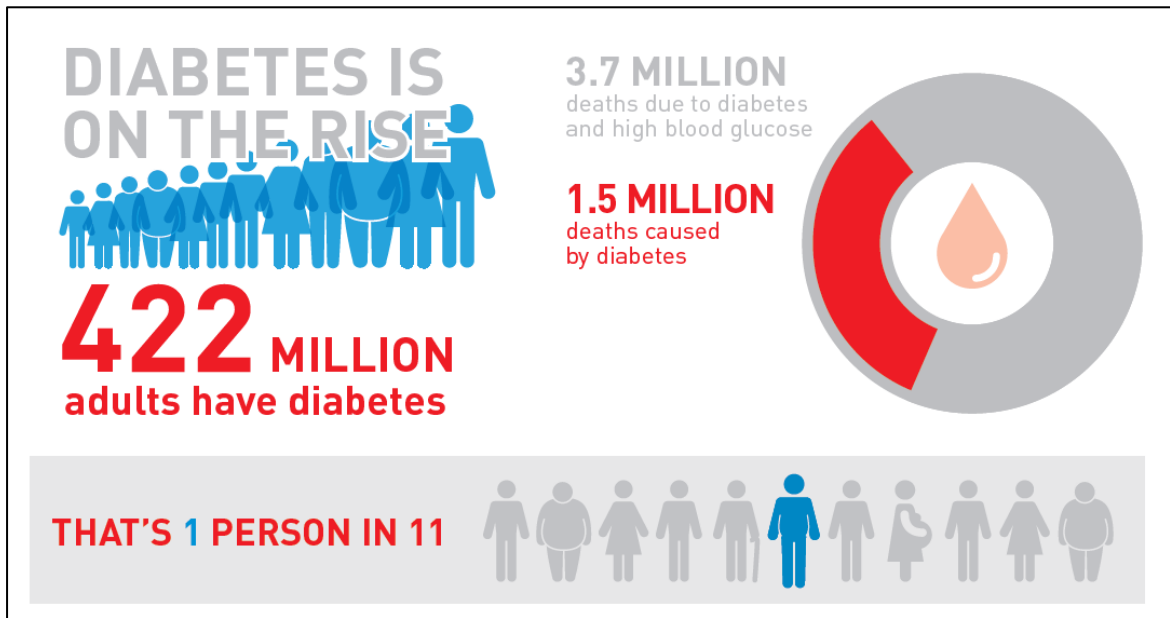


Figure 1: Schematic depiction demonstrating the total number of the diabetic patients, the ratio of the diabetic patients compared to the total population worldwide, and the total mortalities related to diabetes. Picture acquired from WHO website [1].

The symptoms of hyperglycemia would include increased urination (polyuria), excessive thirst (polydipsia), weight loss, excessive hunger (polyphagia), and blurred vision. Additionally, growth abnormalities and susceptibility to certain infections would be observed in some patients. Hence, uncontrolled hyperglycemia is a life-threatening condition that should be corrected according to the type of diabetes.

2. *DM Types:*

DM is classified into three major types: type 1 (T1DM), type 2 (T2DM), and Gestational DM (GDM). Each type is characterized by specific diagnosis, prognosis,

management, and related complications. In the next section, we will be discussing the different types and their characteristics.

a. Type 1 Diabetes Mellitus (T1DM):

T1DM, also known as insulin-dependent or juvenile-onset type, comprises 5 to 10% of the total number of the diabetic patients. This type of diabetes is characterized by insulin deficiency as a result of the β -cells of the pancreas by an autoimmune destruction and requires daily supplementation with insulin (Figure 2). Additionally, T1DM are presented with chronic hyperglycemia that leads to metabolic abnormalities affecting the metabolism of carbohydrates, lipids, and proteins [10].

The exact causes for this mechanism are not well known, and not preventable so far [6]. However, in 85 to 90% of the patients, there are markers for antibodies against self-cells and molecule of the patient upon detecting diabetes. The markers that the self-antibodies are against are β -cells, insulin, glutamic acid decarboxylase, and tyrosine phosphatases IA2 and IA2 β . In addition, T1DM is highly associated with some genes of the Human Leukocyte Antigen (HLA).

The rate of β -cells destruction differs in the patients according to the age at which the onset started. For instance, the rate in infants and children is more than that in adults. Additionally, the predisposition of the patients differs to this type of diabetes. Moreover, β -cells destruction is related to both genetics and environmental factors. Furthermore, T1DM patients are disposed to other autoimmune disorders such as Graves' disease, Hashimoto's thyroiditis, Addison's disease, vitiligo, celiac sprue, autoimmune hepatitis, myasthenia gravis, and pernicious anemia [11].

b. Type 2 Diabetes Mellitus (T2DM):

T2DM, also known as non-insulin-dependent or adult onset, comprises 90 -95 % of the total number of diabetic patients, and most of the patients are adults (Figure 2). Unfortunately, and due to the modern lifestyle, many children are acquiring this type of diabetes. This type of diabetes is characterized by insulin resistance or ineffective use of insulin in the body. Destruction of the β -cells of the pancreas is not a cause of this type of diabetes. However, T2DM is highly associated with age, obesity and physical activity of the patients [6].

Usually, Type 2 diabetes is diagnosed many years after the initial onset, since hyperglycemia in this type of diabetes builds up gradually leading to less prominent symptoms compared to the first type. This type of diabetes barely required insulin-supplementation, and rather many insulin-sensitizing drugs are described to the patients, with lifestyle modification. Additionally, weight reduction, physical activity and/or medication may improve hyperglycemia without restoring the level to normal.

Moreover, there are many factors that would predispose the patient to become T2DM such as women who developed GDM during pregnancy, hypertension, and dyslipidemia. Furthermore, there's more genetic predisposition to the patients of this type of diabetes compared to the first type. Nevertheless, the exact genetic mechanisms are not well understood [11].

c. Gestational Diabetes Mellitus (GDM):

GDM is a temporary state of hyperglycemia that is first developed during the pregnancy. In some cases, this state of diabetes persists after delivery to cause T2DM and may affect the health of the women and their babies [12-14]. GDM is developed in around 1 to 14 % of the pregnancies worldwide [13]. There are some risk factors that increase the predisposition of the women to GDM such as age, weight, developed GDM in a previous pregnancy, and T2DM family history. Additionally, there are some modifiable risk factors such as diet and physical activity of the women [13].

3. *DM complications:*

Hyperglycemia is the common factor in the different types of DM, and if left uncontrolled would lead to injury to many body tissues over time at the micro- and macro-vascular levels [6]. On the microvascular level, DM leads to blindness, end-stage renal failure, and neuropathy. On the macrovascular level, DM promotes atherosclerosis progression in the vessels supplying the body's vital organs, e.g. heart and brain, and extremities leading to myocardial infarcts, strokes, and limb amputations (Figure 2). Clinical studies have shown that hyperglycemia is a risk factor for microvascular complications observed in both types of diabetes [15,16]. On the other hand, both insulin and hyperglycemia serve as risk factors for macrovascular complications in T2DM.

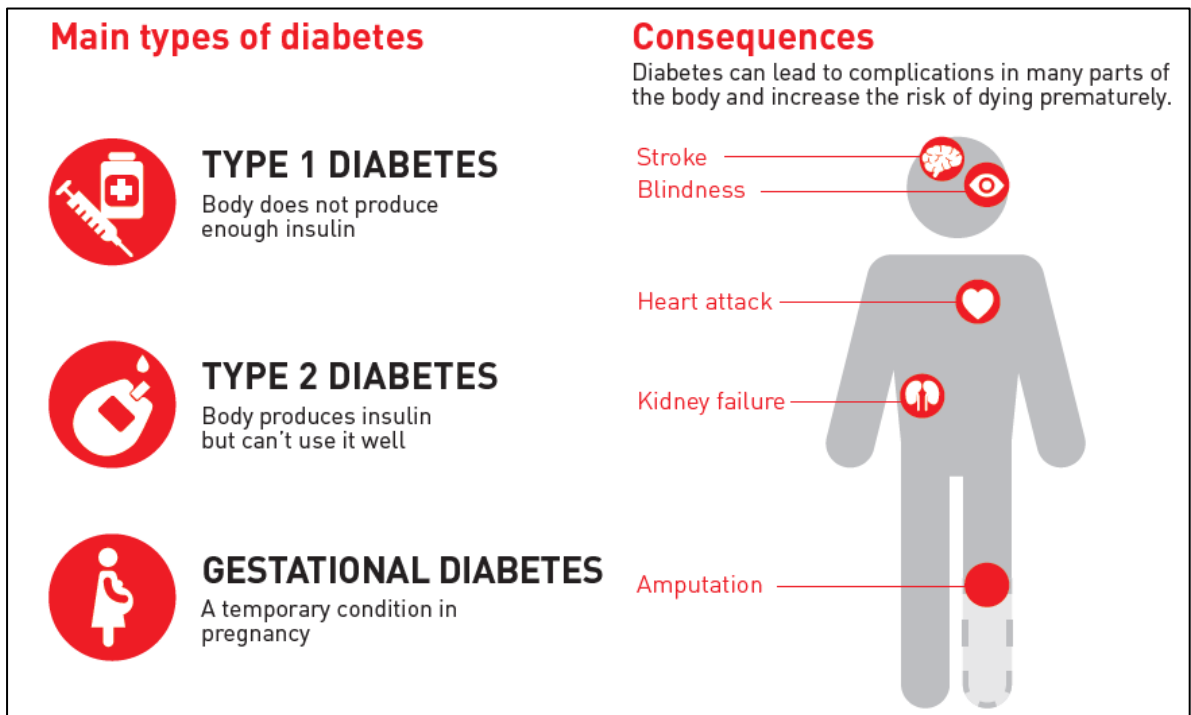


Figure 2: Schematic depiction describing the three most occurring types of diabetes and the diabetes-related complications. Figure acquired from WHO website [1].

- a. DM-Related Complications:
- i. DM-induced inflammation:

As previously discussed, hyperglycemia is the characteristic of all diabetes mellitus patients. Many reports have shown that diabetes is highly correlated with inflammatory processes. For instance, β -cells destruction is a phenomenon driven by the inflammation caused by autoimmunity recognition of this type of cells leading to T1DM. On the other hand, obesity and insulin resistance, the main causes of T2DM, exacerbate the inflammatory process in the patients. Moreover, the modifiable risk factors such as hypertension and dyslipidemia contribute to inflammatory nature of hyperglycemia. These factors lead to the activation of plethora of signaling pathways such as nuclear factor Kappa

B (NF- κ B), advanced glycation endproducts (AGE) receptors, toll-like receptors (TLR), and c-Jun terminal kinase (JNK) that promote β -cells destruction and dysfunction, endothelial injury or dysfunction, and improper vascular dynamics [17].

The mechanisms by which diabetes promote inflammation differ between the two major sites of inflammation, namely the vascular endothelial tissue [18,19] and the adipose tissue [20]. In the following sections, the mechanisms in each tissue will be summarized.

As for the endothelial tissue, the signal starts with chemoattractant molecules, such as monocyte chemoattractant protein (MCP)-1 and macrophage migration inhibition factor (MIF), which induce the expression of adhesion molecules on the endothelial cells and attract monocytes to the injured site and lead to their infiltration and transformation into macrophages [21]. Additionally, macrophages induce the expression of inflammatory cytokines through different pathways such as the induction of reactive oxygen species production, oxidized LDL, reduction in the production and/or bioavailability of nitric oxide, induction of angiotensin 2 production, and the increase in AGE [19,22-24]. Both macrophages and endothelial cells promote the altered vasoreactivity and pro-coagulation state through platelet activation and the induction of coagulation factors such as fibrin and factor VIII [19]. Among the secreted cytokines from the macrophages, IL-6 is the most contributor of inflammation being the inducer of C-reactive protein (CRP), and significant inflammation clinical marker [25,26].

On the other hand, the adipose tissue has a big contribution to the inflammatory process in the overweight and obese patients on the vascular and non-vascular systems in a systematic or local fashion [27]. As for the vascular system, the inflammation process in the adipose tissue starts with activated macrophages in the adipose tissue. Macrophages,

accompanied with adipocytes, secrete chemoattractant and cytokines contributing to insulin resistance [27,28]. However, unlike the vascular tissues, adipocytes produce adiponectin that has antidiabetic and anti-inflammatory effects through sensitizing insulin activity and glucose uptake, increasing nitric oxide production and bioavailability, inhibition of TNF- α production, downregulation of cell adhesion molecules, and in vitro β -cells anti-apoptotic effects [29-31]. Many studies have shown that in obese and diabetic patients, adiponectin levels fall down promoting inflammatory process and cardiovascular diseases in T2DM patients [31].

ii. DM-induced Cardiovascular Diseases:

As previously mentions, the DM-induced inflammation and macrophage infiltration are among the major mechanisms for the development of different cardiovascular diseases (CVD), such as myocardial infarction, stroke, and atherosclerosis. In fact, the CVD is estimated to be four to five times more prevalent in diabetic patients compared to non-diabetic and are the leading cause of morbidity and mortality in DM patients [32-34]. Chronic hyperglycemia is the driving cause of the CVD in DM patients, affecting both the large and the small blood vessels, which is the characteristic of the macro-and micro-vascular lesion, respectively. The mechanisms by which hyperglycemia induces CVD are depicted in Figure 3, and they include endothelial dysfunction, oxidative stress, redox potential imbalance, induction in inflammatory markers, AGE production, and hypercoagulability state [17,35].

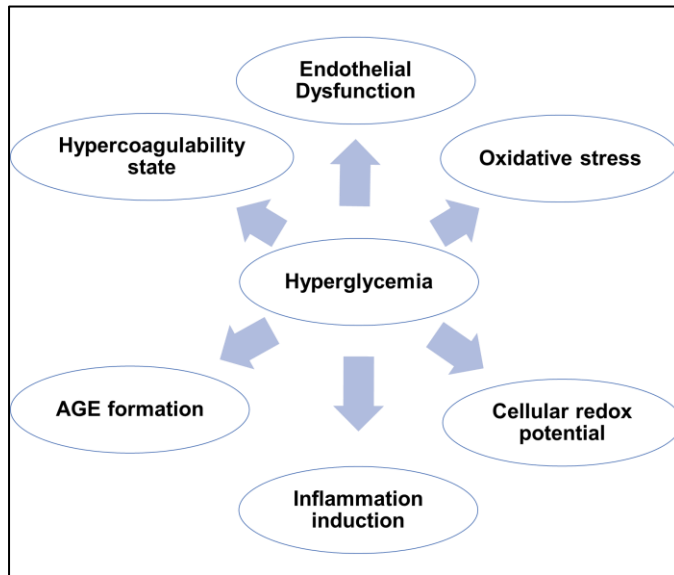


Figure 3: Hyperglycemia-related mechanisms for the development of CVD. Figure modified from [32].

Among the mechanisms of hyperglycemia-induced CVD, endothelial dysfunction could be considered as the leading mechanism for the other complications, since vascular endothelial cell play a crucial physiological barrier between blood flow and the blood vessel media and intima. Additionally, endothelial cells serve as an anticoagulant and fibrinolytic tissue, and as vasodilator through the production of nitric oxide. The latter inhibits vascular smooth muscle cell proliferation and migration [36].

Endothelial cell layer can be injured by hyperglycemia, since circulating blood glucose can passively diffuse and accumulate in the endothelial cells leading to haywire metabolic pathways converting glucose into fructose, on the expense of depleting NADPH and generation of NADH, and subsequently production of AGE [37,38]. The latter imbalance in the NAD molecules promotes cellular oxidative stress, which resembles the effects of hypoxia in inducing protein kinase C (PKC). In turn, activated PKC inhibits nitric oxide synthesis, promotes the production of cytokines and adhesion molecules and subsequently inflammation, induces the expression and deposition of extracellular matrix

(ECM) proteins, and enhances vascular contractility and permeability. The result of these altered pathways are cytotoxic endothelial dysfunction and oxidize low density- lipoprotein (LDL) [38,39]. The destruction of endothelial cells leads to the activation of the inflammatory and adhesion molecules, as discussed in the previous section, promoting both inflammation and coagulation [40]. Moreover, the irreversibly-glycated proteins acquire different biochemical properties to become oxidant molecules, augment oxidative stress through the production of reactive oxygen species, inhibit nitric oxide synthesis, and result in the vascular lesion and compromised vascular dilatation [35,41].

Furthermore, AGE promotes inflammation markers, such as nuclear factor-kappa B (NF- κ B), through the binding and the activation of receptors for advanced glycation end-products (RAGE). RAGE is widely expressed on different cell types such as endothelial cells, smooth muscle cells, fibroblasts, lymphocytes, monocytes and macrophages [38,41]. Activated NF- κ B exerts its coagulability and inflammatory effects through inducing the expression of adhesion molecules, growth factors, and inflammatory cytokines, which aggravate diabetic induced CVD [38,40]. Among the NF- κ B activated growth factors, vascular endothelial growth factor (VEGF) and fibroblast growth factor (FGF) play a substantial role in impairing the hemodynamics of vessels through the promotion of vessel wall remodeling, fibrotic protein and lipid deposition, and basement membrane thickness that cause stiffness of the vessels [38]. The role of the fibrotic proteins in the promotion of CVD will be discussed in later sections.

The previously discussed diabetic-induced alteration in oxidative stress, endothelial dysfunction, proinflammatory markers induction, and adhesion molecule and coagulation markers expression may initiate atherosclerosis and the formation of arterial

thrombosis. Although thrombosis is usually uncommon at the early stages of atherosclerosis, the risk of development of thrombosis increases drastically with the progress of atherosclerosis and the formation of ulceration on the surface of the atherosclerotic plaque, exposing thrombogenic molecules, such as adhesion molecules, to the blood stream. This exposure initiates the activation and aggregation of platelets and leads to the rapid formation of thrombosis and occlusion of the bloodstream [32]. In addition to the thrombosis formation, activated platelets recruit monocytes through the production of the chemoattractants, stimulate the proliferation and the migration of fibroblasts and vascular smooth muscle cells in the vessel wall, and interact with endothelial cells to induce the release of inflammatory cytokines, all of which emphasize the formation of atherosclerosis and inflammatory process [40].

iii. DM-induced renal disease:

In addition to the cardiovascular risks, hyperglycemia is among the major risk factors for developing chronic kidney disease (CKD) [42]. Remarkably, T1DM patients are at higher risk of developing diabetic nephropathy compared to T2DM [32]. Moreover, diabetic nephropathy is the major contributor to end stage renal disease (ESRD) and is an independent risk factor for cardiovascular diseases [32,43].

The mechanisms of diabetic-induced kidney injury have been considerably discussed in many reports. Like the cardiovascular system, hyperglycemia, AGE formation, and oxidative stress alter different metabolic pathways in the kidneys, leading to hemodynamic disequilibrium and the induction of a group of fibrotic and growth factors in

the organ. Among these factors, transforming growth factor beta (TGF- β) and VEGF promote renal fibrosis and proteinuria, which are the fundamental characteristics of diabetic nephropathy [44]. For instance, TGF- β /Smad3 pathway is the major mechanism for causing renal hypertrophy and extracellular matrix deposition in mesangial cells. Additionally, VEGF produced from podocytes is correlated with the development of albuminuria in diabetic patients [36,44].

Similar to the vascular system, the diabetic-induced renal complications are primarily driven by endothelial dysfunction. In addition, insulin resistance, observed in diabetic patients, has been shown to have a role in the exacerbation of the kidney physiology by inducing glomerular hypertension and hyper-filtration [45]. The complex mechanism of glomerular damage could be briefed by the perturbation of the regulation of the vasoactivity of the afferent and the efferent arterioles in the glomeruli. First, insulin resistance leads to induction in nitric oxide and transforming growth factor β 1 (TGF- β 1) production, leading to vasodilation of both arterioles and increasing blood flow in the glomeruli [46,47]. Second, insulin resistance induces the production of the vasoconstrictor Angiotensin II, which has a preferential activity over the efferent arteriole, leading to the escalation of the blood pressure in the glomeruli, and subsequently leading to glomerular cell elongation and damage [48,49]. Additionally, insulin resistance contributes to the observed increase in blood pressure of the patients through the activation of Na⁺ reabsorption in the proximal tubules [50,51].

As previously mentioned, adiponectin production from adipocytes is decreased in obese or insulin resistant patients, which is related to the development of endothelial dysfunction and albuminuria [52]. On the other hand, circulatory levels of leptin are

increased in diabetic patients, which is related to TGF β system activation and has fibrotic and oxidative effects on the glomerular cells [53]. Additionally, leptin was shown to be implicated in inducing the circulatory levels of inflammatory cytokines, such as IL6 and TNF α that induce progression in diabetic kidney disease [54,55].

Furthermore, the role of insulin resistance in nephropathy was recently studied in an in vivo model of podocyte specific insulin receptor null mice. The results showed that the glomerular lesions observed in the animal model resemble those observed in diabetes animal models [56]. Additionally, nephrin, a crucial protein in the slit diaphragm produced by podocytes, was observed to be decreased in diabetes and may contribute to glomerular cell disruption and albuminuria [56,57].

Taken together, endothelial dysfunction, pro-coagulability, induction of fibrotic proteins, insulin resistance, and inflammation play deleterious roles in the diabetes-induced vascular and renal complications. Their role is reflected in the serum levels of their markers in diabetic patients, with augmented levels in the patients with diabetes-induced complications [58,59].

b. Mediators of DM-induced complications:

Due to its huge impact on the population, DM has been extensively studied [1]. Different reports have shown that there are many pathways and proteins that induce the complications of DM. Among the pathways and proteins, we are particularly interested in the role of the Kallikrein Kinin Systems (KKS), connective tissue growth factor (Ctgf), fibronectin (Fn1), and Sphingosine kinase/Sphingosine phosphate pathway. In the

following sections, we will be highlighting the latest findings pertaining these pathways and proteins and diabetes complications.

B. The Kallikrein-Kinin System (KKS):

The kallikrein enzymes belong to the serine proteases family. They are divided into two major categories of plasma kallikrein (PK) and kallikrein-related peptidases (KLKs, Tissue Kallikrein) [60,61]. The location of expression of these two enzymes differs significantly; whereas PK is expressed in the circulating plasma, and KLKs are expressed in tissues. In addition, PK and KLK differ in their molecular weight, substrate specificity, gene structure, and the produced kinins. The vital role of kallikreins is to cleave kininogen to produce kinins, which are short vasoactive peptides. Figure 4 summarizes the activation pathway of the two Kallikrein (PK and KLK) leading to the generation of the vasoactive peptide bradykinin (BK) [62]. Many studies have pointed the involvement of KKS in different pathophysiological processes such as cancer, inflammation, and diabetes-induced complication on renal, cardiovascular, and central nervous systems [63,64].

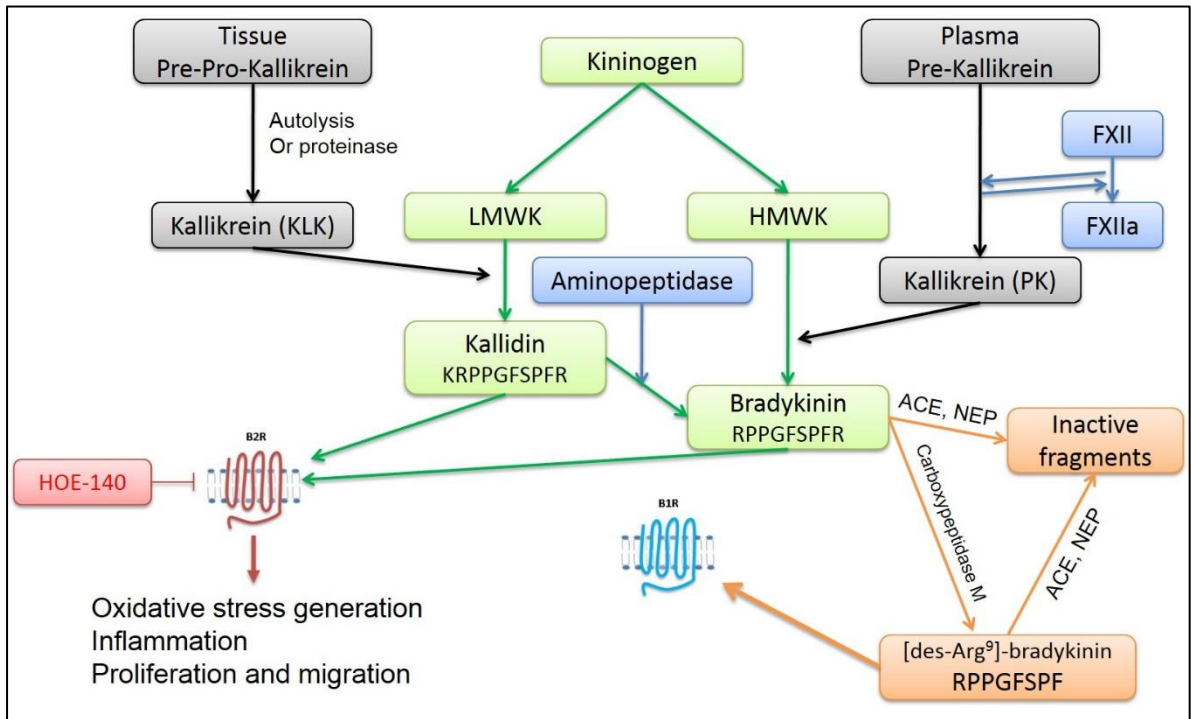


Figure 4: KKS activation pathway. The activation of the two types of Kallikreins (Plasma or Tissue) is different in term of the activation mode. Both active kallikrein cleave Kininogen (High molecular or Low Molecular weight, respectively) to produce vasoactive kinins (Bradykinin, or Kallidin, respectively) that are agonists to kinin receptors (Bdkrb2 or Bdkrb1, respectively). Kallidin is rapidly converted to BK through Aminopeptidase. Moreover, BK is degraded and inactivated by different endopeptidases. Figure modified from [65,66].

1. Kininogens/Kinins:

Kininogens belong to the cystatin superfamily, and they are the precursors of the kinins, mostly the vasoactive kinin Bradykinin (BK). There are two forms of kininogens, namely low molecular weight kininogen (LMWK) and high molecular weight kininogen (HMWK). Both kininogens are substrates for the serine protease activity of kallikreins [67]. LMWK and HMWK are produced by differential splicing of the kininogen gene (symbol *KNG1*). Kininogen proteins have identical N terminus and differ at their C-terminus. Figure 5 schematically illustrates the structural similarities and differences between the two forms of the kininogens.

The mature polypeptide HMWK is a single chain glycoprotein with around 120 kDa of weight and 626 amino acids and composed of 6 domains (D1-D6). Domains 1 through 3 comprise the heavy chain of HMWK, and domain 5 and 6 compose its light chain [64]. Each of the 6 domains encompasses an important characteristic for the function of HMWK. Colman and Schmaier have described the importance of these domains and properties that each domain may contribute to the exerted functions of HMWK. For instance, HMWK interacts with endothelial cell receptor C1q through its D2 domain, it interacts with platelets with its D3 domain, it harbors the vasoactive nonapeptide or BK in the D4 domain, it binds to negatively charged surfaces through D5 domain due to the presence of the histidine-rich region, and it binds to Plasma Kallikrein and Factor XII through its D6 domain [68].

On the other hand, LMWK is a splice variant with around 65 kDa of weight and 409 amino acids in length. It is identical to the heavy chain of the HMWK. The major distinction between the low and high molecular weight kininogens is at their C terminal where LMWK lacks D6 domain. Tissue kallikrein KLK1 interacts and cleaves LMWK to produce Kallidin [69,70].

As defined in Goodman and Gilman's the pharmacologic basis of therapeutics book, 8th edition, Kinins are a group of oligopeptides with similar chemistry and pharmacological characteristics [71]. These polypeptides belong to Autacoids with autocrine or paracrine functions due to their short-lived duration [72]. They are involved in vasodilatation, increased vascular leakage and fluid extravasation, development of angioedema, regulation of blood pressure, electrolyte hemostasis, renal hemodynamics, pain, and prostaglandins generation. Additionally, they exhibit antithrombotic and anti-

fibrotic activities [64]. Therefore, they encompass a diverse group of mediators that play role in inflammatory reaction [73]. Kinins are produced in a variety of tissues in the body. They contribute to various physiological activities in the body, among which they cause vasodilatation or slow smooth muscle contraction in physiological or pathological conditions of the tissues, respectively [74]. This paradox action of kinins could be explained by the fact that kinins lead to vasodilation and relaxation of vessels through the production of nitric oxide (NO) in the endothelial layer of the vessels. However, if this layer of cells has endured any injury jeopardizing its functionality, kinins induce vasoconstriction to the vessels by acting directly on the smooth muscle cell layer [74,75].

Both BK and kallidin belong to the kinins and are produced from HMWK or LMWK, respectively, by the action of kallikreins (Figure 4) [62,76]. Generated kallidin is subsequently transformed into BK by the action of Aminopeptidase floating in the plasma [70,77]. Generated kinins exert their actions through 2 cell surface G-protein coupled receptors: the constitutively expressed Bradykinin 2 receptor (Bdkrb2) with less activity on the inducible Bdkrb1 [72]. Bdkrb1 and Bdkrb2 are primarily coupled to Gq and their activation leads to an intracellular increase in Ca^{2+} by the activation of phospholipase C (PLC) and the subsequent production of IP_3 [78]. Although both kinin receptors (Bdkrb1 and Bdkrb2) signal through similar transduction pathways, their signaling is distinct due to their spatial and conditional distribution.

In vascular endothelial cells, Bdkrb2 activation leads to the release of NO, through the activation of endothelial nitric oxide synthase (eNOS), that will leak outside the endothelium to act on the adjacent smooth muscle cells and lead to their relaxation [79]. On the other hand, Bdkrb1 is absent in physiological conditions. Both receptors are regulated in

different pathologies. For instance, diabetes mellitus leads to the activation of both receptors [80]. Moreover, the expression of the receptors is induced in pathological conditions provoked by tissue injury due to oxidative stress, proinflammatory stimuli such as lipopolysaccharides, endotoxins, and cytokines (IL-1 β and TNF- α), and vasoactive peptide stimuli, such as the renin angiotensin system (RAS) [81-84]. Many studies have shown that the absence of one of the kinin receptors leads to the upregulation of the other receptor as a compensatory mechanism [83,85].

Many enzymes, such as carboxypeptidase-N (also known as Kininase I) and carboxypeptidase- M, modify both BK and kallidin by cutting off the arginine residue from their C terminal generating the des- Arg forms of these kinins, and shifting their specificity from Bdkrb2 to Bdkrb1 [86]. However, angiotensin-I-converting enzyme (ACE, Kininase II) is another carboxypeptidase that converts the inactive angiotensin I to the vasopressor angiotensin II by cutting off two amino acid residues from the C terminal of the angiotensin I [87]. On the other hand, ACE (Kininase II), Neutral endopeptidase 24-11 (NEP, neprilysin), dipeptidyl peptidase IV, Aminopeptidase P and endothelin converting enzyme, inactivate both kinins by cutting off two amino acids residues (Phenylalanine and Arginine) from their C terminal to produce BK (1–7) and kallidin (1–8) from BK and kallidin, respectively [66,88].

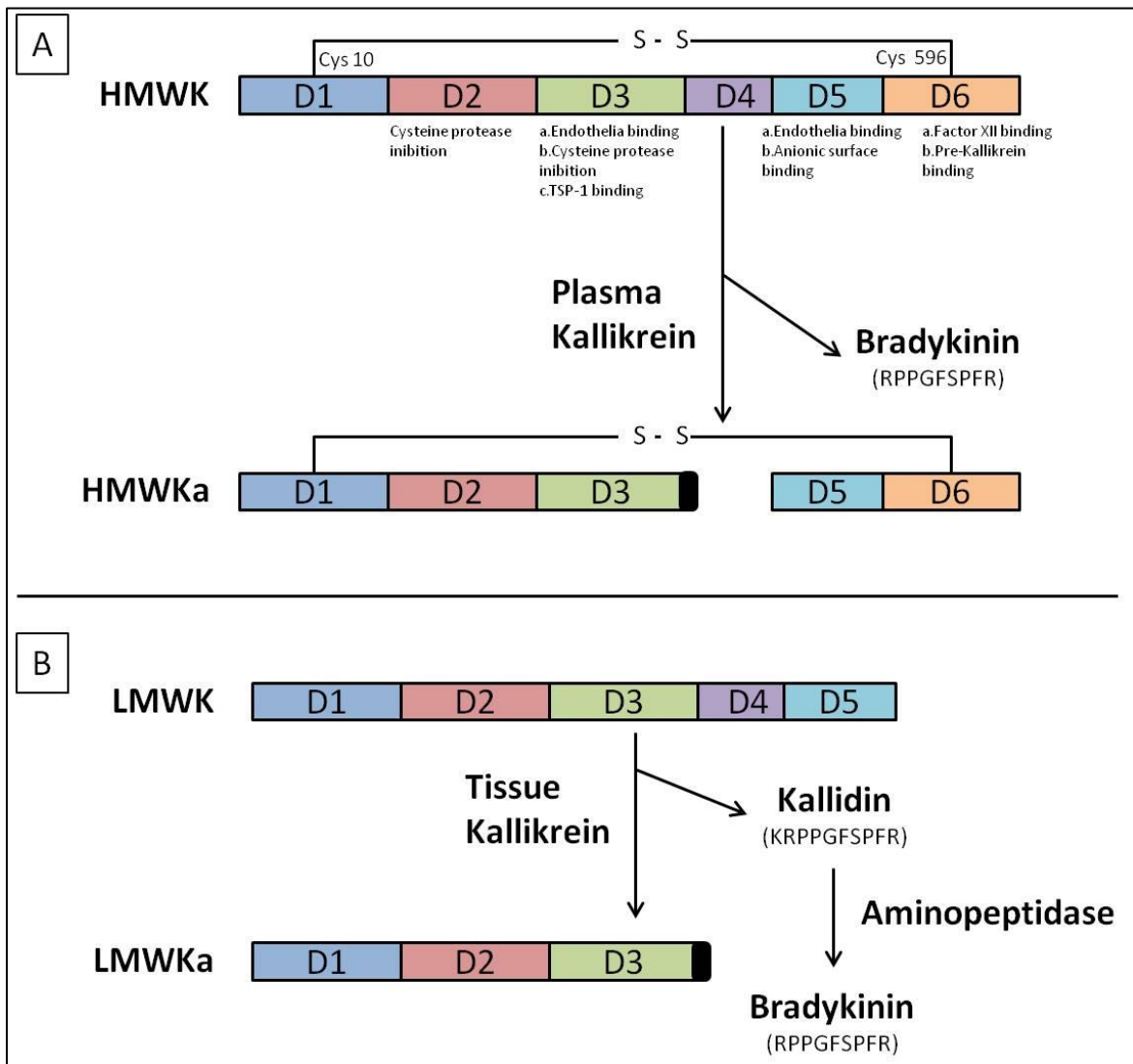


Figure 5: A schematic diagram of the domains of kininogens. A: HMWK is composed of 6 domains (D1-D6). Bradykinin is released from D4 of HMWK upon the action of Plasma Kallikrein on HMWK to yield HMWKa. B: LMWK is a splice variant of HMWK and is composed of 5 domains (D1- D5). Tissue Kallikrein cleaves D4 of LMWK to release Kallidin (Lys- Bradykinin) and LMWKa. Kallidin is then converted to Bradykinin by the action of an aminopeptidase. Figure modified from [65,66].

2. Plasma Kallikrein/Kinin System:

The Plasma Kallikrein/Kinin system (PKKS) consists of three “contact factors” that are the coagulation factor XII (FXII), Plasma Prekallikrein (PPK), and HMWK (Figure 4). Plasma kallikrein (PK, gene symbol KLKB1) is a serine protease that mediates central

roles in blood flow, coagulation, blood pressure regulation, innate inflammation, and pain [62]. PK is generated from the activation of the Plasma prekallikrein, which is abundant primarily in the liver, the pancreas, the kidney, and meagerly in other organs such as the brain, heart, spleen, thymus, testis, and intestine. Due to the fact that active plasma kallikrein is only found in the circulation, PK's effects are exerted through the interaction of plasma with different tissues [89].

a. Activation mechanisms of PK:

Although the activation mechanism of PK is still not well described, there are 2 postulated mechanisms for the activation of plasma kallikrein: contact activation [90], and constitutive activation [91].

i. Contact Activation mechanism:

The physiological events of the contact activation of PK are still not fully clear, the interactions of FXII with an activating surface is a corner stone in this instigation leading to the formation of the active FXIIa [62]. FXIIa, in turn, activates its primary substrates FXI and PPK. The former results in the initiation of the intrinsic coagulation cascade, whereas the latter leads to the formation of active PK. This active serine protease can push the system by additionally activating FXII and also cleaving HMWK and liberating the vasoactive nonapeptide BK that activates Bdkrb2 [92]. Carboxypeptidase M subsequently cleaves BK and generates [des-Arg⁹] Bradykinin, which activates the Bdkrb1.

ii. Constitutive Activation mechanism:

Although the contact activation mechanism was considered as the only route of PK activation for a long time, it did not indicate a pathway for the constitutive activation of PK, and subsequently the generation of BK, in physiological systems. Loza et al. observed an activation mechanism for PK that is independent of the activation of FXII while investigating the activation of urokinase by PK [91]. The events of the constitutive activation of PK can be summarized as follow: HMWK and PK assemble on cell membrane (e.g. platelets [93] and endothelial cells [94]), leading to the PK activity even in the presence of neutralizing antibody to FXII and FXII-deficient plasma, but not PK-deficient plasma [94]. Activated PK results in kinetically-favorable FXII activation after its assembly to cell membranes [95,96]. These findings demonstrate another route for factor XII activation independent of auto-activation on a negatively charged artificial or biologic surface. Two reports have proved the validity of this proposed activation mechanism using two knockout mice models: the C1 INH knockout mice [91], and the factor XII knockout mice [90].

Besides the effects of PK through cleaving HMWK and BK production and Bdkrb2 activation, PK activates other substrates that exert BK receptor independent effects [62]. For instance, PK can activate the contact system, plasminogen, and collagen by cleaving them, and a variety of secreted proteins suggesting that PK interacts with a variety of substrates, however, it's still unclear the physiological significance of many of these interactions [97-99]. Many studies have reported that deficiency in either PK or kininogen in humans showed no significant effect on blood coagulation, however, the results of studies in mouse model systems have documented that contact proteins are vital for

thrombus formation [100-102]. On the other hand, a gain of function mutation in FXII in humans was associated with hereditary angioedema (HAE type III) which is clinically demonstrated as repeated acute skin swelling, abdominal pain, and laryngeal edema [103]. PK can also be activated by an FXII independent mechanism on the surface of endothelial cells by prolyl-carboxypeptidase (PRCP) [104]. Liu *et al.* have demonstrated that PK exacerbates intracerebral hematoma expansion via a BK-independent mechanism and its collagen binding properties, which interferes with collagen-induced platelet activation [105]. Altogether, these findings prove that the plasma PK exerts its effects through both kinin-dependent and kinin-independent mechanisms.

3. *Tissue Kallikrein/Kinin System:*

The Tissue Kallikrein (KLKs) is a family of closely related, single chain, serine proteases that are significantly different from the plasma kallikrein at the physiological and immunological levels. It was first thought that the human KLK family is composed of only 3 genes, which are tissue kallikrein, glandular kallikrein 2, and prostate-specific antigen (PAS) [106]. Later, Murry *et al.* discovered that a cDNA probe from monkey kallikrein gene was able to recognise 19 genomic clones in human samples [107]. After 10 years, Yousef *et al.* have discovered 12 human kallikrein related genes. In addition, they showed that human kallikrein gene family is composed of 15 tandemly related, steroid hormone-regulated, genes located on the same chromosomal locus (19q13.4) [108]. This family comprises the largest cluster of protease in the human genome of any catalytic class [109]. These enzymes were found to be differentially expressed in different tissues such as the prostate gland, salivary glands, pancreas, gut, skin and sweat glands, kidney, liver, central

nervous system, blood vessels, adrenal, neutrophils, and many other tissues. Kallikreins were also present in biological fluids like seminal fluid, serum, and milk of lactating women, which confirms their secretion in physiological conditions [69,110-113]. The expression of tissue kallikreins in broad organisms suggests a paracrine function to these enzymes, where they act principally in the local environment of their tissues of origin.

Each KLK possesses specific function and specificity for its substrate. The different isoforms of KLKs share between 30 and 50% homology among themselves, at the DNA and amino acid residue levels, with approximately 4 to 10 kb of gene size [69] and 230 to 440 amino acid mature proteins [114]. One exception is the KLK2 and KLK3 that share about 80% homology that makes them the most closed members in this family [106]. All KLKs are produced as pre-proenzymes (zymogens), to be then secreted and proteolytically cleaved to create the active enzymes. At their NH₂ terminal, kallikreins contain 16-30 amino acids residues that act as a signal peptide, followed by 4-9 amino acid residues that act as pro-peptide, and then a stretch of amino acid residues forming the catalytic domain that encompasses the enzymatically active mature protein [69]. The chronological cleavage of the signal and pro-peptides leads to the formation of pro- and mature enzyme forms to become active and enter secretory pathway [115,116].

In the human KLK family, KLK1 liberates kinin from kininogen efficiently and the other KLKs possess greatly reduced or no kininogen cleavage activity [69,117]. Therefore, KLK1 is called as 'true tissue kallikrein' [118]. KLK1 has trypsin- and chymotrypsin-like specificity, which unlike PK, hydrolyzes an Arginine and Methionine residues from LMWK to generate Kallidin (Lys-bradykinin) that is subsequently converted to BK by a second aminopeptidase cleavage (Fig. 4) [119]. Aside to the specificity of KLKs

to kininogens, it is expected that KLK to be involved in a broad spectrum of biological processes such as blood pressure regulation, electrolyte homeostasis, remodeling of extracellular-matrix, cellular signal transduction, pro-peptide maturation, neuroplasticity, and desquamation of skin [120,121]. These activities are exerted either solely by KLKs or with coordination of one or more proteolytic cascades. The activation of signal transduction pathways by KLKs pathways could be initiated by cleaving of cell-surface receptors such as protease activated receptors (PARs) by one of the KLK proteins [120,122]. In addition to that, Colman and Schmaier have shown that PSA (KLK3) plays a crucial role in the liberation of sperms by its proteolytic activity on semenogelin and fibronectin [68]. Although many KLK activities and pathways have been documented, the full range of the biological and/or pathophysiological activities and in vivo KLKs' substrates are still not well described.

4. Involvement of KKS in different pathologies:

Despite its clear important physiological activities over different body systems, the involvement of KKS in different pathologies has been studied extensively. For instance, patients with hereditary deficiency of HMWK (Kng1 gene), PK (KLKb1 gene), or FXII (FXII gene), or mouse models with genetic ablation of the aforementioned genes showed a prolonged blood coagulation (aPTT, activated partial thromboplastin time) without any signs of clinical bleeding defects [101,123,124]. Thus, indicating a thrombogenic activity for the activated KKS in different species. In the following sections, we will be discussing

the mechanisms of KKS-induced complications over 2 systems: the cardiovascular and renal systems, in addition to the role of KKs in promoting inflammation.

a. Involvement of KKS in inflammatory process:

Many reports have recognized the inflammatory role that KKS plays on different systems. The mechanisms by which KKS exerts its inflammatory role could be summarized in three broad pathways. In the first pathway, the liberation of BK from kininogen, and its binding and activation of Bdkrb2 leads to vasodilation, increased vascular permeability, and edema through the production and release of nitric oxide and prostacyclin (prostaglandin I₂, PGI₂) from the endothelial cells [125]. Additionally, Bdkrb1 is induced upon inflammatory response in endothelial cells. Moreover, the BK metabolite, des-Arg⁹ BK, preferentially binds and activate Bdkrb1 to augment and maintain the inflammatory response [124,126]. In the second pathway, activated kallikrein cleaves FXII to yield the β form of it. The latter activates the complement system leading to the production of chemoattractants such as C3a and C5a, which attracts monocytes to the site of the complement system activation [127,128]. In the third pathway, kallikrein, independent of the complement system activation, stimulates neutrophil activation, accumulation, and release of elastase from neutrophil to aggravate the inflammatory response [129].

b. Involvement of KKS in CVD:

As previously discussed, the KKS has a key role in controlling blood pressure, thrombosis, fibrinolysis, and inflammation, which rendered this system as a potential target

for therapeutic development, especially for CVD [130]. However, the KKS has opposing effects on the cardiovascular system that will be discussed in the following section.

On the heart, reports have shown that BK decreases heart rate and ameliorates hypertension through nitric oxide production [131,132]. In addition, post myocardial infarction upregulated the components of KKS that contribute to the survival of the patients [18].

However, there are many reports that relate the KKS with different pathophysiological conditions of the cardiovascular system. For instance, in many clinical studies, there was a clear association between the levels of kallikreins and the occurrence of myocardial infarction or stroke [133,134]. Additionally, inhibiting plasma kallikrein showed neuroprotective effects in the early stages of stroke [135]. Moreover, Bdkrb2 was shown to be induced in response to ischemia, and its genetic ablation or inhibiting the receptor in a mouse model resulted in a decrease in infarct size and cerebral edema and enhanced motor function and survival of the mice compared to wild-type controls [136-139].

On the other hand, KKS was shown to be activated in diabetic patients in a hyperglycemia and advanced glycation end products dependent mechanisms [140]. Additionally, several experimental models have shown a clear association between KKS and diabetic-induced microvascular complications [65,141]. Of interest, in the T1DM patients enrolled in the Diabetes Control and Complications Trial/Epidemiology and Diabetes Intervention and Complications (DCCT/EDIC) study there was a markedly increase in the plasma kallikrein levels in the patients, and the levels were associated with hypertension and vascular complications observed in kidneys [142]. Moreover, Ienaga et al.

have shown that BK induces the expression of fibrotic markers, such as connective tissue growth factor [143]. Additionally, Shariat-Madar et al. have shown that genetic ablation of *Bdkrb2* induces the angiotensin 2 receptor mediated nitric oxide production and conferred an anti-thrombogenic activity [66]. Furthermore, Velarde et al. have shown that BK induces proliferation and migration of vascular smooth muscles in a reactive species dependent mechanism, and induces the production of extracellular matrix proteins such as collagen [144]. Taken together, these studies shed a light on the involvement of KKS in the progression of vascular injury, especially arteriosclerosis.

c. Involvement of KKS in renal diseases:

Diabetic nephropathy (DN) is a chief health epidemic complication of diabetes mellitus. It is the leading cause of morbidity and mortality in diabetes, chronic and end-stage renal failure [145]. The renal complication in T1DM is correlated to increased cardiovascular and renal diseases and reduced longevity [146]. Glomerulosclerosis is the initial event and considered as the hallmark of DN development. It is marked by podocyte loss, glomerular basement membrane growth, hyaline arteriosclerosis, and mesangial expansion with the accretion of extracellular matrix (ECM) [83,147]. Furthermore, the signs of DN such as microalbuminuria and reduced glomerular filtration rate (GFR) strongly correlated with the level of mesangial expansion [83,148]. Although genetic factors seem to contribute to the development of glomerular injury, high blood glucose appears to be the incentive for cellular damage [149].

Many investigators have shown that renal KLK production and excretion are significantly decreased in mild renal disease patients and more strikingly diminished in severe renal failure patients [150]. Moreover, KLK administration recovered salt-induced renal fibrosis and glomerular hypertrophy, and reduced infiltration of inflammatory cells in the renal tubules, interstitial tissue, and vasculature of hypertensive rat models, such as Dahl salt-sensitive and spontaneously hypertensive rats (SHR) [70,151,152]. Interestingly, Schneeweiss *et al.* have reported that the administration of aprotinin, a potent KLK inhibitor, after heart surgery induced renal failure and affected the survival of the patients [153]. Collectively, these findings highlight the important role of the KKS in the preservation of renal functionality and protection against the effects of salt-induced and hypertension-induced renal injury by hampering oxidative stress and inflammatory responses.

On the other hand, there are many reports have highlighted a correlation between KKS and renal injury in diabetic settings [154-156]. For example, an increased kinins were observed in urinary secretions of type I diabetic rats with moderate hyperglycemia, and showed decreased vascular resistance of the kidneys and increased GFR and renal plasma flow (RPF) [157]. Moreover, inhibiting kallikrein activity by aprotinin, or Bdkrb2 by HOE-140 normalized the GFR and RPF levels in these hyperfiltration diabetic rats [157,158]. On the contrary, Tschöpe *et al.* have shown there was a decrease in the activity of kallikrein in severe type I hypo-filtrating rats without insulin injections, suggesting a relationship between the activity level of kallikrein and the state of GFR and RPF [159]. These effects of KKS are mainly exerted through the generation of BK [78].

On the other hand, mesangial expansion is a manifestation of glomerulosclerosis. Brownlee et al. studied the mechanisms of the development of DN and showed that hyperglycemia initially provokes mesangial cells proliferation, and then hypertrophy to be ultimately transformed into glomerulosclerosis [160]. This mesangial cell transformation is operated by a different population of renal cells that are stimulated by hyperglycemia, either directly or indirectly, which leads to the secretion of a panel of mediators, such as proinflammatory cytokines and/or growth factors [161]. Among these mediators is transforming growth factor (TGF)- β that has a strong effect on the expansion of mesangial cell ECM deposition [162]. This fibrotic effect of TGF- β intercedes through the stimulating connective tissue growth factor (CTGF) expression [163,164]. It's still not fully clear how KKS beneficially regulates mesangial cells, yet BK was shown to have a paradox effect on renal cell proliferation. For instance, the activation of B2R by BK induces proliferation of quiescent renal cells and inhibits cell growth under proliferative, such as diabetic conditions [165]. This antiproliferative effect was observed in different cell types, including mesangial cells [166]. Insulin-like growth factor-I (IGF-I) and, to a lesser extent, insulin, are the possible link between the KKS and diabetes-induced mesangial cell proliferation. They induce the proliferation of mesangial cell ECM secretion, supposedly through the stimulation of the IGF-I receptor, which makes insulin to be implicated in the initiation of DN [81]. IGF-I is a growth factor produced in many cells and tissues, particularly mesangial cells. It was reported that during the development of diabetic glomerulosclerosis there is an increase in renal IGF-I levels, which promoted cell proliferation and ECM deposition [167]. In addition, it was suggested that BK-induced cell proliferation is dependent on growth factor receptor. IGF-1 significantly stimulates mitogen-activated

protein kinases (MAPKs) like p42/p44 (ERK 1/2) in mesangial cells. On the other hand, it's well demonstrated that BK reduces IGF-I-induced ERK 1/2 stimulation in mesangial cells and IGF-I-induced mesangial cell proliferation. These findings are in favor for delineating the mechanism of crosstalk between the renal KKS and IGF-1, by which renal KKS exerts its antiproliferative effects [166]. Collectively, these opposing proliferative and antiproliferative effects of BK are mainly due to the variability in experimental environments regulating renal KKS in diabetic settings [158,168]. These results propose the potential therapeutic target that B2R may be in DN.

C. Sphingosine Kinase/Sphingosine 1 phosphate pathway:

As previously mentioned, obesity and insulin resistance are risk factors for T2DM [169,170], which is manifested by aberrant lipid metabolism and signaling. Among the signaling molecules, sphingolipids have gained the interest of different investigators for their potential roles in a different array of pathologies, namely cancer, inflammation, and cardiovascular diseases [171]. In the following section, we will be discussing the properties of the sphingosine kinase/sphingosine 1 phosphate pathway, its components, and its mechanism in the involvement in CVD.

Sphingosine kinases (SphKs) are composed of two isoforms (SphK1 and SphK2), each has a distinct cellular localization, biological functions, and protein biochemistry [172]. Both proteins phosphorylate sphingosine to generate sphingosine-1-phosphate (S1P). This phosphorylation process shifts the proapoptotic properties of sphingosine into a pro-survival molecule that favors cell growth, proliferation, and migration (Figure 6) [173,174].

This shift in the properties is very crucial for the biological homeostasis [175,176]. For instance, the imbalance in the levels of sphingosine and S1P would promote insulin resistance if it was in the favor of sphingosine and would promote insulin sensitization if it was in the favor of S1P [177,178]. Additionally, S1P is implicated in many physiological and pathophysiological situations [179,180].

Generated S1P is secreted outside the cells to exert its functions in an autocrine or paracrine fashion through binding to one of the five S1P receptors (S1pr) (Figure 6). All S1pr belong to G protein-coupled receptors family, equipped with different intracellular relaying molecules and mechanisms [181]. Hence, the biological functions of S1P are receptor and cell specific [182].

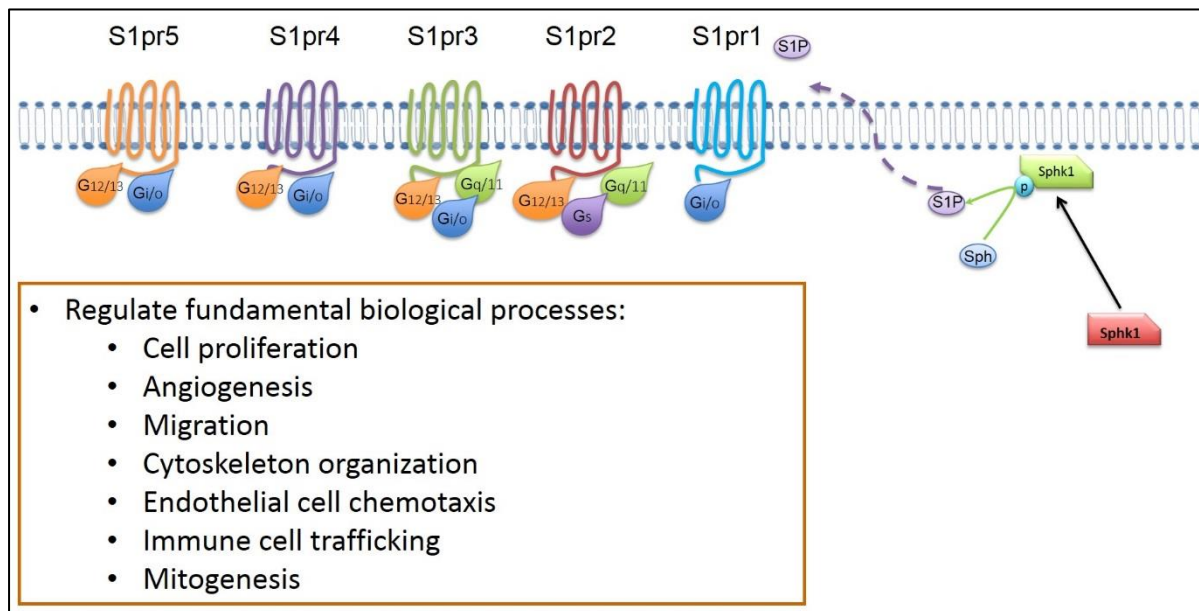


Figure 6: A schematic diagram of the components of the SphK1/S1P pathway. SphK1 is activated by phosphorylation and translocates to the plasma membrane. On the membrane, SphK1 phosphorylates sphingosine to generate S1P, which is exported to the outside of the cells to bind and activate one of the S1P receptors. Each S1P receptor is bound to different types of G proteins that allows these receptors to exert different biological functions.

1. Properties of SphK:

SphK isoforms are structurally related proteins although they are encoded by two distinct genes. Additionally, the two isoforms differ in their protein size, localization, and expression patterns. For instance, SphK1 is the small isoform with a 48 kDa size and cytosolic localization. On the other hand, SphK2 is the big isoform with 69 kDa size and nuclear localization ability [183]. In fact, the difference in the protein size of the two isoforms is due to an extended N-terminal site of SphK2, which contains a nuclear export sequence (NES) responsible for the shuttling property of this isoform between cytosol and nucleus [184].

Furthermore, the tissue distribution of the two isoforms differs. For instance, SphK1 is primarily expressed in the lungs and spleen [173,176], whereas SphK2 is primarily expressed in the heart, brain, and liver [175,177,178]. Additionally, the biological functions of each isoform are different from the other one. For example, SphK1 promotes cell proliferation and survival, whereas SphK2 promotes cell growth arrest and apoptosis [185]. Both isoforms are reported to be involved in the diabetes-induced complications, which will be discussed later.

2. Mechanism of activation of SphK:

Since the substrates of SphK are predominantly localized in the subcellular membrane, translocation of the agonist-stimulated-SphK to close proximity to its substrates is crucial for enzyme activity. As previously mentioned, SphK1 is basally expressed in the cytosol and upon stimulation, it translocates to cell or organelle membrane to regulate

different biological functions. In addition, the translocation destination reflects the functions of SphK1 [185,186]. On the other hand, SphK1 is regulated by phosphorylation on Ser-225, which induces conformational changes to expose the catalytic domain and to promote the subcellular localization from the cytosol to plasma membrane [187]. In fact, there are many growth factors and cytokines are able to induce the phosphorylation of SphK1, mainly through ERK1/2 mediated mechanism [187-189]. In addition to the phosphorylation-mediated translocation of SphK1 to the plasma membrane, some reports have shown that SphK1 translocated to the membrane via a calcium binding site responsible for binding of SphK1 to integrins in the plasma membrane [190].

Unlike SphK1, the activation-associated localization of SphK2 is less understood. Nevertheless, it has been reported that SphK2 has the ability to shuttle between the cytosol and nucleus [190]. On the other hand, SphK2 cellular distribution is cell-type specific, and agonist-mediated [191,192].

As per the activators of SphK2, it was shown that epidermal growth factor (EGF) and phorbol myristate acetate (PMA) activate SphK2 through an ERK1/2-dependent phosphorylation at two residues Ser- 351 and/or Thr- 578 [193]. The EGF- induced phosphorylation. Moreover, EGF-mediated activation of SphK2 was associated with invasiveness and migration of breast cancer cells [193]. The biological functions of SphK2 are exerted mainly by epigenetically modifying the expressions of genes. For instance, activated SphK2 generates S1P in the nucleus, which in turn binds and inhibits histone deacetylase (HDAC 1/2), thus preventing the deacetylation of histone 3 and subsequently the expression of the surrounding genes associated with this histone [180,191].

3. Mechanisms of S1P signaling:

As previously discussed, SphKs exert diverse biological functions mediated through the production of S1P [176,194]. S1P can bind and activate 5 different S1prs, which are transmembrane GPCR. S1pr were originally called endothelial differentiation gene (EDG) receptors. S1prs are coupled to different G proteins, adding to the complexity and diversity of S1P signaling [195]. This mechanism of action of S1P is known as “inside-out” signaling model. In this model, SphK activation and translocation to the plasma membrane is required to generate S1P. S1P is then released to the extracellular area to bind and activate one of the sub-types of its receptors, in an autocrine or paracrine fashion [194]. On the other hand, many reports have shown that S1P has intracellular targets in the cytosol or the nucleus, including HDAC 1/2 [194,196]. Moreover, S1P can bind and regulate prohibitin 2 (PHB2), an inner mitochondrial membrane protein, regulating mitochondrial respiration [197]. Furthermore, S1P also binds to other proteins such as peroxisome proliferator- activated receptor γ (PPAR γ), human telomerase reverse transcriptase (hTERT) and beta- site amyloid precursor protein- cleaving enzyme 1 (BACE1) [198-200].

4. Involvement of SphK/S1P signaling in diabetes and related pathologies:

a. The role of SphK signaling in hepatic insulin resistance:

Insulin resistance is defined as the non-responsiveness of the tissues, such as adipose tissue, skeletal muscle, and liver, to insulin. Insulin resistance, especially in the liver, was shown to be a major risk factor for T2DM initiation [201-203]. SphK activation

was shown to improve insulin signaling in T2DM, through reducing hepatic fat production, albeit a minimal effect on carbohydrates metabolism [204].

b. The role of SphK signaling in pancreatic β -cell death:

Pancreatic β -cell destruction leads to a decrease in insulin production and secretion, which is often driven by high levels of circulating lipids and sphingolipid metabolites in obese or overweight patients [205]. For instance, many reports have shown the involvement of ceramides and caspases activation on the apoptosis of β -cells in *in vivo* animal models and *in vitro* experiments [206-208], however, the mechanism of ceramide actions need further elucidation. On the other hand, SphK/S1P pathway has been shown to improve insulin release and develop islet vasculature [209]. Thus, SphK/S1P pathway exerts a protective role on the β -cells of the pancreas [205].

The favorable effects of SphK/S1P pathway in insulin sensitization is controversial, since many reports show the involvement of this pathway in the proinflammatory process, through inducing the production of pro-inflammatory cytokines (IL6) from the adipocytes [210,211], and inhibiting the expression of anti-inflammatory proteins (IL- 10 and adiponectin) in adipose and muscle tissues [212]. Altogether, these studies suggest regulating SphK/S1p pathway poses a therapeutic potential in the treatment of insulin resistance.

5. The role of SphKs in the progression of diabetes -related complications:

SphK/S1P signaling has been correlated with diabetic-induced macrovascular complications, such as cardiovascular disease [213,214], and correlated with many diabetic-induced microvascular complications, namely neuropathy [215], retinopathy [216], and nephropathy [217]. In the next sections, we will be discussing the mechanisms by which SphK/S1P pathway would induce diabetic induced cardiovascular diseases and diabetic-induced nephropathy.

a. The role of the SphK/S1P pathway in diabetes-induced vascular complications:

Diabetes is a risk factor for the development of different cardiovascular diseases, such as atherosclerosis and heart failure [218-221]. Many studies have shown that sphingomyelin (SM), ceramide, and S1P levels to be elevated in the setting of atherosclerosis and proposed a link between the SphK/S1P pathway and the progression of cardiovascular diseases [222]. For instance, the SphK1/S1P pathway has been shown to promote hypertension, fibronectin deposition, and VSMC proliferation and migration, which rendered S1P to be recognized as pro-inflammatory, proliferative, invasive and migratory agent [223-228]. In this regard, a number of studies implicated SphK1 as a mediator of angiotensin II-induced hypertension [223,229,230]. SphK1 null mice are protected against angiotensin II- and hypoxia-induced hypertension and inhibition of SphK1 reduced the right ventricular hypertrophy pulmonary arterial hypertension mice [231]. Most recently, Siedlinski and colleagues reported a correlation of S1P serum level with higher aortic systolic pressure levels in patients with cardiovascular risk. Also, they

observed elevations of Sphk1 mRNA, protein, and activity in the aorta and mesenteric arteries isolated from AngII-induced hypertensive mice [232]. Furthermore, inhibition of SphK activity protected against atherosclerosis, through abolishing the SphK-induced adhesion molecule expression and the activation of ERK in endothelial cells [233], and against angiotensin-induced hypertension [229,230]. The expression and activation of SphK1 were previously shown to be mediated by BK, and the resulting S1P acting through its receptors induced the expression of Ctgf and fibronectin [191,234].

On the other hand, several studies have shown that SphK/S1P pathway exhibits a cardioprotective role in vivo [235-237]. For instance, SphK1 overexpression was shown to improve cardiac function in a cardiomyopathy diabetic mouse model [235]. In another non-obese diabetic mouse model, S1P was shown to reduce monocyte-endothelial interaction and thus ameliorating atherosclerosis [238]. Moreover, SphK1 was shown to play a protective role in ex vivo experiments on isolated mouse hearts from ischemia-induced injury [239,240]. Taken together, these contradictory outcomes mandate further investigation to decipher the role of the SphK/S1P pathway in physiological and pathophysiological conditions of the vascular system, in order to better intervene with its biological outcomes.

b. The role of SphK/S1P pathway in diabetic-induced nephropathy (DN):

DN is characterized by glomerular cell proliferation and hypertrophy, ECM deposition, and renal fibrosis, all of which promote end stage renal failure. Many reports have shown that the dysregulated levels and metabolism of sphingolipids are implicated in

the progression of diabetic complication, especially the pathogenesis of DN [241]. For instance, S1P induces mesangial cell survival, proliferation and migration [242], and the expression of fibrotic growth factors, collagen and fibronectin production, which are mediated through the Smad pathways [217]. Additionally, S1P has been implicated in promoting renal inflammation and fibrosis through upregulating fibronectin expression [217,243].

Moreover, studies have shown that S1Pr2 and 3 are the receptors involved in relaying the effects of S1P on renal fibrosis, glomerular cell proliferation and pathological angiogenesis [244,245]. On the other hand, the lymphocytes chemoattraction to the site of inflammation is facilitated by the activation of S1pr1 migration [246], which points to the involvement of this pathway in the promotion of the deleterious effects of inflammation on the kidneys and other tissues or organs [247,248]. Nevertheless, there are some reports contradict the involvement of SphK/S1P pathway in promoting inflammation, at least in in vitro experiments, in mesangial cells [249]. In addition, one study has reported that the genetic ablation of SphK2 has a protective role on the kidneys in diabetic mice [250], and SphK1 knock-out aggravated diabetic-induced nephropathy [243]. Altogether, both isoforms of SphK are involved, however, to a different extent, in regulating diabetic-induced microvascular complications, namely DN.

D. Leptin in CVD:

As previously discussed, endothelial dysfunction is the first step in initiation or development of atherosclerosis and plaque progression, thus the manifestations of

atherosclerotic complications and cardiovascular diseases [251]. Among the risk factors for CVD are dyslipidemia, hypertension, hyperglycemia, insulin resistance, and abdominal obesity, which are associated with inflammation and thrombogenicity processes. The sequence of events of atherosclerosis development could be summarized as follow: first endothelial dysfunction occurs accompanied by inflammation and macrophage infiltration to the vessel walls and accumulation of oxidized lipoproteins in the region followed by smooth muscle migration and proliferation, extracellular matrix and fibrotic protein deposition, accumulation of lipid material and fat laden cells, activation of platelets, and promotion of thrombosis [252]. In addition, we previously discussed the involvement of adipose tissue in the development of inflammation. Hence, the notion that adipose tissue has passive biological functions, such as lipids storage sites, is no more valid. Additionally, it is now well established that adipocytes play endocrine functions by producing and secreting many active metabolites that stimulate divers biological processes [253]. The metabolites are primarily divided into inflammatory and anti-inflammatory mediators. Among the inflammatory mediators, adipose tissue produces adipokines, TNF α , IL6, leptin, plasminogen activator inhibitor-1 (PAI-1), angiotensinogen, resistin and C-reactive protein (CRP), which are directly related to vascular injury, insulin resistance, and atherogenesis. On the other hand, adipose tissue also produces anti-inflammatory mediators such as nitric oxide and adiponectin that have an important protective role against inflammation and obesity-induced insulin resistance [254,255].

One of the interesting adipokine produced by adipocytes is leptin, since high circulating leptin levels are associated with the development hypertension, and induces

atherosclerosis [256-258]. We will be discussing leptin, its biochemical properties, and its role in physiological and pathophysiological conditions, especially cardiovascular diseases in the following section.

In 1994, an experimental knock-out mouse model was recognized to be obese and does not feel satiated with a continuous food intake. At first, the researchers called the ablated gene Obese gene (Ob). In the next two years, the gene was sequenced and researchers found that the Ob gene encodes leptin protein, which is predominantly produced and secreted from adipose tissue. In addition, it was shown that leptin is expressed in extra-adipose tissues such as placenta, stomach, mammary glands, and white blood cells [259,260]. Leptin is usually regulated by cytokines and insulin and cortisol [261]. In addition, the levels of leptin in males are less than those in females due to the higher body-fats in female bodies compared to males, and to the hormonal changes between the two genders [262]. Circulating leptin transmits hormonal information to the hypothalamus regarding the state of the stored energy in the adipose tissue, which plays a role in controlling satiety and energy expenditure [263,264].

Leptin induces its functions through its binding to leptin receptor (ObR) that is a single transmembrane receptor, which belongs to cytokine-like receptor superfamily. There are several isoforms of ObR that possess different biological activities [265]. The extracellular binding domain of ObR is similar in all the isoforms. ObR isoform b (ObRb) is the longest and the predominant isoform [266], and genetic ablation of this isoform generates severely obese and leptin resistant mouse model, which is called db/db mouse model [265]. ObRa isoform has a role in transporting leptin through the blood brain barrier to exert its neuroendocrinological effects in the hypothalamus [267]. ObRe isoform is the

exception of all ObR by the fact that ObRe is soluble and lacks the transmembrane domain, and plays a role in binding the circulatory leptin and may regulate its activities [268].

In the following section, we will discuss the mechanisms by which leptin induces its physiological and pathophysiological functions.

1. Leptin receptor signaling:

ObRb belongs to the cytokine receptor family with an extracellular agonist binding domain, a single trans-membrane domain, and intracellular domain. ObRb lacks intrinsic enzymatic activity in its intracellular domain, and depends on the Janus kinase 2 (JAK2) and signal transducer and activator of transcript 3 (STAT3) to transduce its signal (Figure 7) [269]. The mechanism of activation of the JAK/STAT pathway could be summarized as follow: the activation of the receptor leads to the recruitment and activation of JAK2 that phosphorylates ObRb and induces the recruitment of STAT3 to the phosphorylated ObRb, and the phosphorylation of STAT3 by JAK2 [270]. Phosphorylated STAT3 is then translocated to the nucleus and homodimerize to induce its transcriptional activity [271].

On the other hand, JAK2/STAT3 pathway activates cytosolic pathways such as Ras Homolog gene family, member A (RhoA) [272]. On its turn, RhoA activates Rho Associated Kinase (ROCK) leading to phosphorylation of LIM domain Kinase (LIMK) and cofilin, subsequently. This axis regulate cytoskeletal reorganization in different cell types, among which vascular smooth muscle cells [273,274].

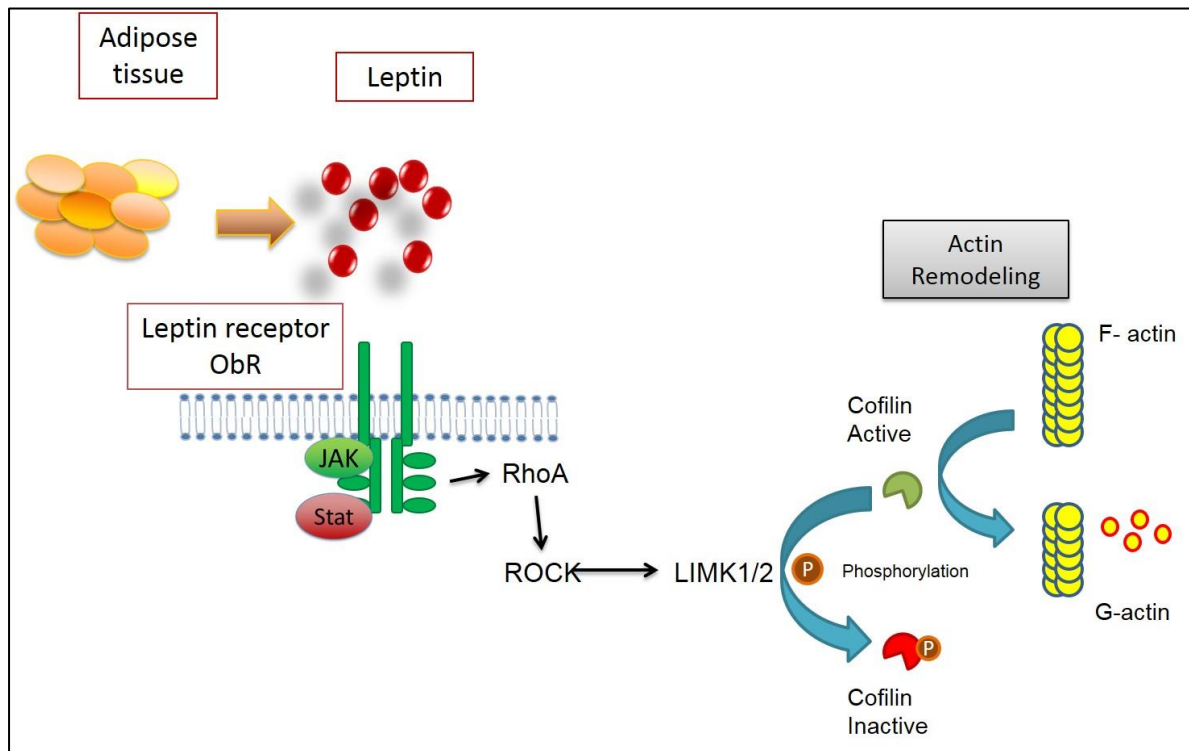


Figure 7: A schematic diagram of the signaling pathway of Leptin receptor (ObRb). Leptin binds to ObR leading to the conformational changes in the receptor and the activation of JAK2. Activated JAK2 phosphorylates the intracellular domains of ObR and recruits STAT3 to the receptor. Among the pathways activated by JAK/STAT mechanism is RhoA/ROCK/LIMK leading to cofilin phosphorylation and inactivation. Active cofilin sieves actin filaments and transforms them into globular actin molecules, contributing to actin remodeling/dynamics.

2. *The role of Leptin in atherosclerosis development:*

a. The role of leptin in hypertension:

High circulating leptin levels are associated with the sympathetic nervous system (SNS)-induced vasoconstriction, and subsequently hypertension, in healthy humans.

Through its binding to the receptors in the central nervous system, leptin induces SNS activity [275], which constitutes the major mechanism of obesity-induced hypertension. In addition, it has been shown that leptin induces the expression of endothelin 1 (ET-1) in endothelial tissues. On its turn, ET-1 is a potent vasoconstrictor through stimulation of the Calcium release from the internal stores in smooth muscle cells [267].

b. The role of leptin in inflammation:

Many reports have described the proinflammatory properties of leptin. High circulating leptin levels induce monocyte-derived expression of TNF α and IL6 and correlate with CRP levels [276]. On its turn, CRP promotes atherosclerosis development by directly inhibiting nitric oxide synthase or indirectly through inducing ROS production, which inhibits nitric oxide production [268].

c. The role of leptin in oxidative stress:

Obesity is associated with an increase in ROS production. Leptin enhances mitochondrial fatty acid oxidation in aortic endothelial cells, thus inducing superoxide production and oxidative stress. Excess superoxide reduces the bioavailability of nitric oxide by inhibiting its synthesis and favoring the formation of peroxynitrite (ONOO⁻), thus attenuating the vasodilation functions of nitric oxide [277].

E. Fibrotic proteins in CVD:

Vascular fibrosis is among the risk factors for the development of atherosclerosis and subsequently CVD [278]. One of the hallmarks of vascular fibrosis is the deposition and accumulation of extracellular matrix (ECM), such as fibronectin and collagen, in the media layer of the vessels promoting vascular remodeling or stiffness and scar formation [279,280]. Vascular fibrosis is the result of the interplay between vascular smooth muscle cells, macrophages, lymphocytes, and endothelial cells to induce ECM production and

deposition and promote fibro-proliferative response [281]. The hemodynamics of blood flow is dependent on the elastic properties of the vessel walls, which in turn are dependent on the constituent of matrix proteins such as elastin and collagen [282]. Any alteration in the relative components of wall matrix proteins in favor of collagen would lead to fibrosis and increased stiffness [283].

1. Risk factors for vascular fibrosis:

Many studies reported an association between vascular fibrosis and cardiovascular disease risk factors including hypertension, hyperglycemia, and dyslipidemia [278]. In addition, renin angiotensin system (RAS), TGF- β , and matrix metalloproteinases (MMPs) were shown to play a role in the development of vascular fibrosis. In the following sections, we will review the mechanisms by which the different risk factors promote fibrosis.

a. Effect of hypertension on vascular fibrosis:

Hypertension is one of the major risk factors for the development of vascular remodeling or stiffness, which is characterized by an increase in extracellular matrix deposition, especially collagen type 1. This fact was supported in an in vivo chronic pressure overload animal model that showed an increase in collagen gene and protein expression [278]. In addition, some observational studies have shown that collagen degradation is repressed in hypertensive patients [278]. Thus, the induction of the collagen production and the inhibition of collagen turn-over would lead to the accumulation of collagen and promotion of vascular fibrosis in hypertensive patients.

Hypertension imposes functional, mechanical, structural changes in the vessel walls that alter the hemodynamics of blood flow [284]. Among the hypertension-induced factors are vessel wall shear stress, and wall circumferential stress [285]. On signaling level, hypertension induces its deleterious effects on the vessel walls through activating RAS, altering the balance between MMP and tissue inhibitors of metalloproteinases (TIMPs), enhancing connective tissue growth factor (CTGF) expression, and abnormal GPCR signaling [286,287]. For instance, reports have shown that angiotensin II plays a fundamental role in executing hypertension-induced fibrosis by promoting endothelial dysfunction and vascular inflammation. In addition, mechanical stretching, because of pressure overload, leads to the upregulation of TGF β and CTGF expression, which regulates collagen deposition in vessel walls [288,289]. Furthermore, hypertension reduces collagen turnover through modifying the activity of the MMP/TIMP [290]. Also, hypertension-induced vascular fibrosis is a result of inflammation and oxidative stress in the vessel walls, and it is affected by endothelial dysfunction, cellular hypertrophy, apoptosis, and migration that are altered in hypertension condition [291].

b. Effect of hyperglycemia on vascular fibrosis:

Hyperglycemia is among the risk factors for the development of atherosclerosis through the vascular fibrosis, which encompasses primarily ECM deposition [292]. Enhanced vascular fibrosis in response to diabetes was described long time ago, and it may affect different organs leading to diabetes-induced complications in the organs [292]. In

addition, vascular fibrosis in diabetes can affect vessels of all sizes from arteries to microvascular beds [293].

Although there has been a huge progress in understanding the mechanisms of vascular diseases in diabetes, the exact mechanisms of vascular stiffness in diabetes are not well established. However, there are indications for the role of metabolic and mechanical alteration in the development of vascular remodeling. Hyperglycemia affects both hemodynamics factors of the vessels and the metabolic properties to promote ECM deposition and inhibit their turn-over [292]. In addition, hyperglycemia induces AGE through the addition of glycated moieties to proteins, such as collagen, which in turn modify the hemodynamic properties of collagen to favor stiffness of the vessels [292]. Moreover, AGE can react with their receptor (RAGE) inducing profibrotic proteins expression, such as TGF β , promoting ECM accumulation, and increasing inflammation. Hence, promoting vascular fibrosis [294,295]. Furthermore, AGE plays a crucial role in ECM regulation by inhibiting the activity of MMP can reduce the [296].

On the other hand, hyperglycemia activates RAS by enhancing AngII activity by upregulating AngII receptor (AT1) and augments ROS generation [292,297]. AngII upregulation in mesangial cells stimulates TGF β production and modifies the regulation of ECM towards accumulation [298,299]. Additionally, many studies reported the upregulation of CTGF, downstream TGF β , which play a role in inducing ECM deposition in diabetes [292,300].

c. Effect of dyslipidemia on vascular fibrosis

Dyslipidemia is a risk factor in for atherosclerosis through promoting vascular fibrosis [301,302]. Many studies have reported that high-fat diet is an inducer of vascular inflammation and fibrosis. Hypercholesterolemia induces an increase in the expression in different forms of collagen (I, III, and IV), fibronectin, and tenascin. Additionally, hypercholesterolemia alters matrix degradation and induces vascular fibrosis [302,303]. The mediated effects of hypercholesterolemia on vascular fibrosis were reversed upon controlling lipid levels through statins [302].

Another mechanism regulated by hypercholesterolemia is the production of ROS and oxidation of LDL in the vasculature, which is a possible mechanism for the development of the hallmarks of vascular remodeling such as endothelial dysfunction, inflammation, hypertrophy, apoptosis, migration, and fibrosis [291]. On its turn, oxidized LDL induces TGF β expression and promotes fibrosis [301,304,305].

2. *Pathogenesis of vascular fibrosis:*

In the following sections, we will review the mechanisms by which CTGF and fibronectin promote in vascular fibrosis pathogenesis.

a. CTGF and vascular fibrosis:

CTGF is relatively a newly discovered growth factor to have a relation to the development of vascular fibrosis. CTGF is a cysteine-rich heparin-binding protein that stimulates ECM formation and deposition [306]. Several studies reported CTGF as a potent

fibrotic factor that induces fibroblast proliferation, adhesion, angiogenesis, and ECM accumulation [278,307]. Additionally, CTGF was shown to activate vascular smooth muscle cells proliferation, migration, and ECM production and deposition, which have a fundamental role in the development of atherosclerosis [308]. In humans with CVD, Ctgf mRNA and protein levels were shown to be elevated in VSMC of advanced atherosclerotic lesions. In addition, Ctgf was aggregated and concentrated near the fibrous cap of the plaque suggesting its potential involvement in atherosclerotic plaque production [309].

Several growth factors and conditions regulate the expression of CTGF, such as TGF β , TNF- α , cAMP, high glucose, coagulation factor VIIa, and mechanical stress [310]. In addition, CTGF was shown to be activated through AngII-induced TGF β pathway, to promote ECM accumulation and fibrosis in different vascular tissues [311,312]. For instance, TGF β -induced CTGF expression falls under the control of different TGF β -induced pathways, such as Smads, Ras/MEK/ERK1/2, Ap-1/JNK, and PKC. On the other hand, TNF- α , cAMP, PGE2, and IL-4 inhibits the expression of CTGF by down-regulating TGF- β [313,314].

One of the mechanisms by which CTGF induces ECM accumulation is through the upregulation of MMP-2, with no effect on TIMPs, in VSMC [315]. Moreover, supplementing mesangial cells with CTGF induces fibronectin production, cell migration, and cytoskeletal rearrangement through the activation of Src, ERK1/2, and Akt [316].

b. Fibronectin and vascular fibrosis:

Another key player in atherosclerosis is Fibronectin, a widely-spread multi-domain glycoprotein existing in the majority of extracellular matrices [317-319]. Fibronectin is particularly abundant in tissues with active morphogenic state, areas of inflammation, and cell migration sites [320]. There are several controversial reports about the implication of Fn1 in atherosclerotic plaque stabilization or its rupture and subsequent thrombosis [318,321-323].

Fibronectin acts as a scaffold for the binding of different ECM molecules such as collagen/gelatin, fibrinogen, heparin, thrombospondin and tenascin, and cells surface integrin receptors [324,325]. Several studies have reported that the interactions of fibronectin and the different molecules have a signal transmission role to the integrin receptors to alter cellular signaling [326]. Hence, it is well-accepted that fibronectin participates in the organization of the basement membranes of the tissues, and plays an important role as a sensor for mechanical changes in the tissue microenvironment to regulate cellular responses [326,327].

The involvement of fibronectin in different pathophysiological conditions in human patients is not well developed [318]. However, there has been a report showing an association between excess, and unstable, deposition of fibronectin and glomerulonephritis due to a mutation in fibronectin gene [328]. In addition, in an in vitro study, there was an association between fibronectin levels and thrombus formation and volume [329,330]. Moreover, the relation between fibronectin circulatory levels and the occurrence of coronary artery disease was studied across different studies. The outcomes of these studies gave contradictory conclusions pertaining the association [326,327,331,332].

On the other hand, some studies have reported that the levels of fibronectin per se are not the best consideration for evaluating the association between fibronectin and different pathophysiological conditions. The proteolytic degradation of fibronectin plays an important role in the abundance of fibronectin and biological functions in response to the degradation. For instance, the metabolites of fibronectin degradation are associated with the promotion of inflammatory lung diseases, namely emphysema and pulmonary fibrosis [333]. As previously discussed, inflammation is a fundamental contributor for CVD, especially atherosclerosis and thrombosis [334].

CHAPTER TWO

HYPOTHESIS AND OBJECTIVES

Diabetes mellitus continues to impose a huge health-care burden worldwide. It is a life threatening condition that alters the life style of the patients and leads to a different array of complication in the patients. Among these complications, diabetic-induced cardiovascular and renal complications are among the major causes for the high morbidity and mortality rates observed in diabetic patients.

Assessing the mechanisms by which diabetes mellitus induces its complication, endothelial dysfunction and inflammation stand-out as the major driving mechanisms. In addition, many reports have discussed the involvement of kallikrein kinin system (KKS), sphingosine kinase pathway, and leptin signaling as mechanisms for the promotion of the complications. Previously, we reported that knocking-out kinin receptor 2 (Bdkrb2) in type 1 diabetic mouse model ameliorated diabetic induced renal complications, pointing to the involvement of KKS in the progression of diabetes-induced complications [83].

Based on these observations, we hypothesize that KKS, especially Bradykinin (BK), contributes to vascular injury through the interaction/cross-talk with different signaling pathways, namely the SphK/S1P pathway and leptin signaling pathway. Therefore, our main objective was to decipher the mechanisms by which BK induces the expression of two fibrotic markers in primary vascular smooth muscle cells.

In this setting, our study was designed as follow:

- 1) A global proteomic profile assessment, using LC MS/MS technique, in type 1 diabetes mellitus animal model, accompanied by an assessment of three

different post-translational modification, namely oxidation, phosphorylation, and acetylation. As specific end-points, we investigated the following points

- a) Assess the effects of hyperglycemia and insulin-supplementation on the global post-translation modification of protein profiles.
 - b) Assess the pathways and/or molecules altered in response to diabetes by employing systems biology analysis
- 2) Cellular signaling assessment of the cross-talk between Bradykinin receptor and SphK/S1P pathway in VSMC. As specific end-points, we investigated the following:
- a) Assess the effect of BK on the gene and protein expression of fibrotic markers.
 - b) Assess the role of ERK1/2 and/or SphK1 activity downstream of Bdkrb2
 - c) Assess the activation of S1pr in response to BK and checked the effect of this activation on the BK-induced expression of fibrotic proteins
- 3) A global proteomic profile assessment in primary VSMC extracted from rat aorta in response to time-point stimulation by BK and leptin. Then we validated the proteomic results and assessed the cellular signaling of the cross-talk between bradykinin receptor and leptin signaling pathway in VSMC. As specific end-points, we investigated the following:
- a) Assess the effect of BK on the gene and protein expression of leptin and its receptor
 - b) Assess the role of leptin receptor in relaying Bdkrb2 effects on fibrotic markers

CHAPTER THREE

RESULTS

A. Proteome Profiling in the Aorta and Kidney of Type 1 Diabetic Rats.

In order to address the questions and the objectives of the study, we designed three approaches. In the first approach, we assessed the global protein regulation/expression in two different tissues in response to diabetes mellitus. We induced Type 1 Diabetes Mellitus in rat model and observed the global expression of the proteins in the denuded aorta and the kidney cortices of the rats through liquid chromatography, mass spectrometry (LC MS/MS). In this model, we were interested to assess the effect of hyperglycemia on the total protein expression in the two tissues. Moreover, we checked the effect of normalizing the blood glucose levels on the different biological processes. In addition, Systems Biology techniques will be employed in order to analyze and connect the regulated proteins to their biological processes.

The outcomes of this study would point to some contributors for the effects of hyperglycemia on the two different tissues, and may identify a new markers or pathway that contribute to the diabetes induced-complications.

1. Abstract

Diabetes is associated with a number of metabolic and cardiovascular risk factors that contribute to a high rate of microvascular and macrovascular complications. The risk factors and mechanisms that contribute to the development of micro- and macrovascular disease in diabetes are not fully explained. In this study, we employed mass spectrometric analysis using tandem LC MS/MS to generate a proteomic profile of protein abundance and post translational modifications (PTM) in the aorta and kidney of diabetic rats. In addition, systems biology analyses were employed to identify key protein markers that can provide insights into molecular pathways and processes that are differentially regulated in the aorta and kidney of type 1 diabetic rats. Our results indicated that 188 (111 downregulated and 77 upregulated) proteins were significantly identified in the aorta of diabetic rats compared to normal controls. A total of 223 (109 downregulated and 114 upregulated) proteins were significantly identified in the kidney of diabetic rats compared to normal controls. When the protein profiles from the kidney and aorta of diabetic and control rats were analyzed by principal component analysis, a distinct separation of the groups was observed. In addition, diabetes resulted in a significant increase in PTM (oxidation, phosphorylation, and acetylation) of proteins in the kidney and aorta and this effect was partially reversed by insulin treatment. Ingenuity pathway analysis performed on the list of differentially expressed proteins depicted mitochondrial dysfunction, oxidative phosphorylation and acute phase response signaling to be among the altered canonical pathways by diabetes in both tissues. The findings of the present study provide a global proteomics view of markers

that highlight the mechanisms and putative processes that modulate renal and vascular injury in diabetes.

Keywords: Post-translational modifications, Proteomics, Systems Biology, kininogen, kidney, Diabetes

2. Introduction:

Diabetes mellitus is a worldwide health burden manifested through hyperglycemia accompanied with insulin deficiency or resistance [5,335]. Hyperglycemia causes irreversible damage to blood vessels and highly vascularized organs at the microvascular and macro-vascular levels, accounting for the highest mortality in diabetic patients, which render diabetes mellitus as an independent risk factor for Cardiovascular Diseases (CVD) and Chronic Kidney Disease (CKD) [336,337]. The diabetes-induced lesions at the microvascular level of the renal glomeruli result in diabetic nephropathy (DN), which constitutes the most recurrent and serious complication of diabetes mellitus [338]. On the other hand, the lesions at the macro-vascular level lead to diabetes-induced atherosclerotic pathophysiology [339,340]. It has been shown that poor control of hyperglycemia at the early stages of diabetes would accelerate the incidence and progression of vascular and renal complications. Outcomes from The Diabetes Control and Complications Trial (DCCT) [15] and the Epidemiology of Diabetes Intervention and Complications (EDIC) [16] have proven that the primary modifiable risk factor for the long-term vascular and renal complications of T1DM is hyperglycemia. [341]

Despite the focus on identifying the mediators of the disease progression in diabetes mellitus, the exact mechanisms for the cardiovascular and renal complications of T1DM are still unclear. Many studies have reported that endothelial dysfunction, oxidative stress, advanced glycation end products, a decrease in nitric oxide production and bioavailability, and deposition of fibrotic proteins are involved in the initiation or development of CVD and CKD [160,342-346]. In this study, we aimed at identifying the global protein changes in response to T1DM-induced hyperglycemia in the aorta and kidney, by employing Liquid chromatography-tandem mass spectrometry (LC-MS/MS) technique to comparatively quantitate the expression of different proteins among the different conditions, and to check the intensities of three different post-translational modifications, namely acetylation, phosphorylation and oxidation. In addition, systems biology analysis (Ingenuity Pathway Analysis, IPA) was used to model the effects of diabetes on different pathways in the two organs, to identify biological processes that are modified by the exposure conditions [347-349]. This approach allows the identification of possible novel biomarkers and development of new mechanisms aimed at defining the interplay of multiple biological pathways involved in the etiology of renal and vascular disease in diabetes.

3. *Methods:*

a. Induction of Diabetes:

Male Sprague-Dawley rats, weighing 250–275 g, were used in all studies. Rats were housed two to three per cage in a light- and temperature-controlled room and had free access to food and water. Diabetes was induced by a single intravenous injection of

streptozotocin (STZ), 65 mg/kg body weight through the tail vein. After 24 h, diabetes was confirmed in STZ-treated rats by tail vein plasma glucose levels. Glucose levels and body weights were measured at predetermined intervals to characterize the diabetic state. Age-matched control (C) rats were also studied. The diabetic rats were divided into two groups. The first group (D) received no insulin treatment and displayed severe hyperglycemia. The second group of diabetic rats was treated twice daily with subcutaneous injections of insulin (3U, HUMULIN N) for 4 weeks, two weeks after induction of diabetes. Rats were sacrificed 6 weeks after induction of diabetes. All animal experiments were approved by the Institutional Animal Care and Use Committee (IACUC) at the American University of Beirut and conducted in accordance with the guidelines of the Animal Care Facility and IACUC.

b. Extraction and Tryptic Digestion of Proteins:

Aorta and kidneys from control, diabetic and insulin-treated diabetic rats were removed under anesthesia, were homogenized using beads beater (Beadbug microtube homogenizer, Benchmark Scientific, Edison, NJ) followed by sonication on ice for 30 min and centrifugation at 14,800 rpm for 10 min. The resulting supernatant was diluted 10x with 50 mM ammonium bicarbonate (ABC) buffer, and the protein concentration was determined by BCA protein assay kit (Thermo Scientific/Pierce, Rockford, IL) according to the user's manual.

Aliquots of 10 μ g extracted proteins from each sample were denatured at 80°C for 10 min followed by adding 200 mM dithiothreitol (DTT) and incubating at 60°C for 45 min.

The resulting reduced proteins were then alkylated by adding 2-6 μ l Indole 3 Acetic Acid (IAA, 200 mM solution) and incubating at 37°C in the dark for 45 min. Excessive IAA was quenched by additional DTT and incubating at 37°C for 30 min. Trypsin (Promega, Madison, WI) was added at a ratio of 1:25 (enzyme: proteins, w/w) into samples and incubated at 37°C for 18 hours followed by addition of formic acid at a final concentration of 0.5% to quench the enzymatic reaction. Samples were then centrifuged at 14,800 rpm for 10 min, and the resulting supernatant containing the digested peptides were dried and then resuspended in an aqueous solution containing 2% acetonitrile (ACN) and 0.1% formic acid (FA) for Liquid Chromatography–Mass Spectroscopy/Mass Spectroscopy (LC-MS/MS) analysis.

c. LC-MS/MS Analysis:

Aliquots (1 μ g) of tryptic digested samples were subjected to Liquid chromatography-electrospray ionization-tandem mass spectrometry (LC-ESI-MS/MS) analysis. The LC-MS/MS data were acquired using a Dionex Ultimate 3000 nano-LC system (Thermo Scientific, San Jose, CA) interfaced to an LTQ Orbitrap Velos mass spectrometer (Thermo Scientific, San Jose, CA) equipped with a nano-ESI source. Injected peptides were first purified online at a flow rate of 3 μ l/min using a C18 Acclaim PepMap 100 trap column (75 μ m I.D. x 2 cm, 3 μ m particle sizes, 100 Å pore sizes, Thermo Scientific, San Jose, CA). Peptides were separated on a C18 Acclaim PepMap RSLC column (75 μ m I.D. x 15 cm, 2 μ m particle sizes, 100 Å pore sizes, Thermo Scientific, San Jose, CA). The column temperature was maintained at 29.5 °C and the flow rate was 350

nl/min during the separation. The mobile phase consisted of solution A (97.9% water/2% ACN/0.1% FA) and solution B (99.9% ACN/0.1% FA). The separation of peptides was achieved by following gradient of solution B: 5% over 10 min, 5%-20% over 55 min, 20-30% over 25 min, 30-50% over 20 min, 50%-80% over 1 min, 80% over 4 min, 80%-5% over 1 min and 5% over 4 min. Data dependent acquisition mode with two scan events was employed for MS/MS analysis. The first scan event was a full MS scan of 400-2000 m/z at a mass resolution of 15,000. In the second scan event, 10 most intense ions detected in the first scan event were selected with an isolation width of 3.0 m/z to perform CID MS/MS. The normalized collision energy (CE) was set to 35%, and an activation Q value was 0.250. The dynamic exclusion was set to have repeat count of 2, repeat duration of the 30s, exclusion list size 200 and exclusion duration of 90s.

d. Post-Translation Modification Analysis:

The raw data obtained from LC-MS/MS analysis were processed with the MaxQuant software version 1.5.4.1. Database search was performed against UniProtKB/Swiss-Prot rat database (35842 entries). The search included cysteine carbamidomethylation as fixed modification and multiple variable modifications, including methionine oxidation, phosphorylation of serine, threonine, and tyrosine, in addition to acetylation of protein N-terminal, histidine and lysine. Corresponding with experimental procedures, trypsin was specified as the proteolysis enzyme and a maximum of 2 miscleavages was allowed. For identification, the peptide precursor mass tolerance was 20 pm in the first search and 8 pm in the main search. As for fragments matching, a deviation

of 0.5 Da was allowed. Only peptides with a minimum length of 7 amino acids were considered for identification. The false discovery rate (FDR) was set to be 0.01 at both peptide and protein levels. The minimum ratio count was set as two to determine the intensities of proteins. Both unique and razor peptides were considered for quantification. Data generated by MaxQuant were further interpreted using Perseus. Filters were applied to eliminate reverse hits and common contaminants for peptide and protein identification, and an additional filter for protein was only identified by sites. Only proteins that were detected in at least 2 replicates of at least one sample group were reported.

e. Systems Biology Assessment:

IPA software (Ingenuity® Systems, Version 33559992) was employed to examine functional correlations within the different treatment groups. IPA is a powerful tool that is widely used in the omics field to suggest/predict the effects of specific conditions or drugs on the biological outcomes [350-352]. Data sets containing protein identifiers (UniProt-KB) and corresponding expression values (Log₂ [Fold change]) of different comparative groups were uploaded. The comparative groups were as follow: diabetic vs. control to analyze the effect of diabetes compared to time-matched control, insulin-treated diabetic vs. control to analyze the effect of insulin treatment compared to time-matched control, and insulin-treated diabetic vs. diabetic to analyze the effect of insulin treatment compared to the diabetic group. Each protein identifier was mapped to its corresponding protein object in the Ingenuity Pathways Knowledge Base. All mapped proteins were differentially expressed with $p < 0.05$ and overlaid onto global molecular networks developed from

information contained in the knowledge base. Networks were then algorithmically generated based on their connectivity. Networks were “named” on the most prevalent functional group(s) present. Canonical pathways, Diseases and Bio Functions, and Ingenuity Tox List tools were overlaid on the networks.

f. Statistical Analysis and LC-MS/MS Data Analysis:

Repeated measure generalized linear mixed models with an intercept as the random effect models were implemented to assess the changes in plasma glucose and body weights between the groups longitudinally over time using SAS proc Glimmix. One way ANOVA, followed by Tukey correction for multiple comparisons was performed to assess the changes between PTM groups. Data are expressed as mean \pm SE and significance were considered at $p < 0.05$.

LC-MS/MS data were used to generate mascot generic format file (*.mgf) by Proteome Discover version 1.2 software (Thermo Scientific, San Jose, CA) then searched using SwissProt database (Rattus) in MaxQuant version 2.4 (Matrix Science Inc., Boston, MA). Iodoacetamide modification of cysteine was set as a fixed modification, while oxidation of methionine was set as a variable modification. An m/z tolerance of 5 ppm was set for the identification of peptides with maximum 2 missed cleavages. Also, tandem MS ion tolerance was set within 0.8 Da with label-free quantification. Scaffold Q+ (Proteome Software, Portland, OR) was employed for spectral counts quantitation. The normalized intensity of target peptides corresponding to each candidate protein was summed up to represent the abundance of the certain protein. Student’s t-tests were performed to

determine the significant proteins in the comparison between every two sample groups with criteria of p-value < 0.05 .

4. Results:

a. Characteristics of the Diabetic State:

Plasma glucose levels and body weights of all three groups of rats over the duration of the study period are shown in Figure 8A and 8B, respectively. The summary statistics conducted at a group level (control, diabetic, and insulin-treated diabetic rats) revealed that the group of diabetic rats had the highest glucose levels 489 ± 31.7 mg/dl with glucose levels ranging between 128-600 mg/dl. The second highest group in plasma glucose was that of insulin-treated diabetic rats with average plasma glucose levels of 305 ± 36 mg/dl and range of 87-600 mg/dl. Controls had the lowest plasma glucose levels with 130.21 ± 3 mg/dl and range of 102-171 mg/dl. To determine if the observed difference in the plasma glucose levels between the groups is of statistical significance and to account for the longitudinal nature of the data we implemented the repeated measure generalized linear mixed models with an intercept as the random effect. This random effect will account for the correlation between the glucose measures repeated for the same rat, referred to as within subject correlation. The outcome glucose was modeled as a function of group and week. In addition, to account for any potential interaction effect, we included in this model an interaction term between week and group. Our longitudinal analysis indicated that group had a significant effect on plasma glucose levels with overall $p < 0.0001$. In addition, a significant interaction between week and group was detected ($p = 0.0002$), hence this interaction term was left in the model to account for its effect modification on the relationship between the group and plasma glucose. Time had a non-significant effect on plasma glucose, indicating that time is not significantly affecting the levels of glucose.

Accordingly, the group is the main factor that is associating with plasma glucose. In specific, the diabetes group had a significantly different (higher) glucose levels compared to controls ($p < 0.0001$), and diabetes with insulin had also significant difference (higher) levels of glucose compared to controls ($p = 0.0003$). Diabetes and diabetes with insulin did not have a significant difference in glucose ($p\text{-value} = 0.2689$).

The body weight for the controls was 354 ± 21 g with values ranging between 178 and 487 g, and that for diabetes were 271 ± 10 g and range of 190 and 341 g, and that for diabetes and insulin were 284 ± 13 g and range of 177 and 393 g. Our longitudinal analysis using the generalized linear mixed models with random effect on the intercept with lognormal distribution and unstructured variance-covariance matrix revealed that there is a significant incremental effect of time (weeks) on weight ($p < 0.0001$), and a significant interaction between time and group ($p < 0.0001$). However, body weight did not significantly differ between the 3 groups with overall P-value of 0.2507, Figure 8B.

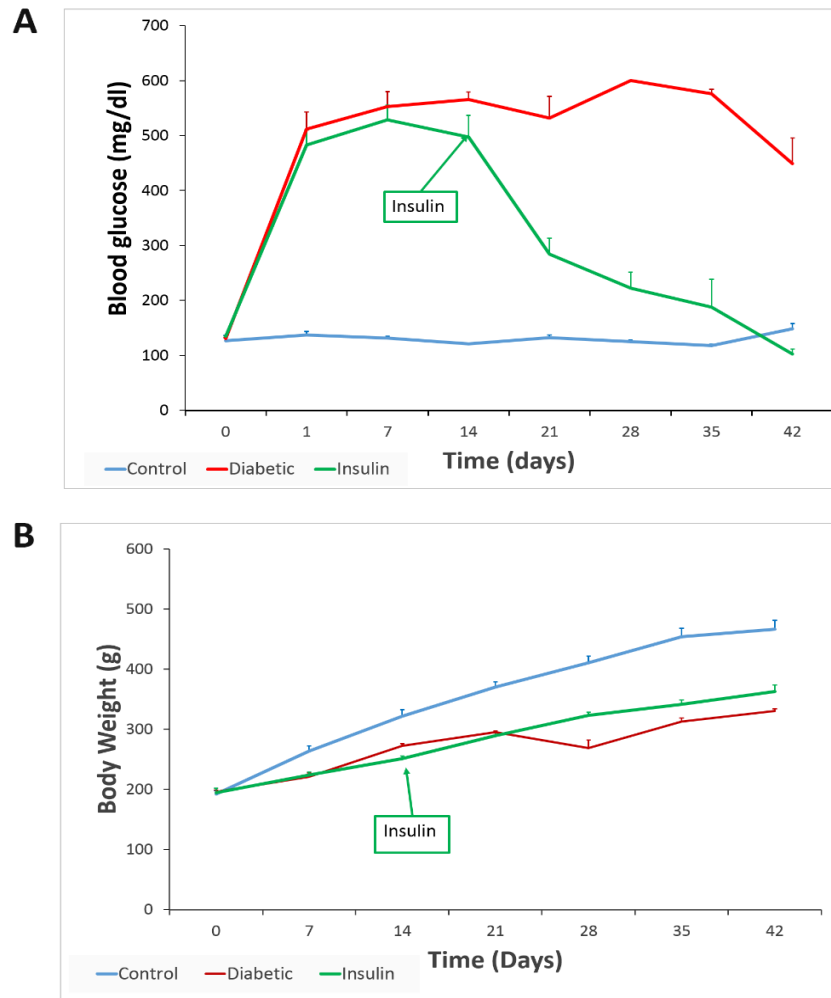


Figure 8: Plasma glucose level and body weigh measurements of the rats. (A) Plasma glucose levels were significantly increased I day after STZ injection in both diabetic groups compared to controls. (B) Initial body weights were not significantly different between diabetic and control rats. Blue line is for Control rats, Red line for Diabetic rats, and Green line is for Insulin-treated diabetic rats.

b. Aorta and Kidney Proteomic Analysis:

Comparative proteomic profiling of kidney and aorta protein abundance was done using LC-ESI-MS/MS followed by MaxQuant analysis of the generated protein spectra. Adopting this approach, 1128 distinct proteins were identified in the aorta of control and

diabetic rats and 1290 distinct proteins were identified in the kidney of control and diabetic rats.

c. Effect of diabetes on proteome profile in the aorta and kidney:

The aorta and kidney responded to the diabetic state differently as evidenced by the proteomic profile in these tissues and as illustrated in the heat maps (Figure 9). Amid the 1128 identified proteins in the aorta, 188 (16.6%) were significantly modified by the diabetic state with $p < 0.05$. Of these, 111 (59%) proteins were significantly downregulated and 77 (41%) proteins were significantly upregulated (list of proteins in Table 1). Among the 1290 proteins identified in the kidney, 223 (17.3%) were significantly modified by the diabetic state with $p < 0.05$. Out of these, 109 (48.8%) proteins were significantly downregulated and 114 (51.1%) proteins were significantly upregulated (list of proteins Table 2). A Venn diagram was generated to determine the common proteins modified by diabetes in the aorta and kidney. Only 12 % of proteins that their expression was significantly modified by the diabetic state were common between the aorta and kidney. The list of common proteins is shown in Table 3 and included proteins related to carbon metabolism, citrate cycle (TCA cycle), metabolic pathways, microbial metabolism in diverse environments, fatty acid degradation, fatty acid metabolism and other pathways.

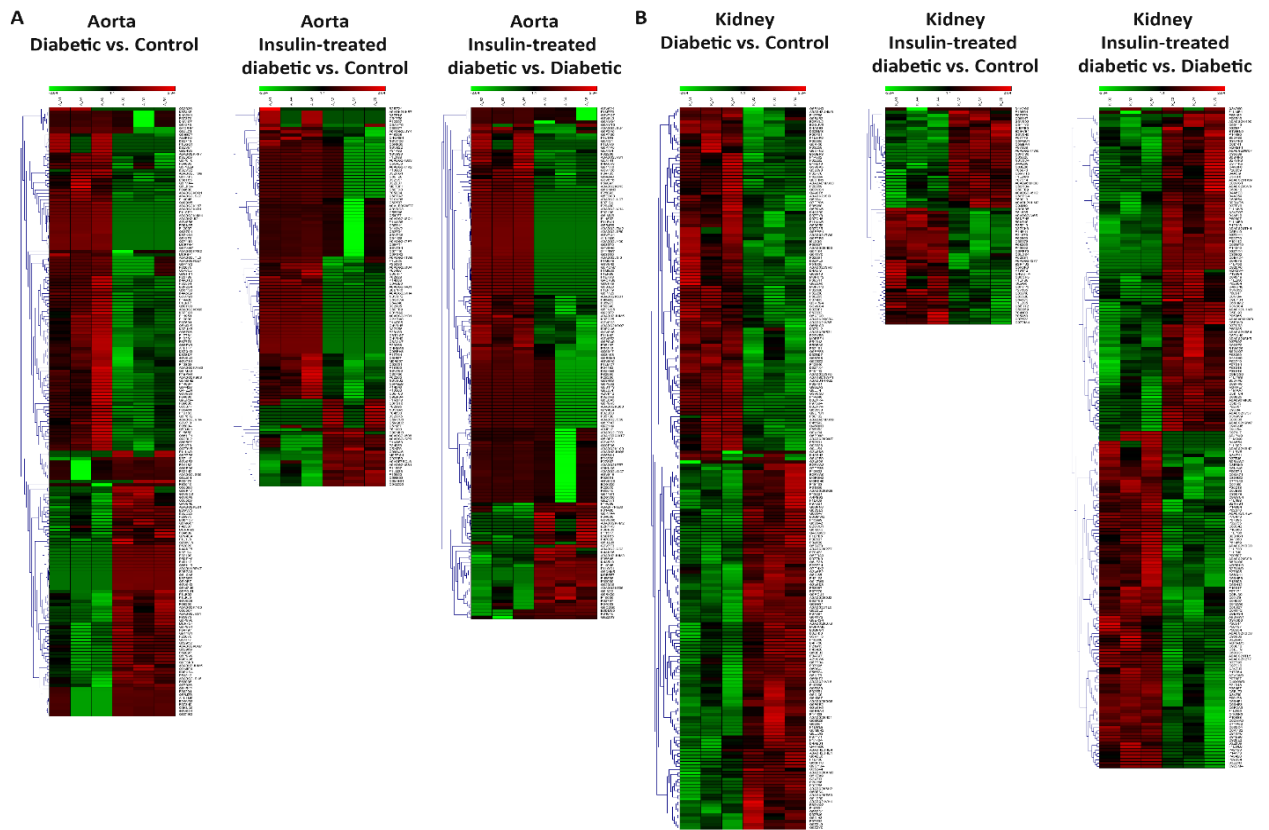


Figure 9: Hierarchical clustering (heat maps) of protein expression profiles in the aorta (A) and kidney (B) among the three groups of rats: The compared groups are Diabetic vs. Control samples, Insulin-treated diabetic vs. Control samples, and Insulin-treated diabetic vs. Diabetic samples. Green color represents downregulation of protein expression, whereas the red color represents upregulation of protein expression. Color intensity reflects the expression level of the proteins. The label on the right-hand side of the heat maps represents the accession number of the proteins.

d. Effect of diabetes on the expression levels of distinct oxidative stress enzymes:

Diabetes resulted in the differential expression of a cluster of oxidative stress related enzymes involved in hydrogen peroxide, electrophilic and superoxide detoxification in the aorta and kidney. In the aorta, diabetes induced the protein expression levels of glutathione peroxidase 1 (3.22 fold, $p = 0.041$) and 3 (2.12 fold, $p = 0.004$), glutathione S-transferase Pi 1 (2.04 fold, $p = 0.021$) and Mu 3 (16.78 fold, $p = 0.039$), monoamine oxidase A (2.67 fold, $p = 0.049$) and reduced the expression of superoxide dismutase 1 (0.7 fold, $p = 0.044$) compared to levels in aorta of control normal rats (Table 1). Whereas in the

kidney, diabetes induced the protein expression levels of glutathione S-transferase Mu 1 (1.55 fold, $p = 0.039$) and Zeta 1 (1.86 fold, $p = 0.005$), peroxiredoxin 3 (1.36 fold, $p = 0.001$) and 6 (1.67 fold, $p = 0.047$) and superoxide dismutase 2 (1.24 fold, $p = 0.018$) compared to levels in kidney of control normal rats (Table 2).

e. Effect of diabetes on matrix proteins in the aorta:

Analysis of the proteomic abundance of proteins indicated that diabetes induced the expressions levels of collagen type VI $\alpha 6$ (4.32 fold, $p = 0.03$), collagen type XVIII $\alpha 1$ (2.75 fold, $p = 0.035$), and fibulin 1 (4.12 fold, $p = 0.013$) compared to control tissues. In addition, diabetes induced the protein expression of integrin beta 1 (2.77 fold, $p = 0.044$), a focal adhesion protein that links the actin cytoskeleton to the extracellular matrix (Table 1).

f. Effect of insulin treatment on proteome profile in the aorta and kidney:

Treatment of diabetic rats with insulin for four weeks resulted in partial reversal of the expression profile of the proteins in aorta and kidney that were significantly modified by the diabetic state as shown in the heat maps Figure 9. Of the 188 proteins significantly modified by diabetes in the aorta, only 42 (22%) proteins responded to insulin treatment by normalizing the expression levels of these proteins (Table 4). Similarly, of the 223 proteins significantly modified by the diabetic state in the kidney, only 101 (45%) responded to insulin treatment by normalizing the expression levels of these proteins (Table 5).

g. Effect of diabetes and insulin on kininogen and angiotensin converting enzyme:

Comparative analysis of the proteomic profile indicated that diabetes induced the protein expression of high molecular weight kininogen in the aorta (2.91-fold, $p = 0.004$) as well as in the kidney (4.61-fold, $p = 0.012$) compared to controls. It is of interest also to point here that insulin treatment resulted in increased expression of angiotensinogen levels by 5.89-fold ($p = 0.025$) and angiotensin converting enzyme by 2.03-fold ($p = 0.007$) in the aorta.

h. Principal component analysis (PCA):

PCA a derivative of multivariate data analysis commonly used to reduce multidimensionality of large data sets and discern features that distinguish the different groups was applied to the proteomic profiles of the aorta and kidney. As shown in Figure 10A & B, PCA efficiently separated the groups, indicating that the proteomic profiles contain structure that is discernable even without considering the identity of individual factors. Importantly, the discriminatory power of the analysis held when considering the aorta and kidney proteome between the three different groups.

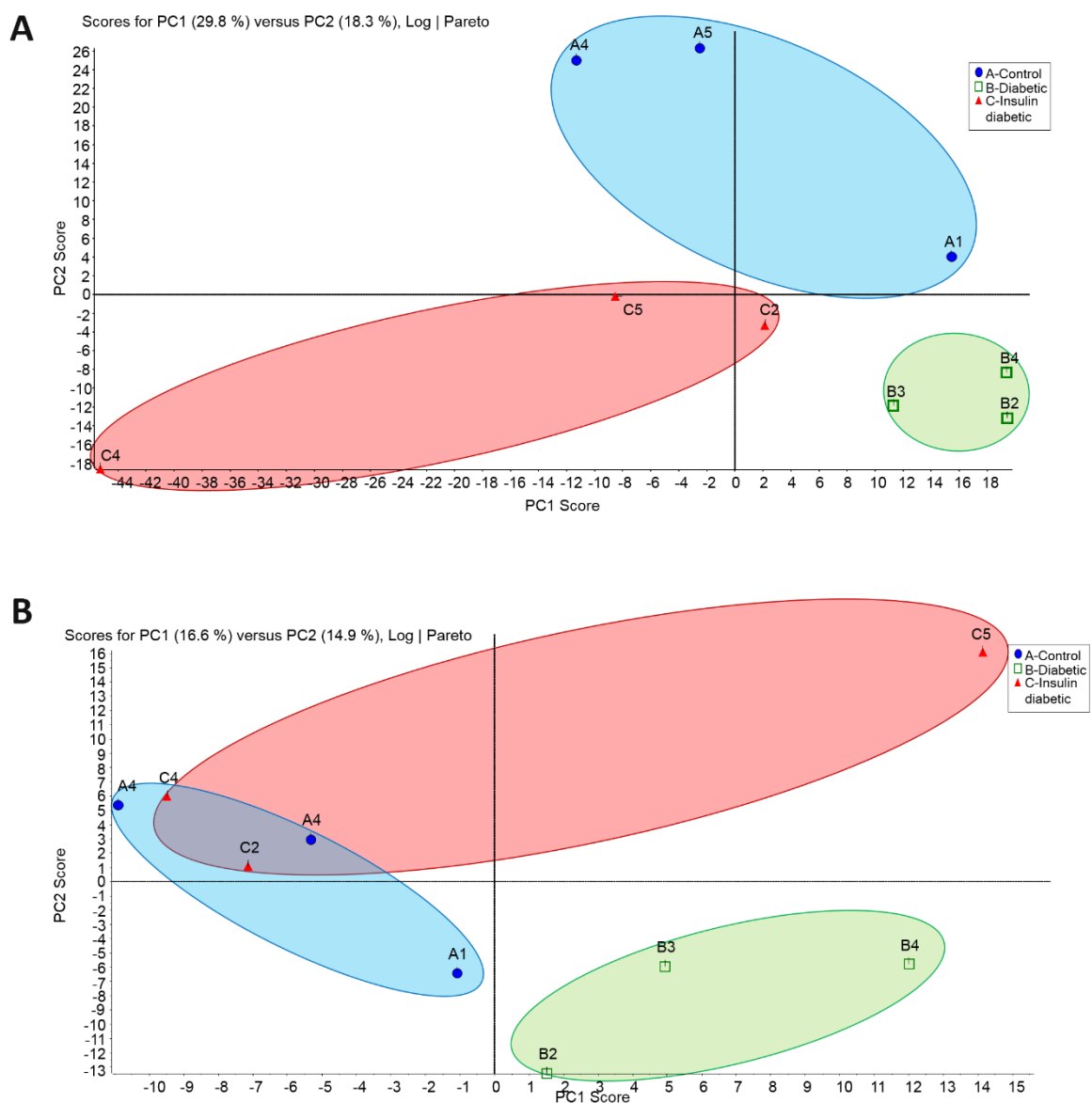


Figure 10: Principal Component Analysis (PCA) of the aorta (A) and kidney (B) samples. The total normalized expression data of the proteins was used to depict the scatter plots of the first (X) and the second (Y) principal components. The numbering of the nodes is an identification of the samples. Abbreviation A (Control), B (Diabetic), and C (Insulin-treated Diabetic). Blue oval encircles the control samples, green oval encircles the diabetic samples, and red oval encircles the Insulin-treated diabetic samples.

i. Effect of Diabetes on PTMs:

Beyond protein abundance, LC MS/MS also determined the intensity of proteins modified by oxidation, phosphorylation, and acetylation in the aorta and kidney of control,

diabetic and insulin-treated diabetic rats. The increased intensity of the PTM proteins we observed was not due to the abundance of the specific proteins but rather to an effect of the diabetic state on the intensity of the modified PTM. The mean intensities of oxidized proteins in control aorta is 7.2 ± 0.93 compared to 18.1 ± 0.71 in diabetic aorta ($p < 0.001$, $n=34$) and 6.3 ± 1.2 in control kidney compared to 18.3 ± 0.85 in diabetic kidney ($p < 0.001$, $n=25$). Treatment of diabetic rats with insulin significantly reduced the increased intensities of oxidized proteins in the aorta to 10.03 ± 1.3 and kidney to 9.96 ± 1.75 of diabetic rats to levels not significantly different from controls (Figure 11A & D). The mean intensities of phosphorylated proteins in control aorta is 6.2 ± 0.5 compared to 17.8 ± 0.44 in the diabetic aorta ($p < 0.001$, $n=100$) and 7.4 ± 0.77 in control kidney compared to 19.9 ± 0.6 in diabetic kidney ($p < 0.001$, $n=72$). Treatment of diabetic rats with insulin significantly reduced the increased intensities of phosphorylated proteins in the aorta to 8.49 ± 0.73 and in the kidney to 13.3 ± 0.97 compared to levels in diabetic rats (Figure 11E & F). The mean intensities of acetylated proteins in control aorta is 6.7 ± 0.42 compared to 18.4 ± 0.39 in the diabetic aorta ($p < 0.001$, $n=128$) and 6.6 ± 0.49 in control kidney compared to 20.1 ± 0.48 in diabetic kidney ($p < 0.001$, $n=105$). Treatment of diabetic rats with insulin significantly reduced the increased intensities of acetylated proteins in the aorta to 9.02 ± 0.6 and in the kidney to 13.99 ± 0.82 compared to levels in diabetic rats (Figure 11C & F).

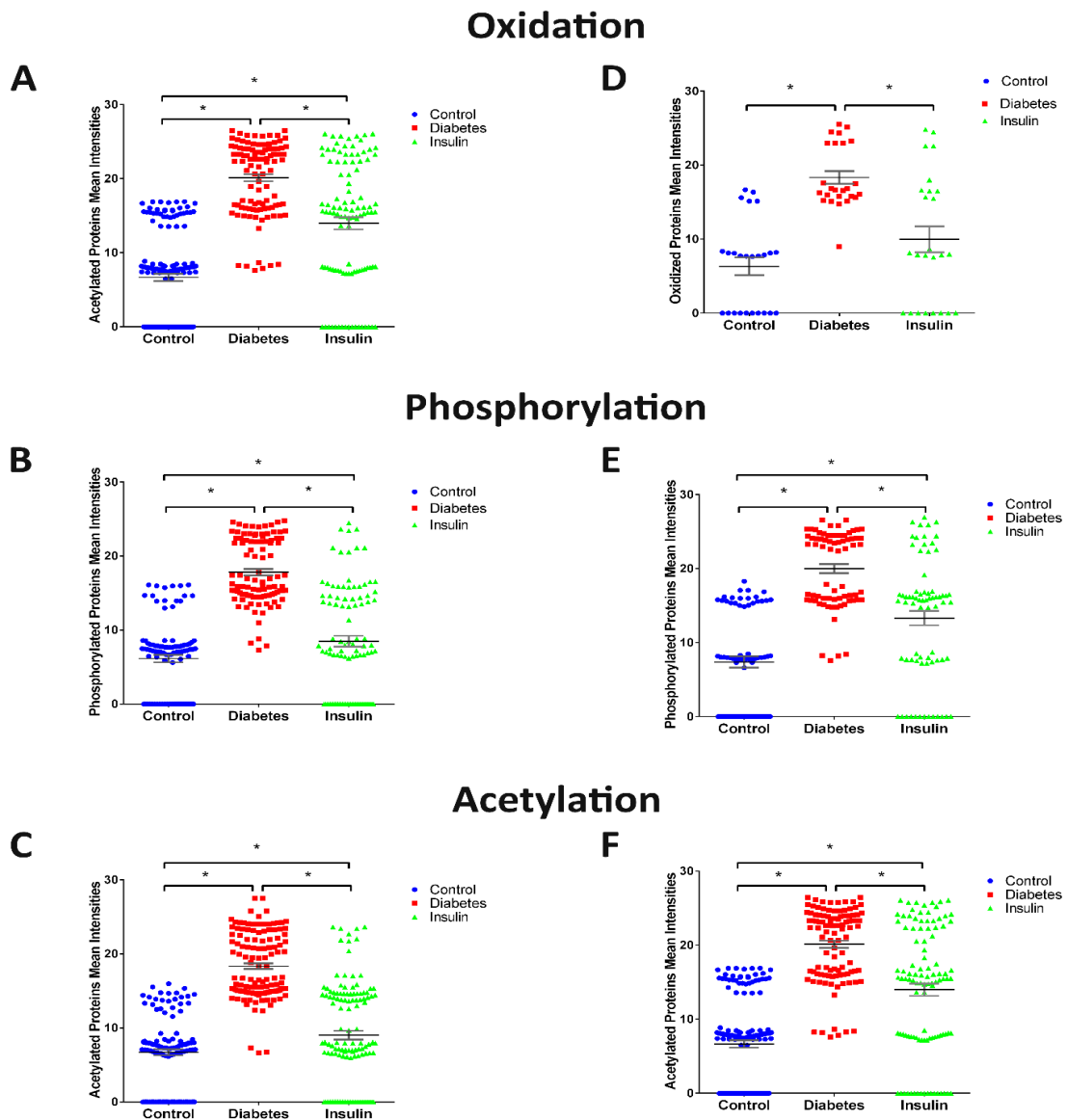


Figure 11: Scatter plot of the mean intensities of the three PTMs in the aorta (A, B and C) and the kidney (D, E, and F) samples. A and C show the scatter of the oxidized proteins among the 3 different groups. B and E show the scatter of the phosphorylated proteins among the 3 different groups. C and F show the scatter of the acetylated proteins among the 3 different groups (* $p < 0.05$).

j. Pathway and network analysis of proteomic profiles:

The proteomic profiles of significantly modified proteins in the aorta and kidney were subjected to IPA analysis. The results shown in Figure 12A-D offer a graphical

representation of the altered canonical pathways of significantly upregulated and downregulated proteins within each tissue and between each group.



Figure 12: Canonical Pathways of the comparative groups in the aorta and the kidney samples. A: top Canonical pathways related to proteins altered in the aorta of Diabetes vs. control samples. B: Top Canonical Pathways related to proteins altered in the aorta of Insulin-treated Diabetic vs. Diabetic samples. C: Top Canonical Pathways related to proteins altered in the kidney of Diabetic vs. Control samples. D: Top Canonical Pathways related to proteins altered in the kidney of Insulin-treated Diabetic vs. Diabetic samples. Bars show the total number of proteins identified in each pathway. The green color represents the down-regulated proteins, and the red color represents the upregulated proteins.

Network analysis of aorta of diabetic rats compared to control (Figure 13A) depicted that Kininogen (KNG1) and Protein Kinase A (PKA) were upregulated by the diabetic state and they were connected to the activation of angiotensin II receptor type 2 (AGTR2), Leptin (LEP), and heme oxygenase 1 (HOX1). In addition, network analysis showed that the modified proteins possessed many aorta toxicity related functions such as cardiac dysfunction, necrosis, fibrosis, hypertrophy, dilatation, proliferation, cell death, movement and migration of connective tissue (Figure 13A & B).

Network analysis of the effect of insulin treatment on the aorta of diabetic rats, showed that angiotensinogen (AGT), and angiotensin converting enzyme (ACE) were upregulated and connected to the inhibition of leptin receptor (LEPR), while alpha-1-microglobulin/bikunin precursor (AMBP) was downregulated and connected to the inhibition of fibronectin 1 (FN1). In addition, insulin altered oxidative stress through the upregulation of glutamate-cysteine ligase modified (GCLM), inhibition of tumor necrosis factor (TNF), nuclear factor kappa-light-chain-enhancer of activated B cells (NF κ B), and superoxide dismutase 2 (SOD2), and activation of CYP (Figure 14A). Toxicity functions involved included cardiac dysfunction, necrosis, fibrosis, hypertrophy, dilatation, and proliferation. Additionally, the list of modified proteins showed activation of cell death, and apoptosis and inhibited the formation of actin filaments as biological functions (Figure 14B).

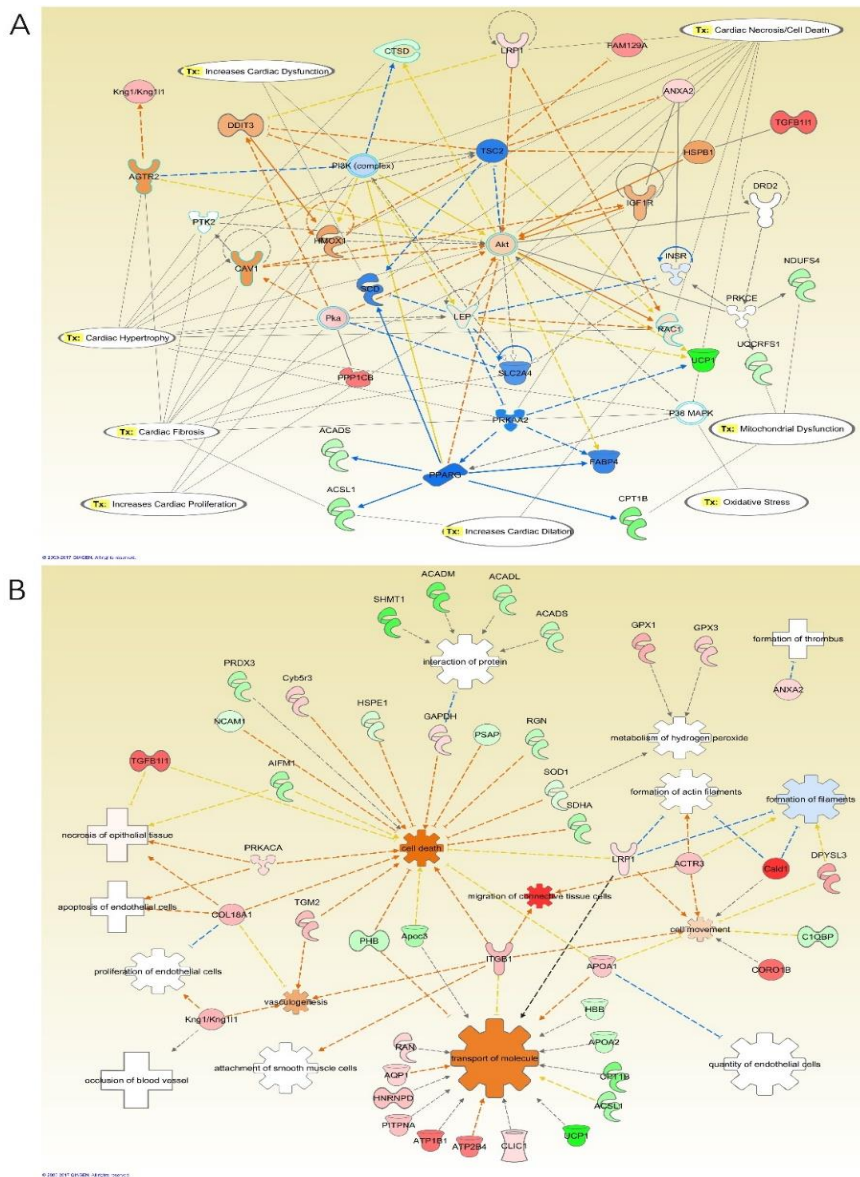


Figure 13: IPA network analysis of the modified proteins in the aorta of diabetic relative to control rats. A: The top diseases and functions related to the modified proteins are Lipid Metabolism, Molecular Transport, and Small Molecule Biochemistry. The top Toxicity and functions predicted by IPA related to the modified proteins are Cardiac Fibrosis, Cardiac Hypertrophy, Cardiac Necrosis/Cell Death, Increased Cardiac Dysfunction, Increased Cardiac Proliferation, Increased Cardiac Dilatation, Mitochondrial Dysfunction, and Oxidative Stress. The main regulated proteins connected in this network were Kng1, AKT, and Leptin. B: Diseases and Biological Functions predicted by IPA related to the differentially expressed proteins in this comparative group. The diseases related to these proteins are apoptosis of endothelial cells, the formation of thrombus, necrosis of epithelial tissue, and occlusion of the blood vessel. The color intensity of the nodes reflects the expression of the proteins. Green nodes are down-regulated proteins, red nodes are upregulated proteins, white nodes are IPA predicted proteins with non-consistent activation pattern, blue nodes are IPA predicted proteins to be inhibited, and orange nodes are IPA predicted proteins to be activated.

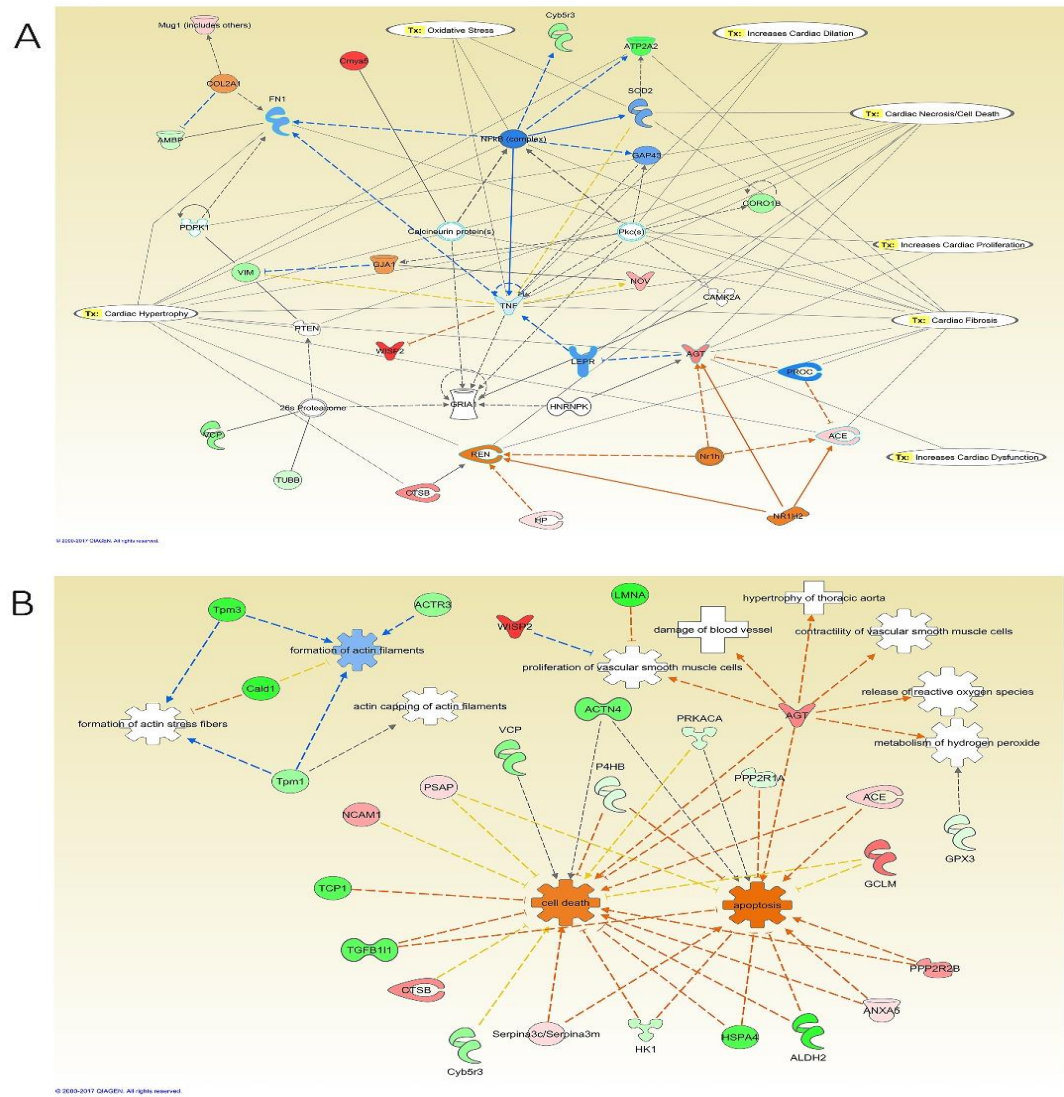


Figure 14: IPA network analysis of the modified proteins in the aorta of insulin-treated diabetic relative to diabetic rats. A: The top Toxicity and functions predicted by IPA related to the modified proteins are Cardiac Fibrosis, Hypertrophy, Necrosis/Cell Death, Oxidative Stress, Increased Cardiac Proliferation, Dilation, and Dysfunction. The main regulated proteins connected in this network are ACE, AGT, and TNF. B: Diseases and Biological Functions predicted by IPA related to the differentially expressed proteins in this comparative group. The main biological functions altered in this network are apoptosis, metabolism of hydrogen peroxide, and release of reactive oxygen species. The diseases related to these proteins are damage of blood vessel, and hypertrophy of thoracic aorta. The color intensity of the nodes reflects the expression of the proteins. Green nodes are down-regulated proteins, red nodes are up-regulated proteins, white nodes are IPA predicted proteins with non-consistent activation pattern, blue nodes are IPA predicted proteins to be inhibited, and orange nodes are IPA predicted proteins to be activated.

Network analysis of the modified proteins in the kidney of diabetic rats revealed that the downregulation of integrin subunit beta 1 (ITGB1) and fatty acid synthase (FASN) to relate to the activation of leptin (LEP), LEPR, matrix metalloproteinase 9 (MMP9), and interleukin 6 (IL6). Diabetes promoted oxidative stress in the kidney through the downregulation of signal transducer and activator of transcription 3 (STAT3), the upregulation of SOD2, glutathione peroxidase 1 (GPX1), and glutathione S-transferase mu 1 (GSTM1), in addition to the activation of IL6 and the inhibition of NFκB activity (Figures 15A). IPA also identified toxicity functions of the detected proteins from the kidneys. These included renal damage, nephritis, necrosis, proliferation, and renal failure. Furthermore, the modified proteins in the kidney of the diabetic relative to control group showed activation of biological functions such as the activation of growth of epithelial tissue and oxidation of long chain fatty acid, and the inhibition of the adhesion of glomerular cells, cell movement, cell proliferation of kidney cell lines, cell spreading of kidney cell lines, generation of reactive oxygen species, metabolism of reactive oxygen species, microtubule dynamics, quantity of lipid peroxide, and quantity of superoxide (Figure 15B).

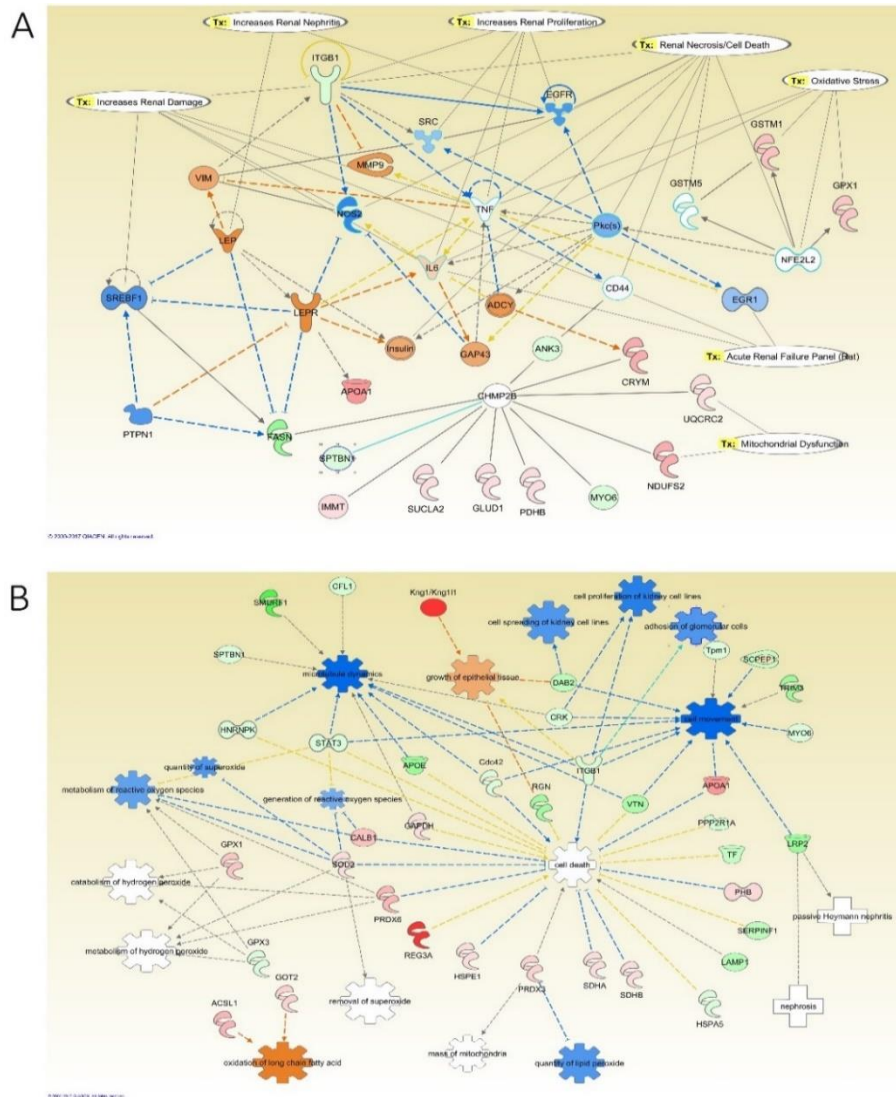


Figure 15: IPA network analysis of the modified proteins in the kidney of diabetic relative to control rats. A: The top Toxicity and functions predicted by IPA related to the modified proteins are Increase Renal Damage, Nephritis, Proliferation, Necrosis/Cell Death, Oxidative Stress, Acute Renal Failure Panel (Rat), and Mitochondrial Dysfunction. The main regulated proteins in this network are EGFR, LEP, LEPR, and TNF. B: Diseases and Biological Functions predicted by IPA related to the differentially expressed proteins in this comparative group. The main biological functions altered in this network are adhesion of glomerular cells, generation of reactive oxygen species, the growth of epithelial tissue, and metabolism of hydrogen peroxide and reactive oxygen species. The diseases related to these proteins are nephrosis and passive Heymann nephritis. The color intensity of the nodes reflects the expression of the proteins. Green nodes are down-regulated proteins, red nodes are upregulated proteins, white nodes are IPA predicted proteins with non-consistent activation pattern, blue nodes are IPA predicted proteins to be inhibited, and orange nodes are IPA predicted proteins to be activated.

Network analysis of the effect of insulin treatment on the kidney of diabetic rats showed that the upregulation of complement C3 (C3) and ITGB1 are connected to the activation of NFκB and TNF (Figure 16A). Additionally, the upregulation of Gamma-Glutamyltransferase 1 (GGT1), the downregulation of GPX1, peroxiredoxin 5 (PRDX5), and SOD2, and the activation of NFκB and TNF regulated oxidative stress in this group. Moreover, the downregulation of Aconitase 2 (ACO2), oxoglutarate dehydrogenase (OGDH), ATP Synthase, H⁺ Transporting, Mitochondrial F1 Complex, Beta Polypeptide (ATP5B), SOD2, Succinate Dehydrogenase Complex Flavoprotein Subunit A (SDHA), PRDX5, NADH dehydrogenase [ubiquinone] iron-sulfur protein 2 (NDUFS2), NADH:ubiquinone oxidoreductase core subunit S7 (NDUFS7), and Cytochrome C Oxidase Subunit 4I1 (COX4I1), and the activation of NFκB, and TNF regulated mitochondrial dysfunction in this group (Figure 16B). Furthermore, the modified proteins in the kidney of this group showed activation of adhesion of glomerular cells, cell death, cell spreading of kidney cell lines, engulfment of cells, metabolism of reactive oxygen species, the quantity of reactive oxygen species, and synthesis of reactive oxygen species as Biological Functions.

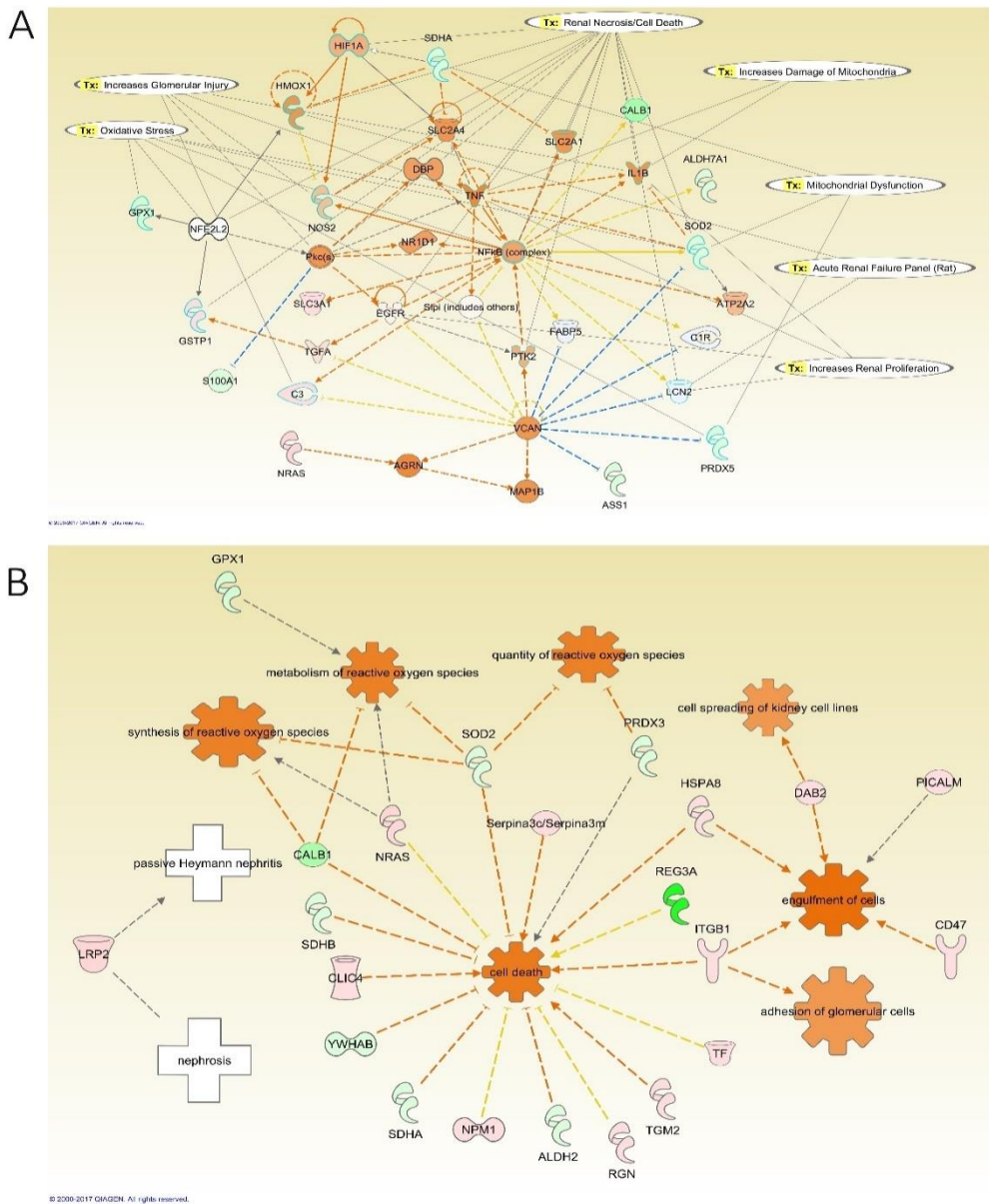


Figure 16: IPA network analysis of the modified proteins in the kidney of insulin-treated diabetic relative to diabetic rats. A: The top Toxicity and functions predicted by IPA related to the modified proteins are Increase Damage to Mitochondria, Glomerular Injury, Renal Proliferation, Necrosis/Cell Death, Oxidative Stress, Acute Renal Failure Panel (Rat), and Mitochondrial Dysfunction. The main regulated proteins in this network are NFkB (complex), PRDX5, and SOD2. B: Diseases and Biological Functions predicted by IPA related to the differentially expressed proteins in this comparative group. The main biological functions altered in this network are adhesion of glomerular cells and metabolism and synthesis of reactive oxygen species. The diseases related to these proteins are nephrosis, passive Heymann nephritis. The color intensity of the nodes reflects the expression of the proteins. Green nodes are down-regulated proteins, red nodes are upregulated proteins, white nodes are IPA predicted proteins with non-consistent activation pattern, and orange nodes are IPA predicted proteins to be activated.

5. *Discussion:*

Discovery proteomic analysis of biological tissues and fluids is increasingly employed in the identification of novel biomarkers. Unlike genomic and transcriptomic approaches for biomarker discovery, proteomics provides significant insights into protein abundance and PTM that modulate protein function and activity [353,354]. In this study, we employed mass spectrometric analysis by using tandem LC MS/MS to generate a proteomic profile that encompasses information on both protein abundance and post translational modification in the aorta and kidney of type 1 diabetic rats. In addition, systems biology analysis was employed on modified proteins to identify key proteins that can highlight mechanisms and pathways involved in diabetic vascular and renal biology.

Our data demonstrated that the aorta and kidney responded to the diabetic state differently as evidenced by the proteomic profile of modified proteins expressed in these tissues. Diabetes induced the expression of fibrotic, inflammatory, oxidative and cytoskeleton-related proteins that are interconnected to cellular networks involved in vascular and renal diseases. Insulin treatment of diabetic rats partially reversed the expression profile of the proteins in aorta and kidney that were significantly modified by the diabetic state, despite normalization of blood glucose levels at study end. This phenomenon is termed “metabolic memory” to specify the continuing persistence of hyperglycemia burden even after glycemic control [355]. Epigenetic modifications of genes caused by the persistent exposure to hyperglycemia may explain some of the enduring detrimental effects of hyperglycemia on causing tissue damage in diabetes [356-359].

It is also conceivable that factors other than hyperglycemia may have contributed to the expression profile of proteins modified by diabetes. In this regard, our data indicated

that the insulin treatment induced the expression of angiotensinogen and ACE in the aorta of diabetic rats, which could result in increased generation of the vasoactive peptide angiotensin II. The generated angiotensin II can act in a paracrine and autocrine manner on vascular cells to mediate a multitude of cellular signaling pathways that result in vascular remodeling [360]. In fact, angiotensin II has been shown to modulate vascular tone and to promote vascular smooth muscle cell proliferation and matrix expansion and contributes to vascular disease in diabetes [361]. Along these lines, analysis of the proteome profile of proteins indicated that diabetes induced the expression levels of matrix proteins such as collagen type VI $\alpha 6$ and type XVIII $\alpha 1$, fibulin 1 and transforming growth factor beta (TGF- β) in the aorta. In this regard, angiotensin II-induced myocardial fibrosis mediated by TGF- β is modulated by fibulin [362]. Moreover, our data indicated that the expression of prohibitin 1 and 2 was reduced in the aorta of diabetic rats, thus increasing the susceptibility to vascular injury. Prohibitin overexpression was associated with inhibition of collagen accumulation and reduction of reactive oxygen species generation in diabetes [363-366]. The downregulation of prohibitin expression in the aorta was associated with the promotion of cell death functions.

Analysis of the proteome profile revealed that diabetes induced the expression of kininogen in both the aorta and kidney and this effect was modulated by hyperglycemia. Kininogen levels were also shown to be upregulated in the liver of T1DM rat model and in the plasma of T1DM patients at risk for renal diabetic disease [367]. Moreover, these findings are in-line with our previous data where we found that the expression and activity of plasma prekallikrein (PK), the serine protease that cleaves kininogen to liberate the vasoactive peptide bradykinin, were elevated in T1DM patients. Furthermore, PK levels

were shown to be associated with macroalbuminuria, and carotid intimal medial thickness implicating a role for PK as a risk factor for vascular and renal disease in T1DM patients [142,368]. In addition, targeted deletion of bradykinin receptor 2 in diabetic mice conferred renoprotection against the development of diabetic nephropathy [83]. It is of interest to point here that network analysis of this group of proteins depicted that kininogen and protein kinase A are connected to the activation of angiotensin II type 2, leptin and heme oxygenase 1, thus linking the kallikrein kinin system and renin-angiotensin system to the inflammatory and oxidative stress processes inherent in the diabetic state.

PTMs have recognized modulators of target protein resulting in their structural conformational changes that influence their activity, spatial localization, and binding to other cellular protein partners [369,370]. Virtually all cellular pathways are regulated by PTMs and their dysregulation has been shown to be related to diseases such as CKD and CVD [371-373]. Our data indicated that diabetes increased the intensities of oxidized, phosphorylated and acetylated proteins in both the aorta and kidney. This increase in PTMs was independent of protein abundance. Hyperglycemia is recognized as one of the main factors that provoke disproportionate reactive oxygen species production in the vasculature, kidney, and heart [374-376]. Oxidative stress causes modifications of protein, lipids, DNA and it activates transcription factors that drive inflammation, fibrosis and cell hypertrophy [356,357,377]. In this regard, our analysis of the proteome profile indicated that diabetes induced the expression of a number of oxidative stress related enzymes involved in hydrogen peroxide, electrophilic and superoxide detoxification such as glutathione peroxidase 1 and 3, glutathione S-transferase Pi 1, Mu 1, Mu 3 and zeta 1 and monoamine

oxidase A, underscoring the oxidative stress condition associated with the exposure of cells to hyperglycemia.

Pathway analysis of our proteome profile indicated that diabetes is associated with activation of inflammatory and oxidative response proteins such as TNF- α , NF κ B, leptin, leptin receptors, and p38 MAPK, factors that have been shown to contribute to micro and macrovascular complications of diabetes [378,379]. In addition, our data indicated that diabetes promotes renal cell necrosis through the alteration of the expression of heat shock protein family A (Hsp70) Member 5 (HSPA5) (or 78 kDa glucose-regulated protein (GRP-78)), superoxide dismutase 2, heme oxygenase 1, peroxiredoxin 3, kininogen, peroxisome proliferator activated receptor gamma (PPAR γ) and calbindin 1. The upregulation of calbindin, a vitamin D binding proteins, is suggested to be related to acute renal failure and long-term renal injury panels [380,381]. In addition, our data indicated that prohibitin 1 and 2 are upregulated in the kidney by diabetes and may have a potential role in early stages of diabetic nephropathy [382].

In summary, we have identified a number of proteins that were differentially expressed and post translationally modified by diabetes in the aorta and kidney. Using informatics analysis of the modified proteome profiles identified key proteins that provided novel insights into biochemical pathways and processes that may be involved in the development of renal and vascular disease in diabetes.

SUPPLEMENTARY DATA FOR STUDY ONE

Table 1: Comparative list of proteins in the aorta of diabetic rats compared to controls.

	Accession Number	Names	Abbreviation	Fold Change	p value
1	A0A0G2JSJ2	Cytidine/Uridine Monophosphate Kinase 1	CMPK1	0.47	0.001
2	A0A0G2JSK5	Integrin Subunit Beta 1	ITGB1	2.77	0.044
3	A0A0G2JSS9	Atlastin-3	Atl3	5.76	0.048
4	G3V9Q3	Heterogeneous Nuclear Ribonucleoprotein H	Hnrnp1	1.94	0.049
5	A0A0G2JTL5	Pyruvate Carboxylase	PC	0.01	0.009
6	A0A0G2JTW9	Hemoglobin Subunit Beta	HBB	0.33	0.034
7	F7EPH4	Pyrophosphatase (Inorganic) 1	PPA1	0.46	0.018
8	A0A0G2JV31	X-Prolyl Aminopeptidase 1	XPNPEP1	3.23	0.007
9	A0A0G2JVH4	Inner Membrane Mitochondrial Protein	IMMT	0.20	0.039
10	F1LUV9	Neural Cell Adhesion Molecule 1	Ncam1	0.57	0.032
11	A0A0G2K0Q7	Myosin Light Chain Kinase	MYLK	10.44	0.046
12	A0A0G2K0Z7	Glycerol-3-Phosphate Dehydrogenase 2	GPD2	0.01	0.006
13	A0A0G2K167	Regulator of Microtubule Dynamics Protein 1	Rmdn1	0.09	0.010
14	A0A0G2K1C0	ARP3 Actin Related Protein 3 Homolog	ACTR3	2.44	0.019
15	F1LQQ1	Malic Enzyme 1	ME1	0.20	0.017
16	A0A0G2K401	Propionyl-CoA Carboxylase Alpha Subunit	PCCA	0.02	0.008
17	A0A0G2K7P7	Mitochondrial Carrier 2	MTCH2	0.11	0.036
18	A0A0G2K4M4	Pro-Epidermal Growth Factor-Like	LOC100910178	0.17	0.023
19	A0A0G2K531	Glutathione Peroxidase 3	GPX3	2.12	0.004
20	D3Z8D7	40s Ribosomal Protein S26	LOC100361854	0.56	0.044
21	A0A0G2K7K2	Apoptosis Inducing Factor Mitochondria Associated 1	AIFM1	0.11	0.044
22	A0A0G2K8Q1	Apolipoprotein C-III	Apoc3	0.13	0.002
23	A0A0G2K8Q8	Ubiquinol-Cytochrome C Reductase, Complex Iii Subunit X	UQCR10	0.41	0.033
24	R9PXU6	Vinculin	VCL	2.95	0.023
25	Q66H18	Synaptophysin-Like 1	Syp11	10.00	0.001
26	A0A0G2KAM3	Pyruvate Dehydrogenase (Lipoamide) Beta	PDHB	0.21	0.040
27	A0A0G2KB63	Prohibitin 2	PHB2	0.42	0.019

28	A0A0H2UHM5	Protein Disulfide Isomerase Family A Member 3	PDIA3	1.64	0.022
29	A0A0H2UI21	Carnitine O-Acetyltransferase	CRAT	0.14	0.023
30	A0A0U1RRV7	Rcg61099, Isoform Cra_B	Srsf3	6.75	0.008
31	A0JPK5	Abhydrolase Domain Containing 5	ABHD5	0.39	0.018
32	A1L114	Fibrinogen Alpha Chain	FGA	0.56	0.034
33	A1L1M0	Protein Kinase Camp-Activated Catalytic Subunit Alpha	PRKACA	1.65	0.022
34	B2GV33	Monoamine Oxidase A	MAOA	2.67	0.049
35	B2GV73	Actin Related Protein 2/3 Complex Subunit 3	ARPC3	3.02	0.004
36	B2RZ24	Succinate-CoA Ligase ADP-Forming Beta Subunit	SUCLA2	0.07	0.005
37	B2RZA6	Tbl1x Protein	Tbl1x	0.55	0.011
38	F1LSP2	Acyl-CoA Dehydrogenase Family, Member 10	Acad10	0.14	0.027
39	B5DEY8	Sorting Nexin	Snx6	1.93	0.021
40	B5DF65	Biliverdin Reductase B	BLVRB	0.42	0.044
41	B6DYQ7	Glutathione S-Transferase Pi 1	GSTP1	2.04	0.021
42	C0KUC5	Lim Zinc Finger Domain Containing 1	LIMS1	3.27	0.037
43	D3ZD09	Cytochrome C Oxidase Subunit 6b1	COX6B1	0.24	0.025
44	D3ZF13	NADH:Ubiquinone Oxidoreductase Subunit AB1	NDUFAB1	0.28	0.020
45	D3ZFQ8	Cytochrome C1	CYC1	0.31	0.048
46	D3ZG43	NADH:Ubiquinone Oxidoreductase Core Subunit S3	NDUFS3	0.08	0.030
47	D3ZIC4	Protein Phosphatase 1, Regulatory (Inhibitor) Subunit 12b	Ppp1r12b	4.20	0.007
48	D3ZJX5	Translocase of Inner Mitochondrial Membrane 50	TIMM50	0.20	0.006
49	D3ZKG1	Methylmalonyl-CoA Mutase	MUT	0.09	0.006
50	D3ZL10	Collagen Type VI Alpha 6 Chain	COL6A6	4.32	0.030
51	D3ZQ25	Fibulin 1	FBLN1	4.12	0.013
52	D3ZS55	Somatomedin B and Thrombospondin Type 1 Domain Containing	SBSPON	3.11	0.026
53	D3ZUX5	Trans-L-3-Hydroxyproline Dehydratase	L3HYPDH	0.15	0.010

54	D3ZV91	NADH:Ubiquinone Oxidoreductase Subunit B10	NDUFB10	0.31	0.046
55	D3ZVS2	L-2-Hydroxyglutarate Dehydrogenase	L2hgdh	0.25	0.042
56	D4A0T0	NADH:Ubiquinone Oxidoreductase Subunit B10	Ndufb10	0.15	0.013
57	D4A197	Methylmalonyl-CoA Epimerase	MCEE	0.10	0.038
58	D4A2K1	4-Hydroxy-2-Oxoglutarate Aldolase 1	HOGA1	0.40	0.033
59	Q4FZZ4	Pyruvate Dehydrogenase (Lipoamide) Alpha 1	PDHA1	0.23	0.018
60	D4A5L9	Uncharacterized Protein	LOC679794	0.21	0.002
61	G3V6A9	Microfibril-Associated Glycoprotein 4-Like	LOC102553715	2.07	0.042
62	D4ADF5	Programmed Cell Death Protein 5-Like	Pdcd5	160	0.011
63	F1LNF7	Isocitrate Dehydrogenase 3 (NAD(+)) Alpha	IDH3A	0.13	0.014
64	F1LR02	Collagen Type XVIII Alpha 1 Chain	COL18A1	2.75	0.035
65	F1LRJ9	Neural Cell Adhesion Molecule 1	NCAM1	2.04	0.037
66	F1LTJ5	Uncharacterized Protein	N/A	2.23	0.019
67	Q6P7A4	Prosaposin	PSAP	0.36	0.026
68	G3V624	Coronin	Coro1c	19.03	0.021
69	O54755	NADH:Ubiquinone Oxidoreductase Subunit V3	NDUFV3	0.06	0.014
70	G3V734	2,4-Dienoyl-CoA Reductase 1	DECR1	0.10	0.048
71	G3V796	Acyl-CoA Dehydrogenase, C-4 To C-12 Straight Chain	ACADM	0.02	0.001
72	G3V7I0	Peroxiredoxin 3	PRDX3	0.14	0.025
73	G3V8R5	Lipase E, Hormone Sensitive Type	LIPE	0.09	0.021
74	G3V928	LDL Receptor Related Protein 1	LRP1	1.47	0.020
75	G3V936	Citrate Synthase	CS	0.25	0.041
76	G3V940	Coronin 1B	CORO1B	8.55	0.007
77	G3V9E3	Caldesmon 1	Cald1	21.46	0.046
78	G3V9U2	Acetyl-CoA Acyltransferase 2	ACAA2	0.08	0.048
79	Q5BJ93	Enolase 1	ENO1	0.70	0.015
80	M0R757	Elongation Factor 1-Alpha	LOC100360413	1.95	0.017
81	M0R7G4	Apolipoprotein O	Apoo	0.08	0.002
82	M0RAM5	Glutathione Peroxidase 1	GPX1	3.22	0.041
83	M0RBF1	Complement C3	C3	0.64	0.016

84	O35077	Glycerol-3-Phosphate Dehydrogenase 1	GPD1	0.05	0.021
85	O35509	Rab11b, Member Ras Oncogene Family	RAB11B	1.49	0.047
86	O35567	5-Aminoimidazole-4-Carboxamide Ribonucleotide Formyltransferase/Imp Cyclohydrolase	ATIC	1.76	0.029
87	O35796	Complement C1q Binding Protein	C1QBP	0.26	0.015
88	O55096	Dipeptidyl Peptidase 3	DPP3	1.73	0.010
89	P04182	Ornithine Aminotransferase	OAT	4.90	0.050
90	P04633	Uncoupling Protein 1	UCP1	0.00	0.004
91	P04636	Malate Dehydrogenase 2	MDH2	0.33	0.035
92	P04638	Apolipoprotein A2	APOA2	0.23	0.004
93	P04639	Apolipoprotein A1	APOA1	2.29	0.032
94	P04797	Glyceraldehyde-3-Phosphate Dehydrogenase	GAPDH	1.70	0.019
95	P07340	ATPase Na ⁺ /K ⁺ Transporting Subunit Beta 1	ATP1B1	8.54	0.025
96	P07379	Phosphoenolpyruvate Carboxykinase 1	PCK1	0.12	0.042
97	Q6LDS4	Superoxide Dismutase 1	SOD1	0.59	0.044
98	P08461	Dihydrolipoamide S-Acetyltransferase	DLAT	0.08	0.013
99	Q6LCA5	Protein Kinase cAMP-Dependent Type I Regulatory Subunit Alpha	PRKAR1A	2.56	0.020
100	P09606	Glutamate-Ammonia Ligase	GLUL	0.24	0.027
101	P0DN35	NADH Dehydrogenase [Ubiquinone] 1 Beta Subcomplex Subunit 1	Ndufb1	0.17	0.012
102	P10888	Cytochrome C Oxidase Subunit 4I1	COX4I1	0.11	0.012
103	Q6TXF3	Diazepam Binding Inhibitor, Acyl-CoA Binding Protein	DBI	0.57	0.024
104	P11951	Cytochrome C Oxidase Subunit Vic	Cox6c	0.22	0.034
105	P12007	Isovaleryl-CoA Dehydrogenase	IVD	0.02	0.002
106	P13803	Electron Transfer Flavoprotein Alpha Subunit	ETFFA	0.11	0.039
107	P14046	Murinoglobulin 1	Mug1 (includes others)	0.25	0.000
108	P14408	Fumarate Hydratase	FH	0.17	0.004
109	P14604	Enoyl-CoA Hydratase, Short Chain 1	ECHS1	0.24	0.021
110	P15650	Acyl-CoA Dehydrogenase, Long Chain	ACADL	0.13	0.013

111	Q6IMX3	Acyl-CoA Dehydrogenase, C-2 To C-3 Short Chain	ACADS	0.20	0.027
112	R9PXS4	Phosphatidylinositol Transfer Protein Alpha	PITPNA	2.50	0.003
113	P17764	Acetyl-CoA Acetyltransferase 1	ACAT1	0.16	0.016
114	P18163	Acyl-CoA Synthetase Long-Chain Family Member 1	ACSL1	0.10	0.024
115	P19234	NADH:Ubiquinone Oxidoreductase Core Subunit V2	NDUFV2	0.15	0.022
116	P20070	Cytochrome B5 Reductase 3	Cyb5r3	2.04	0.018
117	P20788	Ubiquinol-Cytochrome C Reductase, Rieske Iron-Sulfur Polypeptide 1	UQCRC1	0.22	0.008
118	Q6P6T6	Cathepsin D	CTSD	0.41	0.024
119	P97601	Heat Shock Protein Family E (Hsp10) Member 1	HSPE1	0.36	0.025
120	P29975	Aquaporin 1 (Colton Blood Group)	AQP1	1.89	0.018
121	P32198	Carnitine Palmitoyltransferase 1a	CPT1A	8.04	0.007
122	P32551	Ubiquinol-Cytochrome C Reductase Core Protein II	UQCRC2	0.23	0.015
123	P36201	Cysteine Rich Protein 2	Crip2	16.44	0.006
124	P40112	Proteasome Subunit Beta 3	PSMB3	8.27	0.007
125	P40307	Proteasome Subunit Beta 2	PSMB2	4.30	0.035
126	P50475	Alanyl-tRNA Synthetase	AARS	0.31	0.020
127	P54313	G Protein Subunit Beta 2	GNB2	1.89	0.010
128	P62076	Mitochondrial Import Inner Membrane Translocase Subunit Tim13	Timm13	0.06	0.038
129	P62142	Protein Phosphatase 1 Catalytic Subunit Beta	PPP1CB	7.07	0.012
130	P62828	Ran, Member Ras Oncogene Family	RAN	1.86	0.000
131	P67779	Prohibitin	PHB	0.24	0.013
132	P68035	Actin, Alpha, Cardiac Muscle 1	ACTC1	2.12	0.049
133	P68255	Tyrosine 3-Monooxygenase/Tryptophan 5-Monooxygenase Activation Protein Theta	YWHAQ	1.40	0.040
134	P69897	Tubulin Beta Class I	TUBB	2.95	0.005
135	P85515	Alpha-Contractin	Actr1a	3.79	0.012
136	P85834	Elongation Factor Tu, Mitochondrial	Tufm	0.16	0.035
137	P85973	Purine Nucleoside Phosphorylase	PNP	3.39	0.009

138	Q03336	Regucalcin	RGN	0.19	0.026
139	Q07116	Sulfite Oxidase	SUOX	0.06	0.000
140	Q07936	Annexin A2	ANXA2	1.80	0.042
141	Q3MIE4	Synaptic Vesicle Membrane Protein Vat-1 Homolog	Vat1	1.35	0.013
142	Q499N5	Acyl-CoA Synthetase Family Member 2, Mitochondrial	Acsf2	0.03	0.023
143	Q4QRB4	Tubulin Beta 3 Class Iii	TUBB3	0.13	0.002
144	Q4V8N0	Lipocalin 7, Isoform Cra_A	Tinagl1	2.18	0.047
145	Q561S0	NADH:Ubiquinone Oxidoreductase Subunit A10	NDUFA10	0.04	0.001
146	Q56R17	Karyopherin Subunit Alpha 4	KPNA4	0.36	0.048
147	Q5BJZ3	Nicotinamide Nucleotide Transhydrogenase	NNT	15.04	0.034
148	Q5EB77	Rab18, Member Ras Oncogene Family	RAB18	0.68	0.041
149	Q510E7	Transmembrane Emp24 Domain-Containing Protein 9	Tmed9	12.35	0.015
150	Q5M7U6	ARP2 Actin Related Protein 2 Homolog	ACTR2	17.53	0.000
151	Q5M9H2	Acyl-CoA Dehydrogenase, Very Long Chain	ACADVL	0.22	0.024
152	Q5M9I5	Ubiquinol-Cytochrome C Reductase Hinge Protein Like	UQCRHL	0.20	0.014
153	Q5PQU1	Kininogen 1	Kng1/Kng111	2.91	0.004
154	Q5PQZ9	NADH:Ubiquinone Oxidoreductase Subunit C2	NDUFC2	0.06	0.026
155	Q5XI77	Annexin	Anxa11	2.26	0.014
156	Q5XI78	Oxoglutarate Dehydrogenase	OGDH	0.06	0.024
157	Q5XIF3	NADH:Ubiquinone Oxidoreductase Subunit S4	NDUFS4	0.14	0.012
158	Q5XIT9	Methylcrotonoyl-CoA Carboxylase 2	MCCC2	0.05	0.005
159	Q60587	Hydroxyacyl-CoA Dehydrogenase/3-Ketoacyl-CoA Thiolase/Enoyl-CoA Hydratase (Trifunctional Protein), Beta Subunit	HADHB	0.08	0.013
160	Q62952	Dihydropyrimidinase Like 3	DPYSL3	3.89	0.015
161	Q62969	Prostaglandin I2 Synthase	PTGIS	3.75	0.027
162	Q63704	Carnitine Palmitoyltransferase 1b	CPT1B	0.04	0.011

163	Q641Y2	NADH:Ubiquinone Oxidoreductase Core Subunit S2	NDUFS2	0.07	0.044
164	Q64428	Hydroxyacyl-CoA Dehydrogenase/3-Ketoacyl-CoA Thiolase/Enoyl-CoA Hydratase Alpha Subunit	HADHA	0.18	0.019
165	Q64542	ATPase Plasma Membrane Ca ²⁺ Transporting 4	ATP2B4	6.92	0.042
166	Q66HF1	NADH:Ubiquinone Oxidoreductase Core Subunit S1	NDUFS1	0.16	0.012
167	Q68FT1	Coenzyme Q9	COQ9	0.03	0.024
168	Q68FU3	Electron Transfer Flavoprotein Subunit Beta	Etfb	0.08	0.011
169	Q68FY0	Ubiquinol-Cytochrome C Reductase Core Protein I	UQCRC1	0.10	0.008
170	Q6MG61	Chloride Intracellular Channel 1	CLIC1	1.48	0.036
171	Q6P6R2	Dihydrolipoamide Dehydrogenase	DLD	0.15	0.022
172	Q9WVJ6	Transglutaminase 2	TGM2	2.64	0.014
173	Q6P7P5	Basic Leucine Zipper and W2 Domain-Containing Protein 1	Bzw1	0.23	0.002
174	Q6P9V1	CD81 Molecule	CD81	3.49	0.044
175	Q6P9V6	Proteasome Subunit Alpha 5	PSMA5	1.44	0.006
176	Q6P9V9	Tubulin Alpha-1b Chain	Tuba1b	2.42	0.009
177	Q6TXG7	Serine Hydroxymethyltransferase 1	SHMT1	0.01	0.001
178	Q794E4	Heterogeneous Nuclear Ribonucleoprotein F	HNRNPF	1.28	0.023
179	Q91Y81	Septin 2	SEPT2	4.37	0.018
180	Q920L2	Succinate Dehydrogenase Complex Flavoprotein Subunit A	SDHA	0.14	0.013
181	Q924S5	Lon Peptidase 1, Mitochondrial	LONP1	0.20	0.019
182	Q99PD6	Transforming Growth Factor Beta 1 Induced Transcript 1	TGFB1I1	9.85	0.046
183	Q9ER34	Aconitase 2	ACO2	0.14	0.025
184	Q9ESN0	Family with Sequence Similarity 129 Member A	FAM129A	5.12	0.018
185	Q9JJ54	Heterogeneous Nuclear Ribonucleoprotein D	HNRNPD	2.43	0.038
186	Q9JLZ1	Glutaredoxin 3	GLRX3	0.28	0.016
187	Q9Z0V5	Peroxiredoxin 4	PRDX4	0.70	0.014
188	Q9Z1B2	Glutathione S-Transferase Mu 3	GSTM3	16.78	0.039

Table 2: Comparative list of proteins in the kidney of diabetic rats compared to controls.

	Accession Number	Name	Abbreviation	Fold Change	p value
1	A0A0A0MXW3	H2A Histone Family Member Z	H2AFZ	0.76	0.021
2	A0A0A0MXW9	RNA-Binding Motif Protein, X-Linked-Like-1	Rbmx11	0.78	0.014
3	Q95938	Cytochrome C Oxidase Subunit I (Mitochondrion)	COX1	1.21	0.047
4	A0A0G2JSI0	Flavin Containing Monooxygenase 3	FMO3	0.61	0.049
5	A0A0G2JSK5	Integrin Subunit Beta 1	ITGB1	0.74	0.009
6	A0A0G2JSV6	Globin C2	Hba-a2	0.63	0.008
7	A0A0G2JTL5	Pyruvate Carboxylase	PC	1.82	0.004
8	A0A0G2JTW9	Hemoglobin Subunit Beta	HBB	0.49	0.028
9	D4A6E3	Murinoglobulin-1 Precursor	Mug1	0.24	0.011
10	A0A0G2JV65	Tyrosine 3-Monooxygenase/Tryptophan 5-Monooxygenase Activation Protein Zeta	YWHAZ	0.86	0.024
11	A0A0G2JVH4	Inner Membrane Mitochondrial Protein	IMMT	1.16	0.049
12	A0A0G2JVL6	NADH:Ubiquinone Oxidoreductase Subunit A8	NDUFA8	1.66	0.028
13	D3ZFD0	Myosin XVIII A	Myo18a	1.32	0.036
14	A0A0G2K4D0	Ankyrin 3	ANK3	0.79	0.003
15	A0A0G2K0Q8	Alkaline Phosphatase, Liver/Bone/Kidney	ALPL	2.11	0.016
16	A0A0G2K0X8	Alkaline Phosphatase	Alpl	1.37	0.039
17	Q6PAH0	Apolipoprotein E	APOE	0.45	0.039
18	A0A0G2K277	Enoyl-Coenzyme A Delta Isomerase 3	Eci3	1.20	0.002
19	A0A0G2K401	Propionyl-CoA Carboxylase Alpha Subunit	PCCA	1.25	0.031
20	A0A0G2K531	Glutathione Peroxidase 3	GPX3	0.77	0.012
21	A0A0U1RRQ2	Actin Related Protein 2/3 Complex Subunit 5	ARPC5	0.73	0.005
22	G3V9G4	ATP Citrate Lyase	ACLY	0.70	0.032
23	D3ZCF5	SMAD Specific E3 Ubiquitin Protein Ligase 1	SMURF1	0.23	0.003
24	A0A0G2K6H2	Glutathione S-Transferase Zeta 1	GSTZ1	1.86	0.005
25	D3Z8D7	Ribosomal Protein S26	Rps26	0.79	0.013
26	A0A1B0GWP1	ELOVL Fatty Acid Elongase 1	ELOVL1	0.71	0.002

27	A0A0G2K8Q8	Ubiquinol-Cytochrome C Reductase, Complex III Subunit X	UQCR10	1.20	0.017
28	G3V6S0	Spectrin Beta, Non-Erythrocytic 1	SPTBN1	0.79	0.000
29	Q80YG1	Phosphoserine Aminotransferase 1	PSAT1	0.67	0.025
30	A0A0G2K9J2	ATPase H ⁺ Transporting V1 Subunit H	ATP6V1H	1.59	0.005
31	A0A0G2K9W7	LDL Receptor Related Protein 2	LRP2	0.45	0.019
32	A0A0G2KAM3	Pyruvate Dehydrogenase (Lipoamide) Beta	PDHB	1.18	0.032
33	Q7TNX2	Peroxisomal Membrane Protein 2	Pxmp2	2.42	0.039
34	A0A0G2KB63	Prohibitin 2	PHB2	1.15	0.024
35	A0A0G2QC04	Plastin 1	Pls1	0.72	0.026
36	A0A0H2UHE1	Succinate-CoA Ligase Alpha Subunit	SUCLG1	1.36	0.023
37	A0A0H2UHE4	Regenerating Family Member 3 Alpha	REG3A	10.17	0.023
38	A0A0H2UHM3	Haptoglobin	HP	0.67	0.027
39	Q7TP86	Uncharacterized Protein LOC502176	LOC502176	0.78	0.032
40	A2VCW9	Aminoadipate-Semialdehyde Synthase	AASS	2.16	0.037
41	A4PB92	Glycine N-Acyltransferase	Glyat	1.34	0.037
42	B0BMW2	Hydroxysteroid 17-Beta Dehydrogenase 10	HSD17B10	1.51	0.008
43	B0BNG1	Proline Dehydrogenase 2	PRODH2	1.46	0.016
44	B1H216	Hemoglobin, Alpha 1	Hba1/Hba2	0.53	0.046
45	Q5EBA9	Succinate-CoA Ligase GDP-Forming Beta Subunit	SUCLG2	1.32	0.009
46	B2GUV5	Atpase H ⁺ Transporting V1 Subunit G1	ATP6V1G1	0.81	0.008
47	B2GVB1	S100 Calcium Binding Protein A6	S100A6	1.96	0.000
48	B2RYR8	Ribosomal Protein S8	RPS8	0.72	0.003
49	B2RYU2	60S Ribosomal Protein L12	Rpl12	0.77	0.028
50	B2RYW3	NADH: Ubiquinone Oxidoreductase Subunit B9	NDUFB9	1.36	0.041
51	B2RYW9	Fumarylacetoacetate Hydrolase Domain-Containing Protein 2	Fahd2a	1.74	0.013
52	B2RZ24	Succinate-CoA Ligase ADP-Forming Beta Subunit	SUCLA2	1.27	0.031
53	B4F768	Aldehyde Dehydrogenase 4 Family Member A1	ALDH4A1	1.88	0.021

54	B5DER3	Isoamyl Acetate-Hydrolyzing Esterase 1 Homolog	Iah1	0.82	0.045
55	D3ZCH6	Ribonuclease T2 Precursor	Rnaset2	0.74	0.018
56	B5DFA0	Villin-1	Vil1	0.75	0.019
57	B6DYQ2	Glutathione S-Transferase Mu 1	GSTM1	1.55	0.039
58	D3Z8F1	Villin-Like Protein	Vill	0.64	0.010
59	D3Z8M8	TSC22 Domain Family Member 1	TSC22D1	0.76	0.030
60	M0R6N2	MOCO Sulphurase C-Terminal Domain Containing 2	Mosc2	1.55	0.005
61	D4A3B0	Talin 2	TLN2	0.66	0.031
62	D3ZFY8	Ubiquitin-Conjugating Enzyme E2 Variant 1	Ube2v1	0.76	0.042
63	Q6PDW1	Ribosomal Protein S12	RPS12	0.86	0.041
64	D3ZPL5	60S Ribosomal Protein L7a	RGD1562953	0.74	0.035
65	D3ZRJ6	Cell Surface A33 Antigen Precursor	Gpa33	1.39	0.028
66	D3ZSL2	Uncharacterized Protein LOC685045	Abrac1	0.15	0.047
67	D3ZT90	Glutaryl-CoA Dehydrogenase	GCDH	1.39	0.001
68	D3ZTX4	Maltase-Glucoamylase	Mgam	0.28	0.001
69	D3ZXX4	Abhydrolase Domain Containing 11	Abhd11	0.39	0.025
70	D3ZXY4	Aldehyde Dehydrogenase 8 Family Member A1	ALDH8A1	0.32	0.000
71	D3ZZN3	Acyl-CoA Synthetase Short-Chain Family Member 1	ACSS1	1.59	0.012
72	D4A5I9	Myosin VI	MYO6	0.82	0.004
73	D4A8H3	Ubiquitin-Like Modifier-Activating Enzyme 6	Uba6	0.56	0.007
74	D4AB01	Histidine Triad Nucleotide Binding Protein 2	Hint2	1.39	0.036
75	F1LMP9	DAB2, Clathrin Adaptor Protein	DAB2	0.59	0.012
76	F1LMV6	Desmoplakin	DSP	0.67	0.006
77	F1LP30	Methylcrotonoyl-CoA Carboxylase 1	MCCC1	1.53	0.004
78	F1LPD6	Acetyl-CoA Acyltransferase 1	ACAA1	1.52	0.006
79	F1LRJ9	Selenium-Binding Protein 1	Selenbp1	1.65	0.012
80	F1LWL8	Sodium-Coupled Monocarboxylate Transporter 2	Slc5a12	1.32	0.008
81	Q8CHN5	Epididymal Secretory Protein E1 Precursor	Npc2	0.71	0.019

82	G3V6D3	ATP Synthase, H+ Transporting, Mitochondrial F1 Complex, Beta Polypeptide	ATP5B	1.25	0.002
83	G3V6H5	Solute Carrier Family 25 Member 11	SLC25A11	1.28	0.016
84	G3V6P2	Dihydrolipoamide S-Succinyltransferase	DLST	1.22	0.046
85	Q5EBA4	4-Nitrophenylphosphatase	Nipsnap1	1.42	0.014
86	G3V7I0	Peroxiredoxin 3	PRDX3	1.36	0.001
87	G3V7T5	Xylulose Kinase	Xylb	1.21	0.028
88	G3V826	Transketolase	TKT	3.07	0.014
89	G3V8A5	Maternal Embryonic Message 3	Vps35	0.69	0.006
90	G3V8D6	Tripartite Motif Containing 3	TRIM3	0.45	0.047
91	Q6P784	Branched Chain Amino Acid Transaminase 2	BCAT2	1.31	0.050
92	I6L9G6	TAR DNA Binding Protein	Tardbp	0.78	0.028
93	Q5BJ93	Enolase 1	ENO1	0.77	0.011
94	M0R7P0	Protein LOC688784	LOC688784	0.91	0.039
95	M0RAM5	Glutathione Peroxidase 1	GPX1	1.49	0.047
96	M0RBF1	Complement C3	C3	0.50	0.029
97	M0RCY2	Similar to Ribosomal Protein S13	LOC683961	0.67	0.047
98	M0RDH0	Glycine N-Methyltransferase	Gnmt	1.35	0.006
99	O35244	Peroxiredoxin 6	PRDX6	1.67	0.047
100	P00507	Glutamic-Oxaloacetic Transaminase 2	GOT2	1.35	0.006
101	P02091	Hemoglobin Subunit Beta-1	Hbb	0.62	0.031
102	P02680	Fibrinogen Gamma Chain	FGG	0.77	0.018
103	P02761	Alpha-2u-Globulin (L Type) Precursor	Mup5	0.35	0.005
104	P02770	Albumin	ALB	0.64	0.004
105	P04639	Apolipoprotein A1	APOA1	2.13	0.005
106	P04797	Glyceraldehyde-3-Phosphate Dehydrogenase	GAPDH	1.22	0.026
107	Q45QN0	G Protein Subunit Alpha I2	GNAI2	0.71	0.022
108	P05065	Aldolase, Fructose-Bisphosphate A	ALDOA	0.85	0.036
109	P06761	Heat Shock Protein Family A (Hsp70) Member 5	HSPA5	0.90	0.023
110	P07171	Calbindin 1	CALB1	1.55	0.047
111	P07483	Fatty Acid Binding Protein 3	FABP3	0.77	0.012
112	P07687	Epoxide Hydrolase 1	EPHX1	2.35	0.002

113	P07895	Superoxide Dismutase 2	SOD2	1.24	0.018
114	P10860	Glutamate Dehydrogenase 1	GLUD1	1.22	0.010
115	P10888	Cytochrome C Oxidase Subunit 4I1	COX4I1	1.26	0.018
116	P12346	Transferrin	TF	0.63	0.002
117	P12785	Fatty Acid Synthase	FASN	0.43	0.036
118	P13221	Glutamic-Oxaloacetic Transaminase 1	GOT1	1.32	0.024
119	P13803	Electron Transfer Flavoprotein Alpha Subunit	ETF A	1.34	0.013
120	P14046	Murinoglobulin 1	Mug1 (includes others)	0.16	0.000
121	P14408	Fumarate Hydratase	FH	1.22	0.023
122	P14562	Lysosomal Associated Membrane Protein 1	LAMP1	0.57	0.050
123	Q6IMX3	Acyl-CoA Dehydrogenase, C-2 To C-3 Short Chain	ACADS	1.38	0.000
124	P15999	ATP Synthase, H ⁺ Transporting, Mitochondrial F1 Complex, Alpha Subunit 1, Cardiac Muscle	ATP5A1	1.18	0.012
125	P17764	Acetyl-CoA Acetyltransferase 1	ACAT1	1.19	0.041
126	P18163	Acyl-CoA Synthetase Long-Chain Family Member 1	ACSL1	1.70	0.020
127	P19112	Fructose-Bisphosphatase 1	FBP1	0.41	0.000
128	P19804	NME/NM23 Nucleoside Diphosphate Kinase 2	NME2	1.06	0.021
129	P20059	Hemopexin	HPX	0.75	0.017
130	P21913	Succinate Dehydrogenase Complex Iron Sulfur Subunit B	SDHB	1.26	0.003
131	Q68G41	Enoyl-CoA Delta Isomerase 1	Eci1	2.01	0.021
132	P97601	Heat Shock Protein Family E (Hsp10) Member 1	HSPE1	1.26	0.017
133	P29266	3-Hydroxyisobutyrate Dehydrogenase	HIBADH	1.71	0.004
134	P31399	ATP Synthase, H ⁺ Transporting, Mitochondrial Fo Complex Subunit D	ATP5H	1.32	0.013
135	P32551	Ubiquinol-Cytochrome C Reductase Core Protein II	UQCRC2	1.14	0.044
136	P32755	4-Hydroxyphenylpyruvate Dioxygenase	HPD	1.57	0.004
137	P42123	Lactate Dehydrogenase B	LDHB	1.37	0.010
138	P43428	Glucose-6-Phosphatase Catalytic Subunit	G6PC	1.54	0.012
139	P45592	Cofilin 1	CFL1	0.72	0.002

140	P51635	Aldo-Keto Reductase Family 1 Member A1	AKR1A1	0.95	0.017
141	P52631	Signal Transducer and Activator of Transcription 3	STAT3	0.77	0.010
142	P53987	Solute Carrier Family 16 Member 1	SLC16A1	1.51	0.000
143	P54313	G Protein Subunit Beta 2	GNB2	0.85	0.037
144	P55053	Fatty Acid Binding Protein 5	FABP5	0.40	0.011
145	P56574	Isocitrate Dehydrogenase (NADP(+)) 2, Mitochondrial	IDH2	1.16	0.023
146	Q5D059	Heterogeneous Nuclear Ribonucleoprotein K	HNRNPK	0.88	0.014
147	P62161	Calmodulin	Calm1	0.84	0.041
148	P62260	Tyrosine 3-Monooxygenase/Tryptophan 5-Monooxygenase Activation Protein Epsilon	YWHAE	0.89	0.004
149	P62282	Ribosomal Protein S11	RPS11	0.78	0.047
150	P62804	Histone H4 Osteogenic Growth Peptide	Hist2h4	0.74	0.007
151	P62832	Ribosomal Protein L23	RPL23	0.82	0.008
152	P63259	Actin Gamma 1	ACTG1	0.86	0.020
153	P67779	Prohibitin	PHB	1.29	0.016
154	P68182	Protein Kinase cAMP-Activated Catalytic Subunit Beta	PRKACB	0.37	0.032
155	P68255	Tyrosine 3-Monooxygenase/Tryptophan 5-Monooxygenase Activation Protein Theta	YWHAQ	0.84	0.012
156	P68511	Tyrosine 3-Monooxygenase/Tryptophan 5-Monooxygenase Activation Protein Eta	YWHAH	0.56	0.029
157	P69897	Tubulin Beta Class I	TUBB	0.85	0.014
158	P70473	Alpha-Methylacyl-CoA Racemase	AMACR	2.24	0.000
159	P85968	Phosphogluconate Dehydrogenase	PGD	0.72	0.036
160	Q66HP8	Solute Carrier Family 25 Member 20	SLC25A20	1.34	0.014
161	Q66HN6	Solute Carrier Family 27 Member 2	SLC27A2	1.52	0.017
162	P97532	Mercaptopyruvate Sulfurtransferase	MPST	1.16	0.023
163	P97584	Prostaglandin Reductase 1	PTGR1	0.21	0.001
164	Q03336	Regucalcin	RGN	0.47	0.034

165	Q06647	ATP Synthase, H+ Transporting, Mitochondrial F1 Complex, O Subunit	ATP5O	1.17	0.025
166	Q0D2L3	Agmatinase, Mitochondrial	Agmat	1.34	0.012
167	Q3KR94	Vitronectin	VTN	0.52	0.006
168	Q4KM66	Immunoglobulin Kappa Constant	Igkc	1.18	0.050
169	Q6PPF3	Harmonin	Ush1c	0.40	0.028
170	Q4QQW3	Alcohol Dehydrogenase, Iron Containing 1	ADHFE1	3.36	0.000
171	Q4V8F6	Poly(Rc)-Binding Protein 2	Pcbp2	0.56	0.013
172	Q562C4	Methyltransferase-Like Protein 7B	Mettl7b	1.47	0.011
173	Q5BJZ3	Nicotinamide Nucleotide Transhydrogenase	NNT	1.58	0.010
174	Q5HZA9	Transmembrane Protein 126A	Tmem126a	1.36	0.016
175	Q5M9H2	Acyl-CoA Dehydrogenase, Very Long Chain	ACADVL	1.33	0.004
176	Q5PPP1	Clathrin Light Chain A	CLTA	0.24	0.015
177	Q5PQU1	Kininogen 1	Kng1/Kng111	4.61	0.012
178	Q5RJR2	Twinfilin Actin Binding Protein 1	TWF1	0.18	0.049
179	Q5RKI0	WD Repeat-Containing Protein 1	Wdr1	0.73	0.040
180	Q5U2P9	Monocarboxylate Transporter 5	Slc16a4	0.83	0.049
181	Q5XFX0	Transgelin-2	Tagln2	0.80	0.012
182	Q5XI34	Protein Phosphatase 2 Scaffold Subunit Alpha	PPP2R1A	0.72	0.010
183	Q5XI78	Oxoglutarate Dehydrogenase	OGDH	1.26	0.014
184	Q5XI85	Aminomethyltransferase	AMT	1.54	0.016
185	Q5XIC0	Enoyl-CoA Delta Isomerase 2	ECI2	1.74	0.048
186	Q5XIH3	NADH:Ubiquinone Oxidoreductase Core Subunit VI	NDUFV1	1.17	0.042
187	Q62651	Enoyl-CoA Hydratase 1	ECH1	1.94	0.007
188	Q63041	Alpha-1-Macroglobulin Alpha-1-Macroglobulin 45 kDa Subunit	Pzp	0.46	0.031
189	Q63342	Dimethylglycine Dehydrogenase	DMGDH	1.45	0.002
190	Q63530	Phosphotriesterase-Related Protein	Pter	0.73	0.000
191	Q63768	CRK Proto-Oncogene, Adaptor Protein	CRK	0.76	0.036
192	Q63910	Hemoglobin Subunit Alpha 2	HBA1/HBA2	0.37	0.009

193	Q64057	Aldehyde Dehydrogenase 7 Family Member A1	ALDH7A1	1.23	0.011
194	Q641Y0	Dolichyl-Diphosphooligosaccharide--Protein Glycosyltransferase 48 kDa Subunit Precursor	Ddost	0.75	0.002
195	Q641Y2	NADH:Ubiquinone Oxidoreductase Core Subunit S2	NDUFS2	1.78	0.001
196	Q642E6	Tripeptidyl Peptidase 1	TPP1	1.14	0.042
197	Q66HF3	Electron Transfer Flavoprotein-Ubiquinone Oxidoreductase	Etfdh	1.48	0.047
198	Q66HG3	Beta-Ala-His Dipeptidase	Cndp1	0.41	0.038
199	Q68FS4	Cytosol Aminopeptidase	Lap3	1.46	0.009
200	Q68FU3	Electron Transfer Flavoprotein Subunit Beta	Etfb	1.26	0.007
201	Q68FZ8	Propionyl-CoA Carboxylase Beta Subunit	PCCB	1.50	0.024
202	Q68G31	Enoyl-CoA Delta Isomerase 1	ECI1	1.49	0.006
203	Q6JE36	Protein NDRG1	Ndrp1	1.86	0.002
204	Q6P6R2	Dihydrolipoamide Dehydrogenase	DLD	1.32	0.009
205	Q6P7P5	Basic Leucine Zipper and W2 Domain-Containing Protein 1	Bzw1	0.67	0.042
206	Q6P9V6	Proteasome Subunit Alpha 5	PSMA5	0.81	0.035
207	Q812B0	Succinate Dehydrogenase [Ubiquinone] Cytochrome B Small Subunit	Lrrp1	1.18	0.019
208	Q7TP38	Proteasome Activator Subunit 3	PSME3	1.89	0.046
209	Q80ZA3	Serpin Family F Member 1	SERPINF1	0.60	0.003
210	Q8CFN2	Cell Division Cycle 42	Cdc42	0.89	0.040
211	Q9JJI4	Crystallin Mu	CRYM	0.20	0.002
212	Q8VI04	Asparaginase Like 1	ASRGL1	0.70	0.018
213	Q91ZW6	Trimethyllysine Hydroxylase, Epsilon	TMLHE	2.78	0.002
214	Q920A6	Serine Carboxypeptidase 1	SCPEP1	0.64	0.036
215	Q920L2	Succinate Dehydrogenase Complex Flavoprotein Subunit A	SDHA	1.22	0.005
216	Q923Z2	Tropomyosin 1, Alpha	Tpm1	0.82	0.002
217	Q9EPB1	Dipeptidyl Peptidase 7	DPP7	0.61	0.001
218	Q9ER34	Aconitase 2	ACO2	1.42	0.007
219	Q9JJ54	Heterogeneous Nuclear Ribonucleoprotein D	HNRNPD	0.84	0.037

220	Q9JJW3	Up-Regulated During Skeletal Muscle Growth Protein 5	Usmg5	1.11	0.007
221	Q9QYU4	Thiomorpholine-Carboxylate Dehydrogenase	Crym	1.81	0.012
222	Q9Z2L0	Voltage Dependent Anion Channel 1	VDAC1	1.18	0.006
223	Q9Z2Y0	Glycine N-Acyltransferase-Like Protein Keg1	Keg1	1.31	0.016

Table 3: Common proteins between aorta and kidney in diabetic vs. control.

Accession Number	Protein Names
A0A0G2JSK5	Itgb1 - Integrin beta
A0A0G2JTL5	Pc - Pyruvate carboxylase, mitochondrial
A0A0G2JTW9	Hbb-b1 - Hemoglobin, beta adult major chain
A0A0G2JVH4	Immt - MICOS complex subunit MIC60
A0A0G2K401	Pcca - Propionyl-CoA carboxylase alpha chain, mitochondrial
A0A0G2K531	Gpx3 - Glutathione peroxidase
D3Z8D7	Rps26 - ribosomal protein S26
A0A0G2K8Q8	Uqcr10 - Uncharacterized protein
A0A0G2KAM3	Pdhb - Pyruvate dehydrogenase E1 component subunit beta, mitochondrial
A0A0G2KB63	Phb2 - Prohibitin-2
B2RZ24	Sucla2 - succinyl-CoA ligase
F1LRJ9	Selenbp1 - Selenium-binding protein 1
G3V7I0	Prdx3 - thioredoxin-dependent peroxide reductase
Q5BJ93	Eno1 - Alpha-enolase
M0RAM5	Gpx1 - Glutathione peroxidase
M0RBF1	C3 - complement C3 precursor
P04639	Apoa1 - Apolipoprotein A-I
P04797	Gapdh - Glyceraldehyde-3-phosphate dehydrogenase
P10888	Cox4i1 - Cytochrome c oxidase subunit 4 isoform 1
P13803	Etfa - Electron transfer flavoprotein subunit alpha
P14046	Ali3 - alpha-1-inhibitor 3 precursor
P14408	Fh - fumarate hydratase, mitochondrial precursor
Q6IMX3	Acads - Short-chain specific acyl-CoA dehydrogenase
P17764	Acat1 - Acetyl-CoA acetyltransferase
P18163	Acs11 - Long-chain-fatty-acid--CoA ligase 1
P97601	Hspe1 - 10 kDa heat shock protein
P32551	Uqcrc2 - Cytochrome b-c1 complex subunit 2
P54313	Gnb2 - Guanine nucleotide-binding protein G(I)/G(S)/G(T) subunit beta-2
P67779	Phb - Prohibitin
P68255	Ywhaq - 14-3-3 protein theta
P69897	Tubb5 - Tubulin beta-5 chain
Q03336	Rgn - Regucalcin
Q5BJZ3	Nnt - NAD(P) transhydrogenase, mitochondrial
Q5M9H2	Acadv1 - very long-chain specific acyl-CoA dehydrogenase
Q5PQU1	Kng1 - T-kininogen 2 precursor
Q5XI78	Ogdh - 2-oxoglutarate dehydrogenase
Q641Y2	Ndufs2 - NADH dehydrogenase [ubiquinone] iron-sulfur protein 2

Q68FU3	Etfb - Electron transfer flavoprotein subunit beta
Q6P6R2	Dld - Dihydrolipoyl dehydrogenase
Q6P7P5	Bzw1 - Basic leucine zipper and W2 domain-containing protein 1
Q6P9V6	Psma5 - proteasome subunit alpha type-5
Q920L2	Sdha - Succinate dehydrogenase [ubiquinone] flavoprotein subunit
Q9ER34	Aco2 - Aconitate hydratase
Q9JJ54	Hnrpd - Heterogeneous nuclear ribonucleoprotein C

Table 4: Comparative list of proteins in the aorta of insulin-treated diabetic rats compared to diabetic rats.

	Accession Number	Names	Abbreviation	Fold Change	p value
1	A0A0F7RQJ6	D-Dopachrome Tautomerase	DDT	11.92	0.011
2	A0A0G2JSI0	Flavin Containing Monooxygenase 3	FMO3	0.07	0.002
3	Z4YNW7	Protein Phosphatase 2 Regulatory Subunit Bbeta	PPP2R2B	4.49	0.016
4	A0A0G2JSR0	Voltage Dependent Anion Channel 3	VDAC3	0.04	0.000
5	A0A0G2JSS9	Atlastin-3	Atl3	0.16	0.022
6	A0A0G2JSU4	N-Myc Downstream Regulated Gene 2, Isoform CRA_B	Ndrp2	0.60	0.022
7	A0A0G2JT00	Cuta Divalent Cation Tolerance Homolog	CUTA	2.58	0.046
8	G3V9Q3	Heterogeneous Nuclear Ribonucleoprotein H1	Hnrnp1	0.20	0.009
9	D3ZB30	Polypyrimidine Tract Binding Protein 1	PTBP1	0.17	0.038
10	A0A0G2JUC7	Dynactin Subunit 2	DCTN2	0.18	0.040
11	A0A0G2JV31	X-Prolyl Aminopeptidase 1	XPNPEP1	0.43	0.006
12	Q6P7S0	Pyruvate Kinase, Muscle	PKM	0.68	0.042
13	A0A0G2JVH4	Inner Membrane Mitochondrial Protein	IMMT	0.05	0.001
14	D3ZKE6	Sarcolemmal Membrane-Associated Protein	Slmap	0.07	0.010
15	A0A0G2JWC7	Fermitin Family Member 2	FERMT2	0.13	0.010
16	A0A0G2JXC3	Ribosomal Protein S21	RPS21	11.16	0.033
17	G3V9W6	Aldehyde Dehydrogenase 3 Family Member A2	ALDH3A2	5.27	0.010
18	A0A0G2JYD0	Dynein Heavy Chain 7, Axonemal	Dnah7	0.03	0.007
19	Q6IMY8	Heterogeneous Nuclear Ribonucleoprotein U	HNRNPU	0.38	0.032
20	A0A0G2JZM2	Sec23 Homolog A, CoAt Complex II Component	Sec23a	0.27	0.001
21	F1LMC7	Septin 7	SEPT7	0.20	0.040
22	A0A0G2K013	Actinin Alpha 4	ACTN4	0.10	0.001
23	F1LUV9	Neural Cell Adhesion Molecule 1	NCAM1	3.68	0.005
24	A0A0G2K0Q7	Myosin Light Chain Kinase	MYLK	0.09	0.017

25	A0A0G2K1C0	ARP3 Actin Related Protein 3 Homolog	ACTR3	0.19	0.015
26	F1LQQ1	Malic Enzyme 1	ME1	13.38	0.003
27	A0A0G2K506	Lactadherin	Mfge8	3.20	0.040
28	A0A0G2K531	Glutathione Peroxidase 3	GPX3	0.87	0.035
29	A0A0G2K757	Ribophorin II	RPN2	0.27	0.025
30	A0A0G2K7M2	RAD23 Homolog A, Nucleotide Excision Repair Protein	Rad23a	8.13	0.014
31	R9PXU6	Vinculin	VCL	0.31	0.007
32	Q5U1Y3	Filamin Binding LIM Protein 1	FBLIM1	0.13	0.005
33	Q5PQM7	LIM Zinc Finger Domain Containing 2	LIMS2	0.16	0.018
34	A0A0G2KB63	Prohibitin 2	PHB2	0.12	0.036
35	A0A0H2UHM3	Haptoglobin	HP	1.48	0.044
36	A0A0H2UHM5	Protein Disulfide Isomerase Family A Member 3	PDIA3	0.64	0.023
37	A0A0H2UHQ8	40S Ribosomal Protein S17	Rps17	0.45	0.046
38	A0A1B0GWT7	Late Endosomal/Lysosomal Adaptor, MAPK And MTOR Activator 2	Lamtor2	2.88	0.002
39	A0JPJ7	Obg-Like Atpase 1	Ola1	1.45	0.046
40	A1L1M0	Protein Kinase Camp-Activated Catalytic Subunit Alpha	PRKACA	0.53	0.044
41	A2VD12	Pre-B-Cell Leukemia Transcription Factor-Interacting Protein 1	Pbxip1	0.81	0.046
42	D4ACV3	Histone H2A	Hist2h2ac	0.20	0.020
43	F1LXV3	Serine/Threonine Kinase 26	STK26	5.35	0.000
44	B2GUZ5	F-Actin-Capping Protein Subunit Alpha-1	Capza1	0.24	0.010
45	B2GV06	3-Oxoacid CoA-Transferase 1	OXCT1	0.16	0.029
46	B2RYK3	Sepiapterin Reductase (7,8-Dihydrobiopterin:NADP+ Oxidoreductase)	SPR	9.85	0.020
47	B3DM95	Parathymosin	Ptms	19.12	0.043
48	B5DF65	Biliverdin Reductase B	BLVRB	2.43	0.039
49	C0KUC5	LIM Zinc Finger Domain Containing 1	LIMS1	0.30	0.039
50	D3Z8I7	Glutathione S-Transferase, Theta 3	Gstt3	5.17	0.037

51	D3ZCA0	Proline Synthase Co-Transcribed Bacterial Homolog Protein	Prosc	0.27	0.038
52	D3ZF13	NADH:Ubiquinone Oxidoreductase Subunit AB1	NDUFAB1	5.94	0.018
53	D3ZIC4	Protein Phosphatase 1, Regulatory (Inhibitor) Subunit 12B	Ppp1r12b	0.17	0.018
54	D3ZQ25	Fibulin 1	FBLN1	0.21	0.003
55	D3ZS58	NADH:Ubiquinone Oxidoreductase Subunit A2	NDUFA2	6.23	0.047
56	D4A5L9	Protein LOC679794	LOC690675	3.82	0.006
57	D4ADS6	Integrator Complex Subunit 7	Ints7	2.70	0.045
58	F1LN42	Tensin 1	TNS1	0.08	0.008
59	F1LN88	Aldehyde Dehydrogenase 2 Family (Mitochondrial)	ALDH2	0.04	0.000
60	F1LRT9	Dynein Cytoplasmic 1 Heavy Chain 1	DYNC1H1	0.10	0.042
61	F1LRV4	Heat Shock Protein Family A (Hsp70) Member 4	HSPA4	0.07	0.007
62	F1LTF8	Laminin Subunit Alpha 4	LAMA4	0.22	0.023
63	F1M779	Clathrin Heavy Chain	CLTC	0.06	0.032
64	F1M866	Sorbin And SH3 Domain Containing 1	SORBS1	0.30	0.003
65	F1M978	Inositol Monophosphatase 1	IMPA1	0.08	0.001
66	Q6P7A4	Prosaposin	PSAP	1.69	0.015
67	Q8CHN5	Epididymal Secretory Protein E1 Precursor	Npc2	11.08	0.000
68	G3V624	Coronin-1C	Coro1c	0.06	0.003
69	Q5EBC3	Methylenetetrahydrofolate Dehydrogenase, Cyclohydrolase And Formyltetrahydrofolate Synthetase 1	MTHFD1	0.21	0.024
70	G3V6Y6	Glycogen Phosphorylase B	PYGB	0.13	0.001
71	G3V7C6	Tubulin Beta 4B Class Ivb	TUBB4B	0.50	0.014
72	G3V7F3	WNT1 Inducible Signaling Pathway Protein 2	WISP2	17.46	0.043
73	G3V7Q7	IQ Motif Containing GTPase Activating Protein 1	IQGAP1	0.05	0.012
74	G3V7U4	Lamin B1	LMNB1	0.29	0.005
75	G3V818	Parvin Alpha	PARVA	0.11	0.031

76	G3V852	Talin 1	TLN1	0.15	0.024
77	G3V8A5	Maternal Embryonic Message 3	Vps35	0.11	0.047
78	G3V8C3	Vimentin	VIM	0.25	0.019
79	G3V8L3	Lamin A/C	LMNA	0.04	0.038
80	G3V940	Coronin 1B	CORO1B	0.23	0.033
81	G3V9E3	Caldesmon 1	Cald1	0.04	0.031
82	M0R557	Cardiomyopathy Associated 5	Cmya5	15.54	0.005
83	O35814	Stress Induced Phosphoprotein 1	STIP1	0.39	0.019
84	Q6IN22	Cathepsin B	CTSB	5.28	0.021
85	P01015	Angiotensinogen	AGT	5.89	0.025
86	P02651	Apolipoprotein A4	APOA4	0.07	0.039
87	P02767	Transthyretin	TTR	3.26	0.032
88	P04182	Ornithine Aminotransferase	OAT	0.12	0.029
89	P04633	Uncoupling Protein 1	UCP1	17.28	0.036
90	P04638	Apolipoprotein A2	APOA2	2.34	0.036
91	P04785	Prolyl 4-Hydroxylase Subunit Beta	P4HB	0.59	0.030
92	P05197	Eukaryotic Translation Elongation Factor 2	EEF2	0.27	0.036
93	P05545	Serine (Or Cysteine) Proteinase Inhibitor, Clade A, Member 3C	Serpina3c /Serpina3m	1.67	0.015
94	P05708	Hexokinase 1	HK1	0.40	0.036
95	Q5RK05	Matrix Gla Protein	MGP	5.25	0.011
96	Q6LCA5	Protein Kinase Camp-Dependent Type I Regulatory Subunit Alpha	PRKAR1A	0.51	0.047
97	P0DN35	NADH Dehydrogenase [Ubiquinone] 1 Beta Subcomplex Subunit 1	Ndufb1	3.98	0.000
98	P11507	Atpase Sarcoplasmic/Endoplasmic Reticulum Ca ²⁺ Transporting 2	ATP2A2	0.07	0.000
99	P11517	Hemoglobin Subunit Beta-	LOC689064	5.18	0.035
100	P12007	Isovaleryl-CoA Dehydrogenase	IVD	4.75	0.030
101	P14046	Murinoglobulin 1	Mug1 (includes others)	1.96	0.002

102	P14668	Annexin A5	ANXA5	1.41	0.035
103	P16636	Lysyl Oxidase	LOX	9.07	0.034
104	Q6P9V5	Proteasome Subunit Alpha 2	PSMA2	0.68	0.017
105	P20070	Cytochrome B5 Reductase 3	Cyb5r3	0.21	0.028
106	Q4QRB8	Argininosuccinate Lyase	ASL	0.13	0.012
107	P24329	Thiosulfate Sulfurtransferase	TST	0.20	0.032
108	P25093	Fumarylacetoacetate Hydrolase	FAH	0.18	0.007
109	P27867	Sorbitol Dehydrogenase	SORD	0.44	0.044
110	P28480	T-Complex 1	TCP1	0.08	0.011
111	P29266	3-Hydroxyisobutyrate Dehydrogenase	HIBADH	0.19	0.002
112	Q6P2A5	Adenylate Kinase 3	AK3	0.44	0.049
113	P31430	Dipeptidase 1 (Renal)	DPEP1	9.23	0.031
114	P32198	Carnitine Palmitoyltransferase 1A	CPT1A	0.18	0.047
115	P39069	Adenylate Kinase 1	AK1	1.55	0.001
116	P46462	Valosin Containing Protein	VCP	0.16	0.007
117	P47820	Angiotensin I Converting Enzyme	ACE	2.02	0.007
118	P48508	Glutamate-Cysteine Ligase Modifier Subunit	GCLM	7.90	0.044
119	P50398	GDP Dissociation Inhibitor 1	GDI1	0.66	0.048
120	P54313	G Protein Subunit Beta 2	GNB2	0.52	0.019
121	P62260	Tyrosine 3-Monooxygenase/Tryptophan 5-Monooxygenase Activation Protein Epsilon	YWHAE	0.44	0.028
122	P69897	Tubulin Beta Class I	TUBB	0.49	0.001
123	P82995	Heat Shock Protein 90 Alpha Family Class A Member 1	HSP90AA1	0.06	0.013
124	P85515	Alpha-Contractin	Actr1a	0.28	0.000
125	P85973	Purine Nucleoside Phosphorylase	PNP	0.42	0.012
126	Q06647	ATP Synthase, H+ Transporting, Mitochondrial F1 Complex, O Subunit	ATP5O	0.21	0.019
127	Q08163	Adenylate Cyclase Associated Protein 1	CAP1	0.15	0.024
128	Q4V8H5	Aspartyl Aminopeptidase	Dnpep	0.09	0.011

129	Q4V8H8	EH Domain-Containing Protein 2	Ehd2	0.15	0.003
130	Q5BJZ3	Nicotinamide Nucleotide Transhydrogenase	NNT	0.13	0.004
131	Q5FVG5	Tropomyosin 2, Beta	Tpm2	0.06	0.028
132	Q5I0P2	Glycine Cleavage System Protein H	GCSH	4.28	0.042
133	Q5RJR8	Leucine-Rich Repeat-Containing Protein 59	Lrrc59	0.45	0.026
134	Q5UAJ6	Cytochrome C Oxidase Subunit II	MT-CO2	4.38	0.003
135	Q5XI21	Target of Myb Protein 1	Tom1	5.51	0.001
136	Q5XI34	Protein Phosphatase 2 Scaffold Subunit Alpha	PPP2R1A	0.56	0.021
137	Q5XIH1	Asporin Precursor	Aspn	0.48	0.012
138	Q63413	Dexd-Box Helicase 39B	DDX39B	0.09	0.014
139	Q63570	Proteasome 26S Subunit, Atpase 4	PSMC4	1.54	0.030
140	Q63610	Tropomyosin 3	Tpm3	0.05	0.001
141	Q64240	Alpha-1-Microglobulin/Bikunin Precursor	AMBP	0.44	0.019
142	Q68FR9	Eukaryotic Translation Elongation Factor 1 Delta	EEF1D	0.09	0.006
143	Q68FT3	Pyridine Nucleotide-Disulfide Oxidoreductase Domain-Containing Protein 2	Pyroxd2	2.53	0.034
144	Q6AYQ4	Transmembrane Protein 109	Tmem109	0.15	0.031
145	Q6AYT0	Quinone Oxidoreductase	Cryz	1.73	0.012
146	Q6GMN8	Actinin Alpha 1	ACTN1	0.08	0.000
147	Q6P502	Chaperonin Containing TCP1 Subunit 3	CCT3	0.19	0.009
148	Q6P725	Desmin	DES	0.09	0.042
149	Q6P7A7	Dolichyl-Diphosphooligosaccharide--Protein Glycosyltransferase Subunit 1 Precursor	Rpn1	0.09	0.022
150	Q6P7P5	Basic Leucine Zipper and W2 Domain-Containing Protein 1	Bzw1	6.22	0.002
151	Q6P9V9	Tubulin Alpha-1A Chain	Tuba1b	0.46	0.021
152	Q794E4	Heterogeneous Nuclear Ribonucleoprotein F	HNRNPF	0.55	0.034

153	Q811X6	Crystallin Lambda 1	CRYL1	0.32	0.017
154	Q91Y81	Septin 2	SEPT2	0.16	0.026
155	Q920A6	Serine Carboxypeptidase 1	SCPEP1	2.14	0.006
156	Q923Z2	Tropomyosin 1, Alpha	Tpm1	0.23	0.021
157	Q99PD6	Transforming Growth Factor Beta 1 Induced Transcript 1	TGFB1I1	0.09	0.011
158	Q9ESN0	Family with Sequence Similarity 129 Member A	FAM129A	0.07	0.045
159	Q9JJ54	Heterogeneous Nuclear Ribonucleoprotein D	HNRNPD	0.19	0.009
160	Q9QZQ5	Nephroblastoma Overexpressed	NOV	3.40	0.033
161	Q9Z1H9	Protein Kinase C Delta-Binding Protein	Prkcdbp	0.09	0.043
162	Q9Z1X1	Extended Synaptotagmin-1	Esyt1	0.08	0.003
163	Q9Z2G3	ATP Citrate Lyase	ACLY	10.51	0.017

Table 5: Comparative list of proteins in the kidney of the insulin-treated diabetic rats compared to diabetic rats.

	Accession Number	Names	Abbreviation	Fold Change	p value
1	A0A096MK30	Moesin	MSN	1.21	0.004
2	Q8SEZ2	Cytochrome C Oxidase Subunit 3	Mt-cox3	0.94	0.037
3	A0A0A0MXW3	H2A Histone Family Member Z	H2AFZ	1.30	0.049
4	Q95938	Cytochrome C Oxidase Subunit 1	Mt-co1	0.85	0.026
5	Q9Z1J7	Solute Carrier Family 1 Member 5	SLC1A5	2.45	0.006
6	A0A0G2JSK5	Integrin Subunit Beta 1	ITGB1	1.26	0.047
7	A0A0G2JSS8	Peroxiredoxin 5	PRDX5	0.81	0.023
8	A0A0G2JSV6	Hemoglobin, Alpha 1	Hba1/Hba2	2.48	0.039
9	A0A0G2JTH4	CD47 Molecule	CD47	1.30	0.020
10	A0A0G2JTL5	Pyruvate Carboxylase	PC	0.57	0.005
11	Q66WT9	Phosphatidylinositol Binding Clathrin Assembly Protein	PICALM	2.11	0.001
12	A0A0G2JTW9	Hemoglobin Subunit Beta	HBB	3.00	0.023
13	D4A6E3	Murinoglobulin-1 Precursor	Mug1	3.05	0.018
14	F1LPD0	Collagen Type XV Alpha 1 Chain	Col15a1	9.11	0.017
15	D4A1H0	ATPase H ⁺ Transporting V0 Subunit A4	ATP6V0A4	1.23	0.008
16	A0A0G2JWC7	Fermitin Family Member 2	FERMT2	1.20	0.039
17	M0R4L7	Histone H2B	Hist1h2bl	1.39	0.020
18	D4A554	Eukaryotic Translation Initiation Factor 4 Gamma 3	EIF4G3	4.73	0.039
19	A0A0G2K4D0	Ankyrin 3	ANK3	1.14	0.036
20	A0A0G2K0Q8	Sushi Domain-Containing 2	Susd2	0.47	0.001
21	A0A0G2K277	Enoyl-Coenzyme A Delta Isomerase 3	Eci3	0.72	0.000
22	B0BMT6	RCG43995, Isoform CRA_B	Tpmt	1.22	0.032
23	A0A0G2K654	Histone Cluster 1 H1 Family Member C	Hist1h1c	1.50	0.005
24	A0A0G2K6H2	Glutathione S-Transferase Zeta 1	GSTZ1	0.70	0.014
25	D3ZCR3	High Mobility Group Box 1	Gm21596 /Hmgb1	1.57	0.049
26	A0A0G2K737	Thioredoxin Like 1	TXNL1	1.24	0.012
27	D3Z8D7	40S Ribosomal Protein S26	LOC100361854	1.23	0.030

28	FILS02	Nucleoporin 155	NUP155	2.75	0.045
29	A0A0G2K8Q8	Ubiquinol-Cytochrome C Reductase, Complex III Subunit X	UQCR10	0.88	0.024
30	Q80YG1	Phosphoserine Aminotransferase 1	PSAT1	1.52	0.013
31	G3V7K3	Ceruloplasmin	CP	4.30	0.019
32	A0A0G2K9W7	LDL Receptor Related Protein 2	LRP2	2.84	0.006
33	Q7TNX2	Liver Regeneration-Related Protein LRRG01	Pxmp2	0.56	0.010
34	A0A0H2UHE4	Regenerating Family Member 3 Alpha	REG3A	0.13	0.023
35	A0A0H2UHM3	Haptoglobin	HP	1.77	0.010
36	B1WBN9	Pyruvate Kinase, Liver, And RBC	PKLR	1.65	0.029
37	A0JPM9	Eukaryotic Translation Initiation Factor 3 Subunit J	EIF3J	0.30	0.011
38	A2VCW9	Amino adipate-Semialdehyde Synthase	AASS	0.36	0.001
39	A9UMW1	Glutathione S-Transferase, Alpha 4	Gsta4	0.60	0.019
40	B0BMW2	Hydroxysteroid 17-Beta Dehydrogenase 10	HSD17B10	0.70	0.020
41	B0BNG1	Proline Dehydrogenase 2	PRODH2	0.78	0.028
42	B0BNN3	Carbonic Anhydrase 1	CA1	4.95	0.047
43	B1WC26	N-Acetylneuraminase Synthase	NANS	1.15	0.027
44	B2GVB1	S100 Calcium Binding Protein A6	S100A6	0.76	0.029
45	B2RYR8	Ribosomal Protein S8	RPS8	1.33	0.017
46	B2RYW9	Fumarylacetoacetate Hydrolase Domain-Containing Protein 2	Fahd2	0.55	0.008
47	B4F768	Aldehyde Dehydrogenase 4 Family Member A1	ALDH4A1	0.54	0.018
48	B5DF36	Placenta-Specific 8	Plac8	1.56	0.019
49	B5DFA0	Vil1 Protein	Vil1	1.41	0.009
50	B6DYQ0	Glutathione S-Transferase Kappa 1	GSTK1	0.58	0.047
51	B6DYQ7	Glutathione S-Transferase Pi 1	GSTP1	1.38	0.030
52	D3Z8F1	Villin-Like	Vill	1.42	0.048
53	D3ZD09	Cytochrome C Oxidase Subunit 6B1	COX6B1	0.79	0.046
54	F1LZC5	Protein Ndufa13	Ndufa13	0.77	0.008

55	O35802	Inter-Alpha-Trypsin Inhibitor Heavy Chain Family Member 4	ITIH4	5.05	0.026
56	D3ZFY6	Lactamase, Beta	Lactb	0.79	0.043
57	D3ZFY8	Ubiquitin-Conjugating Enzyme E2 Variant 1-Like	LOC100912618	1.27	0.043
58	D3ZG43	NADH:Ubiquinone Oxidoreductase Core Subunit S3	NDUFS3	0.77	0.017
59	D3ZT90	Glutaryl-CoA Dehydrogenase	GCDH	0.63	0.003
60	D3ZTX4	Aldehyde Dehydrogenase 8 Family Member A1	ALDH8A1	3.17	0.000
61	D3ZXY4	Aldehyde Dehydrogenase 8 Family, Member A1	Aldh8a1	3.07	0.000
62	D3ZZN3	Acyl-CoA Synthetase Short-Chain Family Member 1	ACSS1	0.62	0.005
63	D4A269	Uncharacterized Protein	N/A	1.13	0.017
64	D4A5I9	Myosin VI	MYO6	1.18	0.018
65	D4A5L9	Protein LOC679794	LOC679794	1.67	0.004
66	F1LTW8	Similar To Ribosomal Protein S23	RGD1563705	1.21	0.042
67	F1LMF4	Protocadherin Fat 3	Fat3	2.46	0.031
68	Q63654	Ubiquitin B	Ubb	1.10	0.018
69	F1LMP9	DAB2, Clathrin Adaptor Protein	DAB2	1.52	0.014
70	F1LMV6	Desmoplakin	DSP	1.31	0.024
71	F1LN88	Aldehyde Dehydrogenase 2 Family (Mitochondrial)	ALDH2	0.82	0.030
72	F1LP30	Methylcrotonoyl-CoA Carboxylase 1	MCCC1	0.72	0.027
73	F1LPD6	Acetyl-CoA Acyltransferase 1	ACAA1	0.64	0.006
74	F1LRJ9	Selenium-Binding Protein 1	Selenbp1	0.64	0.016
75	F1LRY5	Sarcosine Dehydrogenase	SARDH	0.63	0.028
76	F1LWL8	Solute Carrier Family 5 Member 12	Slc5a12	0.79	0.025
77	F1LZW6	Solute Carrier Family 25 Member 13	Slc25a13	1.17	0.038
78	F1M949	Cytoskeleton Associated Protein 5	CKAP5	0.21	0.009
79	F1MAA7	Laminin Subunit Gamma 1	LAMC1	2.53	0.035
80	Q5BKC4	Complement C9	C9	8.19	0.002
81	G3V6D3	ATP Synthase, H+ Transporting, Mitochondrial F1 Complex, Beta Polypeptide	ATP5B	0.86	0.008

82	G3V741	Solute Carrier Family 25 Member 3	SLC25A3	0.89	0.044
83	G3V7I0	Peroxiredoxin 3	PRDX3	0.76	0.028
84	G3V7J0	Aldehyde Dehydrogenase 6 Family Member A1	ALDH6A1	0.88	0.043
85	G3V7Q7	IQ Motif Containing GTPase Activating Protein 1	IQGAP1	1.27	0.007
86	G3V852	Talin 1	TLN1	1.40	0.017
87	G3V8C4	Chloride Intracellular Channel 4	CLIC4	1.30	0.034
88	G3V960	Guanidinoacetate N-Methyltransferase	GAMT	1.89	0.017
89	G3V9V9	Cysteine And Glycine Rich Protein 2	CSRP2	1.88	0.015
90	M0R3V4	Myeloid-Derived Growth Factor	Mydgf	3.94	0.038
91	Q5BJ93	Enolase 1	ENO1	1.21	0.003
92	M0RAM5	Glutathione Peroxidase 1	GPX1	0.68	0.012
93	M0RBF1	Complement C3	C3	2.11	0.026
94	M0RDH0	Glycine N-Methyltransferase	Gnmt	0.77	0.008
95	O35078	D-Amino Acid Oxidase	DAO	0.78	0.015
96	O35509	RAB11B, Member RAS Oncogene Family	RAB11B	1.17	0.005
97	P00173	Cytochrome B5 Type A	CYB5A	0.75	0.017
98	P00507	Glutamic-Oxaloacetic Transaminase 2	GOT2	0.69	0.007
99	P02761	Alpha-2u-Globulin (L Type) Precursor	Mup5	2.63	0.002
100	P02770	Albumin	ALB	1.63	0.001
101	Q45QN0	G Protein Subunit Alpha I2	GNAI2	1.61	0.012
102	P05065	Aldolase, Fructose-Bisphosphate A	ALDOA	1.18	0.028
103	P05545	Serine (Or Cysteine) Proteinase Inhibitor, Clade A, Member 3C	Serpina3c /Serpina3m	2.39	0.018
104	P07171	Calbindin 1	CALB1	0.48	0.010
105	P07314	Gamma-Glutamyltransferase 1	GGT1	1.62	0.018
106	P07687	Epoxide Hydrolase 1	EPHX1	0.39	0.004
107	P07895	Superoxide Dismutase 2	SOD2	0.82	0.001
108	P09034	Argininosuccinate Synthase 1	ASS1	0.77	0.024
109	P10860	Glutamate Dehydrogenase 1	GLUD1	0.78	0.005
110	P10888	Cytochrome C Oxidase Subunit 4I1	COX4I1	0.75	0.032

111	P12346	Transferrin	TF	1.61	0.003
112	P13084	Nucleophosmin	NPM1	1.17	0.033
113	P13803	Electron Transfer Flavoprotein Alpha Subunit	ETF A	0.81	0.019
114	P14046	Murinoglobulin 1	Mug1 (includes others)	4.72	0.000
115	P14173	DOPA Decarboxylase	DDC	0.66	0.036
116	P14480	Fibrinogen Beta Chain	FGB	2.50	0.039
117	P14604	Enoyl-CoA Hydratase, Short Chain 1	ECHS1	0.79	0.040
118	P16617	Phosphoglycerate Kinase 1	PGK1	0.88	0.030
119	P17764	Acetyl-CoA Acetyltransferase 1	ACAT1	0.84	0.043
120	Q66HM2	Adaptor Related Protein Complex 2 Alpha 2 Subunit	AP2A2	1.19	0.036
121	P19112	Fructose-Bisphosphatase 1	FBP1	1.96	0.001
122	P20059	Hemopexin	HPX	1.25	0.034
123	Q04970	Neuroblastoma RAS Viral Oncogene Homolog	NRAS	2.76	0.021
124	P21913	Succinate Dehydrogenase Complex Iron Sulfur Subunit B	SDHB	0.80	0.026
125	Q68G41	Enoyl-CoA Delta Isomerase 1	ECI1	0.62	0.008
126	P27605	Hypoxanthine Phosphoribosyltransferase 1	HPRT1	0.65	0.015
127	Q6P2A5	Adenylate Kinase 3	AK3	0.70	0.026
128	P32755	4-Hydroxyphenylpyruvate Dioxygenase	HPD	0.59	0.001
129	P35213	Tyrosine 3-Monooxygenase/Tryptophan 5-Monooxygenase Activation Protein Beta	YWHAB	0.88	0.025
130	P35467	S100 Calcium Binding Protein A1	S100A1	0.78	0.009
131	P36511	UDP Glucuronosyltransferase Family 2 Member B7	UGT2B7	0.60	0.044
132	P38918	Aldo-Keto Reductase Family 7 Member A3	AKR7A3	1.41	0.019
133	P42123	Lactate Dehydrogenase B	LDHB	0.73	0.019
134	P43428	Glucose-6-Phosphatase Catalytic Subunit	G6PC	0.73	0.033
135	P50137	Transketolase	TKT	0.88	0.031
136	P50554	4-Aminobutyrate Aminotransferase	ABAT	0.73	0.036

137	P56574	Isocitrate Dehydrogenase (NADP(+)) 2, Mitochondrial	IDH2	0.90	0.031
138	P61459	Pterin-4 Alpha-Carbinolamine Dehydratase 1	PCBD1	0.78	0.008
139	P62076	Mitochondrial Import Inner Membrane Translocase Subunit Tim13	Timm13	0.81	0.048
140	P62749	Hippocalcin-Like Protein 1	Hpcal1	1.29	0.039
141	P62804	Histone H4 Osteogenic Growth Peptide	Hist2h4	1.40	0.007
142	P63018	Heat Shock Protein Family A (Hsp70) Member 8	HSPA8	1.10	0.023
143	P63259	Actin Gamma 1	ACTG1	1.09	0.029
144	P68035	Actin, Alpha, Cardiac Muscle 1	ACTC1	1.45	0.038
145	P68182	Protein Kinase Camp-Activated Catalytic Subunit Beta	PRKACB	2.71	0.042
146	P68511	Tyrosine 3-Monooxygenase/Tryptophan 5-Monooxygenase Activation Protein Eta	YWHAH	1.20	0.024
147	P69897	Tubulin Beta Class I	TUBB	1.28	0.007
148	P70473	Alpha-Methylacyl-CoA Racemase	AMACR	0.43	0.000
149	Q66HP8	Solute Carrier Family 25 Member 20	SLC25A20	0.77	0.007
150	Q03336	Regucalcin	RGN	2.16	0.016
151	Q3B8N9	Biphenyl Hydrolase-Like	Bphl	0.77	0.008
152	Q3T1K5	Capping Actin Protein Of Muscle Z-Line Alpha Subunit 2	CAPZA2	1.43	0.033
153	Q4QQW3	Alcohol Dehydrogenase, Iron Containing 1	ADHFE1	0.29	0.002
154	Q4V8F6	Poly(Rc)-Binding Protein 2	Pcbp2	1.75	0.042
155	Q4V8H5	Aspartyl Aminopeptidase	Dnpep	0.69	0.018
156	Q562C4	Methyltransferase-Like Protein 7B	Mettl7b	0.75	0.022
157	Q5BJT9	Creatine Kinase, Mitochondrial 1B	CKMT1A /CKMT1B	0.67	0.018
158	Q5BJZ3	Nicotinamide Nucleotide Transhydrogenase	NNT	0.66	0.025
159	Q5DT04	UDP Glucuronosyltransferase Family 1 Member A1	UGT1A1	1.62	0.020

160	Q5I0K3	Citrate Lyase Subunit Beta-Like Protein	Clybl	3.62	0.009
161	Q5RJN0	NADH:Ubiquinone Oxidoreductase Core Subunit S7	NDUFS7	0.65	0.042
162	Q5RKI0	WD Repeat-Containing Protein 1	Wdr1	1.26	0.025
163	Q5U3Z7	Serine Hydroxymethyltransferase 2	SHMT2	0.78	0.007
164	Q5UAJ5	ATP Synthase F0 Subunit 8 (Mitochondrion)	ATP8	0.79	0.044
165	Q5XI78	Oxoglutarate Dehydrogenase	OGDH	0.78	0.021
166	Q5XI85	Aminomethyltransferase	AMT	0.60	0.005
167	Q5XIF6	Tubulin Alpha 4a	TUBA4A	1.37	0.026
168	Q63010	Liver Carboxylesterase B-1 Precursor	Ces1f	0.73	0.009
169	Q63025	Alpha-2u-Globulin (L Type) Precursor	Mup5	245.82	0.040
170	Q63342	Dimethylglycine Dehydrogenase	DMGDH	0.67	0.001
171	Q63413	Spliceosome RNA Helicase Ddx39b	Ddx39b	1.32	0.033
172	Q63910	Hemoglobin Subunit Alpha 2	HBA1/HBA2	5.54	0.033
173	Q64057	Aldehyde Dehydrogenase 7 Family Member A1	ALDH7A1	0.81	0.026
174	Q641Y2	NADH:Ubiquinone Oxidoreductase Core Subunit S2	NDUFS2	0.75	0.016
175	Q64319	Solute Carrier Family 3 Member 1	SLC3A1	1.72	0.050
176	Q66H12	Alpha-N-Acetylgalactosaminidase	Naga	0.71	0.011
177	Q66HF1	NADH:Ubiquinone Oxidoreductase Core Subunit S1	NDUFS1	0.79	0.015
178	Q66HF3	Electron Transfer Flavoprotein-Ubiquinone Oxidoreductase	Etfdh	0.74	0.011
179	Q68FR9	Eukaryotic Translation Elongation Factor 1 Delta	EEF1D	1.42	0.028
180	Q68G31	Phenazine Biosynthesis-Like Domain-Containing Protein	Pbld1	0.76	0.013
181	Q6AYS2	Sideroflexin 1	SFXN1	0.71	0.017
182	Q6I7R1	Dehydrogenase/Reductase (SDR Family) Member 7	Dhrs7l1	1.90	0.028

183	Q6JE36	Protein NDRG1	Ndrp1	0.76	0.015
184	Q9WVJ6	Transglutaminase 2	TGM2	1.63	0.026
185	Q6P9V9	Hydroxysteroid 11-Beta Dehydrogenase 1	HSD11B1	1.21	0.034
186	Q812B0	Succinate Dehydrogenase [Ubiquinone] Cytochrome B Small Subunit	Lrrp1	0.78	0.031
187	Q6TUH9	Corticosteroid 11-Beta-Dehydrogenase Isozyme 1	Hsd11b1	1.55	0.012
188	Q6ZMA0	Olfactory Receptor	Olr1868	0.58	0.021
189	Q7TP52	Carboxymethylenebutenolidase Homolog	Cmb1	0.79	0.031
190	Q811X6	Crystallin Lambda 1	CRYL1	0.70	0.011
191	Q9JJI4	Alpha-2u-Globulin (L Type) Precursor	Mup5	4.34	0.002
192	Q8VI04	Asparaginase Like 1	ASRGL1	1.35	0.043
193	Q91ZW6	Trimethyllysine Hydroxylase, Epsilon	TMLHE	0.35	0.029
194	Q920A6	Serine Carboxypeptidase 1	SCPEP1	1.41	0.000
195	Q920L2	Succinate Dehydrogenase Complex Flavoprotein Subunit A	SDHA	0.78	0.038
196	Q923Z2	Tropomyosin 1, Alpha	Tpm1	1.25	0.013
197	Q9EPB1	Dipeptidyl Peptidase 2	Dpp7	1.37	0.027
198	Q9EQS0	Transaldolase 1	TALDO1	1.40	0.006
199	Q9ER34	Aconitase 2	ACO2	0.72	0.004
200	Q9JJ54	Heterogeneous Nuclear Ribonucleoprotein D	HNRNPD	1.28	0.007
201	Q9QX71	Napsin A Aspartic Peptidase Precursor	Napsa	0.86	0.043
202	Q9QYU4	Crystallin Mu	CRYM	0.51	0.016
203	Q9Z2L0	Voltage Dependent Anion Channel 1	VDAC1	0.87	0.015
204	Q9Z2M4	Peroxisomal 2,4-Dienoyl-CoA Reductase	Decr2	0.60	0.008

B. Role of Sphingosine Kinase 1 in Bradykinin Regulation of Fibrotic Markers in Vascular Smooth Muscle Cells

The results of the first study design pointed to the upregulation of KNG1 protein, the precursor and the rate limiting step in the generation of bradykinin in denuded aorta and the kidney cortices. In addition, we observed the induction of the expression of different fibrotic proteins, anti-inflammatory proteins, and adipokines. Taken together, these findings led us to investigate the role of BK on the expression of fibrotic proteins in primary vascular smooth muscle cells (VSMC) extracted from rats' aorta. Moreover, the involvement of sphingolipid signaling molecules in transducing the signal of BK in VSMC was examined.

1. Abstract:

Atherosclerosis is the leading cause of death in diabetes and is also a major source of morbidity and mortality, characterized by endothelial dysfunction, inflammation and vascular smooth muscle cell (VSMC) proliferation and matrix deposition. The cellular and molecular mechanisms responsible for enhanced atherosclerosis are not well understood. In the current study, we aim to understand the cellular mechanisms through which activation of B₂ kinin receptors (Bdkrb2) contribute to factors that modulate vascular remodeling. VSMC treated with bradykinin (BK) resulted in a significant increase in the mRNA and phosphorylation levels of sphingosine kinase 1 (SphK1), and in the mRNA and protein levels of connective tissue growth factor (Ctgf) and fibronectin (Fn1), and these effects were mediated via ERK1/2 activation. VSMC stimulated with BK in the presence of SphK1-inhibitors and/or siRNA targeted against SphK1 significantly inhibited the BK-induced increase in Ctgf and Fn1 protein levels. Furthermore, the basal mRNA levels of Ctgf and Fn1 in VSMC of SphK1 knockout mice were significantly decreased compared to SphK1 wild-type mice. Treatment of HEK293T cells transfected with GFP-tagged sphingosine -1-phosphate receptor 1 (S1pr1) with BK resulted in the internalization of S1pr1 into the cytoplasm and this effect was inhibited with Bdkrb2 antagonist HOE 140. Moreover, the increase in Ctgf and Fn1 protein levels in response to BK was significantly attenuated in the presence of S1pr1 receptor antagonist, thus implicating a role for S1P in modulating the BK response in VSMC. These findings provide new facets of BK signaling pathways that could be linked to the pathogenesis of vascular injury and ascertains potential novel targets for therapy.

Keywords: Sphingosine-1-phosphate, connective tissue growth factor, fibronectin, sphingosine kinase 1 knockout mice, bradykinin 2 receptors.

2. Introduction:

Atherosclerosis continues to pose a global health burden, being one of the leading causes of mortality worldwide, often due to its associated increased risk of strokes and/or myocardial infarctions [383,384]. Atherosclerosis is the result of the build-up of plaque along the inner walls of arteries leading to their narrowing and stiffening [385]. The characteristic vessel stiffening seen in atherosclerosis is primarily the result of lipid accumulation, overproduction of extracellular matrix (ECM) components, particularly fibrotic proteins, and foam cell infiltration of the subendothelial region, leading altogether to a chronic inflammatory response [386,387].

Recently, there has been increasing interest in the understanding of the inflammatory process underlying atherosclerosis, with a particular focus on delineating the signals involved in promoting vessel wall stiffness and foam cell entrapment within the sub-endothelial matrix in the setting of atherosclerosis [344,386]. Moreover, vessel tone and blood flow through the arteries are controlled by the degree of contraction or relaxation of the vascular smooth muscle cells (VSMC) lying within the vessel wall. Therefore, any hyperplastic or hypertrophic changes in VSMC migration, proliferation, or extracellular matrix deposition would affect their tone and consequently alter the blood flow through the vessels. Additionally, VSMC hypertrophy and/or hyperplasia was shown in previous studies to promote atherosclerotic plaque formation [388,389].

Investigating the pro-atherosclerotic roles of various sphingolipids in atherosclerosis is becoming increasingly recognized [213,214]. Several studies showing certain sphingolipids to be elevated in the setting of atherosclerosis, particularly sphingomyelin (SM), ceramide and sphingosine-1-phosphate (S1P) [222]. S1P is

recognized to possess pro-inflammatory, proliferative, invasive and migratory effects [227,228]. S1P is produced intracellularly by two closely related isoforms of sphingosine kinase (SphK): SphK1 and SphK2. The function of SphK1 in different systems has been extensively studied and is consequently better understood than that of SphK2 [390]. For instance, it is well known that many growth factors and hormones activate SphK1 in a biphasic manner: the first phase being rapid and resulting in its translocation to the plasma membrane, followed by the second phase occurring only after a prolonged stimulus leading to transcriptional upregulation of the SphK1 gene [391,392]. After its production, S1P can then bind in a paracrine or autocrine fashion to any of five available G-protein coupled receptors (GPCRs) known as the S1P Receptors (S1pr 1-5) [393,394]. In vascular tissues, however, only S1pr 1, 2, and 3 are expressed, each acting through a different downstream signaling pathway [395,396].

The Kallikrein-Kinin system (KKS) has also been shown to be involved in the inflammatory profile of atherosclerosis [397]. Particularly, it has been shown that bradykinin (BK) is involved in the modulation of resting vascular tone and in the expected flow-induced vasodilation in human arteries through the induction of nitric oxide production in the endothelial cells [398,399]. However, BK was shown to induce vasoconstriction in the absence of intact endothelium through the activation of inositol triphosphate (IP3) and the release of intracellular calcium [19]. BK induces its responses through binding to its Bdkrb2 that are constitutively expressed in most tissues [400-402]. Previous studies conducted in our lab have shown the extracellular signal-regulated kinase 1/2 (ERK1/2) to be among the various signaling pathways activated by Bdkrb2 in VSMC [74,403]. Additionally, we previously reported that knocking out Bdkrb2 ameliorated the

diabetes-induced renal injury [83]. Several other studies have shown that receptor crosstalk is an important mechanism by which Bdkrb2 exerts its effects within cells [404].

Ctgf is a cysteine-rich heparin-binding protein that stimulates ECM formation and deposition [306]. It is upregulated in several fibrotic processes, including atherosclerosis [311]. In fact, Ctgf mRNA and protein levels were shown to be elevated in VSMC of advanced atherosclerotic lesions. In addition, Ctgf was aggregated and concentrated near the fibrous cap of the plaque suggesting its potential involvement in atherosclerotic plaque production [309].

The aim of this study was to investigate the crosstalk between Bdkrb2 and S1pr, delineate the mechanism, and the implications of the interaction in the pathogenesis of atherosclerosis. We are particularly interested in studying the effects of BK on the expression of the profibrotic protein, in an attempt to uncover novel therapeutic intervention targets in vascular injury.

3. *Methods:*

a. Animals:

All the experimental protocols were approved by the Institutional Animal Care and Use Committee at both the American University of Beirut and Medical University of South Carolina (MUSC). Sprague-Dawley rats and mice were housed and handled in the division of laboratory animal resources facility. Animals were maintained under controlled conditions of humidity ($50\% \pm 10\%$), light (12 h light, 12 h dark cycle) and temperature ($23^{\circ}\text{C} \pm 2^{\circ}\text{C}$). SphK1 homozygous knockout mice of the 129SV-C57BL/6 background were a kind gift from Dr. Richard L. Proia (National Institute of Diabetes and Digestive and

Kidney Diseases/National Institutes of Health, Bethesda, Maryland) [229]. Wild-type (WT) mice and Sprague-Dawley rats were purchased from Charles River Laboratories.

b. Primary cell extraction:

Primary rat and murine aortic smooth muscle cells (RASMC and MASMC, respectively) were extracted from the aorta of male Sprague-Dawley rats and from wild-type (SphK1^{+/+}) and SphK1 Knock-out (SphK1^{-/-}) mice respectively, according to the modified technique of Majack and Clowes [405]. RASMC were maintained in DMEM medium supplied with 10% FBS and used between passage 2 and 8. MASMC were maintained in MEM supplied with 20% FBS, and only the first and second passages of MASMC were used for the experiments. Immunocytostaining to Smooth Muscle α -actin (α -SMA, ab7817, Abcam) was used to verify the identity of the primary extracted vascular cells. Quiescent cell stage was achieved at about 80% confluence by serum starving the cells for 24h prior to any treatment.

c. RNA extraction and Real-Time PCR:

Total RNA from VSMC was extracted by using 500 μ l of RiboZol reagent (Amresco) according to the manufacturer's protocol. Total RNA concentration was measured by Nanodrop 1000 (Thermo Scientific) at 260 nm, and the 260/280 ratio was determined. RNA (1 μ g) was reversed transcribed into cDNA using the iScript cDNA synthesis kit (Bio-Rad), according to manufacturer's instructions. cDNA amplification reaction was then performed using the iQ SYBR green mix kit (Bio-Rad) according to the manufacturer's

instructions. Primer sequences for the genes of interest are from TIB Molbiol: Rat GAPDH (Forward: GGGGCTCTCTGCTCCTCCCTG, Reverse: CGGCCAAATCCGTTACACCG), Rat Ctgf (Forward: CCCCCGCCAACCGCAAGATT, Reverse: CGGCCAAATCCGTTACACCG), Rat Fn1 (Forward: CCACAGCCATTCCTGCGCCA, Reverse: TCACCCGCACTCGGTAGCC-A), Rat SphK1 (Forward: GCTAGGGTCAGGGGACGCCA, Reverse: CTTCGGGCACGCGTGGTTCT), Rat SphK2 (Forward: GCCGCACTTCTACGAATTTTG, Reverse: CTAATTCCCC-ATCTACAGTGAGC), Rat S1PR1 (Forward: CGCAGCTTCGTCCCGCTTGA, Reverse: GGCG -AGGTTGAGCGAGCCTT), Rat S1PR2 (Forward: GTCCGGGCCTGTCCTGTCCT, Reverse: AGGTCCCGGCTACGCCATGT), Rat S1PR3 (Forward: GGCAACTTGGCTCTCTGCGA, Reverse: GTGGATGCGCCCAGGGCTAC), Mouse Ctgf (Forward: AATGTCAGTGC-GCAGCCGAAGCA, Reverse: AGGGGTCACGCTCCGTACACAG), Mouse Fn1 (Forward: CCCCAACTGGTTACCCTTCC, Reverse: TGTCCGCCTAAAGCCATGTT), Mouse GAPDH (Forward: AAAGCTGTGGCGTGATGGCCG, Reverse: CGACGGACACATTGGGGGTAGG A).

For each target gene, a standard curve was established by performing a series of 10-fold dilutions. The negative control was made using the same volume of RNase-free water instead of a sample. The master mix was prepared as follows: 2x SYBR Green Supermix 12.5 μ l, forward and reverse primer 0.25 μ l respectively, and ddH₂O 12 μ l. For each well, 22 μ l of master mix was loaded first, followed by 3 μ l of the sample, mixed well to get total reaction volume of 25 μ l. For plate setup, SYBR-490 was chosen as a fluorophore. The plate was covered with a sheet of optical sealing film. PCR was performed using the

CFX96™ Real-Time PCR Detection System (Bio-Rad) programmed for a 1 min of denaturation at 98°C (1 cycle) initially, followed by 40 alternating cycles of 9 sec denaturation at 95°C, 12 sec annealing at 55°C, and 9 sec extension at 72°C. Finally, one cycle of 10 min extension at 72°C was used. After amplification, samples were subjected to melt curve analysis to check the purity and integrity of amplified samples. The annealing temperature for each gene was optimized in the laboratory. The correlation coefficient is between 0.99-1, PCR efficiency is between 80-120%. Quantification of the genes was calculated by the $\Delta\Delta C_t$. mRNA levels were expressed relative to GAPDH mRNA.

d. Protein extraction and western blots:

Quiescent RASMCs grown in 6-well plates were incubated with BK (10^{-7} M, Sigma-Aldrich) or S1P (10^{-9} M, Cayman Chemical), in the absence and presence of PD 98059 (25 μ M, Calbiochem), SphK1 inhibitor (SphKI1, 10^{-5} M, CAS 1177741-83-1 Calbiochem), or W146 (10^{-5} M, Sigma-Aldrich). The inhibitors were added to the cell media 30 minutes prior to the stimulation with the agonists. Quiescent MASMC from SphK1^{+/+} and SphK1^{-/-} were stimulated with BK (10^{-7} M) for 6 and 24h. Cells were washed with PBS containing Ca²⁺/Mg²⁺ and incubated with 100 μ l lysis buffer (25 mM Tris-HCl pH 7.4, 150 mM NaCl, 1 mM EDTA, 1% NP-40, 5% Glycerol, 1 mM PMSF, 1 mM Benzamidine, 2 μ g/ml Aprotinin, 10 mM Sodium Fluoride, 2 mM Sodium Orthovanadate, 1 mM Sodium Pyrophosphate, and 2 μ g/ml Leupeptin) for 15 minutes on ice. Cell lysates were then centrifuged at 14000 x g for 15 minutes at 4°C, and their total protein concentration was subsequently determined using Bradford assay (Bio-Rad) with BSA as

standard. For the determination of protein levels, 30 µg of total protein lysate were mixed with Laemmli buffer, separated in 10% polyacrylamide gel (29:1 acrylamide: bis) and transferred to Nitrocellulose membranes (Bio-Rad). Membranes were then blocked with 5% non-fat milk in TBST1x solution for 1 hour at 37°C. Immunoblot analysis was performed using rabbit anti-rat p-ERK (p44/42 MAPK (T202/Y204), 4370s, Cell Signaling), t-ERK (4695s, Cell Signaling), Fibronectin (ab23750, Abcam), Ctgf (ab6992, Abcam), p-SphK1 (Ser 225, SP1641, ECM Biosciences), and Actin (ab8227, Abcam) and donkey anti-rabbit IgG coupled to HRP (711-035-152, Jackson Immuno Research). Protein band signals were developed by ChemiDoc MP (Bio-Rad) after activation of the HRP by Clarity™ Western ECL Blotting Substrates (Bio-Rad) according to manufacturer's instructions. The fold change of the proteins is expressed as the ratio of Fn1, Ctgf, or p-SphK1 relative to Actin, and that of p-ERK to t-ERK relative to the non-treated control samples.

e. siRNA down-regulation of SphK1 expression:

SphK1 expression was downregulated using rat SphK1 sequence-specific siRNA siGENOME rat SphK1 (170897) siRNA (SMARTpool, M-092434-00-0005) consisting of the following target sequences GAGGUAUCCUUUAAACUGA, CAGCUUCUUUGAACUACUA, GGAGAUUCGUUUCACGGUG, and GUACUUGGUUCA-UGUGCCA, and siGENOME Non-Targeting siRNA Pool #1 (D001206-13-05) consisting of the following target sequence UAGCGACUAAACACAUCAA, UAAGGCUAUGAAGAGAUAC, AUGUAUUGGCCUGUAUUAG, AUGAACGUGAAUUGCUCAA, GE Dharmacon,

Colorado, USA. RASMC were transfected with 20 nM Scrambled siRNA, or 80 nM siGENOME Rat SphK1 siRNA in serum- and antibiotic-free media using Xtreme Gene siRNA Transfection Reagent (Roche), with incubation for 6 hours. After the transfection period, 2x serum solution was added to the media and incubated overnight. Cells were then treated and their total proteins extracted as described earlier.

f. Confocal fluorescence microscopy:

To assess the internalization of S1pr1, a GFP-S1pr1 construct was used as previously described [306,406]. For fluorescent microscopic visualization, 40-50% confluent cultures of HEK293T in 10-cm dishes were transiently transfected with GFP-S1pr1 construct using FuGENE® HD (Promega), according to the manufacturer's protocol. Transfection was verified by the presence of green fluorescent cells, 24 hours post transfection. The cells were then seeded into 35-mm glass-bottom dishes (MatTek) for confocal microscopy and starved overnight in an FBS-free medium. Inhibitors were added to the cells 30 minutes prior to the stimulation with either BK or S1P, which lasted for 30 minutes. Cells were then fixed for 30 minutes with 4% paraformaldehyde diluted in PBS and washed three times with PBS before visualization. Confocal microscopy was then performed using a Zeiss LSM 510 laser-scanning microscope (Carl Zeiss) with 488-nm excitation and 516–560 nm emission filter settings.

g. Statistical Analysis:

Each experiment was performed at least four times. Data are expressed as mean \pm SE with corresponding statistical significance being analyzed with the Sigma Stat software using the Mann-Whitney U test. The differences in the mean between groups were analyzed by student t-test for two tailed unpaired analysis. Significance was considered if $p < 0.05$.

4. Results:

a. BK induces the expression of Fn1, Ctgf, and SphK1 in RASMC:

To assess the effect of BK on the expression of Fn1, Ctgf, SphK1, and SphK2, RASMC were stimulated with BK (10^{-7} M) for 6 and 24 h. Fn1, Ctgf, SphK1, and SphK2 mRNA levels were measured by real-time PCR and expressed relative to GAPDH mRNA levels measured in the same samples at the same time. Results shown in **Figure 17A-D** indicate that stimulation of RASMC with BK resulted in a significant increase in the mRNA levels of Fn1 (2.8 ± 0.4 -fold at 6h, $p=0.002$, and 1.8 ± 0.3 -fold at 24h, $p=0.032$), Ctgf (2.11 ± 0.19 -fold at 6h, $p=0.032$) and SphK1 (2.7 ± 0.34 -fold at 6h, $p=0.016$, and 2.7 ± 0.42 -fold at 24h, $p=0.018$) compared to unstimulated control cells. No effect of BK on the mRNA levels of SphK2 was observed ($p=0.62$ at 6h, and $p=0.12$ at 24h).

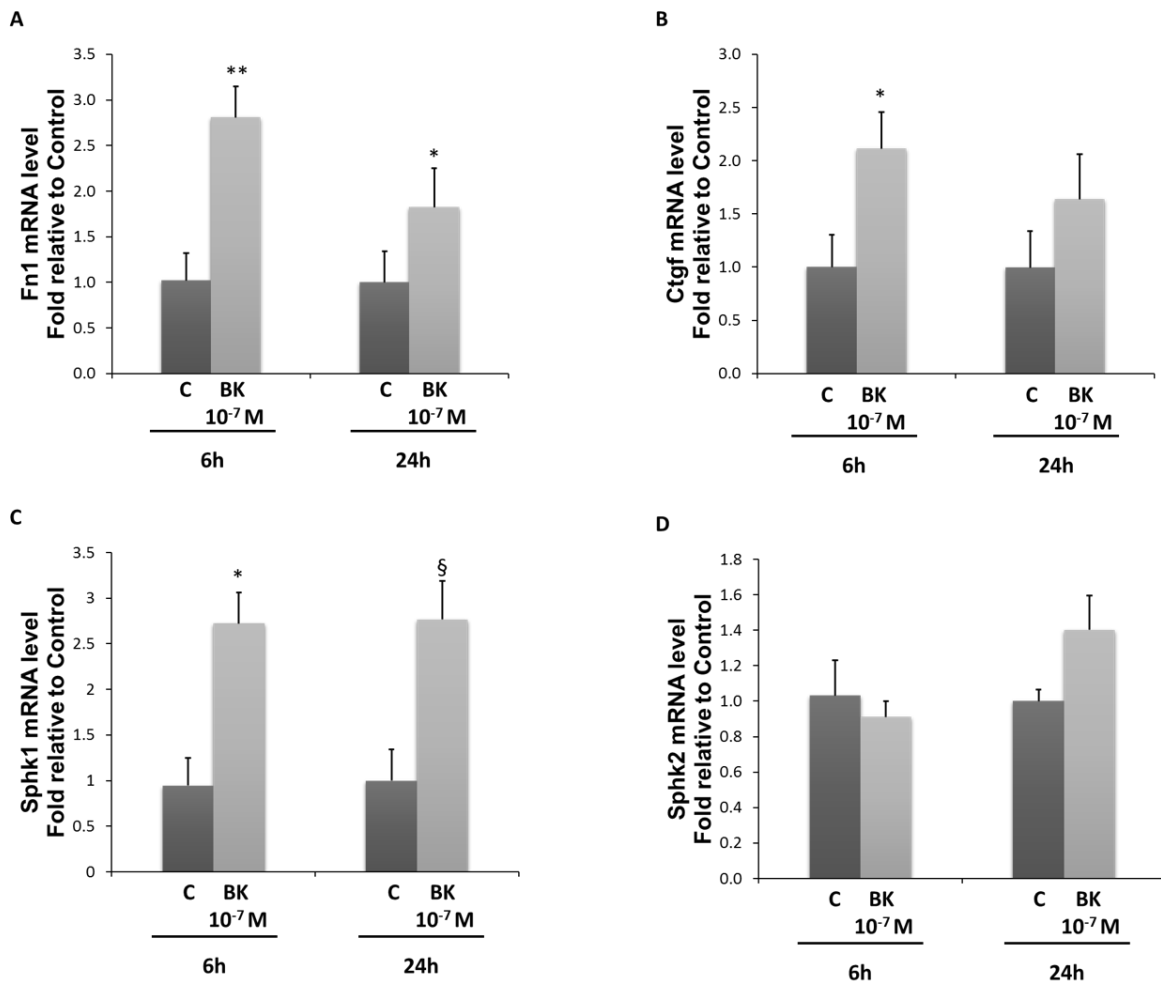


Figure 17: BK induces the expression of Fn1, Ctgf, and SphK1 in RASMC. Quiescent RASMC were stimulated with BK (10^{-7} M) for 6 and 24 h. Fn1 (A), Ctgf (B), SphK1 (C), and SphK2 (D) mRNA levels were measured by RT-qPCR. Bar graph represents the fold change in mRNA levels of Fn1 (** $p=0.002$ BK 6h vs. control, and * $p=0.032$ BK 24h vs. control, $n=5$), Ctgf (* $p=0.032$ BK 6h vs. control, $n=4$), and SphK1 (* $p=0.016$ BK 6h vs. control, and § $p=0.032$ BK 24h vs. control, $n=4$) relative to GAPDH mRNA levels and is the sum of 5 separate experiments.

b. The role of ERK1/2 in BK-induced SphK1 phosphorylation and protein levels of Ctgf and Fn1:

To investigate the involvement of ERK1/2 activity on the phosphorylation of SphK1, and the expression of Ctgf, and Fn1, we first determined the activation of ERK with BK (10^{-7} M) for 5 and 10 mins in the absence and presence of MEK inhibitor, PD98059 (25

μM). Our results showed that BK stimulation induced the phosphorylation of ERK1/2 in RASMC after 5 minutes (2.1 ± 0.27 -fold, $p=0.002$) compared to unstimulated control cells (**Figure 18A**). To test whether activation of ERK is required for BK-induced phosphorylation of SphK1, RASMC were stimulated with BK (10^{-7}M) for 5 and 10 mins in the presence and absence of MEK inhibitor, PD98059 ($25 \mu\text{M}$). Results shown in **Figure 18B** indicate that BK-induced the phosphorylation of SphK1 at 5 and 10 mins (1.9 ± 0.3 fold, $p=0.002$, and 2 ± 0.3 fold, $p=0.026$, $n=6$, respectively) compared to unstimulated cells. However, in the presence of MEK inhibitor, the phosphorylation of SphK1 in response to BK stimulation was significantly decreased compared to BK-stimulated cells (0.8 ± 0.1 -fold, $p=0.004$ at 5 and 10 min). These findings suggest that BK promotes the phosphorylation of SphK1 in RASMC via activation of the ERK1/2 pathway.

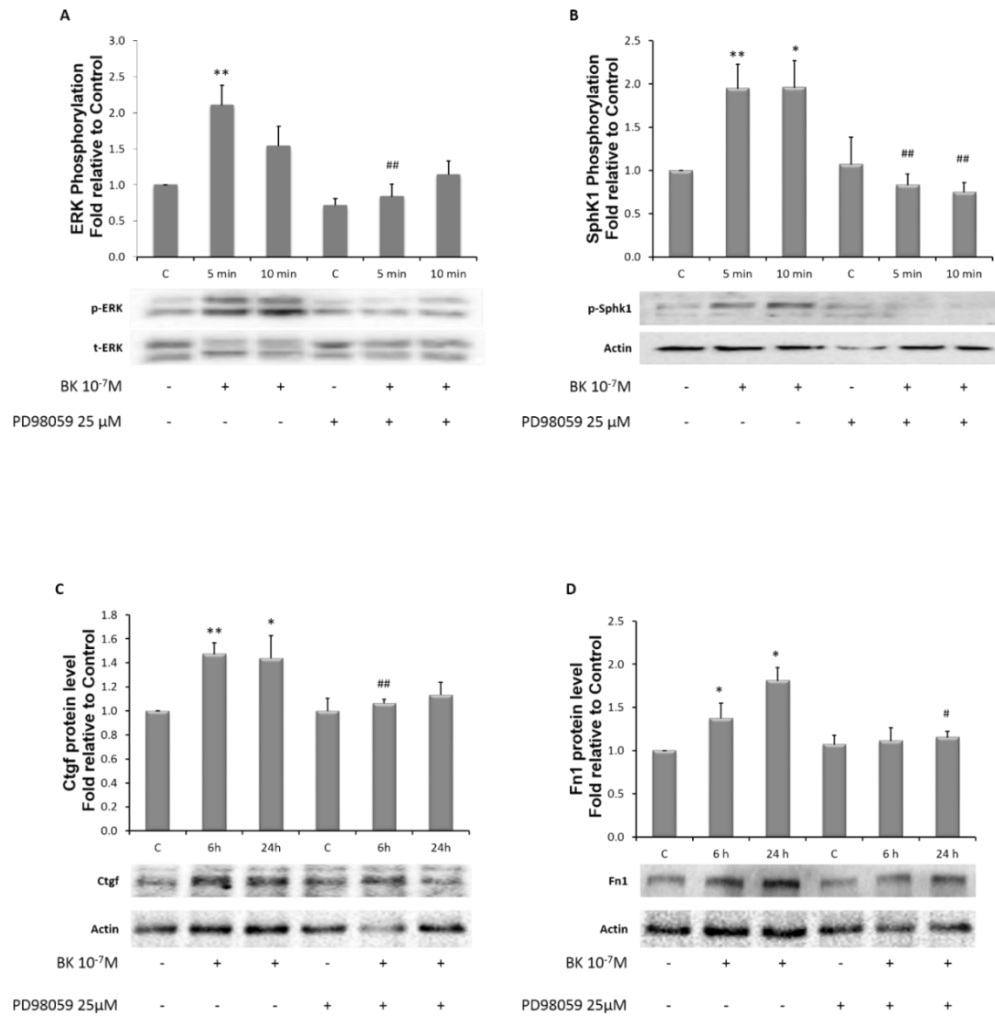


Figure 18: Role of ERK activation in the BK-induced phosphorylation of SphK1 and the protein expression of Ctgf and Fn1 in RASMC. A: quiescent RASMC were stimulated with BK (10^{-7} M) for 5 and 10 mins in the absence and presence of PD98059 (25 μ M). p-ERK (p42/44, Thr 202 and Tyr 204) and t-ERK protein levels were measured by Western Blot, and their fold change is represented in the bar graph (** $p=0.002$ BK 5min vs. control, and ## $p=0.004$ PD98059 + BK 6h vs. BK 6h, $n=6$). B: quiescent RASMC were stimulated with BK (10^{-7} M) for 5 and 10 mins in the absence and presence of PD98059 (25 μ M). p-SphK1 (Ser 225) and β -actin protein levels were measured by Western Blot, and their fold change is represented in the bar graph (** $p=0.001$ BK 5 min vs. control, * $p=0.026$ BK 10 min vs. control, ## $p=0.004$ PD 98059 + BK vs. BK at 5 and 10 min, $n=7$). C: quiescent RASMC were stimulated with BK (10^{-7} M) for 6 and 24 h in the absence and presence of PD98059 (25 μ M). Ctgf and actin protein levels were measured by Western Blot, and their fold change is represented in the bar graph (** $p=0.001$ BK 6h vs. control, * $p=0.026$ BK 24h vs. control, and ## $p=0.006$ PD 98059 + BK 6h vs. BK 6h, $n=4$). D: quiescent RASMC were stimulated with BK (10^{-7} M) for 6 and 24 h in the absence and presence of PD98059 (25 μ M). Fn1 and β -actin protein levels were measured by Western Blot, and their fold change is represented in the bar graph (* $p=0.029$ BK vs. control at 6 and 24h, and # $p=0.029$ PD 98059 + BK 24h vs. BK 24h, $n=4$).

To determine the role of ERK1/2 in the BK-induced expression of Ctgf and Fn1, RASMC were stimulated with BK (10^{-7} M) for 6 and 24h in the presence and absence of the MEK inhibitor PD98059 (25 μ M). Protein levels of Fn1 and Ctgf were measured by western blots and expressed relative to actin protein levels measured in the same blots. Results shown in **Figure 18C and D** demonstrate that BK stimulation significantly increased the protein levels of Ctgf (1.42 \pm 0.07-fold, p=0.001 at 6h, and 1.34 \pm 0.1-fold, p=0.026 at 24h) and Fn1 (1.4 \pm 0.18-fold, p=0.029 at 6h, and 1.8 \pm 0.15-fold, p=0.029 at 24h) compared to levels in control unstimulated cells. However, in the presence of MEK inhibitor significantly abolished the BK-induced increase in Ctgf (1.062 \pm 0.023-fold, p=0.006 at 6h) and Fn1 (1.2 \pm 0.072-fold, p=0.029 at 24h) expression levels compared to BK-stimulated cells. These findings suggest that BK promotes the phosphorylation of SphK1 and the expression of Ctgf and Fn1 in RASMC via activation of the ERK1/2 pathway.

c. The role of SphK1 in the BK-induced protein levels of Ctgf and Fn1:

To determine whether SphK1 plays a role in the BK-induced expression of Ctgf and Fn1, RASMC were stimulated with BK (10^{-7} M) in the presence and absence of SphK1I (10^{-5} M), for 6 and 24 h. The results shown in **Figure 19A and B** demonstrate that inhibition of SphK1 activity significantly decreased the BK-induced increase in Ctgf (0.6 \pm 0.19-fold, p=0.009 at 6h, and 0.7 \pm 0.1-fold, p=0.002 at 24h) and Fn1 (0.61 \pm 0.14-fold, p=0.036 at 24h) protein levels compared to BK-stimulated cells.

Our next series of experiments examined the effect of siRNA directed against SphK1. The first set of experiments examined whether the siRNAs were effective in inhibiting SphK1 protein expression. RASMC were transfected with scrambled or siRNA targeted against SphK1 (80 nM) for 48 hrs. Protein levels of SphK1 were measured by western blots and the results indicated that siRNA resulted in a significant decrease (40%) in SphK1 protein levels compared to cells transfected with scrambled siRNA (p=0.029).

RASMC transfected with scrambled and/or siRNA against SphK1 for 48 h, were then stimulated with BK (10^{-7} M) for 6 and 24h. Ctgf and Fn1 protein levels were determined by western blots and expressed relative to actin protein levels measured in the same cells. Results shown in **Figure 19C and D**, demonstrate that BK stimulation resulted in a significant increase in Ctgf and Fn1 protein levels and this effect of BK was significantly reduced in the presence of SphK1 siRNA (Ctgf, p=0.046 SphK1 siRNA + BK vs. scrambled siRNA + BK at 6h; Fn1, p=0.029 SphK1 siRNA + BK vs. scrambled siRNA + BK at 6h, n=4). The basal expression levels of Ctgf and Fn1 were not significantly altered by SphK1 siRNA compared to scrambled RNA transfected cells (**Figure 19C and D**).

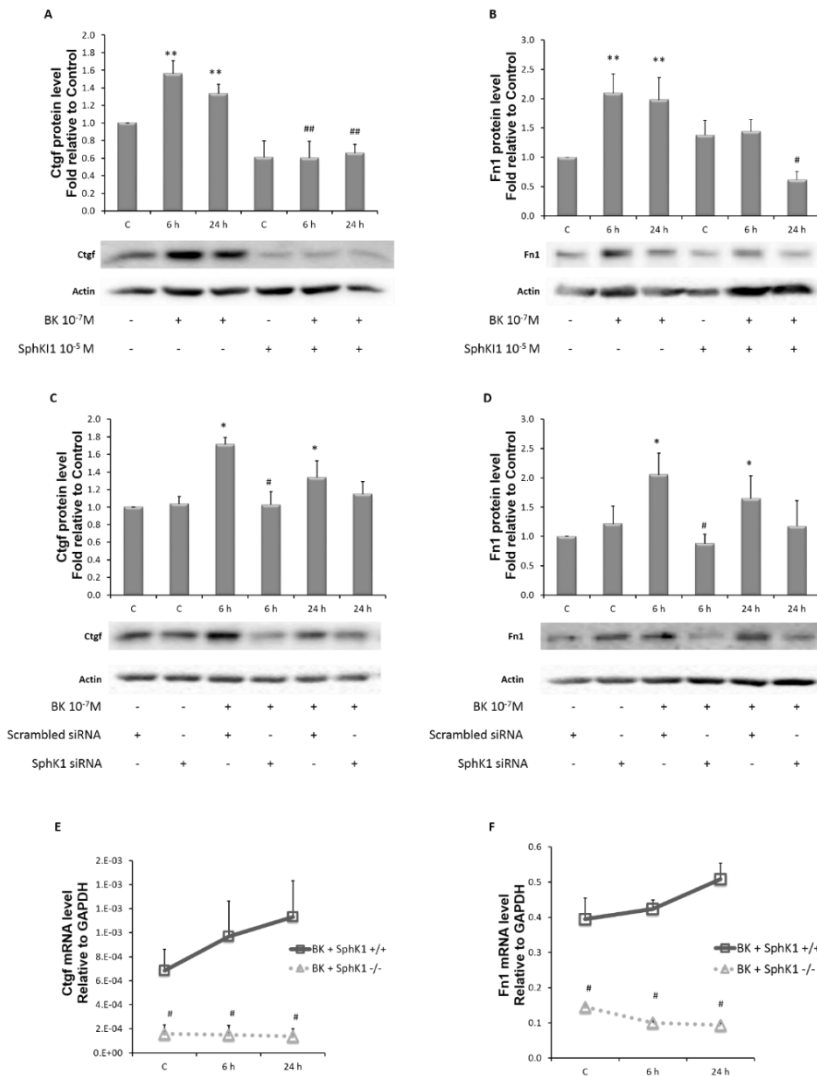


Figure 19: Role of SphK1 in the BK-induced protein expression of Ctgf and Fn1 in RASMC and mouse VSMC. A: quiescent RASMC were stimulated with BK (10⁻⁷ M) for 6 and 24 h in the absence and presence of SphK11 (10⁻⁵ M). Ctgf and β -actin protein levels were measured by Western Blot, and their fold change is represented in the bar graph (** p=0.002 BK vs. control at 6 and 24h, ## p=0.009 SphK11 + BK 6h vs. BK 6h, and ## p=0.002 SphK11 + BK 24h vs. BK 24h, n=6). B: quiescent RASMC were stimulated with BK (10⁻⁷ M) for 6 and 24 h in the absence and presence of SphK11 (10⁻⁵ M). Fn1 and β -actin protein levels were measured by Western Blot, and their fold change is represented in the bar graph (** p=0.008 BK vs. control at 6 and 24h, and # p=0.036 SphK11 + BK 24h vs. BK 24h, n=5). C: quiescent RASMC were stimulated with BK (10⁻⁷ M) for 6 and 24 h in the presence of non-targeting siRNA (20 nM) or SphK1-siRNA (80 nM). Ctgf and β -actin protein levels were measured by Western Blot, and their fold change is represented in the bar graph (* p=0.029 scrambled siRNA + BK vs. scrambled siRNA at 6 and 24h, and # p=0.046 SphK1 siRNA + BK 6h vs. Scrambled siRNA + BK 6h, n=4). D: quiescent RASMC were stimulated with BK (10⁻⁷ M) for 6 and 24 h in the presence of non-targeting siRNA (20 nM) or SphK1-siRNA (80 nM). Fn1 and β -actin protein levels were measured by Western Blot analysis, and their fold change is represented in the bar graph (* p=0.029 scrambled siRNA + BK vs. scrambled siRNA at 6 and 24h, and # p=0.029 SphK1 siRNA + BK 6h vs. Scrambled siRNA + BK 6h, n=4). E: quiescent RASMC were stimulated with BK (10⁻⁷ M) for 6 and 24 h in the presence of non-targeting siRNA (20 nM) or SphK1-siRNA (80 nM). Ctgf mRNA levels were measured by RT-PCR, and their fold change is represented in the line graph. F: quiescent RASMC were stimulated with BK (10⁻⁷ M) for 6 and 24 h in the presence of non-targeting siRNA (20 nM) or SphK1-siRNA (80 nM). Fn1 mRNA levels were measured by RT-PCR, and their fold change is represented in the line graph.

E: quiescent MASMCM from Wild-type (WT) and SphK1 Knock-out (SphK1 KO) were stimulated with BK (10^{-7} M) for 6 and 24 h. Ctgf and GAPDH mRNA levels were measured by RT-qPCR, and the ratio of Ctgf to GAPDH is represented in the line plot (# $p=0.035$ SphK1 KO vs. WT, # $p=0.036$ SphK1 KO + BK 6h vs. WT + BK 6h, and # $p=0.018$ SphK1 KO + BK 24h vs. WT + BK 24h, $n=4$). F: quiescent MASMCM from Wild-type (WT) and SphK1 Knock-out (SphK1 KO) were stimulated with BK (10^{-7} M) for 6 and 24 h. Fn1 and GAPDH mRNA levels were measured by RT-qPCR, and the ratio of Fn1 to GAPDH is represented in the line plot (# $p=0.017$ SphK1 KO vs. WT, # $p=0.015$ SphK1 KO + BK 6h vs. WT + BK 6h, and # $p=0.018$ SphK1 KO + BK 24h vs. WT + BK 24h, $n=4$).

To further explore the role of SphK1 in modulating the expression of Ctgf and Fn1 in response to BK, cultured MASMCM from SphK1^{+/+} and SphK1^{-/-} mice were stimulated with BK (10^{-7} M) for 6 and 24h. The mRNA levels of Ctgf and Fn1 were measured by RT-qPCR and expressed relative to GAPDH mRNA levels measured in the same samples. Results are shown in **Figure 19E and F** demonstrate that the basal, expression of Ctgf and Fn1 were significantly attenuated in MASMCM cultured from SphK1^{-/-} mice compared to those from SphK1^{+/+} mice, $p<0.05$, $n=4$.

Furthermore, stimulation of MASMCM from SphK1^{+/+} with BK produced an increasing trend of Ctgf and Fn1 mRNA levels compared to unstimulated control cells, though they did not reach a significant level. BK significantly increased the mRNA level of Ctgf (2.01 ± 0.76 -fold at 6h, $p=0.036$, and 3.55 ± 0.23 -fold at 24h, $p=0.018$) and Fn1 (2 ± 0.68 -fold at 6h, $p=0.015$, and 2.7 ± 0.9 -fold at 24h, $p=0.018$) in SphK^{+/+} when compared to the SphK1^{-/-} MASMCM (**Figure 19E and F**). However, no increase in Ctgf and/or Fn1 mRNA levels was observed when MASMCM from SphK1^{-/-} null mice were stimulated with BK for 24h.

d. Effect of BK on S1P receptors Regulation and internalization:

The interrelationship between BK and SphK1 were further studied by examining the gene expression of the three receptors by real-time PCR. S1pr 1, 2 and 3 mRNA levels were measured by real-time PCR and expressed relative to GAPDH mRNA levels measured in the same samples at the same time. Results shown in **Figure 20A-C** indicate that stimulation of RASMC with BK resulted in a significant increase in the mRNA levels of S1pr1 (2.2 ± 0.25 -fold at 24h, $p=0.028$), compared to unstimulated control cells. No significant effect of BK treatment was observed on the mRNA levels of S1pr2 (0.85 ± 0.1 fold, $p=0.32$ at 24h) and S1pr3 (0.78 ± 0.08 fold, $p=0.059$ at 24h).

We next sought to determine whether BK will result in the translocation of S1P receptors from the membrane to the cytosol by confocal microscopy. HEK293T cells transfected with GFP-tagged S1pr1 plasmid constructs were stimulated with BK (10^{-7} M) or S1P (10^{-9} M) for 30 min in the presence and absence of Bdkrb2 antagonist HOE 140 (10^{-6} M), SphKII (10^{-5} M), or S1P receptor 1 inhibitor W146 (10^{-5} M). The results shown in Figure 16D, demonstrate that under basal control conditions, the GFP-S1pr1 expression is distributed along the plasma membrane, and this expression pattern was not altered by treatment with HOE 140, SphKII, or W146. Treatment with S1P led to the internalization of GFP-S1pr1, shown as punctate within the cytoplasm of the treated cells compared to controls. Moreover, pretreatment of the cells with HOE 140 or SphKII prior to the stimulation with S1P had no significant effect on S1P-induced GFP-S1pr1 internalization (**Figure 20D**). However, pretreatment of cells with W146 prior to S1P stimulation abolished the S1P-induced internalization of the GFP-S1pr1, indicating the need for S1P binding to S1pr1 to induce its activation. Furthermore, BK stimulation induced the

internalization of GFP-S1pr1 into the cytoplasm compared to basal unstimulated cells, and this BK effect was inhibited in the presence of HOE 140, SphKI1, or W146 (**Figure 20D**).

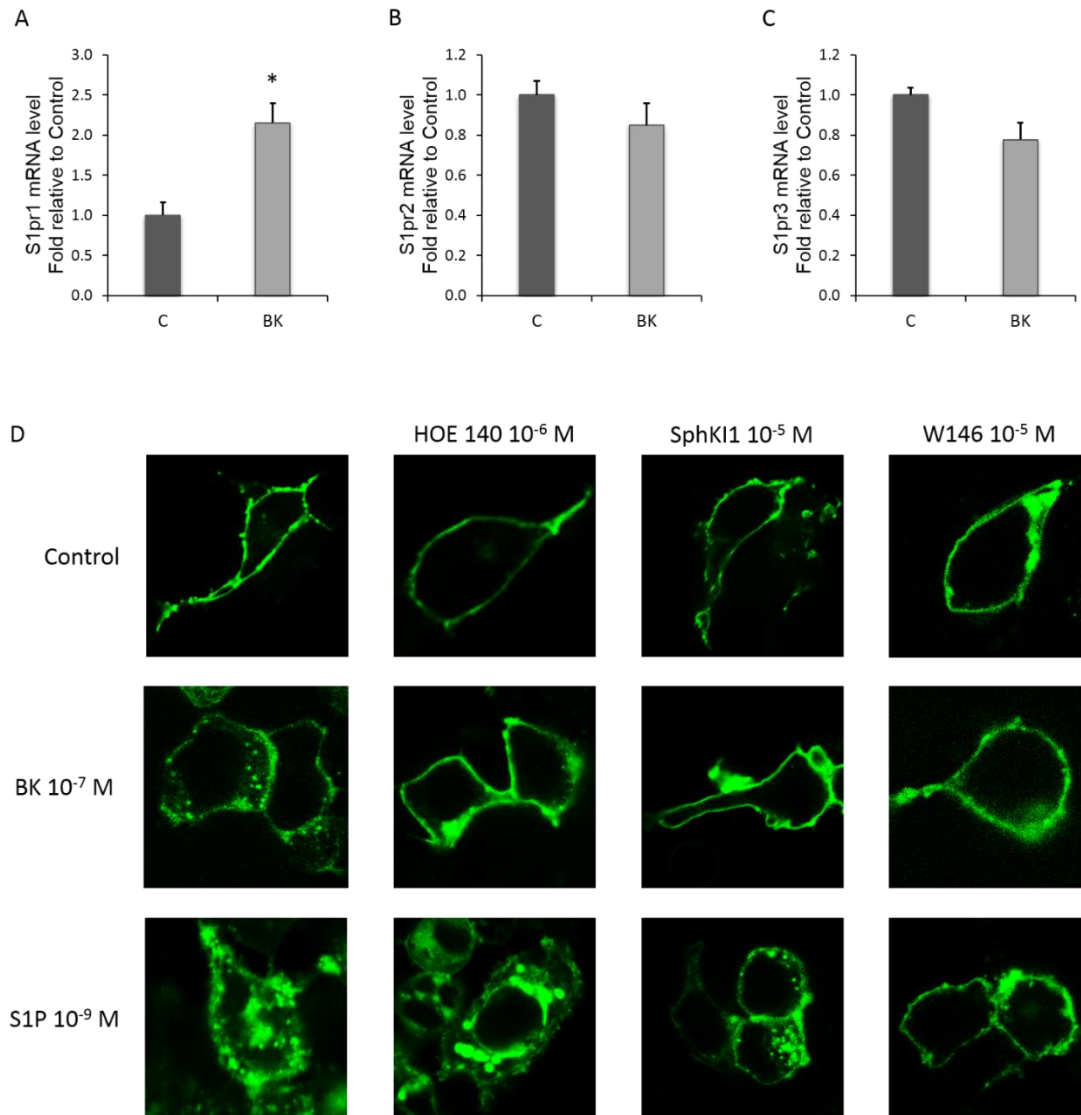


Figure 20: Effect of BK on the expression of S1P receptors and the internalization of S1pr1. Quiescent RASMC were stimulated with BK (10^{-7} M) for 24 h. S1pr1 (A), S1pr2 (B), and S1pr3 (C) mRNA levels were measured by RT-qPCR. Bar graph represents the fold change in mRNA levels of receptors (S1pr1, * $p=0.028$ BK 24h vs. control, $n=4$). D: Quiescent HEK293T cells transfected with GFP-S1pr1 were stimulated with BK (10^{-7} M) and S1P (10^{-9} M) in the absence and presence of HOE 140 (10^{-6} M), SphKI1 (10^{-5} M), and W146 (10^{-5} M). The green color represents the localization of the GFP-S1pr1 fusion protein. Punctate in the cytoplasm represents the internalized GFP-S1pr1 protein.

e. Involvement of S1pr1 in the BK-induced Ctgf and Fn1 expression.

We next sought to determine whether S1pr1 contributes in promoting the expression of Ctgf and Fn1 mediated by BK. The first series of experiments examined the effect of S1P (10^{-9} M) treatment for 6 and 24h on Ctgf and Fn1 protein levels in RASMC in the presence and absence of W146. The results shown in **Figure 21A and B** demonstrate that S1P significantly increased the protein levels of Ctgf (1.7 ± 0.1 -fold, $p=0.008$ at 6h, and 1.5 ± 0.2 -fold, $p=0.008$ at 24h, $n=5$) and Fn1 (1.64 ± 0.2 , $p=0.008$ at 6, $n=5$) compared to unstimulated control cells and W146 significantly inhibited the BK-induced effects on Ctgf (1.1 ± 0.1 -fold, $p=0.008$ at 6h, and 0.9 ± 0.2 -fold, $p=0.032$ at 24h, $n=5$) and Fn1 (0.8 ± 0.17 , $p=0.016$ at 6h, $n=5$).

In the second series of experiments, we assessed whether BK modulates Ctgf and Fn1 expression via S1pr1. RASMC were treated with BK (10^{-7} M) for 6 and 24h in the presence and absence of W 146 (10^{-5} M). Results shown in **Figure 21C and D** demonstrate that W146 significantly inhibited the BK-induced effects Ctgf (0.7 ± 0.1 , $p=0.016$ at 6h, $n=5$) and Fn1 (0.86 ± 0.2 , $p=0.032$ at 24h, $n=5$), indicating that BK stimulates Ctgf and Fn1 expression via S1pr1 ($p < 0.029$ vs. BK, $n=5$).

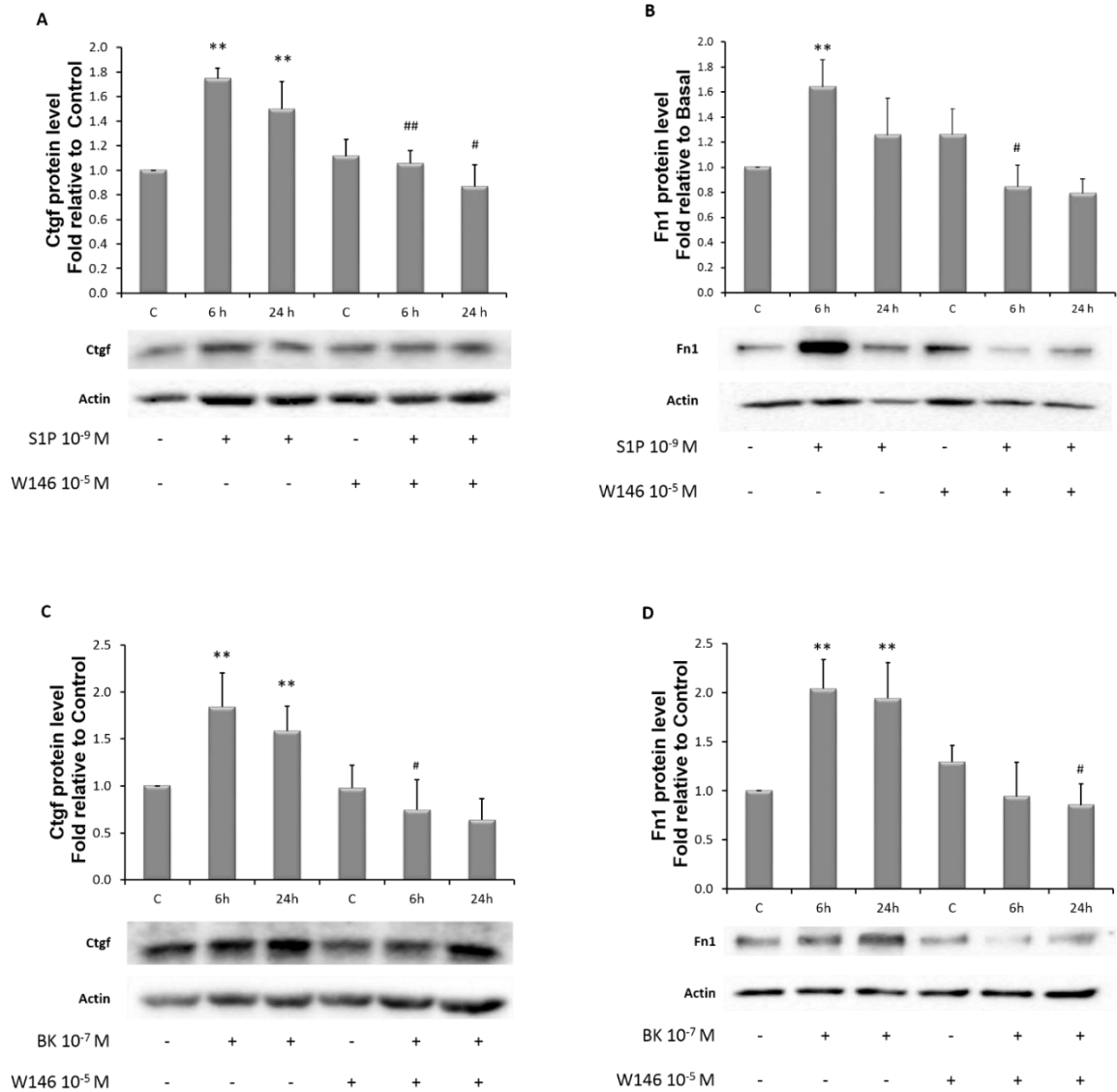


Figure 21: Role of S1pr1 in the BK-induced protein expression of Ctgf and Fn1 in RASMC. A: quiescent RASMC were stimulated with S1P (10^{-9} M) for 6 and 24 h in the absence and presence of W146 (10^{-5} M). Ctgf and β -actin protein levels were measured by Western Blot, and their fold change is represented in the bar graph (** $p=0.008$ S1P vs. control at 6 and 24h, ## $p=0.008$ W146 + S1P 6h vs. control, and # $p=0.032$ W146 + S1P 24h vs. control, $n=5$). B: quiescent RASMC were stimulated with S1P (10^{-9} M) for 6 and 24 h in the absence and presence of W146 (10^{-5} M). Fn1 and β -actin protein levels were measured by Western Blot, and their fold change is represented in the bar graph (* $p=0.026$ S1P vs. control at 6 and 24h, and # $p=0.011$ W146 + S1P 6h vs. control, $n=7$). C: quiescent RASMC were stimulated with BK (10^{-7} M) for 6 and 24 h in the absence and presence of W146 (10^{-5} M). Ctgf and actin protein levels were measured by Western Blot, and their fold change is represented in the bar graph (** $p=0.008$ BK vs. control at 6 and 24h, and # $p=0.016$ W146 + BK 6h vs. control, $n=5$). D: quiescent RASMC were stimulated with BK (10^{-7} M) for 6 and 24 h in the absence and presence of W146 (10^{-6} M). Fn1 and β -actin protein levels were measured by Western Blot, and their fold change is represented in the bar graph (** $p=0.008$ BK vs. control at 6 and 24h, and # $p=0.032$ W146 + BK 6h vs. control, $n=5$).

5. *Discussion:*

Vascular remodeling and endothelial dysfunction are primary inducers of atherogenesis [407]. The factors and mechanisms that cause vascular remodeling leading to pre-atherosclerotic lesion formation are not yet completely defined. In the current manuscript, we demonstrate that BK induces the expression of Ctgf and Fn1, and this is mediated via activation of the SphK1-S1pr1 axis. These findings are based on the observations that the expression and phosphorylation of SphK1 are increased upon stimulation of VSMC with BK. In addition, inhibition of SphK1 activity pharmacologically or knocking-down the SphK1 gene by siRNA attenuated the BK-induced expression of Ctgf and Fn1 in VSMC. Moreover, the basal expression of Ctgf and Fn1 in VSMC cultured from SphK1^{-/-} mice were much lower than levels in wild-type mice. Furthermore, our findings also demonstrate the existence of cross-talk between Bdkrb2 and S1pr1 on modulating the expression of Ctgf and Fn1 in VSMC. This is supported by the observations that BK treatment induced the translocation of S1pr1 from the membrane to the cytosol and this effect was inhibited by receptor antagonists to Bdkrb2 (HOE140) and S1pr1 (W146) and by the SphK1 inhibitor. Moreover, S1pr1 receptor antagonist attenuated the BK-induced expression of Ctgf and Fn1 in VSMC. Taken together, these findings implicate a pivotal role for the SphK1-S1pr1 axis in the BK response to promote the expression of factors that are involved in vascular remodeling. Our findings are in line with the few reports showing the involvement of SphK1-S1pr pathway in the expression of Ctgf and Fn1 in different cell types. We have recently demonstrated that the LDL-induced Ctgf expression in rat mesangial cells is SphK1 and S1pr1 and S1pr3 dependent [306]. In addition, Wunsche et al.

demonstrated that the TGF β ₂-induced Ctgf expression in human mesangial cells is S1pr5 [408].

Our findings in the current study continue to support a role for the kallikrein-kinin system in the pathophysiology of the vascular disease. We have previously demonstrated that the circulating levels of plasma prekallikrein (PK) are associated with increased carotid intima-media thickness and its progression in type 1 diabetic subjects [368]. Additionally, plasma PK influences vascular remodeling by promoting the growth of VSMC through transactivation of epidermal growth factor receptors [409]. Moreover, *Klkb1*^{-/-} mice (prekallikrein-deficient) have delayed arterial thrombosis by increasing protective vascular transcription factors Sirt1 and KLF4 to reduce vessel wall tissue factor and inflammation [393]. On the other hand, activation of Bdkrb2 by BK has been shown to activate a multitude of signaling pathways that result in inflammatory and oxidative stress responses involved in vascular remodeling. In this regard, BK has been shown to stimulate the dysregulation of matrix proteins in VSMC, by enhancing the production of TGF- β 1 and collagens I and III and attenuating the levels of tissue inhibitors of matrix proteins [158,410]. In addition, BK stimulated the generation of reactive oxygen species, the release of intracellular Ca²⁺ from intracellular stores causing contraction, the generation of prostacyclin I₂, and the activation of the MAPK (ERK1/2, P38, and JNK) pathway [74,403,411,412]. In fact, in the current study, we observed that the phosphorylation of ERK1/2 by BK is central to the expression of SphK1, Ctgf, and Fn1 in VSMC. This observation is supported by the finding that inhibition of ERK1/2 activity, attenuated the BK-induced expression of SphK1, Ctgf, and Fn1, implicating that the MAPK pathway is upstream of SphK1. Our findings are consistent with other studies demonstrating an

ERK1/2- dependent mechanism in modulating the expression of Ctgf and Fn1 [158,231,413].

As mentioned earlier, Ctgf has been linked to microvascular and macro-vascular complications of diabetes as well as nondiabetic cardiovascular diseases. For instance, a number of studies have linked Ctgf to diabetic retinopathy, atrial fibrosis, cardiac fibrosis, and vascular fibrosis in atherosclerosis [278]. Moreover, the observed increase in Ctgf expression in the atherosclerotic plaque region of LDL receptor null mice is via a TGF- β dependent mechanism [414]. In addition, plasma and urinary levels Ctgf have been shown to associate with renal and vascular disease risk in diabetic patients [415].

The SphK1-S1P pathway has been shown to promote factors that are linked to vascular diseases such as hypertension, fibronectin deposition, and VSMC proliferation and migration [223-226]. In this regard, a number of studies implicated SphK1 as a mediator of angiotensin II-induced hypertension [223,229,230]. SphK1 null mice are protected against angiotensin II- and hypoxia-induced hypertension and inhibition of SphK1 reduced the right ventricular hypertrophy pulmonary arterial hypertension mice [231]. Most recently, Siedlinski and colleagues reported a correlation of S1P serum level with higher aortic systolic pressure levels in patients with cardiovascular risk. Also, they observed elevations of Sphk1 mRNA, protein, and activity in the aorta and mesenteric arteries isolated from AngII-induced hypertensive mice [232]. Furthermore, inhibition of SphK activity protected against atherosclerosis, through abolishing the SphK-induced adhesion molecule expression and the activation of ERK in endothelial cells [233]. The expression and activation of SphK1 were previously shown to be mediated by BK, and the resulting S1P acting through its receptors induced the expression of Ctgf and fibronectin [191,234].

Our findings support our hypothesis that activation of B₂ receptors contributes to the development of vascular disease. Our findings demonstrate for the first time that BK stimulates the expression of Ctgf and Fn1 in VSMC and this effect is modulated via activation of the SphK1/S1P axis (**Figure 22**). These findings provide new mechanistic insights into new facets of BK signaling in the pathogenesis of vascular remodeling and ascertain novel targets for interventional strategies.

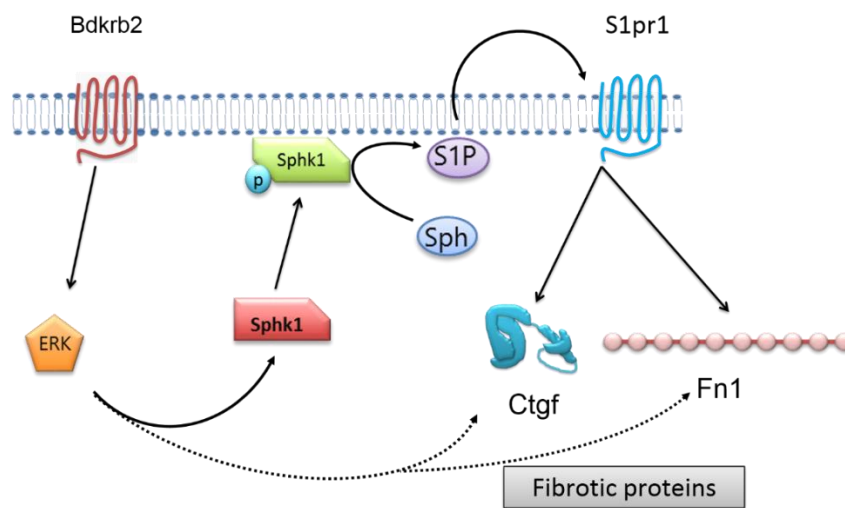


Figure 22: Schematic depiction of the proposed pathway for the BK-induced regulation of Ctgf and Fn1 protein expression. The BK-stimulation induces activation of the ERK and SphK1 downstream of Bdkrb2, which leads to the formation and release of S1P expression, which in turn activates the S1pr1 and subsequently promotes Ctgf and Fn1 expression.

C. Proteome Profiling in the VSMC in response to BK and leptin and cellular signaling assessment of the cross-talk mechanism between Bradykinin receptor and leptin receptor

Results of the second study showed the involvement of Sphingolipid signaling, especially SphK/S1P pathway, in relaying the signal of BK to the fibrotic proteins expression. In addition, the results of the first study indicated the possible activation of leptin and/or leptin receptor in response to diabetes in both the aorta VSMC and the kidney cortices.

These findings led us to investigate the role of leptin and leptin receptor in the induction of fibrotic markers in VSMC in response to BK stimulation. For this purpose, we designed our study to examine the global protein expression profile in primary VSMC in response to BK and leptin to comprehensively assess the protein regulation and the biological processes altered in response to BK and leptin. In addition, we validated the findings of the global proteomic results through assessing the expression of leptin and leptin receptor in response to BK in VSMC.

The outcomes of this objective will indicate to the cross-talk mechanism between BK and leptin in inducing vascular fibrosis in VSMC.

1. Abstract:

Background: Obesity prevalence is exponentially increasing worldwide, especially in the developed countries and the Middle East. The rates of obesity are of high concern due to the high association between obesity and Cardiovascular diseases (CVD), especially atherosclerosis. The latter is a worldwide health burden imposing a huge health toll. Vascular fibrosis and inflammation in the vessel walls are among the risk factors of atherosclerosis development, characterized by vessel stiffness and subsequently loss of elasticity. Bradykinin (BK) and leptin have previously shown to be involved in the development of atherosclerosis through their effect on vascular fibrosis and inflammation processes.

Aim: In this study, we investigate the effect of BK and leptin on the global protein profile in VSMC, employing LC MS/MS technique and systems biology analysis, to have an insight about the different pathways modified by BK and leptin, and the diseases and biological pathways they are involved in. In addition, the effects of BK stimulation were validated through assessing leptin and its receptor expression in VSMC.

Results: In our study, we found that BK induces the modulation of sphingolipid metabolism indicating a role of SphK/S1P downstream of BK signaling. In addition, BK induced the expression of leptin receptor, TGF β , and COX1 in VSMC promoting vascular fibrosis and inflammation. On the other hand, leptin induced the expression of collagen IV, suggesting a role of leptin in development of vascular fibrosis. Furthermore, leptin reduced cofilin expression, confirming the role of leptin in actin remodeling. On the other hand, western blot analysis of BK stimulated VSMC showed the induction in leptin and leptin

receptor expression. Finally, we observed that in the absence of leptin receptor, the BK-induced Ctgf is compromised.

Conclusion(s): BK stimulation showed a proteomic pattern favoring vascular fibrosis, inflammation and leptin pathway. On the other hand, leptin stimulation induced ECM proteins and reduced actin remodeling proteins. Finally, leptin receptor is a requirement for the signaling transduction of BK over fibrotic proteins. These findings point to the interaction between BK and leptin pathways in VSMC to promote vascular injury.

Keywords: Proteomics, Systems Biology, KKS, leptin, atherosclerosis

2. Introduction:

Cardiovascular diseases is a worldwide diseases with high mortality and morbidity rates [416]. Atherosclerosis is an inflammatory process and the leading cause of CVD [417]. It is characterized by entrapment of fat-laden macrophages (foam cells) within the sub-endothelial extracellular matrix in the vessel wall and subsequently the stiffening of large- and medium-sized arteries at different anatomical sites, increasing the risk of acquiring strokes and/or infarction [418]. Lipid accumulation, overproduction of the extracellular matrix, and/or macrophage infiltration of the sub-endothelial region are the major causes of the vessel stiffening observed in atherosclerosis [419].

As a result of vessel stiffness, vessel tone and blood flow dynamics are reported to be modified in response to atherosclerosis [389]. Vessel tone and blood dynamics are controlled by the degree of contraction and/or relaxation of vascular smooth muscle cells (VSMCs). Moreover, the migration, the proliferation, and/or the extracellular matrix deposition of VSMCs play a critical role in atherogenesis by narrowing the lumen of the blood vessels [420,421].

Several studies have reported the involvement of kallikrein kinin system in the development of atherosclerosis, and subsequently CVD [130,142]. Bradykinin is the major end-product of KKS that induces vasorelaxtion for the vessels in the physiological states through production and release of nitric oxide from the endothelial cells [422]. In endothelial dysfunction situations, BK induces vasoconstriction through stimulating calcium release in VSMC [423].

Another contributor for the development of atherosclerosis is adipose tissue through the secretion of diverse metabolites, such as leptin [253]. In addition, leptin was shown to be expressed and secreted from extra-adipose tissues [259,260]. Several studies have reported the association between leptin circulatory levels with different CVD risk factors, such as hypertension, extracellular matrix (ECM) deposition, inflammation, and oxidative stress [276,277].

In this study, we aim at profiling the global protein modification in VSMC in response to time points stimulation by either BK or leptin by LC MS/MS techniques. The comparative data generated between different time point stimulations, compared to the basal levels, will be analyzed through Pathway Studio ® to link the modified proteins. This approach will permit us to identify different effectors and mediators of the signaling pathway of BK or leptin, in an attempt to design a future therapeutic intervention to better understand their involvement in CVD.

3. *Methods:*

a. Animals:

All the experimental protocols were approved by the Institutional Animal Care and Use Committee at both the American University of Beirut. Sprague-Dawley rats were housed and handled in the division of laboratory animal resources facility. Animals were maintained under controlled conditions of humidity ($50\% \pm 10\%$), light (12 h light, 12 h dark cycle) and temperature ($23^{\circ}\text{C} \pm 2^{\circ}\text{C}$). Sprague-Dawley rats were purchased from Charles River Laboratories.

b. Primary cell extraction:

Primary rat aortic smooth muscle cells (RASMC) were extracted from the aorta of male Sprague-Dawley rats according to the modified technique of Majack and Clowes [405]. RASMC were maintained in DMEM medium supplied with 10% FBS and used between passage 2 and 8. Immunocytostaining to Smooth Muscle α -actin (α -SMA, ab7817, Abcam) was used to verify the identity of the primary extracted vascular cells. Quiescent cell stage was achieved at about 80% confluence by serum starving the cells for 24h prior to any treatment.

c. Extraction and Tryptic Digestion of Proteins:

RASMC from control, BK (24h, or 48h), and Leptin (24h, or 48h) were homogenized using beads beater (Beadbug microtube homogenizer, Benchmark Scientific, Edison, NJ) followed by sonication on ice for 30 min and centrifugation at 14,800 rpm for 10 min. The resulting supernatant was diluted 10x with 50 mM ammonium bicarbonate (ABC) buffer, and the protein concentration was determined by BCA protein assay kit (Thermo Scientific/Pierce, Rockford, IL) according to the user's manual.

Aliquots of 10 μ g extracted proteins from each sample were denatured at 80°C for 10 min followed by adding 200 mM dithiothreitol (DTT) and incubating at 60°C for 45 min. The resulting reduced proteins were then alkylated by adding 2-6 μ l Indole 3 Acetic Acid (IAA, 200 mM solution) and incubating at 37°C in the dark for 45 min. Excessive IAA was quenched by additional DTT and incubating at 37°C for 30 min. Trypsin

(Promega, Madison, WI) was added at a ratio of 1:25 (enzyme: proteins, w/w) into samples and incubated at 37°C for 18 hours followed by addition of formic acid at a final concentration of 0.5% to quench the enzymatic reaction. Samples were then centrifuged at 14,800 rpm for 10 min, and the resulting supernatant containing the digested peptides were dried and then resuspended in aqueous solution containing 2% acetonitrile (ACN) and 0.1% formic acid (FA) for Liquid Chromatography–Mass Spectroscopy/Mass Spectroscopy (LC-MS/MS) analysis.

d. Liquid Chromatography –Mass Spectroscopy/Mass Spectroscopy Analysis:

Aliquots (1µg) of tryptic digested samples were subjected to Liquid chromatography-electrospray ionization-tandem mass spectrometry (LC-ESI-MS/MS) analysis. The LC-MS/MS data was acquired using a Dionex Ultimate 3000 nano-LC system (Thermo Scientific, San Jose, CA) interfaced to an LTQ Orbitrap Velos mass spectrometer (Thermo Scientific, San Jose, CA) equipped with a nano-ESI source. Injected peptides were first purified on-line at a flow rate of 3 µl/min using a C18 Acclaim PepMap 100 trap column (75 µm I.D. x 2 cm, 3 µm particle sizes, 100 Å pore sizes, Thermo Scientific, San Jose, CA). Peptides were separated on a C18 Acclaim PepMap RSLC column (75 µm I.D. x 15 cm, 2 µm particle sizes, 100 Å pore sizes, Thermo Scientific, San Jose, CA). The column temperature was maintained at 29.5 °C and flow rate was 350 nl/min during the separation. The mobile phase consisted of solution A (97.9% water/2% ACN/0.1% FA) and solution B (99.9% ACN/0.1% FA). The separation of peptides was achieved by following gradient of solution B: 5% over 10 min, 5%-20% over 55 min, 20-30% over 25 min, 30-

50% over 20 min, 50%-80% over 1 min, 80% over 4 min, 80%-5% over 1 min and 5% over 4 min. Data dependent acquisition mode with two scan events was employed for MS/MS analysis. The first scan event was a full MS scan of 400-2000 m/z at a mass resolution of 15,000. In the second scan event, 10 most intense ions detected in the first scan event were selected with an isolation width of 3.0 m/z to perform CID MS/MS. The normalized collision energy (CE) was set to 35%, and an activation Q value was 0.250. The dynamic exclusion was set to have repeat count of 2, repeat duration of 30s, exclusion list size 200 and exclusion duration of 90s.

e. Systems Biology Assessment:

Pathway Studio® (Elsevier) was employed to examine functional correlations within the different treatment groups. Data sets containing protein identifiers (Uniprot-KB) and corresponding expression values (Log2 [Fold change]) of different comparative groups were uploaded. The comparative groups were as follow: BK 24h vs. control and BK 48h vs. control to analyze the effect of BK treatment compared to time-matched control, leptin 24h vs. control and leptin 48h vs, control to analyze the effect of leptin treatment compared to time-matched control. Each protein identifier was mapped to its corresponding protein object in the Pathway Studio Database. All mapped proteins were differentially expressed with $p < 0.05$ and overlaid onto global molecular networks developed from information contained in the knowledge base. Gene Ontology (GO), Diseases, metabolic process, and signaling process were additionally analyzed.

f. Statistical Analysis and LC-MS/MS Data Analysis:

Repeated measure generalized linear mixed models with intercept as the random effect models were implemented to assess the changes in plasma glucose and body weights between the groups longitudinally over time using SAS proc Glimmix. Oneway ANOVA, followed by Tukey correction for multiple comparisons was performed to assess the changes between PTM groups. Data are expressed as mean \pm SE and significance was considered at $p < 0.05$.

LC-MS/MS data was used to generate mascot generic format file (*.mgf) by Proteome Discover version 1.2 software (Thermo Scientific, San Jose, CA) then searched using SwissProt database (Rattus) in MaxQuant version 2.4 (Matrix Science Inc., Boston, MA). Iodoacetamide modification of cysteine was set as a fixed modification, while oxidation of methionine was set as a variable modification. An m/z tolerance of 5 ppm was set for the identification of peptides with maximum 2 missed cleavages. Also, tandem MS ion tolerance was set within 0.8 Da with label-free quantification. Scaffold Q+ (Proteome Software, Portland, OR) was employed for spectral counts quantitation. The normalized intensity of target peptides corresponding to each candidate protein was summed up to represent the abundance of the certain protein. Student's t-tests were performed to determine the significant proteins in the comparison between every two sample groups with a criterial of p-value < 0.05 .

g. Primary cell extraction:

Primary rat aortic smooth muscle cells (RASMC) were extracted from the aorta of male Sprague-Dawley rats, according to the modified technique of Majack and Clowes [332]. RASMC were maintained in DMEM medium supplied with 10% FBS and used between passage 2 and 8. Immunocytostaining to Smooth Muscle α -actin (α -SMA, ab7817, Abcam) was used to verify the identity of the primary extracted vascular cells. Quiescent cell stage was achieved at about 80% confluence by serum starving the cells for 24h prior to any treatment.

h. Treatment of RASMC:

After starvation, cells were incubated with BK (10^{-7} M) or leptin (3.1 nM or 50 μ g/ml), in the absence or presence of Sphki (10^{-5} M), or N-Acetylcystaien NAC (10^{-4} M). The inhibitors were added to the cell-media 30 minutes prior to the stimulation with BK or leptin.

i. Protein extraction:

After incubation, cells were washed with PBS containing Ca^{2+}/Mg^{2+} and incubated with 100 μ l lysis buffer (25 mM Tris-HCl pH 7.4, 150 mM NaCl, 1 mM EDTA, 1% NP-40, 5% Glycerol, 1 mM PMSF, 1 mM Benzamidine, 2 μ g/ml Aprotinin, 10 mM Sodium Floride, 2 mM Sodium Orthovanadate, 1 mM Sodium Pyrophosphate, and 2 μ g/ml Leupeptin) for 15 minutes on ice. Cell lysates were centrifuged at 14000 x g for 15 minutes at 4oC. Total protein concentration was determined using Bradford assay with BSA as standard.

j. Western Blot:

30 µg of total protein lysate were mixed with Laemmli buffer and then heated for 5 minutes at 95°C. Protein lysates were separated in 10% polyacrylamide gel (29:1 acrylamide:bis) and then transferred to Nitrocellulose membrane. Membranes were blocked with 5% non-fat milk in TBST1x solution for 1 hour at 37°C. Immunoblot analysis was performed using rabbit anti-rat leptin (ab3583, Abcam), Leptin receptor ObR (ab177469, Abcam), Ctgf (ab6992, Abcam), Actin (ab8227, Abcam) and donkey anti-rabbit IgG coupled to HRP (711-035-152, Jackson Immuno Research). Protein band signals were developed by ChemiDoc MP (Bio-Rad) after activation of the HRP by Clarity™ Western ECL Blotting Substrates (Bio-Rad) according to manufacturer's instructions. The fold change of the proteins is expressed as the ratio of Ctgf relative to GAPDH relative to the non-treated control samples.

k. RNA extraction and RT-qPCR:

After incubation, total RNA from cells was extracted using RiboZol (Amresco) according to the manufacturer's instructions. RNA concentration was measured by Nanodrop 1000 (Thermo Scientific) at 260 nm, and 260/280 ratio was determined. 1 µg of total RNA were reverse transcribed into cDNA using the iScript cDNA synthesis kit, according to manufacturer's instructions. cDNA amplification reaction was performed using the iQ SYBR green mix kit, according to the manufacturer's instructions. Primer sequences for the genes of interest are from TIB Molbiol: Rat GAPDH (Forward:

GGGGCTCTCTGCTCCTCCCTG, Reverse: CGGCCAAATCCGTTACACCG), Rat leptin (Forward: GAGACCTCCTCCATGTGCTG, Reverse: CATTCAAGGGCTAAGGTCCAA), Rat leptin receptor (Forward: TGACCACTCCAGATTCCACA, Reverse: CCACTGTTTTACGTTGCTG), and Rat Ctgf (Forward: CCCCCGCAACCGCAAGATT, Reverse: CGGCCAAATCCGTTACACCG). For each target gene, a standard curve was established by performing a series of 10-fold dilutions. The negative control was made using the same volume of RNase-free water instead of a cDNA. The master mix was prepared as follows: 2x SYBR Green Supermix 12.5 μ l, forward and reverse primer 0.25 μ l respectively, and ddH₂O 12 μ l. For each well, 22 μ l of master mix was loaded first, followed by 3 μ l of the sample, mixed well to get total reaction volume of 25 μ l. For plate setup, SYBR-490 was chosen as a fluorophore. The plate was covered with a sheet of optical sealing film. PCR was performed using the CFX96™ Real-Time PCR Detection System (Bio-Rad) programmed for a 1 min of denaturation at 98°C (1 cycle) initially, followed by 40 alternating cycles of 9 sec denaturation at 95°C, 12 sec annealing at 55°C, and 9 sec extension at 72°C. Finally, one cycle of 10 min extension at 72°C was used. After amplification, samples were subjected to melt curve analysis to check the purity and integrity of amplified samples. The annealing temperature for each gene was optimized in the laboratory. The correlation coefficient is between 0.99-1, PCR efficiency is between 80-120%. Quantification of the genes was calculated by the $\Delta\Delta$ Ct. mRNA levels were expressed relative to GAPDH mRNA.

l. siRNA transfection:

RASMCs were double-transfected with 20 nM Scrambled non-targeting sequences: (UAGCGACUAAACACAUCAA, UAAGGCUAUGAAGAGAUAC, AUGUAUUGGCCUGUAUUAG, AUGAACGUGAAUUGCUCAA), or 80 nM leptin receptor siRNA (target sequences: GGACUGGGUAUUGGAGUA, GGAGAGUUGUUCACACUUU, CGAAUGUCAUGUACCAGUA, GGAAGACACACGAGGUAUU) in serum and antibiotic free media using Xtreme Gene siRNA transfection Reagent, for 6 hours. After the transfection period, 2x serum solution was added and incubated overnight. Cells were then treated and total proteins were extracted as described earlier.

m. Ctgf release from RASMC:

After stimulation, cell media were collected and quantified for total protein content as previously discussed. 30µg of total protein from the media samples was prepared for western blotting analysis as previously discussed. Western blot analysis of Ctgf was performed and reported as fold change of Ctgf to total protein content ratio, relative to control sample.

4. Results:

a. RASMC Proteomic Analysis:

Comparative proteomic profiling of RASMC protein abundance in response to either BK or leptin time point stimulations were done using LC-ESI-MS/MS followed by

MaxQuant analysis of the generated protein spectra. Adopting this approach, 1837 distinct proteins were identified in the control samples of RASMC.

b. Effect of BK stimulation on proteome profile in RASMC:

The effect of time point BK-stimulation (24h or 48h) of RASMC showed a temporal profile of protein expression in response to BK as illustrated in the heat maps (Figure 23A). Although there were more than 1800 identified proteins in the control samples, 70 (3.8%) proteins were significantly modified after 24h of BK stimulation with $p < 0.05$, and of these 28 were upregulated and 44 were downregulated. In addition, 120 (6.5%) proteins were significantly modified after 48h of BK stimulation with $p < 0.05$, and the number of the upregulated and downregulated proteins was almost the same (list of proteins in Tables 6 and 7).

c. Effect of leptin stimulation on proteome profile in RASMC:

The effect of time point leptin-stimulation (24h or 48h) of RASMC showed a temporal profile of protein expression in response to leptin as illustrated in the heat maps (Figure 23B). Although there were more than 1800 identified proteins in the control samples, 189 (10.2%) proteins were significantly modified after 24h of BK stimulation with $p < 0.05$, and of these 108 were upregulated and 81 we downregulated. In addition, 127 (6.5%) proteins were significantly modified after 48h of BK stimulation with $p < 0.05$, and of these 78 were upregulated and 49 we downregulated (list of proteins in Tables 8 and 9).

d. Principal component analysis (PCA):

PCA a derivative of multivariate data analysis, commonly used to reduce multidimensionality kidney of large datasets and discern features that distinguish the different groups was applied to the proteomic profiles of the BK- and leptin-stimulated samples. As shown in Figure 24A & B, PCA efficiently separated the groups, indicating that the proteomic profiles are distinct due to the time point stimulation.

e. Pathway and network analysis of proteomic profiles:

The proteomic profiles of significantly modified proteins in response to time point stimulations with BK or leptin were subjected to Pathway Studio analysis. The results shown in Figure 25A-D offer a graphical representation of the altered canonical pathways of significantly upregulated and downregulated proteins within each tissue and between each group.

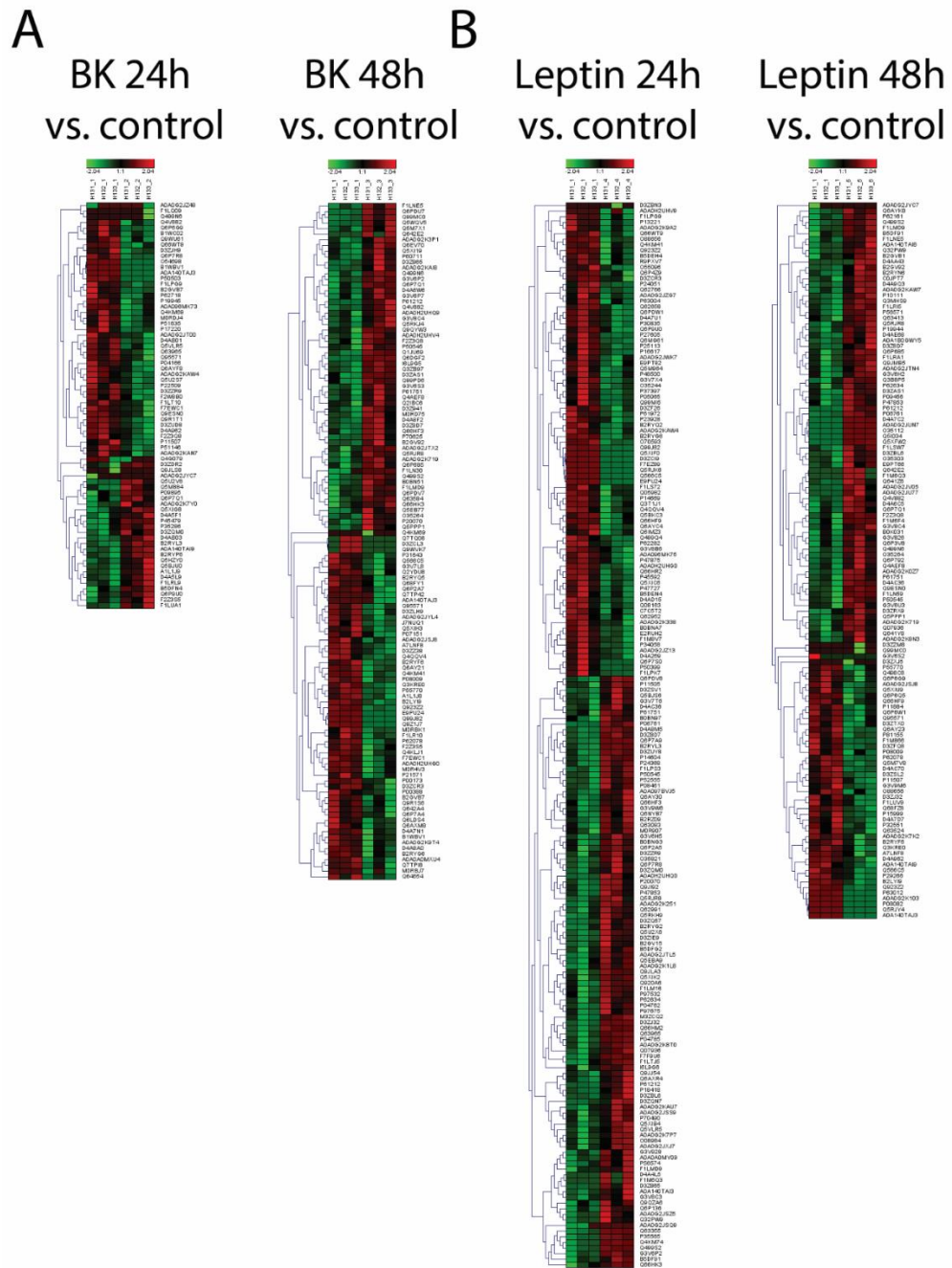


Figure 23: Hierarchical clustering (heat maps) of protein expression profiles in RASM cells stimulated by (A) BK (24h or 48h) and (B) Leptin (24h or 48h). Green color represents downregulation of protein expression, whereas the red color represents upregulation of protein expression. Color intensity reflects the expression level of the proteins. The label on the right-hand side of the heat maps represents the accession number of the proteins.

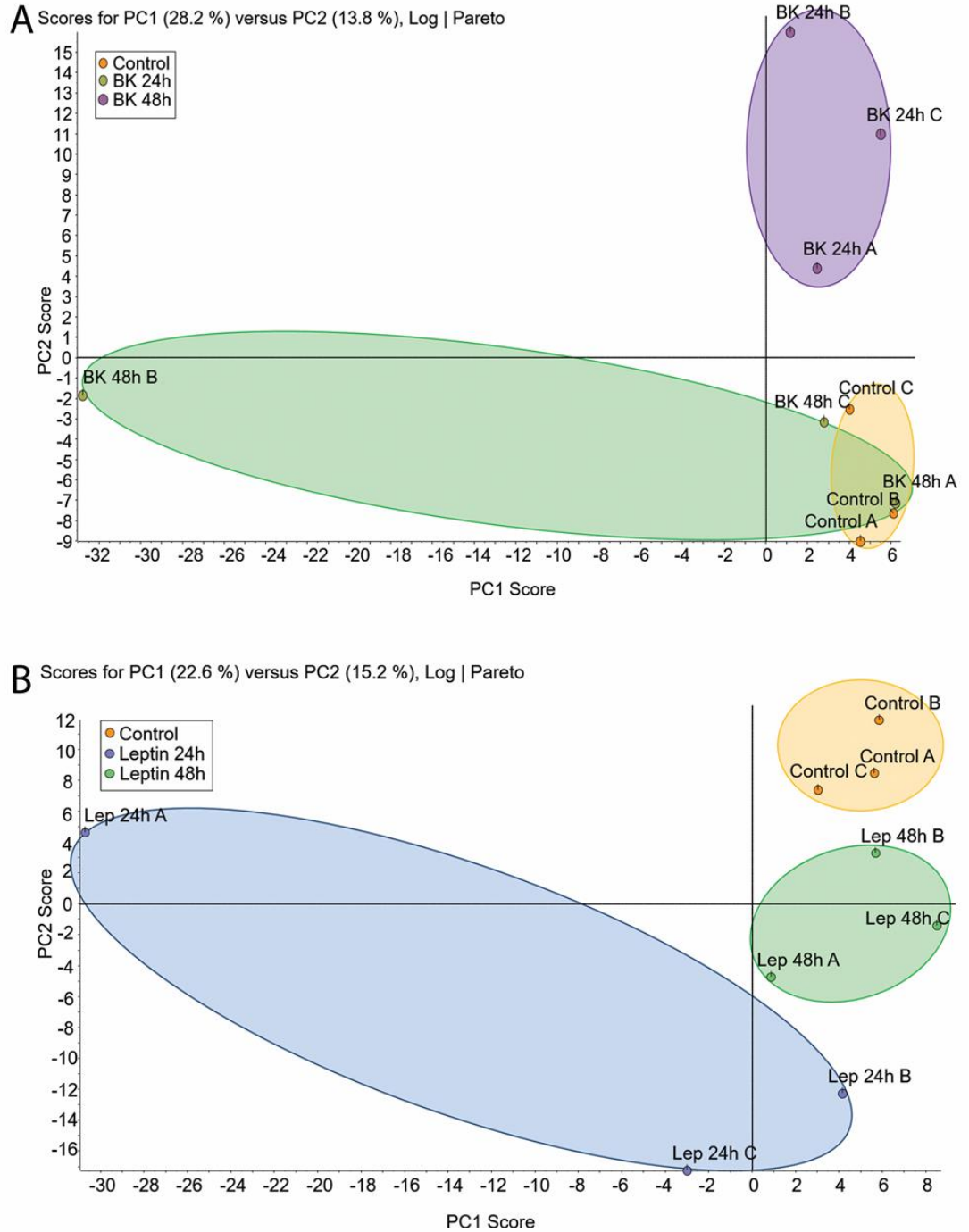


Figure 24: Principal Component Analysis (PCA) of the BK-stimulated (A) and Leptin-stimulated (B) RASMCM samples. The total normalized expression data of the proteins was used to depict the scatter plots of the first (X) and the second (Y) principal components. The numbering of the nodes is an identification of the samples. Letters used in the labels of the nodes represent the repeat. Yellow oval encircles the control samples, violet oval encircles the BK 24h stimulated samples, green oval encircles the BK 48h stimulated samples, blue oval encircles leptin 24h stimulated samples, and pale green oval encircles the leptin 48h stimulated samples.



Figure 25: Canonical Pathways of the comparative groups in the BK-stimulated and leptin-stimulated RSMC samples. A: Top Canonical pathways related to proteins altered in the BK 24h stimulated vs. control samples. B: Top Canonical Pathways related to proteins altered in the BK 48h stimulated vs. control samples. C: Top Canonical Pathways related to proteins altered in the leptin 24h stimulated vs. control samples. D: Top Canonical Pathways related to proteins altered in the kidney of the leptin 48h stimulated vs. control samples. Bars show the total number of proteins identified in each pathway. The green color represents the down-regulated proteins, and the red color represents the upregulated proteins.

Network analysis of BK stimulation for 24h compared to control (Figure 26) depicted that Leptin receptor (LEPR) (1.83 ± 0.21 -fold, $p=0.005$) and Ras-related protein Rab-13 (RAB13) (1.168 ± 0.06 -fold, $p=0.04$) were upregulated by the BK stimulation and they were connected to the activation of PI3K, Lep, IGF1, and STAT3. In addition, network analysis showed that the modified proteins possessed many cardiovascular disease risk factors such as hypertrophy, fibrosis, and obesity.

Network analysis of the effect of BK stimulation for 48h compared to control (Figure 27), showed that Caveolin (Cav1) (1.74 ± 0.23 -fold, $p=0.047$), Zonula occludens 2 protein (ZO-2) (1.47 ± 0.26 -fold, $p=0.023$), Prostaglandin G/H synthase 1 (Ptgs1) (1.45 ± 0.12 -fold, $p=0.034$), Synaptopodin (Synpo) (1.41 ± 0.15 -fold, $p=0.037$), Ptges3 protein (Ptges3) (1.37 ± 0.27 -fold, $p=0.049$), and Transforming growth factor beta-1-induced transcript 1 protein (Tgfb1i1) (1.28 ± 0.05 -fold, $p=0.022$) were upregulated and connected to the leptin receptor (LEPR), CTGF, Fn1, CFL1, and SphK1, while Vasodilator-stimulated phosphoprotein (Vasp) and Tropomyosin 1, alpha (Tpm1) were downregulated.

Network analysis of the effect of leptin stimulation for 24h compared to control (Figure 28), showed that Collagen type IV alpha 2 chain (Col4a2) ($3.53\pm .35$ -fold, $p=0.027$) and Plasminogen activator inhibitor 1 (Serpin1) (1.65 ± 0.14 -fold, $p=0.028$) were upregulated, while Cofilin-1 (Cfl1) (0.77 ± 0.06 -fold, $p=0.009$), Peroxiredoxin-6 (Prdx6) (0.69 ± 0.13 -fold, $p=0.023$), Tropomyosin 1, alpha (Tpm1) (0.42 ± 0.69 -fold, $p=0.035$), Myosin light chain 10 (Myl10) (0.12 ± 0 -fold, $p=0.003$) were downregulated.

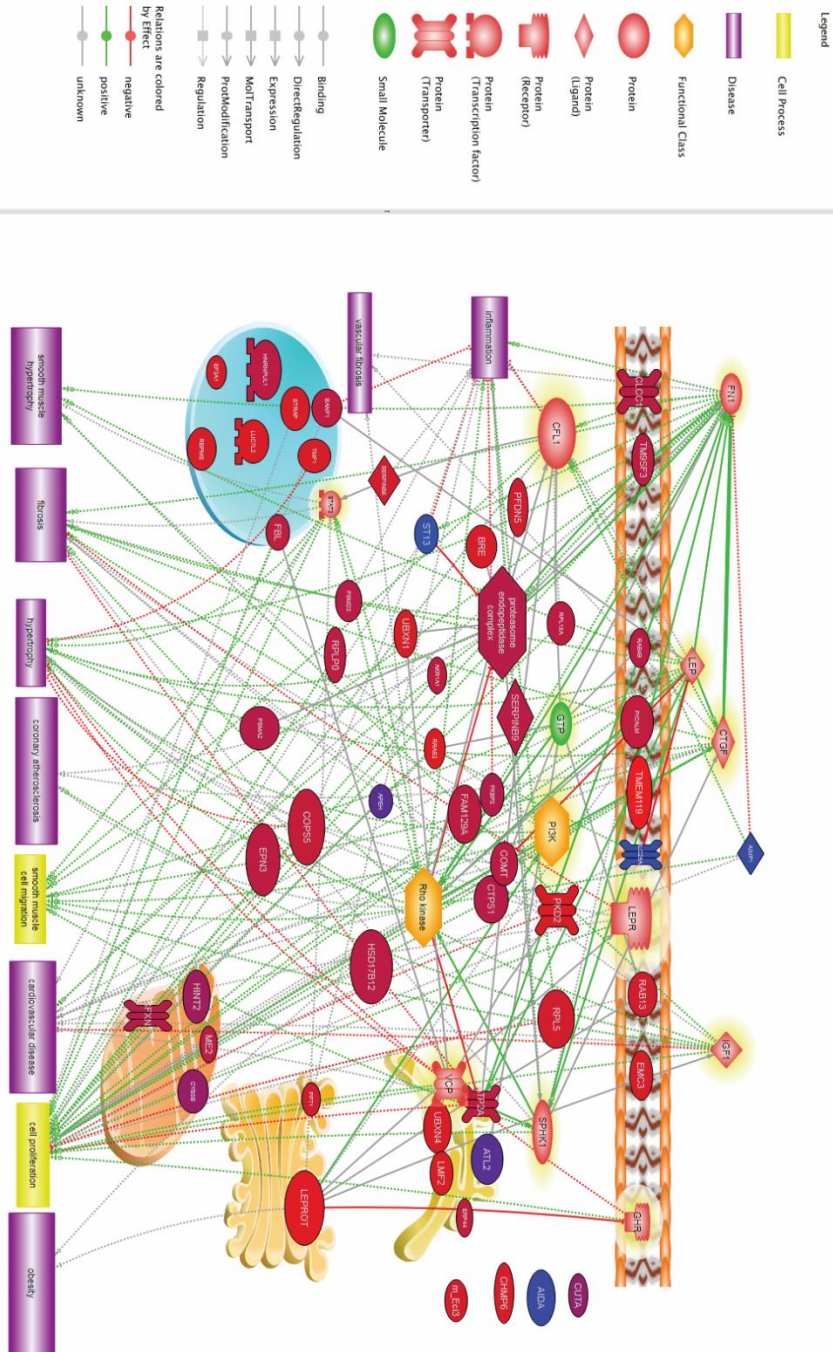


Figure 26: Pathway studio network analysis of the modified proteins in response to BK 24h treatment relative to control in RASM. **A:** The top diseases related to the modified proteins are smooth muscle hypertrophy, fibrosis, coronary atherosclerosis, inflammation, vascular fibrosis, cardiovascular disease, and obesity. The cellular processes related to the modified proteins are smooth muscle migration and cell proliferation. The main regulated proteins connected in this network were LEPROT and RAB13, which are predicted to have a relation with LEPR, PI3K, IGF1, LEP, and STAT3. Red color indicates an upregulated protein, and blue color indicates a down-regulated proteins. The color intensity represents the level of expression.

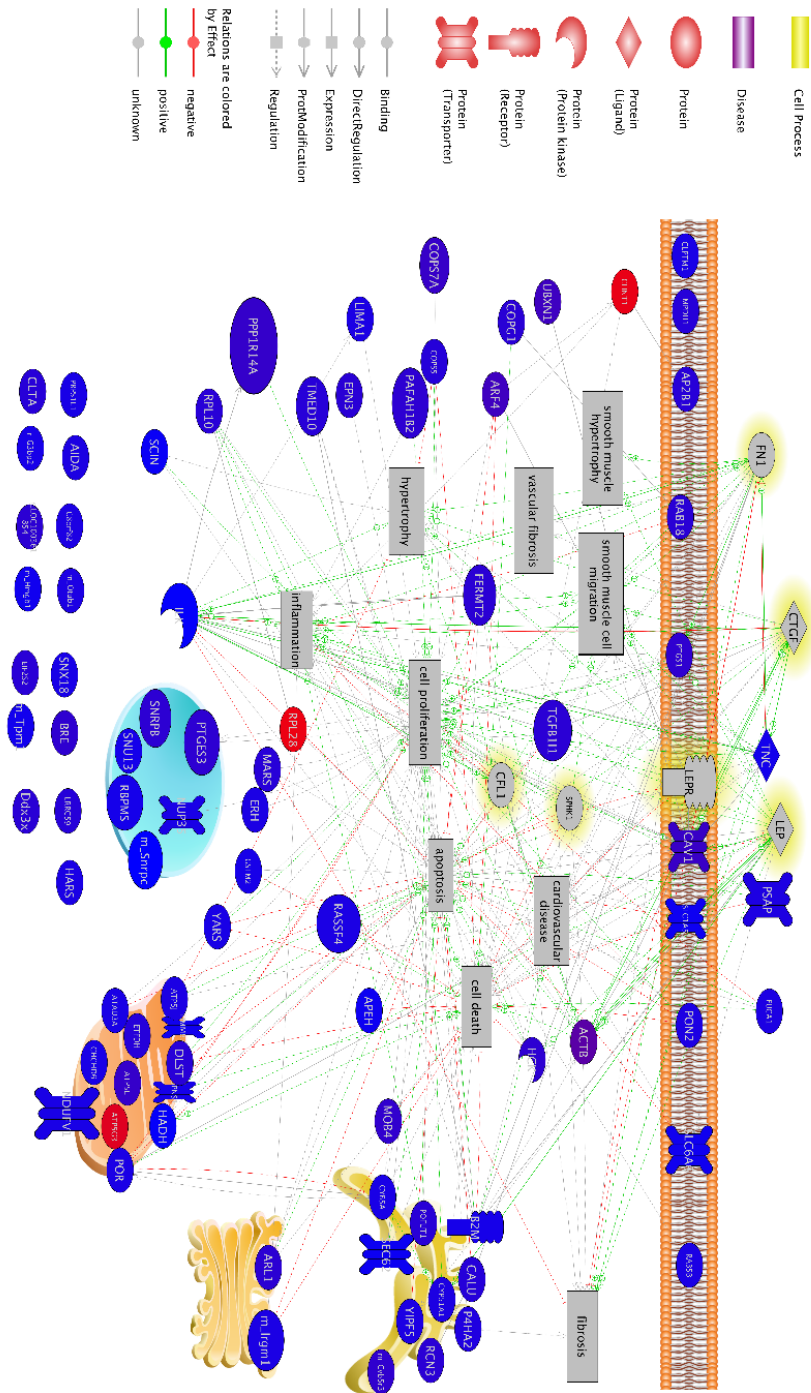


Figure 27: Pathway studio network analysis of the modified proteins in response to BK 48h treatment relative to control in RASMC. **A:** The top diseases related to the modified proteins are smooth muscle hypertrophy, fibrosis, inflammation, vascular fibrosis, and cardiovascular disease. The cellular processes related to the modified proteins are smooth muscle migration, cell proliferation, apoptosis, and cell death. The main regulated proteins connected in this network were PTGS1 and PTGS3, which are predicted to have a relation with LEP and Fn1. Red color indicates an upregulated protein, and blue color indicates a down-regulated proteins. The color intensity represents the level of expression.

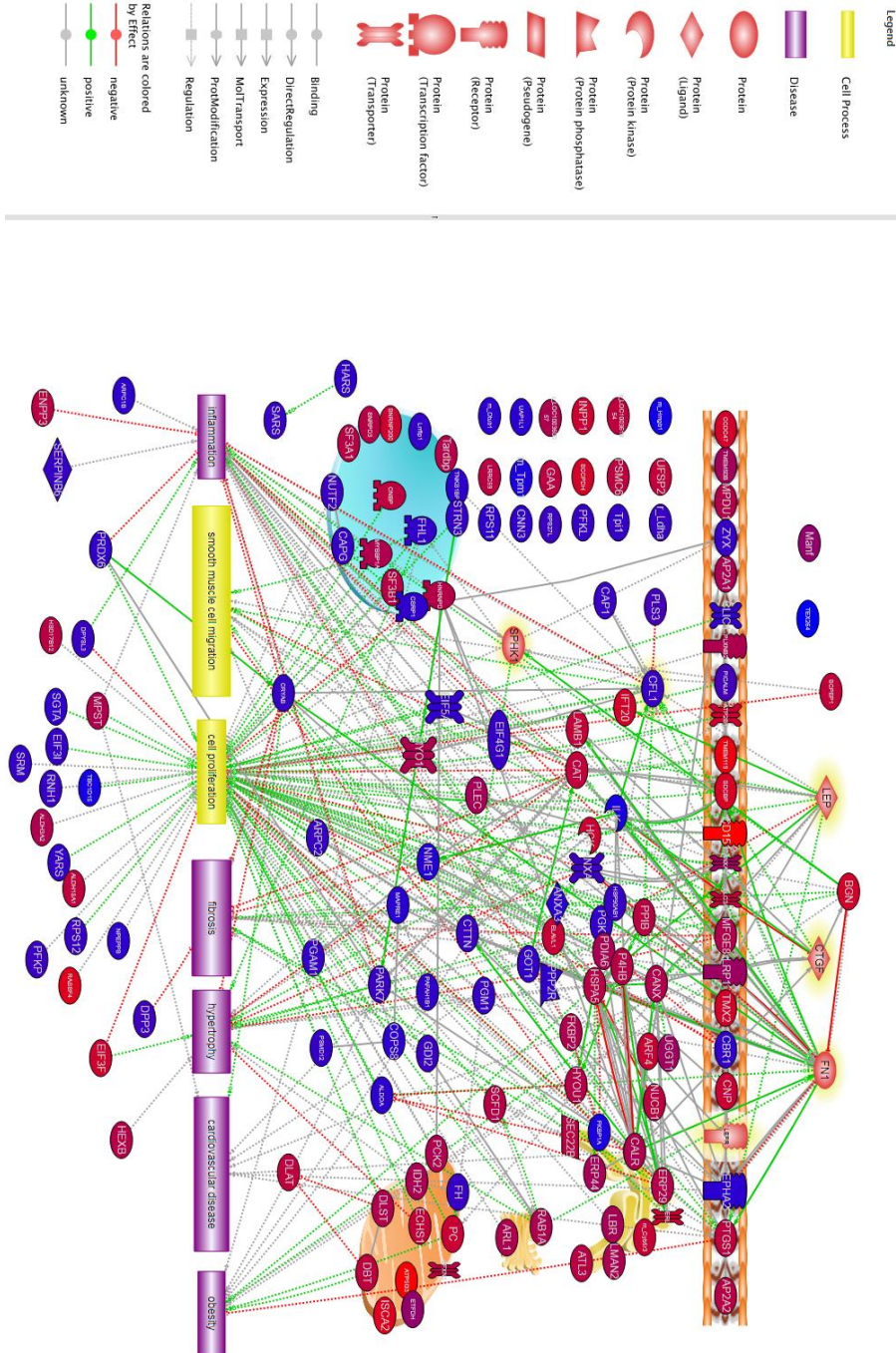


Figure 28: Pathway studio network analysis of the modified proteins in response to leptin 24h treatment relative to control in RASM. **A:** The top diseases related to the modified proteins are hypertrophy, fibrosis, inflammation, obesity, and cardiovascular disease. The cellular processes related to the modified proteins are smooth muscle migration and cell proliferation. The main regulated proteins connected in this network were CFL1 and ILK, which are predicted to have a relation with LEP and CTGF. Red color indicates an upregulated protein, and blue color indicates a down-regulated proteins. The color intensity represents the level of expression.

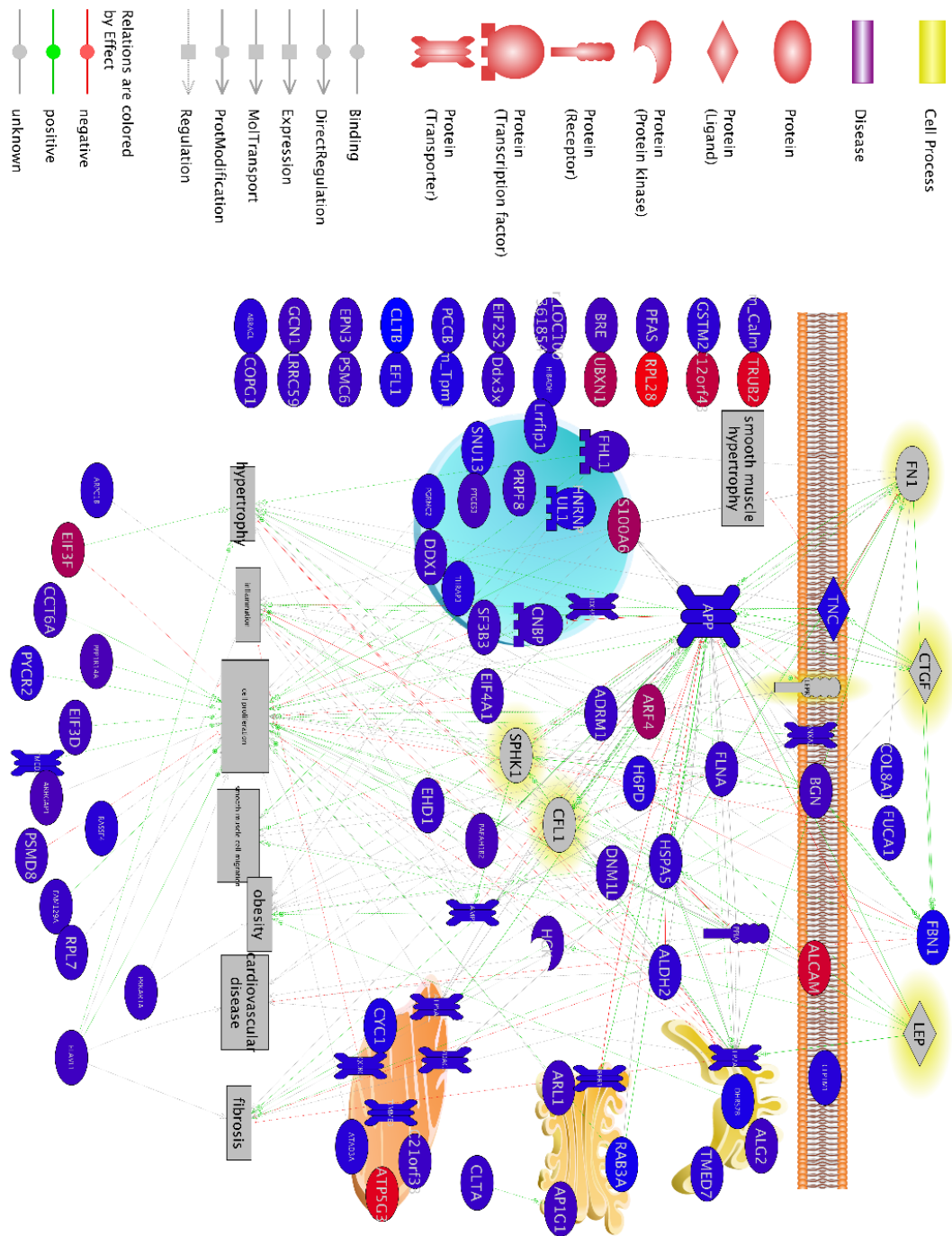


Figure 29: Pathway studio network analysis of the modified proteins in response to leptin 24h treatment relative to control in RASM. **A:** The top diseases related to the modified proteins are smooth muscle hypertrophy, fibrosis, inflammation, obesity, and cardiovascular disease. The cellular processes related to the modified proteins are smooth muscle migration and cell proliferation. The main regulated proteins connected in this network were APP, HSPA5 and FBN1, which are predicted to have a relation with Fn1 and CTGF. Red color indicates an upregulated protein, and blue color indicates a down-regulated proteins. The color intensity represents the level of expression.

Network analysis of the effect of leptin stimulation for 48h compared to control (Figure 29) showed that Thioredoxin reductase 1 (Txnrd1) (8.13 ± 0.23 -fold, $p=0.0006$), Collagen type IV alpha 2 chain (Col4a2) (1.97 ± 0.97 -fold, $p=0.015$), Ptges3 protein (Ptges3) (1.43 ± 0.24 -fold, $p=0.023$), and Tyrosine-protein kinase HCK (Hck) (1.40 ± 0.11 -fold, $p=0.021$) were upregulated. Moreover, Leptin receptor overlapping transcript-like 1 (Leprotl1) (0.76 ± 0.14 -fold, $p=0.039$), Collagen alpha-1(VIII) chain precursor (Col8a1) (0.73 ± 0.037 -fold, $p=0.009$), Tropomyosin 1, alpha (Tpm1) (0.56 ± 0.06 -fold, $p=7.9788E-05$), and Fibrillin-1 precursor (Fbn1) (0.31 ± 0.27 -fold, $p=0.035$) were downregulated.

f. BK induced leptin and leptin receptor expression in RASMC:

In our previous work, we observed an upregulation of Leptin receptor upon assessing the proteomic profile of RASMC in response to BK time points. To validate this observation, we assessed the effect of BK on the expression of leptin and leptin receptor in RASMC stimulated with BK. Results in **Figure 30** showed an increase mRNA levels of leptin (6.85 ± 0.71 -fold at 6h with $p=0.01$ and 4.1 ± 0.81 -fold at 24h with $p=0.028$) and leptin receptor ObRb (3.67 ± 0.46 -fold at 6h with $p=0.01$ and 3.48 ± 0.75 -fold at 24h with $p=0.028$). In addition, BK stimulated the protein expression of leptin (1.64 ± 0.43 -fold at 6h with $p=0.03$ and 2.5 ± 0.37 -fold at 24h with $p=0.006$) and leptin receptor ObR (2.5 ± 0.27 -fold at 24h with $p=0.008$) in RASMC.

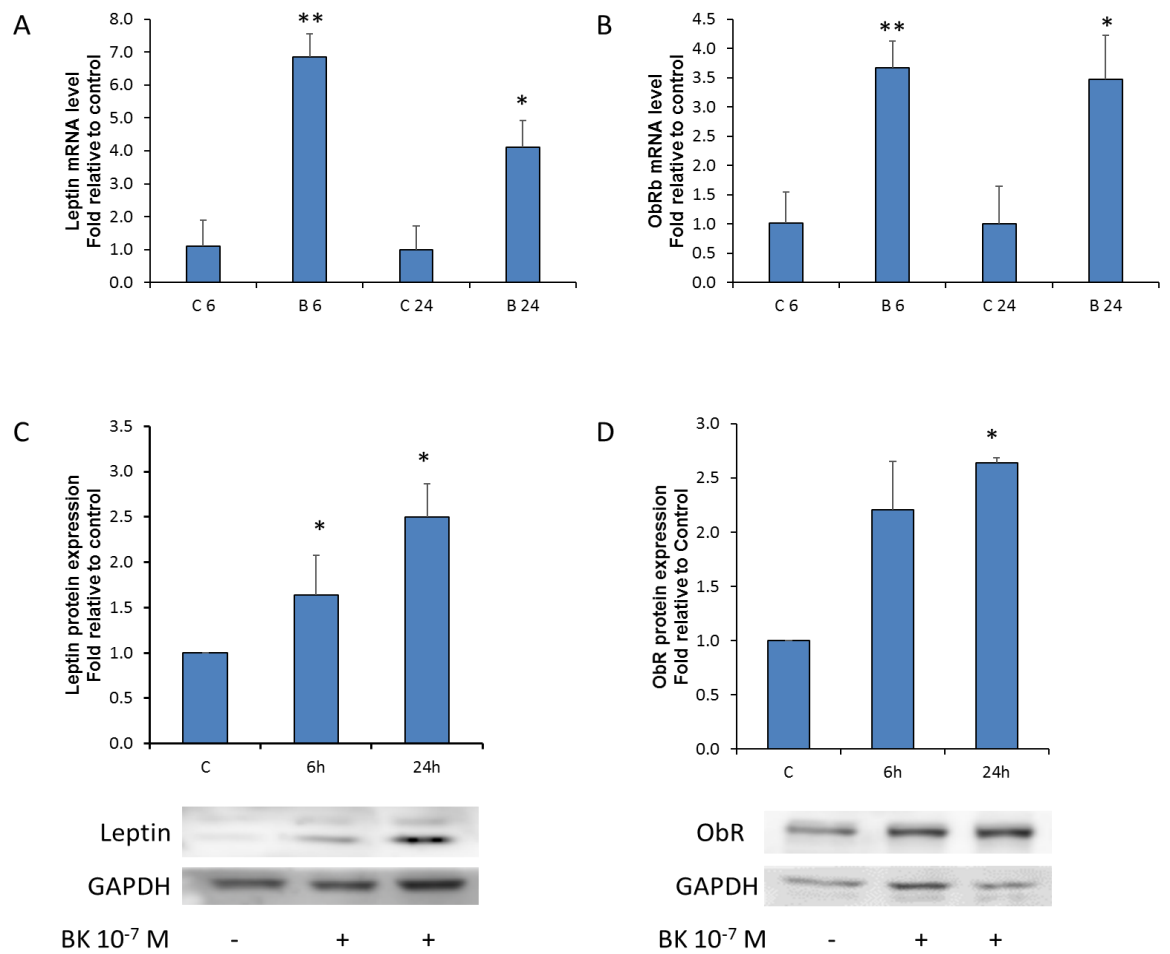


Figure 30: *BK* induced leptin and leptin receptor expression in RASMC. Quiescent RASMC were stimulated with BK (10^{-7} M) for 6 and 24 h. A: Leptin and GAPDH mRNA levels were measured by RT-qPCR and leptin fold change is represented in the Bar graph (6.85 ± 0.71 -fold, ** BK 6 vs. C6, $n=4$, $p=0.01$, and 4.1 ± 0.81 -fold, * BK 24 vs C 24 $p=0.028$, Student t.test, $n=5$). B: Leptin receptor and GAPDH mRNA levels were measured by RT-qPCR, and leptin receptor fold change is represented in the Bar graph (3.67 ± 0.46 -fold, ** BK 6 vs. C6, $n=5$, $p=0.01$, and 3.48 ± 0.75 -fold, * BK 24 vs C 24 $p=0.028$, Student t.test, $n=5$). C: Leptin and Actin protein levels were measured by Western blot, and leptin fold change is represented in the Bar graph (1.64 ± 0.43 -fold, * BK 6 vs. C, $n=4$, $p=0.03$, and 2.5 ± 0.37 -fold, * BK 24 vs C $p=0.006$, Student t.test, $n=4$). D: Leptin receptor and Actin protein levels were measured by Western blot, and leptin receptor fold change is represented in the Bar graph (2.5 ± 0.27 -fold, * BK 24 vs C $p=0.008$, Student t.test, $n=4$).

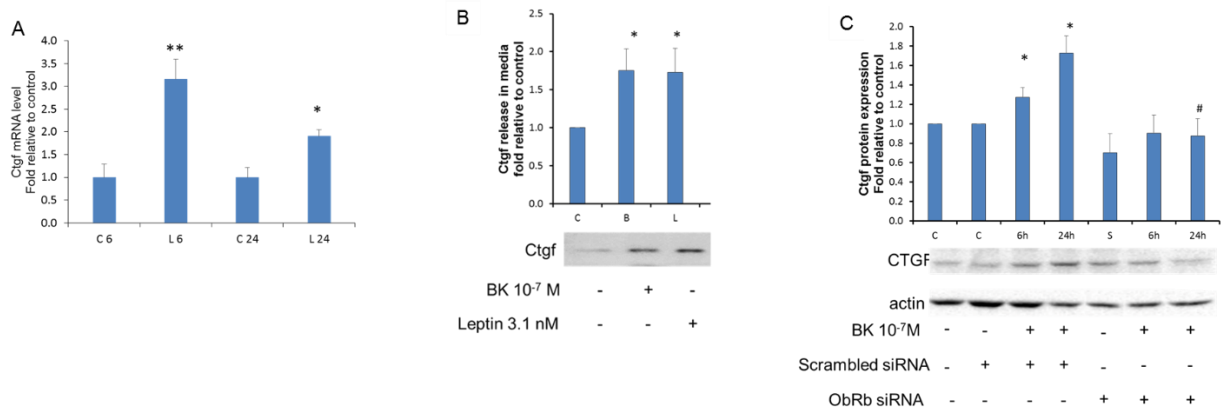


Figure 31: Leptin receptor signaling is a mediator of BK-induced Ctgf expression. A: Quiescent RASMC were stimulated with leptin (3.1 nM) for 6 and 24h. Ctgf and GAPDH mRNA levels were measured by RT-qPCR and Ctgf fold change is represented in the Bar graph (3.16±0.43-fold, ** Lep 6 vs. C6, n=6, p=0.004, and 1.91±0.14-fold, * Lep 24 vs C 24 p=0.013, Student t.test, n=4). B: Quiescent RASMC were stimulated with BK (10⁻⁷M) or leptin (3.1 nM). Ctgf protein release from RASMC was measured by Western blot and Ctgf to total protein loading fold change is represented in the Bar graph (1.75±0.28-fold, * BK 24h vs. C, n=3, p=0.027, 1.73±0.32-fold, * Lep 24h vs. C, n=3, p=0.042, Student t.test). C: Quiescent RASMC were stimulated with BK (10⁻⁷M) in the presence and absence of scrambled siRNA, or Leptin receptor siRNA. Ctgf and Actin protein levels were measured by Western blot and Ctgf fold change is represented in the Bar graph (1.66±0.28-fold, * BK 6h+ scrambled siRNA vs. C, n=4, p=0.024, 2.48±0.2-fold, * BK 24h + scrambled siRNA vs. C, n=4, p=0.009, and 0.98±0.14-fold, # BK 24h + ObR siRNA vs. BK 24h + scrambled siRNA, n=4, p=0.012, Student t.test).

g. Leptin induced CTGF, Fn1, and NOX1 expression in RASMC:

We sought the effect of leptin stimulation in RASMC. We first checked the effect of leptin time points on the expression Ctgf as a fibrotic marker. Results in Figure 31A showed that leptin increased the mRNA levels of Ctgf (3.16±0.43-fold at 6h with p=0.004 and 1.91±0.14-fold at 24h with p=0.013) in RASMC. In addition, BK and leptin stimulated the protein release of Ctgf (1.75±0.28-fold by BK, p=0.027, and 1.73±0.32-fold by leptin, p=0.42) to the extracellular space of the RASMC after 24h stimulation (Figure 31B). Finally, we explored the involvement of leptin receptor as a mediator of BK response on Ctgf expression. We uses leptin receptor specific siRNA to knock down the expression of Leptin receptor in RASMC. Results presented in **Figure 31C** showed that knocking down

the expression of leptin receptor dampened the BK-induced expression of Ctgf (from 2.48±0.2 to 0.98±0.14-fold at 24h with p=0.012).

5. Discussion:

Atherosclerosis continues to be the major contributor of CVD and its exact mechanisms of development are not well defined. Employing proteomic approaches to study the global protein profile modification in different pathologies proved the strength of this approach over other global profiling approaches, such as genomics and transcriptomics, for the significance of studying the relationship of diseases and the biochemical end-product, i.e. the protein. In addition, proteomic approaches aided in the discovery of biomarkers of diseases or their etiology or stage [353,354]. In this study, LC MS/MS technique was employed to assess the global protein modifications in primary RASMC stimulated for two-time points (24 and 48 h) with either BK or leptin. In addition, systems biology analysis was used to link the modified proteins, and to point on the biological processes that they have a link with.

Our data showed that time is a factor affecting the BK or leptin stimulation in VSMC as evidenced by the number of modified proteins, compared to control, in BK or leptin stimulated conditions. For instance, there were more proteins modified after 48h stimulation by BK compared to the 24h stimulated samples. In addition, the altered canonical pathways of BK time points showed different modified pathways between the two conditions. After 24h stimulation, BK induced an increase in the activity of Ceramide degradation and Sphingosine and Sphingosine-1-phosphate metabolism, which is pointing to the involvement of the SphK/S1P pathway in the signaling pathway of BK (Figure 25A).

We have previously demonstrated the involvement of SphK1/S1pr1 as mediator of the signaling process of BK to promote the expression of fibrotic markers [424]. Whereas, after 48h stimulation, BK induced the activity of the signaling of the Rho Family GTPases (Figure 25B).

On the other hand, the pattern of modified proteins in response of the time point stimulations by leptin was different. For instance, stimulating VSMC with leptin for 24h modified more protein than at 48h time point. In addition, the altered canonical pathways of leptin time points showed different modified pathways between the two conditions. For example, leptin 24h stimulated the regulation of actin-based motility by Rho among other pathways. The involvement of Rho-A signaling downstream leptin receptor (ObRb) is well established in the literature [425] (Figure 25C). Moreover, leptin 48h stimulation showed a different pattern of altered pathways (Figure 25D).

To further comprehend the effects of BK or leptin time points stimulation in RASMC, we linked the modified proteins with their biological processes and the diseases that they may be involved in development. For instance, we have observed an increase in the expression of Leptin receptor ObR after 24h BK stimulation and a decrease in vasodilator-stimulated phosphoprotein (VASP) after 24 and 48h of BK stimulation. This is the first report in the literature to describe the regulation of leptin receptor and VASP in response to BK. In one of the reports, Nevelsteen et al. studied the involvement of leptin or leptin receptor in the BK-induced vasorelaxation in aortic rings. They have demonstrated that the genetic ablation of leptin or its receptor aggravated the endothelial dysfunction and dampened the vascular reactivity of BK [426]. As for the VASP activity, it has been reported that VASP is a requirement for endothelial cells to promote vasodilatation in

mesenteric arteries [427]. Our data shows that BK induces a down-regulation of VASP expression in RASMC, which is an indication for the aggravation of vasodilatation impairment upon the direct effect of BK on VSMC.

In addition, we observed an increase in TGF β post BK stimulation for 48h. This finding of the regulation of TGF β downstream of BK stimulation is in line with our previous reports. We have previously shown that BK promotes vascular fibrosis through the induction of ECM protein expression and secretion of Tissue Inhibitor of Metalloproteinase 1 (TIMP1) via TGF β pathway [410].

Moreover, our results show an upregulation of Ptg1 (COX1) in VSMC, indicating to the relationship between BK and inflammation. COX1 induces platelets activation and aggregation through the production of thromboxane A2 [428]. In addition, thromboxane A2 produced in VSMC can be released to the circulation to activate platelets [429]. Furthermore, thromboxane A2 was shown to induce cell proliferation and migration of VSMC [430].

On the other hand, upon analyzing the protein modifications of the leptin stimulated samples, we observed an induction of collagen IV alpha 2 protein at the two time points of leptin treatment. Previous reports have shown the importance of collagen IV protein to transduce the mechanical stretching effects from the extracellular matrix area into a signal transduction intracellularly. Additionally, they have shown that this mechanotransduction communication is RhoA dependent in VSMC. Moreover, the increase in Collagen IV expression is reflective of an increase of stress fiber and focal adhesion rearrangement in VSMC, and the rearrangement of the ECM protein components in the development of vascular fibrosis [410,425,431].

Furthermore, leptin stimulation showed a down regulation in the expression of cofilin-1 and Peroxiredoxin-6 expression. The downregulation of cofilin goes in line with the well-established role of leptin in actin remodeling. Leptin activates RhoA-LIMK pathway to phosphorylate and inhibit the activity of cofilin. Active, non-phosphorylated, cofilin catalyzes the actin depolarization from the filamentous form into the globular form [432]. Leptin, upon inhibiting cofilin, preserves the filamentous type of actin aiding the functions of actin polymerization in mobility and proliferation [433]. The downregulation of cofilin by leptin, is another pathway by which leptin regulates actin remodeling in VSMC. On the other hand, the downregulation of peroxiredoxin-6 is a mechanism of oxidative stress promotion by leptin in VSMC [434]. This mechanism is not well-established and worth to be further investigated.

One remarkable finding of this study is the downregulation of tropomyosin in response to each BK and leptin at both time points. Previously, King-Briggs et al. studies have found a reduction of VSMC tropomyosin because of balloon-induced carotid injury. In addition, these studies have linked the vascular injury to TGF β pathway [435].

Another remarkable finding of this study is the upregulation of leptin and leptin receptor in response to BK stimulation in VSMC. The regulation of leptin and leptin receptor by BK in RASMC is, to our knowledge, the first report to show and validate the regulatory effect of BK on leptin and leptin receptor expression. Previously, Abe et al. have shown that the genetic ablation of leptin in ob/ob mouse model is associated with an increased mRNA expression of Bdkrb1 in some of the mouse tissues, such as adipose tissue, liver, abdominal aorta, and stomach [436]. In addition, Chiu et al. have shown that leptin expression in cardiomyocytes is induced by AngII, ROS, and ERK activity [437].

Moreover, inhibiting ROS production, by using Ursolic acid, dampened the leptin-mediated atherogenesis [438]. ROS generation was shown to be downstream of BK and leptin stimulation, and it is a requirement for ERK activation downstream of these two systems.

On the other hand, leptin induced the expression of one of the fibrotic markers in RASMC. For instance, leptin induced Ctgf expression, which is in line with previous reports investigating the effect of leptin on vascular fibrosis in the aorta and the heart [439,440]. The involvement of Ctgf in different pathophysiological conditions has been documented in different studies. Mainly, Ctgf was linked to the development of vascular fibrosis, and subsequently atherosclerosis [278]. Moreover, type1 diabetic patients presented with high renal and cardiovascular risk exhibited high Ctgf circulating levels [415]. Furthermore, there is a strong evidence in the literature that Ctgf expression is regulated by TGF β downstream of BK receptor [292,300].

Taken together, our global proteomic profile in response to BK stimulation showed an induction in leptin receptor, fibrotic proteins, and inflammatory protein expression. On the other hand, leptin stimulation induced ECM proteins and reduced actin remodeling proteins. Furthermore, the results show an evidence of the BK receptor and leptin receptor cross talk to modulate actin remodeling and induce vascular fibrosis in VSMC.

SUPPLEMENTARY DATA FOR CHAPTER FOUR

Table 6: Comparative list of proteins in the BK-stimulated for 24h compared to controls.

Number	Accession	Name	p-value	Fold change
1	B2RYL3	Tmem119 - Transmembrane protein 119 precursor	0.002	6.18
2	A0A140TAI9	Leprotl1 - Leptin receptor overlapping transcript-like 1	0.006	1.83
3	Q9JLS8	Leprot - Leptin receptor gene-related protein	0.040	1.82
4	D4A5L9	LOC690675 - Electron carrier protein	0.033	1.66
5	Q5BJU0	Rras2 - Ras-related protein R-Ras2	0.044	1.62
6	B2RYP6	Luc7l2 - LUC7-like 2	0.011	1.56
7	A1L1J9	Lmf2 - Lipase maturation factor 2	0.020	1.51
8	F1LRL9	Map1b - Microtubule-associated protein 1B	0.045	1.50
9	D4AB03	Fam120a - Constitutive coactivator of PPAR-gamma-like protein 1	0.007	1.44
10	Q499N6	Ubxn1 - UBX domain-containing protein 1	0.023	1.40
11	Q5HZY0	Ubxn4 - UBX domain-containing protein 4	0.036	1.39
12	D4A5F1	Pkd2 - Polycystin-2	0.036	1.38
13	Q6P7Q1	Bre - BRCA1-A complex subunit BRE	0.042	1.35
14	Q5U2V8	Emc3 - ER membrane protein complex subunit 3	0.003	1.35
15	F2Z3S5	Rbpms - RNA-binding protein with multiple-splicing	0.050	1.32
16	A0A0G2JZ48	Tmf1 - TATA element modulatory factor 1	0.012	1.31
17	Q5XIG8	Strap - Serine-threonine kinase receptor-associated protein	0.024	1.30
18	A0A0G2JYC7	Hdgfrp2 - Uncharacterized protein	0.035	1.30
19	F1LUA1	Eea1 - Early endosome antigen 1	0.050	1.28
20	D3ZDR2	Chmp6 - Charged multivesicular body protein 6	0.030	1.27
21	Q5M884	Eci3 - enoyl-Coenzyme A delta isomerase	0.025	1.23
22	Q6P9U0	Serpib6 - Serpin B6	0.040	1.20
23	D3ZQM0	Sf3a1 - Splicing factor 3A subunit 1	0.049	1.18

24	A0A0G2K7Y0	Cr1l - Complement component receptor 1-like protein	0.042	1.18
25	P35286	Rab13 - Ras-related protein Rab-13	0.040	1.17
26	P09895	Rpl5 - 60S ribosomal protein L5	0.040	1.17
27	B5DFN4	Pfdn5 - Prefoldin 5	0.038	1.12
28	P45479	Ppt1 - Palmitoyl-protein thioesterase 1	0.015	1.09
29	Q4KM69	Cops5 - COP9 (Constitutive photomorphogenic) homolog, subunit 5 (Arabidopsis thaliana)	0.034	0.93
30	Q66WT9	Picalm - Clathrin-assembly lymphoid myeloid leukemia protein	0.011	0.87
31	P11507	Atp2a2 - Sarcoplasmic/endoplasmic reticulum calcium ATPase 2 isoform b	0.036	0.87
32	P51635	Akr1a1 - Alcohol dehydrogenase [NADP(+)]	0.037	0.87
33	Q9R1T1	Banf1 - Barrier-to-autointegration factor	0.003	0.86
34	Q5VLR5	Erp44 - Endoplasmic reticulum resident protein 44 precursor	0.026	0.86
35	A0A0G2KAN7	Gls - Glutaminase kidney isoform, mitochondrial	0.049	0.86
36	P22509	Fbl - rRNA 2'-O-methyltransferase fibrillar	0.031	0.86
37	A0A0G2KAW4	Thop1 - Thimet oligopeptidase	0.024	0.85
38	F2Z3Q8	Kpnb1 - Importin subunit beta-1	0.049	0.85
39	P19945	Rplp0 - 60S acidic ribosomal protein P0	0.027	0.84
40	D3ZUD8	Tm9sf3 - Protein Tm9sf3	0.009	0.84
41	Q9ESN0	Fam129a - Protein Niban	0.048	0.83
42	P62718	Rpl18a - 60S ribosomal protein L18a	0.041	0.83
43	Q4V882	Epn3 - Epsin-3	0.012	0.83
44	D3ZJH9	Me2 - Malic enzyme	0.019	0.83
45	D4A962	Hnrnpul1 - Heterogeneous nuclear ribonucleoprotein U-like protein 1	0.032	0.83
46	F7EWC1	Vasp - Vasodilator-stimulated phosphoprotein	0.034	0.82
47	F2W8B0	Comt - Catechol-O-methyltransferase	0.046	0.82
48	Q95571	RT1.A(u) - RT1.A(U) alpha chain	0.042	0.81
49	Q6AYF8	Serpib9 - Serpin B9	0.031	0.81

50	Q9WU61	Clcc1 - Chloride channel CLIC-like protein 1 precursor	0.046	0.81
51	P51146	Rab4b - Ras-related protein Rab-4B	0.017	0.81
52	Q6P7R8	Hsd17b12 - Estradiol 17-beta-dehydrogenase 12	0.003	0.81
53	F1LPG9	Washc2c - WASH complex subunit 2C	0.014	0.79
54	Q5U2S7	Psmc3 - 26S proteasome non-ATPase regulatory subunit 3	0.039	0.79
55	A0A096MK73	Stmn1 - Stathmin	0.035	0.78
56	B1WC02	Ctps - CTP synthase 1	0.028	0.78
57	P17220	Psmc2 - Proteasome subunit alpha type-2	0.048	0.78
58	Q63965	Sfxn1 - Sideroflexin-1	0.025	0.77
59	D3ZZR9	Fkbp2 - Peptidyl-prolyl cis-trans isomerase FKBP2 precursor	0.016	0.76
60	Q6P6G9	Hnrnpa1 - Heterogeneous nuclear ribonucleoprotein A1	0.009	0.76
61	M0RDJ4	Gmfb - Glia maturation factor beta	0.030	0.76
62	F1LT10	Afdn - Afadin	0.044	0.73
63	D4AB01	Hint2 - Histidine triad nucleotide binding protein 2	0.007	0.69
64	P04166	Cyb5b - Cytochrome b5 type B	0.020	0.68
65	A0A0G2JT00	Cuta - Divalent cation tolerant protein CUTA, isoform CRA_c	0.038	0.68
66	B2GVB7	Apeh - N-acylaminoacyl-peptide hydrolase	0.026	0.64
67	F1LQ09	Atl2 - ADP-ribosylation factor-like 6 interacting protein 2	0.004	0.64
68	A0A140TAJ3	Fubp1 - Far upstream element-binding protein 1	0.014	0.22
69	B1WBV1	Aida - Axin interactor, dorsalization-associated protein	0.010	0.21
70	Q4G079	Aimp1 - Aminoacyl tRNA synthase complex-interacting multifunctional protein 1	0.011	0.20
71	O54698	Slc29a1 - Equilibrative nucleoside transporter 1	0.005	0.15
72	P50503	St13 - Hsc70-interacting protein	0.040	0.07

Table 7: Comparative list of proteins in the BK-stimulated for 48h compared to controls.

Number	Accession	Name	p-value	fold change
1	F1LN30	Sumo4 - Small ubiquitin-related modifier	0.000	32.60
2	Q642E2	Rpl28 - 60S ribosomal protein L28	0.046	11.82
3	Q6DGF2	Clint1 - Clathrin interactor 1	0.002	10.22
4	Q499S2	Atp5g3 - ATP synthase F(0) complex subunit C3, mitochondrial	0.003	6.78
5	P60711	Actb - Actin	0.032	2.40
6	P61751	Arf4 - ADP-ribosylation factor 4	0.035	1.92
7	Q499N6	Ubxn1 - UBX domain-containing protein 1	0.003	1.90
8	A0A0G2K3P1	Transcription factor BTF3	0.023	1.78
9	Q2IBC6	Cav1 - Caveolin	0.047	1.74
10	F1LMD9	Gak - Cyclin-G-associated kinase	0.020	1.73
11	Q1JU69	Cops7a - ZH11 protein	0.001	1.70
12	D3ZAS1	ENSRNOG00000032289 - Protein RGD1562399	0.015	1.67
13	Q6PDU7	Atp5l - ATP synthase subunit g, mitochondrial	0.002	1.64
14	Q99MC0	Ppp1r14a - Protein phosphatase 1 regulatory subunit 14A	0.003	1.61
15	D4A8F2	Rsu1 - Ras suppressor protein 1	0.019	1.57
16	Q9QYW3	Mob4 - MOB-like protein phocein	0.035	1.50
17	P20070	Cyb5r3 - NADH-cytochrome b5 reductase 3	0.019	1.48
18	P70625	ZO-2 - Zonula occludens 2 protein	0.023	1.48
19	F1LNE5	Memo1 - Protein MEMO1	0.009	1.47
20	Q66HK3	Ptgs1 - Prostaglandin G/H synthase 1	0.035	1.45
21	Q6P7Q1	Bre - BRCA1-A complex subunit BRE	0.012	1.42
22	A0A0H2UHQ9	Synpo - Synaptopodin	0.038	1.41
23	Q5RKJ4	Fnta - Farnesyltransferase, CAAX box, alpha	0.045	1.39
24	A0A0G2JTX2	Praf2 - PRA1 family protein	0.016	1.38
25	O35264	Pafah1b2 - Platelet-activating factor acetylhydrolase IB subunit beta	0.031	1.37
26	B2GV92	Ptges3 - Ptges3 protein	0.049	1.37
27	P50545	Hck - Tyrosine-protein kinase HCK	0.039	1.36

28	A0A0G2KAI8	Drg2 - Developmentally-regulated GTP-binding protein 2	0.039	1.35
29	B0BN51	Snrpb - Small nuclear ribonucleoprotein-associated protein	0.015	1.34
30	D3Z8D7	Rps26 - Ribosomal protein S26	0.025	1.32
31	P61212	Arl1 - ADP-ribosylation factor-like protein 1	0.007	1.32
32	Q5XI19	Fermt2 - Fermitin family homolog 2	0.028	1.29
33	Q99PD6	Tgfb1i1 - Transforming growth factor beta-1-induced transcript 1 protein	0.022	1.28
34	I6L9G5	Rcn3 - Reticulocalbin 3	0.003	1.27
35	M0RD75	ENSRNOG00000049025 - 40S ribosomal protein S6	0.028	1.26
36	Q4V882	Epn3 - Epsin-3	0.014	1.25
37	A0A0G2K719	Ddx3x - DEAD-box helicase 3, X-linked	0.017	1.25
38	Q4AEF8	Copg1 - Coatomer subunit gamma-1	0.039	1.25
39	Q5EB77	Rab18 - Ras-related protein Rab-18	0.033	1.25
40	Q6P685	Eif2s2 - Eukaryotic translation initiation factor 2 subunit 2	0.035	1.24
41	Q5WQV5	Rdx - Radixin	0.011	1.23
42	Q6EV70	Pofut1 - GDP-fucose protein O-fucosyltransferase 1	0.028	1.21
43	G3V6P2	Dlst - Dihydrolipoamide S-succinyltransferase	0.004	1.20
44	Q6PDV7	Rpl10 - 60S ribosomal protein L10	0.031	1.19
45	D4A6W6	RGD1561333 - Protein RGD1561333	0.020	1.19
46	A0A0H2UHV4	Eif5b - Eukaryotic translation initiation factor 5B	0.022	1.19
47	D3Z941	Mars - methionine--tRNA ligase, cytoplasmic	0.022	1.18
48	F2Z3Q8	Kpnb1 - Importin subunit beta-1	0.035	1.17
49	Q5PPP1	Clta - Clathrin light chain	0.049	1.17
50	G3V8C4	Clic4 - Chloride intracellular channel protein	0.043	1.17
51	Q63584	Tmed10 - Transmembrane emp24 domain-containing protein 10	0.011	1.16
52	Q3ZB97	Ap2b1 - AP complex subunit beta	0.004	1.16

53	Q5RJR8	Lrrc59 - Leucine-rich repeat-containing protein 59	0.022	1.14
54	D3Z865	Mpdu1 - mannose-P-dolichol utilization defect 1 protein	0.021	1.13
55	Q4KM69	Cops5 - COP9 (Constitutive photomorphogenic) homolog, subunit 5	0.020	1.12
56	G3V6S3	Calu - Calumenin	0.010	1.11
57	Q66HF3	Etfdh - Electron transfer flavoprotein-ubiquinone oxidoreductase	0.047	1.10
58	Q5M7X1	Copb2 - Coatomer subunit beta'	0.032	1.10
59	G3V6P7	Myh9 - Myosin, heavy polypeptide 9, non-muscle	0.029	1.09
60	Q6LDS4	Sod1 - Superoxide dismutase [Cu-Zn]	0.034	0.91
61	A0A0G2JYL4	P4ha2 - Prolyl 4-hydroxylase subunit alpha 2	0.010	0.90
62	Q6P2A7	Flot1 - Flot1 protein	0.037	0.90
63	A7LNF8	RT1.A - MHC class I antigen	0.011	0.87
64	D3ZLH9	LOC680385 - Protein LOC680385	0.012	0.86
65	Q6P7A4	Psap - Prosaposin	0.047	0.85
66	Q64654	Cyp51 - Lanosterol 14-alpha demethylase	0.049	0.82
67	B1WBV1	Aida - Axin interactor	0.036	0.82
68	Q6AXM8	Pon2 - Serum paraoxonase/arylesterase 2	0.036	0.82
69	Q642A4	MGC94207 - UPF0598 protein C8orf82 homolog	0.039	0.82
70	Q95571	RT1.A(U) - RT1.A(U) alpha chain	0.005	0.81
71	A0A0A0MXU4	Emc2 - ER membrane protein complex subunit 2	0.011	0.81
72	Q9R1S6	Cd1d1 - CD1 antigen	0.045	0.80
73	B2RYG6	Otub1 - Ubiquitin thioesterase OTUB1	0.045	0.80
74	A0A0G2JSJ8	Fuca1 - Fucosidase, alpha-L-1, tissue, isoform CRA_a	0.021	0.80
75	Q7TPI8	Yip5 - Protein YIPF5	0.042	0.80
76	B2RYQ5	Erh - Enhancer of rudimentary homolog	0.032	0.79

77	F1LR10	Lima1 - LIM domain and actin-binding protein 1	0.032	0.79
78	A1L1J8	Rab5b - Ras-related protein Rab-5B	0.007	0.78
79	Q566C5	Rassf4 - Ras association domain-containing protein 4	0.027	0.78
80	J7NUQ1	Irgm - Interferon-gamma-inducible GTPase Irgg3 protein	0.019	0.77
81	P21571	Atp5j - ATP synthase-coupling factor 6, mitochondrial	0.040	0.77
82	M0R4V3	Snap23 - Synaptosomal-associated protein	0.037	0.76
83	G3V7L8	Atp6v1e1 - ATPase, H ⁺ transporting, V1 subunit E isoform 1	0.030	0.76
84	Q4KM41	Ewsr1 - Ewing sarcoma breakpoint region 1	0.003	0.75
85	F7EWC1	Vasp - Vasodilator-stimulated phosphoprotein	0.020	0.75
86	P00388	Por - NADPH--cytochrome P450 reductase	0.044	0.75
87	Q4QQV4	Hars - histidyl-tRNA synthetase	0.023	0.74
88	A0A0G2K9T4	Macf1 - Microtubule-actin cross-linking factor 1	0.044	0.74
89	Q3KRE0	Atad3a - ATPase family AAA domain-containing protein 3	0.002	0.73
90	D4A7N1	Chchd6 - Coiled-coil-helix-coiled-coil-helix domain-containing protein 6	0.030	0.73
91	P00173	Cyb5a - Cytochrome b5	0.022	0.73
92	Q4KLJ1	Srsf7 - RCG61762, isoform CRA_a	0.021	0.73
93	Q68FY1	Nup35 - Nucleoporin NUP53	0.034	0.73
94	B2RYF6	Clptm1 - Cleft lip and palate associated transmembrane protein 1	0.005	0.72
95	Q5XIH3	Ndufv1 - NADH dehydrogenase	0.015	0.71
96	A0A0H2UHGO	Yars - Tyrosine--tRNA ligase	0.019	0.70
97	M0RBK1	Prps11 - Phosphoribosyl pyrophosphate synthetase 1-like 1	0.018	0.70
98	D3ZZ38	Snx18 - Sorting nexin-18	0.013	0.68
99	D4A8A0	Cad - CAD protein	0.037	0.68
100	P08009	Gstm7 - Glutathione S-transferase Yb-3	0.005	0.67

101	Q6AY21	G3bp2 - Ras GTPase-activating protein-binding protein 2	0.003	0.66
102	Q2YDU8	Spns1 - Protein spinster homolog 1	0.041	0.64
103	P07151	B2m - Beta-2-microglobulin	0.047	0.63
104	F2Z3S5	Rbpms - RNA-binding protein with multiple-splicing	0.035	0.62
105	P55770	Nhp2l1 - NHP2-like protein 1	0.002	0.61
106	B2LYI9	Tnc - Tenascin C	0.001	0.55
107	Q923Z2	Tpm1 - Tropomyosin 1, alpha, isoform CRA_a	0.000	0.54
108	P62078	Timm8b - Mitochondrial import inner membrane translocase subunit Tim8 B	0.007	0.49
109	P31643	Slc6a6 - Sodium- and chloride-dependent taurine transporter	0.022	0.48
110	D3ZCR3	Hmg1l1 - Protein RGD1560584	0.040	0.48
111	B2GVB7	Apeh - N-acylaminoacyl-peptide hydrolase	0.038	0.42
112	Q9Z1J7	Slc1a5 - Amino acid transporter	0.034	0.41
113	Q7TP42	Sec62 - Translocation protein SEC62	0.046	0.40
114	M0RBJ7	C3 - Complement C3	0.045	0.36
115	E9PU24	Dnah11 - Dynein-like protein 11	0.002	0.34
116	Q7TQ08	Scin - Scinderin	0.007	0.33
117	Q9WVK7	Hadh - Hydroxyacyl-coenzyme A dehydrogenase	0.020	0.26
118	Q99J82	Ilk - Integrin-linked protein kinase	0.003	0.25
119	D3ZCL3	Snrpc - U1 small nuclear ribonucleoprotein C	0.002	0.21
120	A0A140TAJ3	Fubp1 - Far upstream element-binding protein 1	0.047	0.20

Table 8: Comparative list of proteins in the leptin-stimulated for 24h compared to controls.

Number	Accession	Name	p-value	fold change
1	Q9QZA6	Cd151 - CD151 antigen	0.047	9.55
2	Q499S2	Atp5g3 - ATP synthase F(0) complex subunit C3, mitochondrial	0.001	7.92
3	B2RYL3	Tmem119 - Transmembrane protein 119 precursor	0.001	4.26
4	F1M6Q3	Col4a2 - Collagen type IV alpha 2 chain	0.027	3.53
5	Q566C5	Rassf4 - Ras association domain-containing protein 4	0.012	2.62
6	D4A4L5	Hbld1 - Uncharacterized protein LOC500694	0.015	2.61
7	F1LPS3	Nolc1 - Nucleolar and coiled-body phosphoprotein 1	0.005	2.42
8	A0A0H2UHV9	Copg2 - Coatomer subunit gamma	0.017	2.27
9	Q9JI92	Sdcbp - Syntenin-1	0.017	2.15
10	A0A0G2JSQ9	Pelp1 - Proline-, glutamic acid- and leucine-rich protein 1	0.023	2.15
11	Q6AY30	Sccpdh - Saccharopine dehydrogenase (putative)	0.022	1.96
12	D3ZSV1	lft20 - Intraflagellar transport protein 20 homolog	0.010	1.94
13	Q5XIK2	Tmx2 - Thioredoxin-related transmembrane protein 2	0.021	1.93
14	Q5U2X6	Ccdc47 - Coiled-coil domain-containing protein 47	0.005	1.89
15	P47853	Bgn - Biglycan	0.019	1.86
16	D4AC36	Eif3f - Eukaryotic translation initiation factor 3 subunit F	0.037	1.74
17	M3ZCQ2	Snrnp200 - U5 small nuclear ribonucleoprotein 200 kDa helicase	0.005	1.69
18	P11505	Atp2b1 - Plasma membrane calcium-transporting ATPase 1	0.026	1.68
19	P50545	Hck - Tyrosine-protein kinase HCK	0.009	1.68
20	Q5RJK6	Inpp1 - Inositol polyphosphate 1-phosphatase	0.028	1.67
21	Q5RKH9	Der1 - Derlin	0.024	1.67
22	F1LMD9	Gak - Cyclin-G-associated kinase	0.043	1.66

23	F1LM16	Serpine1 - Plasminogen activator inhibitor 1	0.029	1.65
24	A0A0G2JTL5	Pc - Pyruvate carboxylase, mitochondrial	0.012	1.58
25	P61751	Arf4 - ADP-ribosylation factor 4	0.048	1.57
26	F1LTJ5	Uncharacterized protein	0.029	1.57
27	P20070	Cyb5r3 - NADH-cytochrome b5 reductase 3	0.013	1.57
28	A0A097BVJ5	Cnp - 2',3'-cyclic-nucleotide 3'-phosphodiesterase	0.010	1.57
29	A0A0G2K8T0	Asah1 - Acid ceramidase	0.008	1.56
30	B5DF91	Elavl1 - ELAV-like protein 1	0.025	1.51
31	D3ZQN7	Lamb1 - Laminin B1	0.046	1.47
32	A0A0H2UHQ0	Slc3a2 - 4F2 cell-surface antigen heavy chain	0.016	1.45
33	A0A0G2KAU7	Ltbp2 - Latent-transforming growth factor beta-binding protein 2	0.026	1.44
34	D3ZBL6	Nup160 - Nuclear pore complex protein Nup160	0.044	1.44
35	Q920A6	Scpep1 - Retinoid-inducible serine carboxypeptidase	0.014	1.44
36	P14604	Echs1 - Short-chain enoyl-CoA hydratase	0.004	1.43
37	P04762	Cat - Catalase	0.017	1.42
38	Q5XIB4	Ufsp2 - Ufm1-specific protease 2	0.039	1.42
39	D3ZIE9	Aldh18a1 - Delta-1-pyrroline-5-carboxylate synthase	0.014	1.37
40	Q66HK3	Ptgs1 - Prostaglandin G/H synthase 1	0.050	1.36
41	P08461	Dlat - Dihydrolipoyllysine-residue acetyltransferase component of pyruvate dehydrogenase complex	0.017	1.35
42	D3ZJ32	Esy2 - Extended synaptotagmin-like protein 2	0.000	1.35
43	D3Z8D7	Rps26 - Ribosomal protein S26	0.001	1.35
44	B2GV15	Dbt - Lipoamide acyltransferase component of branched-chain alpha-keto acid dehydrogenase complex	0.038	1.34
45	Q32PW9	Psmc6 - Psmc6 protein	0.049	1.34
46	A0A0G2K7P7	Mtch2 - Mitochondrial carrier 2	0.025	1.33
47	Q63083	Nucb1 - Nucleobindin-1	0.046	1.33

48	Q6P7A9	Gaa - Lysosomal alpha-glucosidase precursor	0.000	1.32
49	P62634	Cnbp - Cellular nucleic acid-binding protein	0.034	1.32
50	Q4KM74	Sec22b - Vesicle-trafficking protein SEC22b	0.001	1.30
51	Q63965	Sfxn1 - Sideroflexin-1	0.003	1.29
52	B5DFG2	Hnrnpl - Hnrnpl protein	0.036	1.29
53	Q5RJR8	Lrrc59 - Leucine-rich repeat-containing protein 59	0.046	1.29
54	Q5EBA9	Sucg2 - Succinate-CoA ligase subunit beta	0.037	1.29
55	A0A0G2K251	Abcg3l1 - ATP-binding cassette, subfamily G (WHITE), member 3-like 1	0.010	1.28
56	P24368	Ppib - Peptidyl-prolyl cis-trans isomerase B	0.005	1.28
57	A0A0G2JSS9	Atl3 - Atlastin-3	0.039	1.28
58	D4A8M5	Snrpe - Small nuclear ribonucleoprotein E	0.001	1.27
59	D3ZQM0	Sf3a1 - Splicing factor 3A subunit 1	0.036	1.27
60	P97675	Enpp3 - Ectonucleotide pyrophosphatase/phosphodiesterase family member 3 Alkaline phosphodiesterase I Nucleotide pyrophosphatase	0.048	1.27
61	Q66HM2	Ap2a2 - AP-2 complex subunit alpha-2	0.001	1.27
62	Q6P7R8	Hsd17b12 - Estradiol 17-beta-dehydrogenase 12	0.017	1.27
63	M0R907	Snrpd3 - Small nuclear ribonucleoprotein D3	0.048	1.26
64	Q62991	Scfd1 - Sec1 family domain-containing protein 1	0.022	1.25
65	P04785	P4hb - Protein disulfide-isomerase	0.004	1.25
66	P06761	Hspa5 - 78 kDa glucose-regulated protein	0.000	1.25
67	G3V7T6	Sf3b1 - Splicing factor 3b, subunit 1	0.036	1.24
68	A0A0G2JXJ7	Esyt1 - Extended synaptotagmin-1	0.049	1.24
69	Q6AXR4	Hexb - Beta-hexosaminidase subunit beta	0.038	1.24

70	Q6P136	Hyou1 - Hyou1 protein	0.032	1.23
71	I6L9G6	Tardbp - TAR DNA binding protein	0.049	1.23
72	P52555	Erp29 - Endoplasmic reticulum resident protein 29	0.009	1.23
73	G3V8C3	Vim - Vimentin	0.048	1.22
74	Q9JJ54	Hnrpd - Heterogeneous nuclear ribonucleoprotein C	0.024	1.22
75	D3Z865	Mpdu1 - mannose-P-dolichol utilization defect 1 protein	0.043	1.21
76	A0A140TAI3	Hnrnpc - Heterogeneous nuclear ribonucleoprotein C	0.037	1.20
77	P70490	Mfge8 - Lactadherin	0.047	1.20
78	G3V6P2	Dlst - Dihydrolipoamide S-succinyltransferase	0.004	1.20
79	P35565	Canx - Calnexin	0.001	1.20
80	P97532	Mpst - 3-mercaptopyruvate sulfurtransferase	0.042	1.19
81	D3ZZR9	Fkbp2 - Peptidyl-prolyl cis-trans isomerase FKBP2 precursor	0.031	1.18
82	B2RYG2	Pck2 - Pck2 protein	0.035	1.18
83	G3V9W6	Aldh3a2 - Aldehyde dehydrogenase	0.028	1.17
84	O35821	Mybbp1a - Myb-binding protein 1A	0.021	1.17
85	A0A0A0MY09	Hsp90b1 - Endoplasmin	0.027	1.17
86	D3ZQ57	Plxnb2 - plexin-B2 precursor	0.019	1.17
87	G3V6H5	Slc25a11 - Mitochondrial 2-oxoglutarate/malate carrier protein	0.008	1.17
88	P61212	Arl1 - ADP-ribosylation factor-like protein 1	0.009	1.17
89	Q6PDV8	LOC100360057 - RCG31311	0.005	1.17
90	P18418	Calr - Calreticulin	0.030	1.17
91	A0A0G2K1L8	Basp1 - Brain acid soluble protein 1	0.046	1.16
92	Q63355	Myo1c - Unconventional myosin-Ic	0.000	1.16
93	Q6NYB7	Rab1A - Ras-related protein Rab-1A	0.042	1.16
94	B0BNG3	Lman2 - Vesicular integral-membrane protein VIP36 precursor	0.021	1.16
95	D3ZUY8	Ap2a1 - AP-2 complex subunit alpha-1	0.004	1.15
96	P56574	Idh2 - Isocitrate dehydrogenase [NADP]	0.033	1.15
97	A0A0G2JSZ5	Pdia6 - Protein disulfide-isomerase A6	0.040	1.14

98	F7F9U6	Plec - Plectin	0.007	1.13
99	Q6P2A5	Ak3 - GTP:AMP phosphotransferase AK3, mitochondrial	0.027	1.13
100	B0BN97	Txndc12 - Txndc12 protein	0.036	1.13
101	O08984	Lbr - Lamin-B receptor	0.039	1.13
102	Q5VLR5	Erp44 - Endoplasmic reticulum resident protein 44 precursor	0.040	1.12
103	Q5BJS6	Tmem50b - Transmembrane protein 50B	0.035	1.12
104	Q07936	Anxa2 - Annexin A2	0.010	1.11
105	Q9JLA3	Uggt1 - UDP-glucose:glycoprotein glucosyltransferase 1	0.010	1.10
106	G3V928	Lrp1 - Prolow-density lipoprotein receptor-related protein 1 precursor	0.023	1.09
107	B2RZ09	Pdia6 - Protein disulfide-isomerase A6	0.043	1.08
108	Q66HF3	Etfdh - Electron transfer flavoprotein-ubiquinone oxidoreductase	0.039	1.08
109	Q66WT9	Picalm - Clathrin-assembly lymphoid myeloid leukemia protein	0.008	0.91
110	F1LPK7	Pls3 - Plastin 3 (T-isoform), isoform CRA_a	0.049	0.90
111	Q4KM41	Ewsr1 - Ewing sarcoma breakpoint region 1	0.030	0.90
112	O55096	Dpp3 - Dipeptidyl peptidase 3	0.018	0.86
113	Q6IMZ3	Anxa6 - Annexin	0.048	0.85
114	G3V8B6	Psmd1 - 26S proteasome non- ATPase regulatory subunit 1	0.032	0.84
115	P24051	Rps27l - 40S ribosomal protein S27- like	0.032	0.83
116	P61972	Nutf2 - Nuclear transport factor 2	0.012	0.82
117	A0A096MK75	Rhog - Ras homolog family member G	0.015	0.82
118	C7C5T2	Pfkp - ATP-dependent 6- phosphofruktokinase	0.045	0.82
119	P50399	Gdi2 - Rab GDP dissociation inhibitor beta	0.033	0.82
120	A0A0G2KAW 4	Thop1 - Thimet oligopeptidase	0.020	0.81
121	Q5BKC3	Park7 - Park7 protein	0.024	0.81

122	Q08163	Cap1 - Adenylyl cyclase-associated protein 1	0.042	0.80
123	P27605	Hprt1 - Hypoxanthine-guanine phosphoribosyltransferase	0.006	0.80
124	Q62952	Dpysl3 - Dihydropyrimidinase-related protein 3	0.047	0.80
125	Q6PDW1	Rps12 - 40S ribosomal protein S12	0.009	0.79
126	B5DEN4	Ldha - L-lactate dehydrogenase	0.047	0.79
127	Q5M964	Fh - Fumarate hydratase 1	0.033	0.79
128	A0A0G2JZG7	Sars - Serine--tRNA ligase, cytoplasmic	0.041	0.79
129	A0A0G2JZ13	Ctnn - Src substrate cortactin	0.032	0.78
130	E2RUH2	Rnh1 - Ribonuclease inhibitor	0.009	0.78
131	P45592	Cfl1 - Cofilin-1	0.009	0.78
132	D4A7U1	Zyx - Zyxin	0.009	0.77
133	P30835	Pfkl - 6-phosphofructokinase	0.010	0.77
134	A0A0G2K9A2	Arpc2 - Arp2/3 complex 34 kDa subunit	0.039	0.77
135	P34058	Hsp90ab1 - Heat shock protein HSP 90-beta	0.017	0.77
136	P23928	Cryab - Alpha-crystallin B chain	0.022	0.77
137	Q499Q4	Pgm1 - Phosphoglucomutase 1	0.020	0.76
138	Q6AYC4	Capg - Macrophage-capping protein	0.008	0.76
139	Q6P9U0	Serpinb6 - Serpin B6	0.043	0.76
140	Q5XIC6	Psmd12 - 26S proteasome non-ATPase regulatory subunit 12	0.010	0.76
141	E9PT82	Strn3 - Striatin-3	0.039	0.76
142	P48500	Tpi1 - Triosephosphate isomerase 1	0.038	0.75
143	D4AD15	Eif4g1 - Eukaryotic translation initiation factor 4 gamma, 1	0.036	0.75
144	P25113	Pgam1 - Phosphoglycerate mutase 1	0.022	0.75
145	B0BNA7	Eif3i - Eukaryotic translation initiation factor 3 subunit I	0.008	0.74
146	Q6P7S0	Pkm - Pyruvate kinase	0.029	0.74
147	Q99MI5	Srm - Spermidine synthase	0.045	0.74
148	Q66HF9	Lrrfip1 - Leucine-rich repeat flightless-interacting protein 1	0.028	0.74
149	D4A269	ENSRNOG00000005630 - Uncharacterized protein	0.042	0.74
150	Q6MG61	Clic1 - Chloride intracellular channel protein 1	0.010	0.74

151	G3V7X4	Abca2 - ATP-binding cassette sub-family A member 2	0.022	0.73
152	Q3T1J1	Eif5a - Eukaryotic translation initiation factor 5A-1	0.033	0.73
153	P13221	Got1 - Aspartate aminotransferase, cytoplasmic	0.017	0.72
154	P16617	Pgk1 - Phosphoglycerate kinase 1	0.044	0.72
155	A0A0H2UHG0	Yars - Tyrosine--tRNA ligase	0.002	0.71
156	A0A0G2K338	Fhl1 - Four and a half LIM domains protein 1	0.038	0.71
157	B2RYQ2	Ppp2r4 - Serine/threonine-protein phosphatase 2A activator	0.018	0.71
158	P47727	Cbr - Carbonyl reductase [NADPH] 1	0.024	0.71
159	P63004	Pafah1b1 - Platelet-activating factor acetylhydrolase IB subunit alpha	0.042	0.70
160	Q4QQV4	Hars - histidyl-tRNA synthetase, cytoplasmic	0.039	0.70
161	O35244	Prdx6 - Peroxiredoxin-6	0.024	0.70
162	P37397	Cnn3 - Calponin-3	0.022	0.70
163	R9PXV7	Ppp1r7 - Protein phosphatase 1 regulatory subunit 7	0.040	0.69
164	P47875	Csrp1 - Cysteine and glycine-rich protein 1	0.043	0.69
165	F1LPG9	Washc2c - WASH complex subunit 2C	0.031	0.69
166	D3ZF26	Tnks1bp1 - Protein Tnks1bp1	0.014	0.68
167	O70593	Sgta - Small glutamine-rich tetratricopeptide repeat-containing protein alpha	0.001	0.68
168	P62282	Rps11 - 40S ribosomal protein S11	0.036	0.68
169	A0A0G2JWK7	Tagln - Transgelin	0.037	0.68
170	O88656	Arpc1b - Actin-related protein 2/3 complex subunit 1B	0.006	0.67
171	F1M9V7	Npepps - Puromycin-sensitive aminopeptidase precursor	0.013	0.66
172	P05065	Aldoa - Fructose-bisphosphate aldolase A	0.034	0.66
173	Q6P4Z9	Cops8 - COP9 signalosome complex subunit 8	0.025	0.65
174	Q62766	kap12 - SSeCKS	0.033	0.64
175	D3ZBN3	Epha2 - Ephrin type-A receptor 2 precursor	0.023	0.64

176	B5DEH4	Uap1l1 - UDP-N-acetylhexosamine pyrophosphorylase-like protein 1	0.028	0.63
177	B2RYG6	Otub1 - Ubiquitin thioesterase OTUB1	0.001	0.63
178	P14669	Anxa3 - Annexin A3	0.012	0.63
179	Q66HR2	Mapre1 - Microtubule-associated protein RP/EB family member 1	0.005	0.61
180	F1LS72	Uba2 - SUMO-activating enzyme subunit 2	0.036	0.59
181	Q05982	Nme1 - Nucleoside diphosphate kinase A	0.036	0.54
182	Q923Z2	Tpm1 - Tropomyosin 1, alpha, isoform CRA_a	0.036	0.42
183	Q62658	Fkbp1a - Peptidyl-prolyl cis-trans isomerase FKBP1A	0.007	0.39
184	Q99J82	Ilk - Integrin-linked protein kinase	0.030	0.39
185	E9PU24	Dnah11 - Dynein-like protein 11	0.039	0.36
186	F7EZ89	Tbc1d15 - Protein Tbc1d15	0.010	0.34
187	D3ZCR3	Hmg1l1 - Protein RGD1560584	0.041	0.28
188	Q5XIF0	Tex264 - Testis-expressed sequence 264 protein	0.000	0.15
189	D3ZCI9	Myl10 - Myosin light chain 10	0.004	0.12

Table 9: Comparative list of proteins in the leptin-stimulated for 48h compared to controls.

Number	Accession	Name	p-value	fold change
1	D4A7C2	RGD1306349 - Formin 1	0.000	45.09
2	Q642E2	Rpl28 - 60S ribosomal protein L28	0.008	16.37
3	A0A0G2JUN7	Txnrd1 - Thioredoxin reductase 1, cytoplasmic	0.001	8.13
4	Q499S2	Atp5g3 - ATP synthase F(0) complex subunit C3	0.003	6.94
5	Q5XFW2	Trub2 - Probable tRNA pseudouridine synthase 2	0.018	5.81
6	D4AA43	Kbtbd5 - Kelch repeat and BTB domain-containing protein 5	0.016	5.62
7	O35112	Alcam - CD166 antigen	0.008	3.79
8	Q5I034	RGD1311899 - Uncharacterized protein C12orf43 homolog	0.010	2.74
9	F1LMD9	Gak - Cyclin-G-associated kinase	0.009	2.23
10	Q499N6	Ubxn1 - UBX domain-containing protein 1	0.005	2.15
11	D4AC36	Eif3f - Eukaryotic translation initiation factor 3 subunit F	0.005	2.05
12	B2GVB1	S100a6 - Protein S100	0.042	1.99
13	F1M6Q3	Col4a2 - Collagen type IV alpha 2 chain	0.016	1.97
14	P61751	Arf4 - ADP-ribosylation factor 4	0.019	1.97
15	D3ZAS1	ENSRNOG00000032289 - Protein RGD1562399	0.016	1.84
16	A0A0G2KAW7	Eif4h - Eukaryotic translation initiation factor 4H	0.038	1.63
17	Q99MC0	Ppp1r14a - Protein phosphatase 1 regulatory subunit 14A	0.041	1.56
18	D4A6C5	Arhgap1 - Rho GTPase activating protein 1	0.013	1.55
19	O35264	Pafah1b2 - Platelet-activating factor acetylhydrolase IB subunit beta	0.007	1.48
20	B2GV92	Ptges3 - Ptges3 protein	0.023	1.43
21	Q6P7Q1	Bre - BRCA1-A complex subunit BRE	0.045	1.43
22	F1LSW7	Rpl14 - 60S ribosomal protein L14	0.009	1.42
23	D4AE68	Gnaq - Guanine nucleotide binding protein, alpha q polypeptide	0.017	1.41
24	P50545	Hck - Tyrosine-protein kinase HCK	0.021	1.40
25	P47853	Bgn - Biglycan	0.039	1.38

26	Q6AYK8	Eif3d - Eukaryotic translation initiation factor 3 subunit D	0.005	1.37
27	Q3MHS9	Cct6a - T-complex protein 1 subunit zeta	0.005	1.36
28	F1LRI5	Gcn1l1 - GCN1 general control of amino-acid synthesis 1-like 1	0.006	1.36
29	A0A0G2JU77	Eif3k - Eukaryotic translation initiation factor 3 subunit K	0.040	1.34
30	Q6P792	Fhl1 - Four and a half LIM domains 1	0.017	1.34
31	B2RYN6	Ap1g1 - Adaptor-related protein complex 1, gamma 1 subunit, isoform CRA_b	0.023	1.33
32	B5DF91	Elavl1 - ELAV-like protein 1	0.031	1.33
33	P10111	Ppia - Peptidyl-prolyl cis-trans isomerase A	0.005	1.30
34	A0A140TAI8	Ahcy1l - S-adenosylhomocysteine hydrolase-like protein 1	0.029	1.30
35	Q6P3V8	Eif4a1 - Eukaryotic initiation factor 4A-I	0.045	1.30
36	O35303	Dnm1l - Dynamin-1-like protein	0.017	1.30
37	Q3B8P5	Psm8 - Psm8 protein	0.007	1.29
38	E9PT66	Sf3b3 - Splicing factor 3B subunit 3	0.042	1.29
39	G3V6U3	Alg2 - Alpha-1,3-mannosyltransferase ALG2	0.049	1.28
40	D3Z8D7	Rps26 - Ribosomal protein S26	0.039	1.28
41	F1LNE5	Memo1 - Protein MEMO1	0.020	1.28
42	Q32PW9	Psmc6 - Psmc6 protein	0.006	1.27
43	P61212	Arl1 - ADP-ribosylation factor-like protein 1	0.002	1.27
44	D3ZRX9	Cnn2 - Calponin 2	0.034	1.27
45	Q6P685	Eif2s2 - Eukaryotic translation initiation factor 2 subunit 2	0.018	1.26
46	A0A0G2K9N3	Ddx3 - DEAD (Asp-Glu-Ala-Asp) box polypeptide 3	0.049	1.26
47	F1M6F4	RGD1564597 - Protein RGD1564597	0.019	1.26
48	P62634	Cnbp - Cellular nucleic acid-binding protein	0.031	1.25
49	A0A0G2JTN4	Pfas - Phosphoribosylformylglycinamide synthase-like	0.039	1.25

50	A0A1B0GWY5	Arhgef2 - Rho guanine nucleotide exchange factor 2	0.021	1.25
51	G3V6H2	Prpf8 - pre-mRNA-processing-splicing factor 8	0.048	1.24
52	P56571	RGD1303003 - ES1 protein homolog	0.011	1.24
53	P19944	Rplp1 - 60S acidic ribosomal protein P1	0.014	1.22
54	F2Z3Q8	Kpnb1 - Importin subunit beta-1	0.015	1.22
55	Q4V882	Epn3 - Epsin-3	0.024	1.22
56	Q641Y8	Ddx1 - ATP-dependent RNA helicase DDX1	0.027	1.21
57	Q9JMB5	Adrm1 - Proteasomal ubiquitin receptor ADRM1	0.028	1.21
58	P09456	Prkar1a - cAMP-dependent protein kinase type I-alpha regulatory subunit	0.022	1.21
59	D4A9Q3	RGD1563570 - Protein RGD1563570	0.007	1.20
60	G3V826	Tkt - Transketolase	0.035	1.20
61	Q4AEF8	Copg1 - Coatomer subunit gamma-1	0.048	1.20
62	Q5RJR8	Lrrc59 - Leucine-rich repeat-containing protein 59	0.012	1.20
63	A0A0G2JV05	Mroh1 - Maestro heat-like repeat family member 1	0.019	1.19
64	F1LN59	Eif4g2 - Eukaryotic translation initiation factor 4 gamma, 2	0.010	1.19
65	A0A0G2K719	Ddx3x - DEAD-box helicase 3, X-linked	0.036	1.18
66	Q63413	Ddx39b - Spliceosome RNA helicase Ddx39b	0.039	1.18
67	Q9ESN0	Fam129a - Protein Niban	0.005	1.17
68	Q641Z6	Ehd1 - EH domain-containing protein 1	0.039	1.16
69	D3ZBL6	Nup160 - Nuclear pore complex protein Nup160	0.014	1.16
70	B0K031	Rpl7 - 60S ribosomal protein L7	0.036	1.16
71	F1LRA1	Lman1 - Protein ERGIC-53	0.019	1.16
72	A0A0G2K0Z7	Gpd2 - Glycerol-3-phosphate dehydrogenase, mitochondrial	0.011	1.15
73	Q5PPP1	Clta - Clathrin light chain	0.014	1.14
74	COJPT7	Flna - filamin-A	0.015	1.14

75	G3V8C4	Clic4 - Chloride intracellular channel protein	0.041	1.13
76	P62161	Calm1 - Calmodulin	0.005	1.11
77	Q07936	Anxa2 - Annexin A2	0.039	1.07
78	P06761	Hspa5 - 78 kDa glucose-regulated protein	0.001	1.06
79	O88656	Arpc1b - Actin-related protein 2/3 complex subunit 1B	0.041	0.96
80	Q66HF9	Lrrfip1 - Leucine-rich repeat flightless-interacting protein 1	0.047	0.93
81	P11884	Aldh2 - Aldehyde dehydrogenase, mitochondrial precursor	0.013	0.92
82	P15999	Atp5a1 - ATP synthase subunit alpha, mitochondrial precursor	0.035	0.92
83	A0A0G2K7K2	Aifm1 - Apoptosis-inducing factor 1, mitochondrial	0.019	0.90
84	D3ZJ32	Esyt2 - Extended synaptotagmin-like protein 2	0.032	0.89
85	P81155	Vdac2 - Voltage-dependent anion-selective channel protein 2	0.010	0.89
86	P08009	Gstm7 - Glutathione S-transferase Yb-3	0.050	0.87
87	A0A0G2JYC7	Hdgfrp2 - Uncharacterized protein	0.009	0.84
88	P29266	Hibadh - 3-hydroxyisobutyrate dehydrogenase	0.024	0.83
89	Q6P6W1	Lamp2 - Lysosome-associated membrane glycoprotein 2	0.022	0.83
90	F1LUV9	Ncam1 - Neural cell adhesion molecule 1	0.037	0.82
91	P11507	Atp2a2 - Sarcoplasmic/endoplasmic reticulum calcium ATPase 2 isoform b	0.026	0.81
92	D3ZTX0	Tmed7 - Transmembrane emp24 domain-containing protein 7	0.049	0.81
93	Q6AY23	Pycr2 - Pyrroline-5-carboxylate reductase 2	0.004	0.81
94	Q566C5	Rassf4 - Ras association domain-containing protein 4	0.023	0.80
95	D3ZYM8	LOC680432 - Uncharacterized protein	0.027	0.80

96	Q68FZ8	Pccb - Propionyl coenzyme A carboxylase, beta polypeptide	0.004	0.80
97	A0A0G2JSJ8	Fuca1 - Fucosidase, alpha-L-1, tissue, isoform CRA_a	0.017	0.79
98	Q5XIU9	Pgrmc2 - Membrane-associated progesterone receptor component 2	0.020	0.78
99	Q95571	RT1.A(u) - RT1.A(U) alpha chain	0.031	0.78
100	Q498C8	Rer1 - Protein RER1	0.034	0.77
101	D3ZSL2	Abrac1 - Uncharacterized protein LOC685045	0.003	0.76
102	A0A140TAI9	Leprotil1 - Leptin receptor overlapping transcript-like 1	0.039	0.76
103	Q3KRE0	Atad3a - ATPase family AAA domain-containing protein 3	0.033	0.76
104	D4A7D7	H6pd - GDH/6PGL endoplasmic bifunctional protein precursor	0.036	0.75
105	Q6P6G9	Hnrnpa1 - Heterogeneous nuclear ribonucleoprotein A1	0.034	0.75
106	B2RYF6	Clptm1 - Cleft lip and palate associated transmembrane protein 1	0.028	0.74
107	A7LNF8	RT1.A - MHC class I antigen	0.034	0.73
108	P32551	Uqcrc2 - Cytochrome b-c1 complex subunit 2, mitochondrial	0.037	0.73
109	D4AC70	Col8a1 - Collagen alpha-1(VIII) chain precursor	0.009	0.73
110	Q6P6Q5	App - Amyloid beta A4 protein	0.042	0.71
111	Q5M7V8	Thrap3 - Thyroid hormone receptor-associated protein 3	0.002	0.68
112	F1M866	Sorbs1 - Sorbin and SH3 domain-containing protein 1	0.014	0.68
113	Q63524	Tmed2 - Transmembrane emp24 domain-containing protein 2	0.039	0.65
114	P55770	Nhp2l1 - NHP2-like protein 1	0.033	0.65
115	D3ZXJ5	Eftud1 - Elongation factor Tu GTP-binding domain-containing protein 1	0.006	0.65
116	D4A962	Hnrnpul1 - Heterogeneous nuclear ribonucleoprotein U-like protein 1	0.012	0.63

117	P62078	Timm8b - Mitochondrial import inner membrane translocase subunit Tim8 B	0.001	0.63
118	Q923Z2	Tpm1 - Tropomyosin 1, alpha, isoform CRA_a	0.000	0.56
119	B2LYI9	Tnc - Tenascin C	0.003	0.54
120	D3ZFQ8	Cyc1 - Cytochrome c-1	0.016	0.49
121	Q5RJY4	Dhrs7b - Dehydrogenase/reductase SDR family member 7B	0.011	0.43
122	AOA0G2K103	Sptlc2 - Serine palmitoyltransferase, long chain base subunit 2	0.020	0.33
123	G3V9M6	Fbn1 - Fibrillin-1 precursor	0.035	0.31
124	P63012	Rab3a - Ras-related protein Rab-3A	0.001	0.27
125	G3V6S2	Aco1 - Aconitate hydratase	0.030	0.27
126	AOA140TAJ3	Fubp1 - Far upstream element-binding protein 1	0.050	0.24
127	P08082	Cltb - Clathrin light chain B	0.000	0.08

CHAPTER FOUR

DISCUSSION

In this study, we aimed at deciphering the mechanisms altered in response to diabetes mellitus that lead to vascular diseases. For that purpose, we divided our aim into four sub-objectives. In the first objective, we assessed the global protein profile in Type 1 DM on the expression and the post-translational modification of the proteins in the aorta and the kidney of the T1DM rat model. The results out of this objective showed that diabetes altered the expression of proteins involved in the oxidative stress and vascular fibrosis. In addition, we observed a total increase in the oxidation of proteins, assessed through the PTM analysis, which was decreased by normalizing blood glucose.

Moreover, the results of this objective showed an interesting regulation on the components of the Kallikrein Kinin system and the Renin angiotensin systems. For instance, diabetes induced kininogen, the precursor of bradykinin, in both the aorta and the kidney. This is among the first studies to report a direct effect of DM on the kininogen expression in the aorta and the kidney. This finding has an important significance since it supports previous reports demonstrating the association of different components of KKS with diabetes and its complications [83,142,368]. However, in all our previous work, we could not show a direct association between DM and kininogen. Also, insulin showed an induction in the expression of angiotensinogen (AGT) and angiotensin converting enzyme (ACE). The induction of AGT and ACE expression lead to high angiotensin II production that induces hypertension. In addition, AngII has been shown to be involved in vascular

remodeling and development of vascular fibrosis, through its effects on VSMC proliferation and migration [360,361].

Furthermore, we observed a modification of proteins that promote the development of cellular hypertrophy, which is associated with the development of diabetes-induced CVD [441]. For instance, we observed a downregulation of the expression of cofilin in diabetic kidneys. Cofilin is an actin depolarizing protein that transforms actin from the filamentous type into globular type [442]. So, a decrease in the expression of cofilin would preserve the F-actin more, leading to cellular hypertrophy [441].

In the second objective, we were interested in studying the effect of BK on vascular fibrosis since the outcomes of the first objective showed an increase in the expression of BK, which points to a relation of BK in the development of CVD. For this objective, we studied the signaling pathway altered downstream of BK receptor 2 in VSMC. We assessed the expression of two fibrotic proteins in response to BK stimulation in VSMC. In addition, we examined the role of sphingolipids in mediating the signal of BK. The outcomes of this objective showed that BK induces the expression of connective tissue growth factor (Ctgf) and fibronectin (Fn1) in VSMC. Additionally, BK induced the activity of SphK1 leading to the translocation of S1pr1. Furthermore, the activity of SphK1/S1pr1 pathway is required for BK to induce its effects on the expression of Ctgf and Fn1. The outcomes of this objective support our previous findings demonstrating a role of KKS in promoting vascular fibrosis and involvement in the development of pathophysiological conditions leading to diabetes-induced CVD [158,368,393,409,410]. In addition, the SphK1/S1P pathway was previously related to the development of hypertension,

atherosclerosis and vascular fibrosis [191,232-234]. Therefore, these results point to a possible mechanism for the development of diabetic induced CVD through BK signaling.

In the third objective, to have a complete figure of the modifications that BK induces in VSMC, we assessed the global protein profile of the modified proteins in VSMC in response to BK stimulation and analyzed the link between the proteins through systems biology. The outcomes from this objective showed that BK upregulates proteins related to Sphingosine kinase and sphingosine 1 phosphate metabolism, which is in line with the finding of the second objective. In addition, Bk induced an upregulation in the expression of leptin receptor in VSMC. Moreover, many proteins involved in vascular fibrosis, inflammatory, and endothelial dysfunction were modified by BK. on the other hand, we assessed the effect of leptin on VSMC. The results showed that leptin induced the expression of proteins involved in ECM production and reduced proteins related to actin remodeling.

In addition, we observed a possible regulation of nitric oxide production through the modification of Caveolin1. BK induced Cav 1 expression that has a role in binding to eNOS inhibiting its nitric oxide production [443,444]. Moreover, SIRT1 is a deacetylase protein responsible for activating eNOS through deacetylation. Cav1 is known to bind to SIRT1 and inhibit its deacetylation properties, thus exerting another inhibitory function on eNOS [445]. Hence, less nitric oxide production induces imbalance in the ability for the vessels to vasodilate and contribute to endothelial dysfunction [446]. Furthermore, BK was involved in downregulating anti-oxidant proteins, such as SOD1 and Gstm3, which proves the involvement of BK in promoting oxidative stress in VSMC [447].

In the last objective, we were interested to validate the observed modulation of leptin pathway in response to BK in VSMC and the role of such interaction on the expression of fibrotic proteins. The outcomes of this objective showed that BK induced the expression of both leptin and leptin receptor. Additionally, both BK and leptin induced the expression of NOX1 and the generation of ROS in VSMC. This finding is in line with previous reports about the involvement of ROS production as a signaling transduction mechanism, especially upstream of ERK1/2 activation [437,438]. Moreover, both BK and leptin induced inhibition in the activity of cofilin which led to a modulation in actin remodeling in the cells and SphK1 plays a role in relaying the signal of both BK and leptin. This divergence of BK signaling through the activation of SphK1 is a good example of signal amplification. In this manner, BK activates its receptor and leads to the activation of SphK1, which in turn can produce SIP and lead to the activation of Leptin pathway. Finally, we confirmed that leptin receptor is a mediator of the signaling pathway of BK on Ctgf and Fn1. There is a strong evidence of the involvement of Ctgf and Fn1 in the development of different pathophysiologies, among which CVD [278,329,330,415,448].

The physiological vasodilatory effects of the KKS was of great interest for the research community trying to find a mechanism to counteract the hypertensive effects of RAS [449,450]. In physiological conditions, the endothelium is intact and lines the vessel walls, which makes the endothelium the first tissue to have contact with the circulation in the vessels. In such conditions, it is well established that BK stimulates Bdkrb2 in endothelial cells leading to Ca^{2+} release from the intracellular stores of the endothelial cells. Ca^{2+} leads to the activation of eNOS and nitric oxide production, and the activation of phospholipase A₂ (PLA₂) and prostaglandin I₂ (PGI₂) in the endothelial cells [450]. Both

nitric oxide and PGI₂ is released from endothelial cells to VSMC to activate the production of cGMP and cAMP, respectively. Both cGMP and cAMP inhibit the release of Ca²⁺ from the internal stores of the VSMC and decrease the contraction of VSMC leading to the vasodilatory effects of BK [451,452].

On the other hand, endothelial tissue can suffer from injury leading to dysfunction. Many pathophysiological conditions are reported to induce endothelial dysfunction, such as obesity, oxidative stress, dyslipidemia, and diabetes [453]. Endothelial dysfunction is characterized by a decrease in nitric oxide production and disability to induce vasodilation [454]. In addition, the association of endothelial dysfunction with CVD is well established [455]. In such conditions, BK loses its ability to induce vasodilation, and rather it interacts directly with Bdkrb2 receptors expressed on VSMC. In the VSMC, Bdkrb2 stimulates the release of Ca²⁺ from the sarcoplasmic reticulum leading to the contraction of the cells. In addition, Bdkrb2 also induces the activation of different pathways leading to the activation of MAPK and PKB (AKT) and their corresponding pathways to induce VSMC proliferation and migration and to alter the ability of the cells to produce more fibrotic proteins [144,456].

We observed in our results that kininogen is highly expressed in the denuded aorta, which indicates a direct production of BK in VSMC of the aorta by tissue kallikrein. On its turn, BK can be released from the VSMC to stimulate Bdkrb2 in an autocrine or paracrine fashion, overcoming the role of BK on endothelial cells, if they were physiologically functional. Additionally, upon examining the effects of BK directly on VSMC, we confirmed the involvement of BK in the promotion of vascular fibrosis through the upregulation of Ctgf and Fn1. Moreover, Ctgf and Fn1's implication in vascular fibrosis

was extensively investigated, and the reports showed that rat aortic smooth muscle cells responded to high glucose by upregulating the expression of Ctgf and Fn1, in ERK1/2 dependent mechanism. Furthermore, Ctgf expression was indispensable for production and accumulation of collagen proteins (1 and 3), and VSMC proliferation [457]. Our results add to this mechanism by identifying SphK1/S1pr1 pathway as a requirement for the expression of both Ctgf and Fn1 in the same type of cells.

Further, we assessed the global pathways that are altered in VSMC stimulated with BK to gain a wider insight on the modified pathways in response to BK. Our results showed a novel modified protein by BK stimulation which is leptin receptor. Previously in the literature there was no reports linking the expression of leptin receptor to BK or KKS. However, there were few reports linking the physiological functions of BK in the endothelial cells with the existence of leptin or its receptor [426]. In addition, the outcomes of the proteomic response of BK in VSMC showed an impaired nitric oxide production pathway and enhanced vascular fibrosis through TGF β -mediated pathways [410].

Finally, we sought to validate the proposed relationship between BK and leptin pathways in VSMC. Indeed, BK induced the expression of leptin and its receptor in VSMC, and this regulation is required for BK to induce the expression of Ctgf and Fn1. Additionally, SphK1 was shown to be mediator of BK and leptin signaling on actin remodeling promoting vascular hypertrophy. This observation adds to the pathophysiological roles of BK in VSMC by linking the detrimental effects of pro-inflammatory adipokines to the cardiovascular system and CVD [438].

In summary, the results of this study show a strong evidence about the role of BK in promoting the development of diabetes-induced CVD through its actions in VSMC. First,

we observed that diabetes effects on VSMC eradicate the vasodilatory effects of BK on the vessels, since it is increasing BK precursors in VSMC. Additionally, BK induced the expression of two fibrotic proteins through SphK1/S1pr1 and leptin/leptin receptor pathways in VSMC. Further investigation and research focusing on targeting these signaling pathways would result in ameliorating the development of CVD in diabetic patients.

A. Significance of the study:

The outcomes of this study support the involvement of KKS in the promotion of CVD in diabetic situations. It's the first study to show the regulation of kininogen, the direct precursor of BK, by diabetes in the aorta and the kidney. In addition, this study showed that BK stimulates the expression of two fibrotic proteins, well known to be involved in vascular fibrosis in different pathophysiological conditions, among which atherosclerosis. The effect of BK on fibrotic proteins passes through the activation of two pathways, namely the SphK1/S1P/S1pr1 pathway and leptin/leptin receptor pathway. These cross-talk mechanisms prove the complexity of biological functions and pathologies that BK is involved in. Finally, we observed that Ctgf has a signaling role involved in modulating actin remodeling in VSMC. This is a novel finding about the activity of this growth factor, which may shed a light on the involvement of it in the development of CVD.

B. Limitation of the study:

Having said that, we must acknowledge some of the limitations of this study.

1. Global proteomic profiling of T1DM mouse model:

In our first objective, we studied the effect of hyperglycemia induction on the aorta and kidney samples of the mouse models. This type of diabetes constitutes only 10% of the total diabetic patients. So, the observed results of objective one on the expression of Kininogen was not tested in T2DM model. In addition, this animal model (STZ-induced hyperglycemia in rats) is not the perfect model to study CVD, especially atherosclerosis, since these rats do not develop atherosclerosis at all. Moreover, we did not collect data to show the effect of T1DM on the kidney function, such as AER.

2. Assessing the cross-talk between BK and S1P pathways:

In the second objective, we showed a cross-talk between Bdkrb2 and S1pr1 through the activity of SphK1. We proved the activation of SphK1 through its phosphorylation and translocation to the membrane of the cells. However, we did not measure the production or the release of S1P from the cells. Although we did not observe any modification of the expression of S1pr2, S1pr3, and SphK2 in our results, we did not prove that they are not involved in the signaling pathway of BK. In addition, we assessed the gene expression of Ctgf and Fn1 in cells extracted from mouse VSMC of WT and SphK1^{-/-}, but could not measure the protein expression of them due to the low yield of extraction of VSMC from these mice and their slow rate of growing. Finally, we did not study or assess the development of CVD, such as atherosclerotic plaque formation or size, in these SphK1^{-/-} due to their disability of atherosclerosis development.

3. *Assessing the cross-talk between BK and leptin:*

In the fourth objective, we showed that BK induced leptin and leptin receptor expression. Additionally, we observed that SphK1 play a mediator role downstream of BK and leptin leading to actin remodeling effects. The involvement of SphK1 was assessed through using the pharmacological inhibitor of SphK1 activity, at relatively high concentration. Moreover, we assessed the effect of BK and leptin on the ratio of actin types inside the cells as an indication of hypertrophy of cells without relying on other techniques such as cellular staining on actin bundles or measure wet-to-dry weight of the cells. Furthermore, the effect of BK and leptin cross-talk on the expression of Ctgf and Fn1 was not validated in ob/ob or db/db mouse models.

C. Future perspectives:

To better understand and validate the results of this study, animal models should be used. For instance, confirming the findings of the cross-talk between BK and Sp1r pathways requires the use of atherosclerosis animal model, such as ApoE^{-/-}. This model will aid in assessing the number and the volume of atherosclerotic plaque or lesions inside the major vessels. Different experimental designs could be used to study the effects of diabetes on atherosclerosis, such as assessing the effect of vasoactive molecules on ex vivo aortic rings. Moreover, the ApoE^{-/-} mouse model could be crossed with Bdkrb2^{-/-}, SphK1^{-/-}, or S1pr1^{-/-} models to assess their involvement in inducing the diabetes observed cardiovascular outcomes.

Additionally, employing ob/ob or db/db mouse models in confirming the cross-talk between BK and leptin would be of great significance for the outcomes. These mouse models would be used to generate primary VSMC to examine if BK signaling in these cells is altered due to the absence of leptin pathway components. Furthermore, these models could be crossed with *Bdkrb2* and diabetes could be induced in the double knock-out models. The anticipated results out of the diabetic-double knocked out mice would be a less diabetes induced vascular injury.

Finally, confirming the involvement of SphK1 in the regulation of BK and leptin pathway is crucial. This aim could be studied in a pharmacologically altered and genetically ablated SphK1 models. The outcomes of this aim would point to the deleterious role the sphingolipids are potentially playing in VSMC-observed inflammation, fibrosis, and acting remodeling, which renders SphK1 as a potential therapeutic target to focus on in order to enhancing the cardiovascular physiology in diabetic patients.

D. Possible therapeutic interventions:

The outcomes of this study point to the involvement of sphingolipid signaling in the possible initiation or development of vascular diseases. Further studies are needed to investigate the role of this signaling system, for instance SphK or the S1P receptors, on vascular fibrosis. Currently, there are many clinical trials targeting the components of the sphingolipid signaling pathway over different pathophysiologies [458,459]. Only one study focused on vascular complication, which studied the effect of inhibiting S1pr1, by FTY720, on acute stroke. The molecule has passed phase II clinical trial.

On the other hand, there is no clinical studies to evaluate the effects of attenuating the enzymatic activity of SphK1 on CVD patients. In our opinion and based on the results of this study, inhibiting SphK1 in patients with CVD would ameliorate the development of atherosclerosis.

REFERENCES:

1. Desmedt L, Hotier L, Giurfa M, Velarde R, de Brito Sanchez MG (2016) Absence of food alternatives promotes risk-prone feeding of unpalatable substances in honey bees. *Sci Rep* 6: 31809.
2. Cho NH (2016) Q&A: Five questions on the 2015 IDF Diabetes Atlas. *Diabetes Research and Clinical Practice* 115: 157-159.
3. da Rocha Fernandes J, Ogurtsova K, Linnenkamp U, Guariguata L, Seuring T, et al. (2016) IDF Diabetes Atlas estimates of 2014 global health expenditures on diabetes. *Diabetes Research and Clinical Practice* 117: 48-54.
4. (CDC) CfDCaP (2014) 2014 National Diabetes Statistics Report.
5. da Rocha Fernandes J, Ogurtsova K, Linnenkamp U, Guariguata L, Seuring T, et al. (2016) IDF Diabetes Atlas estimates of 2014 global health expenditures on diabetes. *Diabetes Res Clin Pract* 117: 48-54.
6. Yalcin GC, Velarde C, Robledo A (2015) Entropies for severely contracted configuration space. *Heliyon* 1: e00045.
7. (2013) Economic costs of diabetes in the U.S. in 2012. *Diabetes Care* 36: 1033-1046.
8. Wong E, Stevenson C, Backholer K, Woodward M, Shaw JE, et al. (2015) Predicting the risk of physical disability in old age using modifiable mid-life risk factors. *Journal of Epidemiology and Community Health* 69: 70-76.
9. Wong E, Woodward M, Stevenson C, Backholer K, Sarink D, et al. (2016) Prevalence of disability in Australian elderly: Impact of trends in obesity and diabetes. *Preventive Medicine* 82: 105-110.
10. Papadopoulou-Marketou N, Chrousos GP, Kanaka-Gantenbein C (2017) Diabetic nephropathy in type 1 diabetes: a review of early natural history, pathogenesis, and diagnosis. *Diabetes Metab Res Rev* 33.
11. American Diabetes A (2009) Diagnosis and Classification of Diabetes Mellitus. *Diabetes Care* 32: S62-S67.
12. Aroda VR, Christophi CA, Edelstein SL, Zhang P, Herman WH, et al. (2015) The effect of lifestyle intervention and metformin on preventing or delaying diabetes among women with and without gestational diabetes: the Diabetes Prevention Program outcomes study 10-year follow-up. *J Clin Endocrinol Metab* 100: 1646-1653.

13. Bain E, Crane M, Tieu J, Han S, Crowther CA, et al. (2015) Diet and exercise interventions for preventing gestational diabetes mellitus. *Cochrane Database Syst Rev*: CD010443.
14. Kasher-Meron M, Grajower MM (2017) Preventing Progression from Gestational Diabetes Mellitus to Diabetes: A Thought-filled Review. *Diabetes Metab Res Rev*.
15. (1993) The effect of intensive treatment of diabetes on the development and progression of long-term complications in insulin-dependent diabetes mellitus. The Diabetes Control and Complications Trial Research Group. *N Engl J Med* 329: 977-986.
16. Holman RR, Paul SK, Bethel MA, Matthews DR, Neil HA (2008) 10-year follow-up of intensive glucose control in type 2 diabetes. *N Engl J Med* 359: 1577-1589.
17. Goldberg RB (2009) Cytokine and cytokine-like inflammation markers, endothelial dysfunction, and imbalanced coagulation in development of diabetes and its complications. *J Clin Endocrinol Metab* 94: 3171-3182.
18. Cardozo AK, Kruhoffer M, Leeman R, Orntoft T, Eizirik DL (2001) Identification of novel cytokine-induced genes in pancreatic beta-cells by high-density oligonucleotide arrays. *Diabetes* 50: 909-920.
19. Ballantyne CM, Nambi V (2005) Markers of inflammation and their clinical significance. *Atheroscler Suppl* 6: 21-29.
20. Christiansen T, Richelsen B, Bruun JM (2005) Monocyte chemoattractant protein-1 is produced in isolated adipocytes, associated with adiposity and reduced after weight loss in morbid obese subjects. *Int J Obes (Lond)* 29: 146-150.
21. Libby P (2002) Inflammation in atherosclerosis. *Nature* 420: 868-874.
22. Ehses JA, Boni-Schnetzler M, Faulenbach M, Donath MY (2008) Macrophages, cytokines and beta-cell death in Type 2 diabetes. *Biochem Soc Trans* 36: 340-342.
23. Griendling KK, FitzGerald GA (2003) Oxidative stress and cardiovascular injury: Part I: basic mechanisms and in vivo monitoring of ROS. *Circulation* 108: 1912-1916.
24. Ceriello A, Motz E (2004) Is oxidative stress the pathogenic mechanism underlying insulin resistance, diabetes, and cardiovascular disease? The common soil hypothesis revisited. *Arterioscler Thromb Vasc Biol* 24: 816-823.
25. Libby P, Ridker PM (2004) Inflammation and atherosclerosis: role of C-reactive protein in risk assessment. *Am J Med* 116 Suppl 6A: 9S-16S.
26. Papanicolaou DA, Vgontzas AN (2000) Interleukin-6: the endocrine cytokine. *J Clin Endocrinol Metab* 85: 1331-1333.

27. Rajala MW, Scherer PE (2003) Minireview: The adipocyte--at the crossroads of energy homeostasis, inflammation, and atherosclerosis. *Endocrinology* 144: 3765-3773.
28. Suganami T, Nishida J, Ogawa Y (2005) A paracrine loop between adipocytes and macrophages aggravates inflammatory changes: role of free fatty acids and tumor necrosis factor alpha. *Arterioscler Thromb Vasc Biol* 25: 2062-2068.
29. Berg AH, Combs TP, Du X, Brownlee M, Scherer PE (2001) The adipocyte-secreted protein Acrp30 enhances hepatic insulin action. *Nat Med* 7: 947-953.
30. Ouchi N, Kihara S, Arita Y, Okamoto Y, Maeda K, et al. (2000) Adiponectin, an adipocyte-derived plasma protein, inhibits endothelial NF-kappaB signaling through a cAMP-dependent pathway. *Circulation* 102: 1296-1301.
31. Rakatzi I, Mueller H, Ritzeler O, Tennagels N, Eckel J (2004) Adiponectin counteracts cytokine- and fatty acid-induced apoptosis in the pancreatic beta-cell line INS-1. *Diabetologia* 47: 249-258.
32. Domingueti CP, Dusse LM, Carvalho M, de Sousa LP, Gomes KB, et al. (2016) Diabetes mellitus: The linkage between oxidative stress, inflammation, hypercoagulability and vascular complications. *J Diabetes Complications* 30: 738-745.
33. Domingueti CP, Dusse LM, Carvalho M, Gomes KB, Fernandes AP (2013) Hypercoagulability and cardiovascular disease in diabetic nephropathy. *Clin Chim Acta* 415: 279-285.
34. Sosnowska B, Penson P, Banach M (2017) The role of nutraceuticals in the prevention of cardiovascular disease. *Cardiovasc Diagn Ther* 7: S21-s31.
35. Wautier J-L, Guillausseau P-J (1998) Diabetes, advanced glycation endproducts and vascular disease. *Vascular Medicine* 3: 131-137.
36. Karnib HH, Ziyadeh FN (2010) The cardiorenal syndrome in diabetes mellitus. *Diabetes Research and Clinical Practice* 89: 201-208.
37. Goldberg RB (2009) Cytokine and Cytokine-Like Inflammation Markers, Endothelial Dysfunction, and Imbalanced Coagulation in Development of Diabetes and Its Complications. *The Journal of Clinical Endocrinology & Metabolism* 94: 3171-3182.
38. Giannini C, Mohn A, Chiarelli F, Kelnar CJH (2011) Macrovascular angiopathy in children and adolescents with type 1 diabetes. *Diabetes/Metabolism Research and Reviews* 27: 436-460.
39. Kessler L, Wiesel ML, Attali P, Mossard JM, Cazenave JP, et al. (1998) Von Willebrand factor in diabetic angiopathy. *Diabetes Metab* 24: 327-336.

40. Margetic S (2012) Inflammation and haemostasis. *Biochem Med (Zagreb)* 22: 49-62.
41. Yamagishi S-i, Matsui T (2010) Advanced Glycation end Products, Oxidative Stress and Diabetic Nephropathy. *Oxidative Medicine and Cellular Longevity* 3.
42. Karalliedde J, Gnudi L (2016) Diabetes mellitus, a complex and heterogeneous disease, and the role of insulin resistance as a determinant of diabetic kidney disease. *Nephrol Dial Transplant* 31: 206-213.
43. Domingueti CP, Dusse LMSA, Carvalho MdG, Gomes KB, Fernandes AP (2013) Hypercoagulability and cardiovascular disease in diabetic nephropathy. *Clinica Chimica Acta* 415: 279-285.
44. Ziyadeh FN (2008) Different roles for TGF-beta and VEGF in the pathogenesis of the cardinal features of diabetic nephropathy. *Diabetes Res Clin Pract* 82 Suppl 1: S38-41.
45. Sasson AN, Cherney DZ (2012) Renal hyperfiltration related to diabetes mellitus and obesity in human disease. *World J Diabetes* 3: 1-6.
46. De Vriese AS, Stoenoiu MS, Elger M, Devuyst O, Vanholder R, et al. (2001) Diabetes-induced microvascular dysfunction in the hydronephrotic kidney: role of nitric oxide. *Kidney Int* 60: 202-210.
47. Sharma K, Cook A, Smith M, Valancius C, Inscho EW (2005) TGF-beta impairs renal autoregulation via generation of ROS. *Am J Physiol Renal Physiol* 288: F1069-1077.
48. Raij L (2005) The pathophysiologic basis for blocking the renin-angiotensin system in hypertensive patients with renal disease. *Am J Hypertens* 18: 95s-99s.
49. Arima S, Ito S (2003) The mechanisms underlying altered vascular resistance of glomerular afferent and efferent arterioles in diabetic nephropathy. *Nephrol Dial Transplant* 18: 1966-1969.
50. Wilding JP (2014) The role of the kidneys in glucose homeostasis in type 2 diabetes: clinical implications and therapeutic significance through sodium glucose co-transporter 2 inhibitors. *Metabolism* 63: 1228-1237.
51. Cherney DZ, Perkins BA, Soleymanlou N, Maione M, Lai V, et al. (2014) Renal hemodynamic effect of sodium-glucose cotransporter 2 inhibition in patients with type 1 diabetes mellitus. *Circulation* 129: 587-597.
52. Deng G, Long Y, Yu YR, Li MR (2010) Adiponectin directly improves endothelial dysfunction in obese rats through the AMPK-eNOS Pathway. *Int J Obes (Lond)* 34: 165-171.

53. Hunley TE, Ma LJ, Kon V (2010) Scope and mechanisms of obesity-related renal disease. *Curr Opin Nephrol Hypertens* 19: 227-234.
54. Wisse BE (2004) The inflammatory syndrome: the role of adipose tissue cytokines in metabolic disorders linked to obesity. *J Am Soc Nephrol* 15: 2792-2800.
55. Otero M, Lago R, Lago F, Casanueva FF, Dieguez C, et al. (2005) Leptin, from fat to inflammation: old questions and new insights. *FEBS Lett* 579: 295-301.
56. Welsh GI, Hale LJ, Eremina V, Jeansson M, Maezawa Y, et al. (2010) Insulin signaling to the glomerular podocyte is critical for normal kidney function. *Cell Metab* 12: 329-340.
57. Fornoni A (2010) Proteinuria, the podocyte, and insulin resistance. *N Engl J Med* 363: 2068-2069.
58. Dubin R, Cushman M, Folsom AR, Fried LF, Palmas W, et al. (2011) Kidney function and multiple hemostatic markers: cross sectional associations in the multi-ethnic study of atherosclerosis. *BMC Nephrology* 12: 3.
59. Sahakyan K, Klein BE, Lee KE, Tsai MY, Klein R (2010) Inflammatory and endothelial dysfunction markers and proteinuria in persons with type 1 diabetes mellitus. *Eur J Endocrinol* 162: 1101-1105.
60. Clements JA, Willemsen NM, Myers SA, Dong Y (2004) The tissue kallikrein family of serine proteases: functional roles in human disease and potential as clinical biomarkers. *Crit Rev Clin Lab Sci* 41: 265-312.
61. Yousef GM, Obiezu CV, Luo LY, Magklara A, Borgono CA, et al. (2005) Human tissue kallikreins: from gene structure to function and clinical applications. *Adv Clin Chem* 39: 11-79.
62. Sainz IM, Pixley RA, Colman RW (2007) Fifty years of research on the plasma kallikrein-kinin system: from protein structure and function to cell biology and in-vivo pathophysiology. *Thromb Haemost* 98: 77-83.
63. Kayashima Y, Smithies O, Kakoki M (2012) The kallikrein-kinin system and oxidative stress. *Curr Opin Nephrol Hypertens* 21: 92-96.
64. Tomita H, Sanford RB, Smithies O, Kakoki M (2012) The kallikrein-kinin system in diabetic nephropathy. *Kidney Int* 81: 733-744.
65. Phipps JA, Feener EP (2008) The kallikrein-kinin system in diabetic retinopathy: lessons for the kidney. *Kidney Int* 73: 1114-1119.

66. Shariat-Madar Z, Mahdi F, Warnock M, Homeister JW, Srikanth S, et al. (2006) Bradykinin B2 receptor knockout mice are protected from thrombosis by increased nitric oxide and prostacyclin. *Blood* 108: 192-199.
67. Kaplan AP, Joseph K, Shibayama Y, Nakazawa Y, Ghebrehiwet B, et al. (1998) Bradykinin formation. Plasma and tissue pathways and cellular interactions. *Clin Rev Allergy Immunol* 16: 403-429.
68. Colman RW, Schmaier AH (1997) Contact system: a vascular biology modulator with anticoagulant, profibrinolytic, antiadhesive, and proinflammatory attributes. *Blood* 90: 3819-3843.
69. Yousef GM, Diamandis EP (2001) The new human tissue kallikrein gene family: structure, function, and association to disease. *Endocr Rev* 22: 184-204.
70. Zhang JC, Claffey K, Sakthivel R, Darzynkiewicz Z, Shaw DE, et al. (2000) Two-chain high molecular weight kininogen induces endothelial cell apoptosis and inhibits angiogenesis: partial activity within domain 5. *FASEB J* 14: 2589-2600.
71. Bergmann S, Zheng D, Barredo J, Abboud MR, Jaffa AA (2006) Renal kallikrein: a risk marker for nephropathy in children with sickle cell disease. *J Pediatr Hematol Oncol* 28: 147-153.
72. Leeb-Lundberg LM, Marceau F, Muller-Esterl W, Pettibone DJ, Zuraw BL (2005) International union of pharmacology. XLV. Classification of the kinin receptor family: from molecular mechanisms to pathophysiological consequences. *Pharmacol Rev* 57: 27-77.
73. Gilman AG (1990) *Pharmacological Basis of Therapeutics*; 8, editor. New York: Pergamon Press. 1811 p.
74. Webb JG, Tan Y, Jaffa MA, Jaffa AA (2010) Evidence for prostacyclin and cAMP upregulation by bradykinin and insulin-like growth factor 1 in vascular smooth muscle cells. *J Recept Signal Transduct Res* 30: 61-71.
75. Rivilla F, Vallejo S, Peiro C, Sanchez-Ferrer CF (2012) Characterization of endothelium-dependent relaxations in the mesenteric vasculature: a comparative study with potential pathophysiological relevance. *J Pediatr Surg* 47: 2044-2049.
76. Shesely EG, Hu CB, Alhenc-Gelas F, Meneton P, Carretero OA (2006) A second expressed kininogen gene in mice. *Physiol Genomics* 26: 152-157.
77. Hassan S, Sainz IM, Khan MM, Bradford HN, Isordia-Salas I, et al. (2007) Antithrombotic activity of kininogen is mediated by inhibitory effects of domain 3 during arterial injury in vivo. *Am J Physiol Heart Circ Physiol* 292: H2959-2965.

78. Marceau F, Regoli D (2004) Bradykinin receptor ligands: therapeutic perspectives. *Nat Rev Drug Discov* 3: 845-852.
79. Kakoki M, Smithies O (2009) The kallikrein-kinin system in health and in diseases of the kidney. *Kidney Int* 75: 1019-1030.
80. Ignjatovic T, Tan F, Brovkovich V, Skidgel RA, Erdos EG (2002) Activation of bradykinin B1 receptor by ACE inhibitors. *Int Immunopharmacol* 2: 1787-1793.
81. Tschope C, Schultheiss HP, Walther T (2002) Multiple interactions between the renin-angiotensin and the kallikrein-kinin systems: role of ACE inhibition and AT1 receptor blockade. *J Cardiovasc Pharmacol* 39: 478-487.
82. Sabourin T, Morissette G, Bouthillier J, Levesque L, Marceau F (2002) Expression of kinin B(1) receptor in fresh or cultured rabbit aortic smooth muscle: role of NF-kappa B. *Am J Physiol Heart Circ Physiol* 283: H227-237.
83. Jaffa MA, Kobeissy F, Al Hariri M, Chalhoub H, Eid A, et al. (2012) Global renal gene expression profiling analysis in B2-kinin receptor null mice: impact of diabetes. *PLoS One* 7: e44714.
84. Bossi F, Fischetti F, Regoli D, Durigutto P, Frossi B, et al. (2009) Novel pathogenic mechanism and therapeutic approaches to angioedema associated with C1 inhibitor deficiency. *J Allergy Clin Immunol* 124: 1303-1310 e1304.
85. Westermann D, Walther T, Savvatis K, Escher F, Sobirey M, et al. (2009) Gene deletion of the kinin receptor B1 attenuates cardiac inflammation and fibrosis during the development of experimental diabetic cardiomyopathy. *Diabetes* 58: 1373-1381.
86. Fryer RM, Segreti J, Banfor PN, Widomski DL, Backes BJ, et al. (2008) Effect of bradykinin metabolism inhibitors on evoked hypotension in rats: rank efficacy of enzymes associated with bradykinin-mediated angioedema. *Br J Pharmacol* 153: 947-955.
87. Tang SC, Leung JC, Lai KN (2011) The kallikrein-kinin system. *Contrib Nephrol* 170: 145-155.
88. Cyr M, Lepage Y, Blais C, Jr., Gervais N, Cugno M, et al. (2001) Bradykinin and des-Arg(9)-bradykinin metabolic pathways and kinetics of activation of human plasma. *Am J Physiol Heart Circ Physiol* 281: H275-283.
89. Fink E, Bhoola KD, Snyman C, Neth P, Figueroa CD (2007) Cellular expression of plasma prekallikrein in human tissues. *Biol Chem* 388: 957-963.
90. Iwaki T, Castellino FJ (2006) Plasma levels of bradykinin are suppressed in factor XII-deficient mice. *Thromb Haemost* 95: 1003-1010.

91. Han ED, MacFarlane RC, Mulligan AN, Scafidi J, Davis AE, 3rd (2002) Increased vascular permeability in C1 inhibitor-deficient mice mediated by the bradykinin type 2 receptor. *J Clin Invest* 109: 1057-1063.
92. Maas C, Renne T (2012) Regulatory mechanisms of the plasma contact system. *Thromb Res* 129 Suppl 2: S73-76.
93. Gustafson EJ, Schutsky D, Knight LC, Schmaier AH (1986) High molecular weight kininogen binds to unstimulated platelets. *J Clin Invest* 78: 310-318.
94. Motta G, Rojkaer R, Hasan AA, Cines DB, Schmaier AH (1998) High molecular weight kininogen regulates prekallikrein assembly and activation on endothelial cells: a novel mechanism for contact activation. *Blood* 91: 516-528.
95. Mahdi F, Madar ZS, Figueroa CD, Schmaier AH (2002) Factor XII interacts with the multiprotein assembly of urokinase plasminogen activator receptor, gC1qR, and cytokeratin 1 on endothelial cell membranes. *Blood* 99: 3585-3596.
96. Mahdi F, Shariat-Madar Z, Schmaier AH (2003) The relative priority of prekallikrein and factors XI/XIa assembly on cultured endothelial cells. *J Biol Chem* 278: 43983-43990.
97. Selvarajan S, Lund LR, Takeuchi T, Craik CS, Werb Z (2001) A plasma kallikrein-dependent plasminogen cascade required for adipocyte differentiation. *Nat Cell Biol* 3: 267-275.
98. Joseph K, Kaplan AP (2005) Formation of bradykinin: a major contributor to the innate inflammatory response. *Adv Immunol* 86: 159-208.
99. Maas C, Oschatz C, Renne T (2011) The plasma contact system 2.0. *Semin Thromb Hemost* 37: 375-381.
100. Revenko AS, Gao D, Crosby JR, Bhattacharjee G, Zhao C, et al. (2011) Selective depletion of plasma prekallikrein or coagulation factor XII inhibits thrombosis in mice without increased risk of bleeding. *Blood* 118: 5302-5311.
101. Merkulov S, Zhang WM, Komar AA, Schmaier AH, Barnes E, et al. (2008) Deletion of murine kininogen gene 1 (mKng1) causes loss of plasma kininogen and delays thrombosis. *Blood* 111: 1274-1281.
102. Kleinschnitz C, Stoll G, Bendszus M, Schuh K, Pauer HU, et al. (2006) Targeting coagulation factor XII provides protection from pathological thrombosis in cerebral ischemia without interfering with hemostasis. *J Exp Med* 203: 513-518.
103. Cichon S, Martin L, Hennies HC, Muller F, Van Driessche K, et al. (2006) Increased activity of coagulation factor XII (Hageman factor) causes hereditary angioedema type III. *Am J Hum Genet* 79: 1098-1104.

104. Zhao Y, Qiu Q, Mahdi F, Shariat-Madar Z, Rojkjaer R, et al. (2001) Assembly and activation of HK-PK complex on endothelial cells results in bradykinin liberation and NO formation. *Am J Physiol Heart Circ Physiol* 280: H1821-1829.
105. Liu J, Gao BB, Clermont AC, Blair P, Chilcote TJ, et al. (2011) Hyperglycemia-induced cerebral hematoma expansion is mediated by plasma kallikrein. *Nat Med* 17: 206-210.
106. Diamandis EP, Yousef GM, Luo LY, Magklara A, Obiezu CV (2000) The new human kallikrein gene family: implications in carcinogenesis. *Trends Endocrinol Metab* 11: 54-60.
107. Murray SR, Chao J, Lin FK, Chao L (1990) Kallikrein multigene families and the regulation of their expression. *J Cardiovasc Pharmacol* 15 Suppl 6: S7-16.
108. Yousef GM, Chang A, Scorilas A, Diamandis EP (2000) Genomic organization of the human kallikrein gene family on chromosome 19q13.3-q13.4. *Biochem Biophys Res Commun* 276: 125-133.
109. Yousef GM, Kopolovic AD, Elliott MB, Diamandis EP (2003) Genomic overview of serine proteases. *Biochem Biophys Res Commun* 305: 28-36.
110. Kapadia C, Chang A, Sotiropoulou G, Yousef GM, Grass L, et al. (2003) Human kallikrein 13: production and purification of recombinant protein and monoclonal and polyclonal antibodies, and development of a sensitive and specific immunofluorometric assay. *Clin Chem* 49: 77-86.
111. Yousef GM, Polymeris ME, Grass L, Soosaipillai A, Chan PC, et al. (2003) Human kallikrein 5: a potential novel serum biomarker for breast and ovarian cancer. *Cancer Res* 63: 3958-3965.
112. Komatsu N, Takata M, Otsuki N, Toyama T, Ohka R, et al. (2003) Expression and localization of tissue kallikrein mRNAs in human epidermis and appendages. *J Invest Dermatol* 121: 542-549.
113. Kishi T, Soosaipillai A, Grass L, Little SP, Johnstone EM, et al. (2004) Development of an immunofluorometric assay and quantification of human kallikrein 7 in tissue extracts and biological fluids. *Clin Chem* 50: 709-716.
114. Charlesworth MC, Young CY, Miller VM, Tindall DJ (1999) Kininogenase activity of prostate-derived human glandular kallikrein (hK2) purified from seminal fluid. *J Androl* 20: 220-229.
115. Brattsand M, Egelrud T (1999) Purification, molecular cloning, and expression of a human stratum corneum trypsin-like serine protease with possible function in desquamation. *J Biol Chem* 274: 30033-30040.

116. Gomis-Ruth FX, Bayes A, Sotiropoulou G, Pampalakis G, Tsetsenis T, et al. (2002) The structure of human prokallikrein 6 reveals a novel activation mechanism for the kallikrein family. *J Biol Chem* 277: 27273-27281.
117. Yousef GM, Diamandis EP (2002) Human tissue kallikreins: a new enzymatic cascade pathway? *Biol Chem* 383: 1045-1057.
118. Clements JA (2008) Reflections on the tissue kallikrein and kallikrein-related peptidase family - from mice to men - what have we learnt in the last two decades? *Biol Chem* 389: 1447-1454.
119. Li HX, Hwang BY, Laxmikanthan G, Blaber SI, Blaber M, et al. (2008) Substrate specificity of human kallikreins 1 and 6 determined by phage display. *Protein Sci* 17: 664-672.
120. Gao L, Smith RS, Chen LM, Chai KX, Chao L, et al. (2010) Tissue kallikrein promotes prostate cancer cell migration and invasion via a protease-activated receptor-1-dependent signaling pathway. *Biol Chem* 391: 803-812.
121. Petraki CD, Karavana VN, Revelos KI, Luo LY, Diamandis EP (2002) Immunohistochemical localization of human kallikreins 6 and 10 in pancreatic islets. *Histochem J* 34: 313-322.
122. de Veer SJ, Swedberg JE, Parker EA, Harris JM (2012) Non-combinatorial library screening reveals subsite cooperativity and identifies new high-efficiency substrates for kallikrein-related peptidase 14. *Biol Chem* 393: 331-341.
123. Kolte D, Shariat-Madar Z (2016) Plasma Kallikrein Inhibitors in Cardiovascular Disease: An Innovative Therapeutic Approach. *Cardiology in Review* 24: 99-109.
124. Bird JE, Smith PL, Wang X, Schumacher WA, Barbera F, et al. (2012) Effects of plasma kallikrein deficiency on haemostasis and thrombosis in mice: murine ortholog of the Fletcher trait. *Thromb Haemost* 107: 1141-1150.
125. Kolte D, Osman N, Yang J, Shariat-Madar Z (2011) High molecular weight kininogen activates B2 receptor signaling pathway in human vascular endothelial cells. *J Biol Chem* 286: 24561-24571.
126. Marceau F (1995) Kinin B1 receptors: a review. *Immunopharmacology* 30: 1-26.
127. DiScipio RG (1982) The activation of the alternative pathway C3 convertase by human plasma kallikrein. *Immunology* 45: 587-595.
128. Ghebrehiwet B, Silverberg M, Kaplan AP (1981) Activation of the classical pathway of complement by Hageman factor fragment. *J Exp Med* 153: 665-676.

129. Schapira M, Despland E, Scott CF, Boxer LA, Colman RW (1982) Purified human plasma kallikrein aggregates human blood neutrophils. *J Clin Invest* 69: 1199-1202.
130. Bryant JW, Shariat-Madar Z (2009) Human plasma kallikrein-kinin system: physiological and biochemical parameters. *Cardiovasc Hematol Agents Med Chem* 7: 234-250.
131. Costa-Neto CM, Dillenburg-Pilla P, Heinrich TA, Parreiras-e-Silva LT, Pereira MG, et al. (2008) Participation of kallikrein-kinin system in different pathologies. *Int Immunopharmacol* 8: 135-142.
132. Tirapelli CR, Bonaventura D, de Oliveira AM (2007) Functional characterization of the mechanisms underlying bradykinin-induced relaxation in the isolated rat carotid artery. *Life Sci* 80: 1799-1805.
133. Cooper JA, Miller GJ, Bauer KA, Morrissey JH, Meade TW, et al. (2000) Comparison of novel hemostatic factors and conventional risk factors for prediction of coronary heart disease. *Circulation* 102: 2816-2822.
134. Grundt H, Nilsen DW, Hetland O, Valente E, Fagertun HE (2004) Activated factor 12 (FXIIa) predicts recurrent coronary events after an acute myocardial infarction. *Am Heart J* 147: 260-266.
135. Storini C, Bergamaschini L, Gesuete R, Rossi E, Maiocchi D, et al. (2006) Selective inhibition of plasma kallikrein protects brain from reperfusion injury. *J Pharmacol Exp Ther* 318: 849-854.
136. Groger M, Lebesgue D, Pruneau D, Relton J, Kim SW, et al. (2005) Release of bradykinin and expression of kinin B2 receptors in the brain: role for cell death and brain edema formation after focal cerebral ischemia in mice. *J Cereb Blood Flow Metab* 25: 978-989.
137. Ding-Zhou L, Margail I, Palmier B, Pruneau D, Plotkine M, et al. (2003) LF 16-0687 Ms, a bradykinin B2 receptor antagonist, reduces ischemic brain injury in a murine model of transient focal cerebral ischemia. *Br J Pharmacol* 139: 1539-1547.
138. Zausinger S, Lumenta DB, Pruneau D, Schmid-Elsaesser R, Plesnila N, et al. (2002) Effects of LF 16-0687 Ms, a bradykinin B(2) receptor antagonist, on brain edema formation and tissue damage in a rat model of temporary focal cerebral ischemia. *Brain Res* 950: 268-278.
139. Relton JK, Beckey VE, Hanson WL, Whalley ET (1997) CP-0597, a selective bradykinin B2 receptor antagonist, inhibits brain injury in a rat model of reversible middle cerebral artery occlusion. *Stroke* 28: 1430-1436.

140. Maas C, Govers-Riemslog JW, Bouma B, Schiks B, Hazenberg BP, et al. (2008) Misfolded proteins activate factor XII in humans, leading to kallikrein formation without initiating coagulation. *J Clin Invest* 118: 3208-3218.
141. Gao BB, Clermont A, Rook S, Fonda SJ, Srinivasan VJ, et al. (2007) Extracellular carbonic anhydrase mediates hemorrhagic retinal and cerebral vascular permeability through prekallikrein activation. *Nat Med* 13: 181-188.
142. Jaffa AA, Durazo-Arvizu R, Zheng D, Lackland DT, Srikanth S, et al. (2003) Plasma prekallikrein: a risk marker for hypertension and nephropathy in type 1 diabetes. *Diabetes* 52: 1215-1221.
143. Ienaga K, Sohn M, Naiki M, Jaffa AA (2014) Creatinine metabolite, HMH (5-hydroxy-1-methylhydantoin; NZ-419), modulates bradykinin-induced changes in vascular smooth muscle cells. *J Recept Signal Transduct Res* 34: 195-200.
144. Velarde V, de la Cerda PM, Duarte C, Arancibia F, Abbott E, et al. (2004) Role of reactive oxygen species in bradykinin-induced proliferation of vascular smooth muscle cells. *Biol Res* 37: 419-430.
145. Bodin S, Chollet C, Goncalves-Mendes N, Gardes J, Pean F, et al. (2009) Kallikrein protects against microalbuminuria in experimental type I diabetes. *Kidney Int* 76: 395-403.
146. (1995) Effect of intensive therapy on the development and progression of diabetic nephropathy in the Diabetes Control and Complications Trial. The Diabetes Control and Complications (DCCT) Research Group. *Kidney Int* 47: 1703-1720.
147. Blazquez-Medela AM, Lopez-Novoa JM, Martinez-Salgado C (2010) Mechanisms involved in the genesis of diabetic nephropathy. *Curr Diabetes Rev* 6: 68-87.
148. Drummond K, Mauer M (2002) The early natural history of nephropathy in type 1 diabetes: II. Early renal structural changes in type 1 diabetes. *Diabetes* 51: 1580-1587.
149. Balakumar P, Arora MK, Reddy J, Anand-Srivastava MB (2009) Pathophysiology of diabetic nephropathy: involvement of multifaceted signalling mechanism. *J Cardiovasc Pharmacol* 54: 129-138.
150. Chiang WC, Lin SL, Chen YM, Wu KD, Tsai TJ (2008) Urinary kallikrein excretion is related to renal function change and inflammatory status in chronic kidney disease patients receiving angiotensin II receptor blocker treatment. *Nephrology (Carlton)* 13: 198-203.
151. Churchill PC, Churchill MC, Bidani AK, Rabito SF (1995) Kallikrein excretion in Dahl salt-sensitive and salt-resistant rats with native and transplanted kidneys. *Am J Physiol* 269: F710-717.

152. Wang C, Chen YP, Chao L, Chao J (1995) Regulatory elements in the promoter region of the renal kallikrein gene in normotensive vs hypertensive rats. *Biochem Biophys Res Commun* 217: 113-122.
153. Schneeweiss S, Seeger JD, Landon J, Walker AM (2008) Aprotinin during coronary-artery bypass grafting and risk of death. *N Engl J Med* 358: 771-783.
154. Jaffa AA, Rust PF, Mayfield RK (1995) Kinin, a mediator of diabetes-induced glomerular hyperfiltration. *Diabetes* 44: 156-160.
155. Moreau ME, Garbacki N, Molinaro G, Brown NJ, Marceau F, et al. (2005) The kallikrein-kinin system: current and future pharmacological targets. *J Pharmacol Sci* 99: 6-38.
156. Harvey JN, Edmundson AW, Jaffa AA, Martin LL, Mayfield RK (1992) Renal excretion of kallikrein and eicosanoids in patients with type 1 (insulin-dependent) diabetes mellitus. Relationship to glomerular and tubular function. *Diabetologia* 35: 857-862.
157. Harvey JN, Jaffa AA, Margolius HS, Mayfield RK (1990) Renal kallikrein and hemodynamic abnormalities of diabetic kidney. *Diabetes* 39: 299-304.
158. Tan Y, Wang B, Keum JS, Jaffa AA (2005) Mechanisms through which bradykinin promotes glomerular injury in diabetes. *Am J Physiol Renal Physiol* 288: F483-492.
159. Tschöpe C, Reinecke A, Seidl U, Yu M, Gavrilluk V, et al. (1999) Functional, biochemical, and molecular investigations of renal kallikrein-kinin system in diabetic rats. *Am J Physiol* 277: H2333-2340.
160. Brownlee M (2001) Biochemistry and molecular cell biology of diabetic complications. *Nature* 414: 813-820.
161. Tsutsumi Y, Matsubara H, Masaki H, Kurihara H, Murasawa S, et al. (1999) Angiotensin II type 2 receptor overexpression activates the vascular kinin system and causes vasodilation. *J Clin Invest* 104: 925-935.
162. Sharma K, Ziyadeh FN (1994) The emerging role of transforming growth factor-beta in kidney diseases. *Am J Physiol* 266: F829-842.
163. Ziyadeh FN, Sharma K (1995) Role of transforming growth factor-beta in diabetic glomerulosclerosis and renal hypertrophy. *Kidney Int Suppl* 51: S34-36.
164. Ziyadeh FN (1994) Role of transforming growth factor beta in diabetic nephropathy. *Exp Nephrol* 2: 137.

165. Godin C, Smith AD, Riley PA (1991) Bradykinin stimulates DNA synthesis in competent Balb/c 3T3 cells and enhances inositol phosphate formation induced by platelet-derived growth factor. *Biochem Pharmacol* 42: 117-122.
166. Alric C, Pecher C, Cellier E, Schanstra JP, Poirier B, et al. (2002) Inhibition of IGF-I-induced Erk 1 and 2 activation and mitogenesis in mesangial cells by bradykinin. *Kidney Int* 62: 412-421.
167. Schreiber BD, Hughes ML, Groggel GC (1995) Insulin-like growth factor-1 stimulates production of mesangial cell matrix components. *Clin Nephrol* 43: 368-374.
168. El-Dahr SS, Dipp S, Baricos WH (1998) Bradykinin stimulates the ERK-->Elk-1-->Fos/AP-1 pathway in mesangial cells. *Am J Physiol* 275: F343-352.
169. Shao S, Yang Y, Yuan G, Zhang M, Yu X (2013) Signaling molecules involved in lipid-induced pancreatic beta-cell dysfunction. *DNA Cell Biol* 32: 41-49.
170. Newsholme P, Keane D, Welters HJ, Morgan NG (2007) Life and death decisions of the pancreatic beta-cell: the role of fatty acids. *Clin Sci (Lond)* 112: 27-42.
171. Ng ML, Wadham C, Sukocheva OA (2017) The role of sphingolipid signalling in diabetes-associated pathologies (Review). *Int J Mol Med* 39: 243-252.
172. Alemany R, van Koppen CJ, Danneberg K, Ter Braak M, Meyer Zu Heringdorf D (2007) Regulation and functional roles of sphingosine kinases. *Naunyn Schmiedebergs Arch Pharmacol* 374: 413-428.
173. Olivera A, Spiegel S (1993) Sphingosine-1-phosphate as second messenger in cell proliferation induced by PDGF and FCS mitogens. *Nature* 365: 557-560.
174. Van Brocklyn JR, Lee MJ, Menzeleev R, Olivera A, Edsall L, et al. (1998) Dual actions of sphingosine-1-phosphate: extracellular through the Gi-coupled receptor Edg-1 and intracellular to regulate proliferation and survival. *J Cell Biol* 142: 229-240.
175. Pyne S, Chapman J, Steele L, Pyne NJ (1996) Sphingomyelin-derived lipids differentially regulate the extracellular signal-regulated kinase 2 (ERK-2) and c-Jun N-terminal kinase (JNK) signal cascades in airway smooth muscle. *Eur J Biochem* 237: 819-826.
176. Cuvillier O, Pirianov G, Kleuser B, Vanek PG, Coso OA, et al. (1996) Suppression of ceramide-mediated programmed cell death by sphingosine-1-phosphate. *Nature* 381: 800-803.
177. Qi Y, Chen J, Lay A, Don A, Vadas M, et al. (2013) Loss of sphingosine kinase 1 predisposes to the onset of diabetes via promoting pancreatic beta-cell death in diet-induced obese mice. *Faseb j* 27: 4294-4304.

178. Bruce CR, Risis S, Babb JR, Yang C, Kowalski GM, et al. (2012) Overexpression of sphingosine kinase 1 prevents ceramide accumulation and ameliorates muscle insulin resistance in high-fat diet-fed mice. *Diabetes* 61: 3148-3155.
179. Pyne S, Pyne NJ (2011) Translational aspects of sphingosine 1-phosphate biology. *Trends Mol Med* 17: 463-472.
180. Maceyka M, Spiegel S (2014) Sphingolipid metabolites in inflammatory disease. *Nature* 510: 58-67.
181. Mendelson K, Evans T, Hla T (2014) Sphingosine 1-phosphate signalling. *Development* 141: 5-9.
182. Hla T, Dannenberg AJ (2012) Sphingolipid signaling in metabolic disorders. *Cell Metab* 16: 420-434.
183. Pitson SM (2011) Regulation of sphingosine kinase and sphingolipid signaling. *Trends Biochem Sci* 36: 97-107.
184. Don AS, Rosen H (2009) A lipid binding domain in sphingosine kinase 2. *Biochem Biophys Res Commun* 380: 87-92.
185. Hait NC, Allegood J, Maceyka M, Strub GM, Harikumar KB, et al. (2009) Regulation of histone acetylation in the nucleus by sphingosine-1-phosphate. *Science* 325: 1254-1257.
186. Giussani P, Maceyka M, Le Stunff H, Mikami A, Lepine S, et al. (2006) Sphingosine-1-phosphate phosphohydrolase regulates endoplasmic reticulum-to-golgi trafficking of ceramide. *Mol Cell Biol* 26: 5055-5069.
187. Pitson SM, Moretti PA, Zebol JR, Lynn HE, Xia P, et al. (2003) Activation of sphingosine kinase 1 by ERK1/2-mediated phosphorylation. *Embo j* 22: 5491-5500.
188. Barr RK, Lynn HE, Moretti PA, Khew-Goodall Y, Pitson SM (2008) Deactivation of sphingosine kinase 1 by protein phosphatase 2A. *J Biol Chem* 283: 34994-35002.
189. Sutherland CM, Moretti PA, Hewitt NM, Bagley CJ, Vadas MA, et al. (2006) The calmodulin-binding site of sphingosine kinase and its role in agonist-dependent translocation of sphingosine kinase 1 to the plasma membrane. *J Biol Chem* 281: 11693-11701.
190. Siow D, Wattenberg B (2011) The compartmentalization and translocation of the sphingosine kinases: mechanisms and functions in cell signaling and sphingolipid metabolism. *Crit Rev Biochem Mol Biol* 46: 365-375.

191. Maceyka M, Sankala H, Hait NC, Le Stunff H, Liu H, et al. (2005) SphK1 and SphK2, sphingosine kinase isoenzymes with opposing functions in sphingolipid metabolism. *J Biol Chem* 280: 37118-37129.
192. Ding G, Sonoda H, Yu H, Kajimoto T, Goparaju SK, et al. (2007) Protein kinase D-mediated phosphorylation and nuclear export of sphingosine kinase 2. *J Biol Chem* 282: 27493-27502.
193. Hait NC, Bellamy A, Milstien S, Kordula T, Spiegel S (2007) Sphingosine kinase type 2 activation by ERK-mediated phosphorylation. *J Biol Chem* 282: 12058-12065.
194. Alvarez SE, Milstien S, Spiegel S (2007) Autocrine and paracrine roles of sphingosine-1-phosphate. *Trends Endocrinol Metab* 18: 300-307.
195. Strub GM, Maceyka M, Hait NC, Milstien S, Spiegel S (2010) Extracellular and intracellular actions of sphingosine-1-phosphate. *Adv Exp Med Biol* 688: 141-155.
196. Maceyka M, Harikumar KB, Milstien S, Spiegel S (2012) Sphingosine-1-phosphate signaling and its role in disease. *Trends Cell Biol* 22: 50-60.
197. Artal-Sanz M, Tavernarakis N (2009) Prohibitin and mitochondrial biology. *Trends Endocrinol Metab* 20: 394-401.
198. Takasugi N, Sasaki T, Suzuki K, Osawa S, Isshiki H, et al. (2011) BACE1 activity is modulated by cell-associated sphingosine-1-phosphate. *J Neurosci* 31: 6850-6857.
199. Panneer Selvam S, De Palma RM, Oaks JJ, Oleinik N, Peterson YK, et al. (2015) Binding of the sphingolipid S1P to hTERT stabilizes telomerase at the nuclear periphery by allosterically mimicking protein phosphorylation. *Sci Signal* 8: ra58.
200. Parham KA, Zebol JR, Tooley KL, Sun WY, Moldenhauer LM, et al. (2015) Sphingosine 1-phosphate is a ligand for peroxisome proliferator-activated receptor-gamma that regulates neoangiogenesis. *Faseb j* 29: 3638-3653.
201. Tao C, Sifuentes A, Holland WL (2014) Regulation of glucose and lipid homeostasis by adiponectin: effects on hepatocytes, pancreatic beta cells and adipocytes. *Best Pract Res Clin Endocrinol Metab* 28: 43-58.
202. Osawa Y, Seki E, Kodama Y, Suetsugu A, Miura K, et al. (2011) Acid sphingomyelinase regulates glucose and lipid metabolism in hepatocytes through AKT activation and AMP-activated protein kinase suppression. *Faseb j* 25: 1133-1144.
203. Lee SY, Hong IK, Kim BR, Shim SM, Sung Lee J, et al. (2015) Activation of sphingosine kinase 2 by endoplasmic reticulum stress ameliorates hepatic steatosis and insulin resistance in mice. *Hepatology* 62: 135-146.

204. Kowalski GM, Kloehn J, Burch ML, Selathurai A, Hamley S, et al. (2015) Overexpression of sphingosine kinase 1 in liver reduces triglyceride content in mice fed a low but not high-fat diet. *Biochim Biophys Acta* 1851: 210-219.
205. Boslem E, Meikle PJ, Biden TJ (2012) Roles of ceramide and sphingolipids in pancreatic beta-cell function and dysfunction. *Islets* 4: 177-187.
206. Zhu Q, Shan X, Miao H, Lu Y, Xu J, et al. (2009) Acute activation of acid ceramidase affects cytokine-induced cytotoxicity in rat islet beta-cells. *FEBS Lett* 583: 2136-2141.
207. Véret J, Coant N, Berdyshev Evgeny V, Skobeleva A, Therville N, et al. (2011) Ceramide synthase 4 and *de novo* production of ceramides with specific N-acyl chain lengths are involved in glucolipototoxicity-induced apoptosis of INS-1 β -cells. *Biochemical Journal* 438: 177-189.
208. Boslem E, MacIntosh G, Preston AM, Bartley C, Busch AK, et al. (2011) A lipidomic screen of palmitate-treated MIN6 beta-cells links sphingolipid metabolites with endoplasmic reticulum (ER) stress and impaired protein trafficking. *Biochem J* 435: 267-276.
209. Jessup CF, Bonder CS, Pitson SM, Coates PT (2011) The sphingolipid rheostat: a potential target for improving pancreatic islet survival and function. *Endocr Metab Immune Disord Drug Targets* 11: 262-272.
210. Zhang W, Mottillo EP, Zhao J, Gartung A, VanHecke GC, et al. (2014) Adipocyte lipolysis-stimulated interleukin-6 production requires sphingosine kinase 1 activity. *J Biol Chem* 289: 32178-32185.
211. Tous M, Ferrer-Lorente R, Badimon L (2014) Selective inhibition of sphingosine kinase-1 protects adipose tissue against LPS-induced inflammatory response in Zucker diabetic fatty rats. *Am J Physiol Endocrinol Metab* 307: E437-446.
212. Wang J, Badeanlou L, Bielawski J, Ciaraldi TP, Samad F (2014) Sphingosine kinase 1 regulates adipose proinflammatory responses and insulin resistance. *Am J Physiol Endocrinol Metab* 306: E756-768.
213. Borodzicz S, Czarzasta K, Kuch M, Cudnoch-Jedrzejewska A (2015) Sphingolipids in cardiovascular diseases and metabolic disorders. *Lipids Health Dis* 14: 55.
214. Jiang XC, Liu J (2013) Sphingolipid metabolism and atherosclerosis. *Handb Exp Pharmacol*: 133-146.
215. Janes K, Little JW, Li C, Bryant L, Chen C, et al. (2014) The development and maintenance of paclitaxel-induced neuropathic pain require activation of the sphingosine 1-phosphate receptor subtype 1. *J Biol Chem* 289: 21082-21097.

216. Xie B, Shen J, Dong A, Rashid A, Stoller G, et al. (2009) Blockade of sphingosine-1-phosphate reduces macrophage influx and retinal and choroidal neovascularization. *J Cell Physiol* 218: 192-198.
217. Lan T, Liu W, Xie X, Xu S, Huang K, et al. (2011) Sphingosine kinase-1 pathway mediates high glucose-induced fibronectin expression in glomerular mesangial cells. *Mol Endocrinol* 25: 2094-2105.
218. Schnell O, Cappuccio F, Genovese S, Standl E, Valensi P, et al. (2013) Type 1 diabetes and cardiovascular disease. *Cardiovasc Diabetol* 12: 156.
219. Paneni F, Beckman JA, Creager MA, Cosentino F (2013) Diabetes and vascular disease: pathophysiology, clinical consequences, and medical therapy: part I. *Eur Heart J* 34: 2436-2443.
220. Fioretto P, Dodson PM, Ziegler D, Rosenson RS (2010) Residual microvascular risk in diabetes: unmet needs and future directions. *Nat Rev Endocrinol* 6: 19-25.
221. Li H, Horke S, Forstermann U (2014) Vascular oxidative stress, nitric oxide and atherosclerosis. *Atherosclerosis* 237: 208-219.
222. Keul P, Lucke S, von Wnuck Lipinski K, Bode C, Graler M, et al. (2011) Sphingosine-1-phosphate receptor 3 promotes recruitment of monocyte/macrophages in inflammation and atherosclerosis. *Circ Res* 108: 314-323.
223. Ahmad M, Long JS, Pyne NJ, Pyne S (2006) The effect of hypoxia on lipid phosphate receptor and sphingosine kinase expression and mitogen-activated protein kinase signaling in human pulmonary smooth muscle cells. *Prostaglandins & Other Lipid Mediators* 79: 278-286.
224. Chen J, Tang H, Sysol JR, Moreno-Vinasco L, Shioura KM, et al. (2014) The sphingosine kinase 1/sphingosine-1-phosphate pathway in pulmonary arterial hypertension. *Am J Respir Crit Care Med* 190: 1032-1043.
225. Harijith A, Pendyala S, Reddy NM, Bai T, Usatyuk PV, et al. (2013) Sphingosine Kinase 1 Deficiency Confers Protection against Hyperoxia-Induced Bronchopulmonary Dysplasia in a Murine Model. *The American Journal of Pathology* 183: 1169-1182.
226. Milara J, Navarro R, Juan G, Peiro T, Serrano A, et al. (2012) Sphingosine-1-phosphate is increased in patients with idiopathic pulmonary fibrosis and mediates epithelial to mesenchymal transition. *Thorax* 67: 147-156.
227. Ammit AJ, Hastie AT, Edsall LC, Hoffman RK, Amrani Y, et al. (2001) Sphingosine 1-phosphate modulates human airway smooth muscle cell functions that promote inflammation and airway remodeling in asthma. *FASEB J* 15: 1212-1214.

228. Spiegel S, Milstien S (2002) Sphingosine 1-phosphate, a key cell signaling molecule. *J Biol Chem* 277: 25851-25854.
229. Wilson PC, Fitzgibbon WR, Garrett SM, Jaffa AA, Luttrell LM, et al. (2015) Inhibition of Sphingosine Kinase 1 Ameliorates Angiotensin II-Induced Hypertension and Inhibits Transmembrane Calcium Entry via Store-Operated Calcium Channel. *Mol Endocrinol* 29: 896-908.
230. Furuya H, Wada M, Shimizu Y, Yamada PM, Hannun YA, et al. (2013) Effect of sphingosine kinase 1 inhibition on blood pressure. *Faseb j* 27: 656-664.
231. MacRitchie N, Volpert G, Al Washih M, Watson DG, Futerman AH, et al. (2016) Effect of the sphingosine kinase 1 selective inhibitor, PF-543 on arterial and cardiac remodelling in a hypoxic model of pulmonary arterial hypertension. *Cell Signal* 28: 946-955.
232. Siedlinski M, Nosalski R, Szczepaniak P, Ludwig-Galezowska AH, Mikolajczyk T, et al. (2017) Vascular transcriptome profiling identifies Sphingosine kinase 1 as a modulator of angiotensin II-induced vascular dysfunction. *Sci Rep* 7: 44131.
233. Xia P, Vadas MA, Rye KA, Barter PJ, Gamble JR (1999) High density lipoproteins (HDL) interrupt the sphingosine kinase signaling pathway. A possible mechanism for protection against atherosclerosis by HDL. *J Biol Chem* 274: 33143-33147.
234. Karliner JS (2009) Sphingosine kinase and sphingosine 1-phosphate in cardioprotection. *J Cardiovasc Pharmacol* 53: 189-197.
235. Ma MM, Chen JL, Wang GG, Wang H, Lu Y, et al. (2007) Sphingosine kinase 1 participates in insulin signalling and regulates glucose metabolism and homeostasis in KK/Ay diabetic mice. *Diabetologia* 50: 891-900.
236. Karliner JS (2013) Sphingosine kinase and sphingosine 1-phosphate in the heart: a decade of progress. *Biochim Biophys Acta* 1831: 203-212.
237. Karliner JS (2009) Sphingosine kinase regulation and cardioprotection. *Cardiovasc Res* 82: 184-192.
238. Whetzel AM, Bolick DT, Hedrick CC (2009) Sphingosine-1-phosphate inhibits high glucose-mediated ERK1/2 action in endothelium through induction of MAP kinase phosphatase-3. *Am J Physiol Cell Physiol* 296: C339-345.
239. Vessey DA, Kelley M, Li L, Huang Y (2009) Sphingosine protects aging hearts from ischemia/reperfusion injury: Superiority to sphingosine 1-phosphate and ischemic pre- and post-conditioning. *Oxid Med Cell Longev* 2: 146-151.

240. Jin ZQ, Karliner JS, Vessey DA (2008) Ischaemic postconditioning protects isolated mouse hearts against ischaemia/reperfusion injury via sphingosine kinase isoform-1 activation. *Cardiovasc Res* 79: 134-140.
241. Liu Y (2006) Renal fibrosis: new insights into the pathogenesis and therapeutics. *Kidney Int* 69: 213-217.
242. Klawitter S, Hofmann LP, Pfeilschifter J, Huwiler A (2007) Extracellular nucleotides induce migration of renal mesangial cells by upregulating sphingosine kinase-1 expression and activity. *Br J Pharmacol* 150: 271-280.
243. Yaghobian D, Don AS, Yaghobian S, Chen X, Pollock CA, et al. (2016) Increased sphingosine 1-phosphate mediates inflammation and fibrosis in tubular injury in diabetic nephropathy. *Clin Exp Pharmacol Physiol* 43: 56-66.
244. Liu W, Lan T, Xie X, Huang K, Peng J, et al. (2012) S1P2 receptor mediates sphingosine-1-phosphate-induced fibronectin expression via MAPK signaling pathway in mesangial cells under high glucose condition. *Exp Cell Res* 318: 936-943.
245. Imasawa T, Kitamura H, Ohkawa R, Satoh Y, Miyashita A, et al. (2010) Unbalanced expression of sphingosine 1-phosphate receptors in diabetic nephropathy. *Exp Toxicol Pathol* 62: 53-60.
246. Xia P, Wang L, Gamble JR, Vadas MA (1999) Activation of sphingosine kinase by tumor necrosis factor-alpha inhibits apoptosis in human endothelial cells. *J Biol Chem* 274: 34499-34505.
247. Vessey DA, Kelley M, Li L, Huang Y, Zhou HZ, et al. (2006) Role of sphingosine kinase activity in protection of heart against ischemia reperfusion injury. *Med Sci Monit* 12: Br318-324.
248. Jin ZQ, Karliner JS (2006) Low dose N, N-dimethylsphingosine is cardioprotective and activates cytosolic sphingosine kinase by a PKCepsilon dependent mechanism. *Cardiovasc Res* 71: 725-734.
249. Besler C, Heinrich K, Rohrer L, Doerries C, Riwanto M, et al. (2011) Mechanisms underlying adverse effects of HDL on eNOS-activating pathways in patients with coronary artery disease. *J Clin Invest* 121: 2693-2708.
250. Park SW, Kim M, Kim JY, Brown KM, Haase VH, et al. (2012) Proximal tubule sphingosine kinase-1 has a critical role in A1 adenosine receptor-mediated renal protection from ischemia. *Kidney Int* 82: 878-891.
251. Bonetti PO, Lerman LO, Lerman A (2003) Endothelial Dysfunction. A Marker of Atherosclerotic Risk 23: 168-175.

252. Vincent MA, Montagnani M, Quon MJ (2003) Molecular and physiologic actions of insulin related to production of nitric oxide in vascular endothelium. *Current Diabetes Reports* 3: 279-288.
253. Ferroni P, Basili S, Falco A, Davì G (2004) Inflammation, insulin resistance, and obesity. *Current Atherosclerosis Reports* 6: 424-431.
254. Yan H, Aziz E, Shillabeer G, Wong A, Shanghavi D, et al. (2002) Nitric oxide promotes differentiation of rat white preadipocytes in culture. *J Lipid Res* 43: 2123-2129.
255. Kubota N, Terauchi Y, Yamauchi T, Kubota T, Moroi M, et al. (2002) Disruption of adiponectin causes insulin resistance and neointimal formation. *J Biol Chem* 277: 25863-25866.
256. Beltowski J (2006) Leptin and atherosclerosis. *Atherosclerosis* 189: 47-60.
257. Beltowski J (2006) Role of leptin in blood pressure regulation and arterial hypertension. *J Hypertens* 24: 789-801.
258. Koleva DI, Orbetzova MM, Nikolova JG, Deneva TI (2016) Pathophysiological Role of Adiponectin, Leptin and Asymmetric Dimethylarginine in the Process of Atherosclerosis. *Folia Med (Plovdiv)* 58: 234-240.
259. Mantzoros CS (1999) The role of leptin in human obesity and disease: a review of current evidence. *Ann Intern Med* 130: 671-680.
260. Matarese G, Moschos S, Mantzoros CS (2005) Leptin in immunology. *J Immunol* 174: 3137-3142.
261. Chan JL, Heist K, DePaoli AM, Veldhuis JD, Mantzoros CS (2003) The role of falling leptin levels in the neuroendocrine and metabolic adaptation to short-term starvation in healthy men. *J Clin Invest* 111: 1409-1421.
262. Saad MF, Damani S, Gingerich RL, Riad-Gabriel MG, Khan A, et al. (1997) Sexual dimorphism in plasma leptin concentration. *J Clin Endocrinol Metab* 82: 579-584.
263. Brennan AM, Mantzoros CS (2006) Drug Insight: the role of leptin in human physiology and pathophysiology--emerging clinical applications. *Nat Clin Pract Endocrinol Metab* 2: 318-327.
264. Friedman JM, Halaas JL (1998) Leptin and the regulation of body weight in mammals. *Nature* 395: 763-770.
265. Lee GH, Proenca R, Montez JM, Carroll KM, Darvishzadeh JG, et al. (1996) Abnormal splicing of the leptin receptor in diabetic mice. *Nature* 379: 632-635.

266. Elmquist JK, Bjorbaek C, Ahima RS, Flier JS, Saper CB (1998) Distributions of leptin receptor mRNA isoforms in the rat brain. *J Comp Neurol* 395: 535-547.
267. Bjorbaek C, Elmquist JK, Michl P, Ahima RS, van Bueren A, et al. (1998) Expression of leptin receptor isoforms in rat brain microvessels. *Endocrinology* 139: 3485-3491.
268. Chan JL, Bluher S, Yiannakouris N, Suchard MA, Kratzsch J, et al. (2002) Regulation of circulating soluble leptin receptor levels by gender, adiposity, sex steroids, and leptin: observational and interventional studies in humans. *Diabetes* 51: 2105-2112.
269. Zhou Y, Rui L (2013) Leptin signaling and leptin resistance. *Frontiers of medicine* 7: 207-222.
270. Morris DL, Rui L (2009) Recent advances in understanding leptin signaling and leptin resistance. *Am J Physiol Endocrinol Metab* 297: E1247-1259.
271. Xu AW, Ste-Marie L, Kaelin CB, Barsh GS (2007) Inactivation of signal transducer and activator of transcription 3 in proopiomelanocortin (Pomc) neurons causes decreased pomc expression, mild obesity, and defects in compensatory refeeding. *Endocrinology* 148: 72-80.
272. Huang H, Kong D, Byun KH, Ye C, Koda S, et al. (2012) Rho-kinase regulates energy balance by targeting hypothalamic leptin receptor signaling. *Nat Neurosci* 15: 1391-1398.
273. Zeidan A, Paylor B, Steinhoff KJ, Javadov S, Rajapurohitam V, et al. (2007) Actin cytoskeleton dynamics promotes leptin-induced vascular smooth muscle hypertrophy via RhoA/ROCK- and phosphatidylinositol 3-kinase/protein kinase B-dependent pathways. *J Pharmacol Exp Ther* 322: 1110-1116.
274. Peelman F, Tavernier J (2013) ROCKing the JAKs. *JAK-STAT* 2: e24074.
275. Fei H, Okano HJ, Li C, Lee GH, Zhao C, et al. (1997) Anatomic localization of alternatively spliced leptin receptors (Ob-R) in mouse brain and other tissues. *Proc Natl Acad Sci U S A* 94: 7001-7005.
276. Schwartz MW, Peskind E, Raskind M, Boyko EJ, Porte D, Jr. (1996) Cerebrospinal fluid leptin levels: relationship to plasma levels and to adiposity in humans. *Nat Med* 2: 589-593.
277. Ren D, Li M, Duan C, Rui L (2005) Identification of SH2-B as a key regulator of leptin sensitivity, energy balance, and body weight in mice. *Cell Metab* 2: 95-104.
278. Lan TH, Huang XQ, Tan HM (2013) Vascular fibrosis in atherosclerosis. *Cardiovasc Pathol* 22: 401-407.

279. Touyz RM (2005) Intracellular mechanisms involved in vascular remodelling of resistance arteries in hypertension: role of angiotensin II. *Exp Physiol* 90: 449-455.
280. Shirwany NA, Zou MH (2010) Arterial stiffness: a brief review. *Acta Pharmacol Sin* 31: 1267-1276.
281. Katsuda S, Kaji T (2003) Atherosclerosis and extracellular matrix. *J Atheroscler Thromb* 10: 267-274.
282. Jacob MP (2003) Extracellular matrix remodeling and matrix metalloproteinases in the vascular wall during aging and in pathological conditions. *Biomed Pharmacother* 57: 195-202.
283. Arribas SM, Hinek A, González MC (2006) Elastic fibres and vascular structure in hypertension. *Pharmacology & Therapeutics* 111: 771-791.
284. Montezano AC, Nguyen Dinh Cat A, Rios FJ, Touyz RM (2014) Angiotensin II and vascular injury. *Curr Hypertens Rep* 16: 431.
285. Shafer I, Nancollas R, Boes M, Sieminski AL, Geddes JB (2011) Stability of a microvessel subject to structural adaptation of diameter and wall thickness. *Math Med Biol* 28: 271-286.
286. Savoia C, Burger D, Nishigaki N, Montezano A, Touyz RM (2011) Angiotensin II and the vascular phenotype in hypertension. *Expert Rev Mol Med* 13: e11.
287. Meissner A, Miro F, Jimenez-Altayo F, Jurado A, Vila E, et al. (2017) Sphingosine-1-phosphate signalling-a key player in the pathogenesis of Angiotensin II-induced hypertension. *Cardiovasc Res* 113: 123-133.
288. Ryan ST, Koteliensky VE, Gotwals PJ, Lindner V (2003) Transforming growth factor-beta-dependent events in vascular remodeling following arterial injury. *J Vasc Res* 40: 37-46.
289. de las Heras N, Ruiz-Ortega M, Ruperez M, Sanz-Rosa D, Miana M, et al. (2006) Role of connective tissue growth factor in vascular and renal damage associated with hypertension in rats. Interactions with angiotensin II. *J Renin Angiotensin Aldosterone Syst* 7: 192-200.
290. Frenay AR, Yazdani S, Boersema M, van der Graaf AM, Waanders F, et al. (2015) Incomplete Restoration of Angiotensin II-Induced Renal Extracellular Matrix Deposition and Inflammation Despite Complete Functional Recovery in Rats. *PLoS One* 10: e0129732.
291. Touyz RM, Briones AM (2011) Reactive oxygen species and vascular biology: implications in human hypertension. *Hypertens Res* 34: 5-14.

292. Ban CR, Twigg SM (2008) Fibrosis in diabetes complications: pathogenic mechanisms and circulating and urinary markers. *Vasc Health Risk Manag* 4: 575-596.
293. Song W, Ergul A (2006) Type-2 diabetes-induced changes in vascular extracellular matrix gene expression: relation to vessel size. *Cardiovasc Diabetol* 5: 3.
294. Cooper ME (2004) Importance of advanced glycation end products in diabetes-associated cardiovascular and renal disease. *Am J Hypertens* 17: 31S-38S.
295. Reddy GK (2004) AGE-related cross-linking of collagen is associated with aortic wall matrix stiffness in the pathogenesis of drug-induced diabetes in rats. *Microvasc Res* 68: 132-142.
296. Newby AC (2006) Matrix metalloproteinases regulate migration, proliferation, and death of vascular smooth muscle cells by degrading matrix and non-matrix substrates. *Cardiovasc Res* 69: 614-624.
297. Lavrentyev EN, Estes AM, Malik KU (2007) Mechanism of high glucose induced angiotensin II production in rat vascular smooth muscle cells. *Circ Res* 101: 455-464.
298. Zou H, Wu G, Lv J, Xu G (2017) Relationship of angiotensin I-converting enzyme (ACE) and bradykinin B2 receptor (BDKRB2) polymorphism with diabetic nephropathy. *Biochim Biophys Acta* 1863: 1264-1272.
299. Sagar SK, Zhang C, Guo Q, Yi R (2013) Role of expression of endothelin-1 and angiotensin-II and hypoxia-inducible factor-1alpha in the kidney tissues of patients with diabetic nephropathy. *Saudi J Kidney Dis Transpl* 24: 959-964.
300. Russo I, Frangogiannis NG (2016) Diabetes-associated cardiac fibrosis: Cellular effectors, molecular mechanisms and therapeutic opportunities. *J Mol Cell Cardiol* 90: 84-93.
301. Chade AR, Mushin OP, Zhu X, Rodriguez-Porcel M, Grande JP, et al. (2005) Pathways of renal fibrosis and modulation of matrix turnover in experimental hypercholesterolemia. *Hypertension* 46: 772-779.
302. Figarola JL, Loera S, Weng Y, Shanmugam N, Natarajan R, et al. (2008) LR-90 prevents dyslipidaemia and diabetic nephropathy in the Zucker diabetic fatty rat. *Diabetologia* 51: 882-891.
303. Eddy AA (1998) Interstitial fibrosis in hypercholesterolemic rats: role of oxidation, matrix synthesis, and proteolytic cascades. *Kidney Int* 53: 1182-1189.
304. Lee HS (2012) Paracrine role for TGF-beta-induced CTGF and VEGF in mesangial matrix expansion in progressive glomerular disease. *Histol Histopathol* 27: 1131-1141.

305. Song CY, Kim BC, Hong HK, Lee HS (2005) Oxidized LDL activates PAI-1 transcription through autocrine activation of TGF-beta signaling in mesangial cells. *Kidney Int* 67: 1743-1752.
306. El-Shewy HM, Sohn M, Wilson P, Lee MH, Hammad SM, et al. (2012) Low-density lipoprotein induced expression of connective tissue growth factor via transactivation of sphingosine 1-phosphate receptors in mesangial cells. *Mol Endocrinol* 26: 833-845.
307. Sanchez-Lopez E, Rodriguez-Vita J, Cartier C, Ruperez M, Esteban V, et al. (2008) Inhibitory effect of interleukin-1beta on angiotensin II-induced connective tissue growth factor and type IV collagen production in cultured mesangial cells. *Am J Physiol Renal Physiol* 294: F149-160.
308. Leask A (2011) CCN2/decorin interactions: a novel approach to combating fibrosis? *J Cell Commun Signal* 5: 249-250.
309. Oemar BS, Werner A, Garnier JM, Do DD, Godoy N, et al. (1997) Human connective tissue growth factor is expressed in advanced atherosclerotic lesions. *Circulation* 95: 831-839.
310. Lau LF (2016) Cell surface receptors for CCN proteins. *J Cell Commun Signal* 10: 121-127.
311. Lipson KE, Wong C, Teng Y, Spong S (2012) CTGF is a central mediator of tissue remodeling and fibrosis and its inhibition can reverse the process of fibrosis. *Fibrogenesis Tissue Repair* 5: S24.
312. Purohit T, Qin Z, Quan C, Lin Z, Quan T (2017) Smad3-dependent CCN2 mediates fibronectin expression in human skin dermal fibroblasts. *J Cell Commun Signal* 12: e0173191.
313. Cheng Y, Lin CH, Chen JY, Li CH, Liu YT, et al. (2016) Induction of Connective Tissue Growth Factor Expression by Hypoxia in Human Lung Fibroblasts via the MEKK1/MEK1/ERK1/GLI-1/GLI-2 and AP-1 Pathways. *PLoS One* 11: e0160593.
314. Leask A, Abraham DJ (2003) The role of connective tissue growth factor, a multifunctional matricellular protein, in fibroblast biology. *Biochem Cell Biol* 81: 355-363.
315. Droppelmann CA, Gutierrez J, Vial C, Brandan E (2009) Matrix metalloproteinase-2-deficient fibroblasts exhibit an alteration in the fibrotic response to connective tissue growth factor/CCN2 because of an increase in the levels of endogenous fibronectin. *J Biol Chem* 284: 13551-13561.
316. Crean JK, Finlay D, Murphy M, Moss C, Godson C, et al. (2002) The role of p42/44 MAPK and protein kinase B in connective tissue growth factor induced extracellular matrix protein production, cell migration, and actin cytoskeletal rearrangement in human mesangial cells. *J Biol Chem* 277: 44187-44194.

317. Kostourou V, Papalazarou V (2014) Non-collagenous ECM proteins in blood vessel morphogenesis and cancer. *Biochimica et Biophysica Acta (BBA) - General Subjects* 1840: 2403-2413.
318. Maurer LM, Tomasini-Johansson BR, Mosher DF (2010) Emerging roles of fibronectin in thrombosis. *Thromb Res* 125: 287-291.
319. Mao Y, Schwarzbauer JE (2005) Fibronectin fibrillogenesis, a cell-mediated matrix assembly process. *Matrix Biol* 24: 389-399.
320. Singh P, Schwarzbauer JE (2012) Fibronectin and stem cell differentiation - lessons from chondrogenesis. *J Cell Sci* 125: 3703-3712.
321. Ni H, Yuen PS, Papalia JM, Trevithick JE, Sakai T, et al. (2003) Plasma fibronectin promotes thrombus growth and stability in injured arterioles. *Proc Natl Acad Sci U S A* 100: 2415-2419.
322. Cho J, Mosher DF (2006) Role of fibronectin assembly in platelet thrombus formation. *J Thromb Haemost* 4: 1461-1469.
323. Davi G, Patrono C (2007) Platelet activation and atherothrombosis. *N Engl J Med* 357: 2482-2494.
324. Massam-Wu T, Chiu M, Choudhury R, Chaudhry SS, Baldwin AK, et al. (2010) Assembly of fibrillin microfibrils governs extracellular deposition of latent TGF beta. *J Cell Sci* 123: 3006-3018.
325. Hynes RO (2007) Cell-matrix adhesion in vascular development. *J Thromb Haemost* 5 Suppl 1: 32-40.
326. Smith ML, Gourdon D, Little WC, Kubow KE, Eguiluz RA, et al. (2007) Force-induced unfolding of fibronectin in the extracellular matrix of living cells. *PLoS Biol* 5: e268.
327. Schiller HB, Hermann MR, Polleux J, Vignaud T, Zanivan S, et al. (2013) beta1- and alpha5-class integrins cooperate to regulate myosin II during rigidity sensing of fibronectin-based microenvironments. *Nat Cell Biol* 15: 625-636.
328. Astrof S, Crowley D, George EL, Fukuda T, Sekiguchi K, et al. (2004) Direct test of potential roles of EIIIA and EIIIB alternatively spliced segments of fibronectin in physiological and tumor angiogenesis. *Mol Cell Biol* 24: 8662-8670.
329. McDonald JA, Quade BJ, Broekelmann TJ, LaChance R, Forsman K, et al. (1987) Fibronectin's cell-adhesive domain and an amino-terminal matrix assembly domain participate in its assembly into fibroblast pericellular matrix. *J Biol Chem* 262: 2957-2967.

330. Fruh SM, Schoen I, Ries J, Vogel V (2015) Molecular architecture of native fibronectin fibrils. *Nat Commun* 6: 7275.
331. Takahashi S, Leiss M, Moser M, Ohashi T, Kitao T, et al. (2007) The RGD motif in fibronectin is essential for development but dispensable for fibril assembly. *J Cell Biol* 178: 167-178.
332. Franz M, Brehm BR, Richter P, Gruen K, Neri D, et al. (2010) Changes in extra cellular matrix remodelling and re-expression of fibronectin and tenascin-C splicing variants in human myocardial tissue of the right atrial auricle: implications for a targeted therapy of cardiovascular diseases using human SIP format antibodies. *J Mol Histol* 41: 39-50.
333. Carpenter B, Lin Y, Stoll S, Raffai RL, McCuskey R, et al. (2005) VEGF is crucial for the hepatic vascular development required for lipoprotein uptake. *Development* 132: 3293-3303.
334. Abbott NJ, Ronnback L, Hansson E (2006) Astrocyte-endothelial interactions at the blood-brain barrier. *Nat Rev Neurosci* 7: 41-53.
335. Cho NH (2016) Q&A: Five questions on the 2015 IDF Diabetes Atlas. *Diabetes Res Clin Pract* 115: 157-159.
336. Ding Y, Sun X, Shan PF (2017) MicroRNAs and Cardiovascular Disease in Diabetes Mellitus. *Biomed Res Int* 2017: 4080364.
337. Bannier K, Lichtenauer M, Franz M, Fritzenwanger M, Kabisch B, et al. (2015) Impact of diabetes mellitus and its complications: survival and quality-of-life in critically ill patients. *J Diabetes Complications* 29: 1130-1135.
338. Mogensen CE (1997) How to protect the kidney in diabetic patients: with special reference to IDDM. *Diabetes* 46 Suppl 2: S104-111.
339. Kilpatrick ES (2012) The rise and fall of HbA(1c) as a risk marker for diabetes complications. *Diabetologia* 55: 2089-2091.
340. Nathan DM, Group DER (2014) The diabetes control and complications trial/epidemiology of diabetes interventions and complications study at 30 years: overview. *Diabetes Care* 37: 9-16.
341. Larusch GA, Merkulova A, Mahdi F, Shariat-Madar Z, Sitrin RG, et al. (2013) Domain 2 of uPAR regulates single-chain urokinase-mediated angiogenesis through beta1-integrin and VEGFR2. *Am J Physiol Heart Circ Physiol* 305: H305-320.
342. Zheng H, Wu J, Jin Z, Yan LJ (2017) Potential Biochemical Mechanisms of Lung Injury in Diabetes. *Aging Dis* 8: 7-16.

343. Hsueh WA, Law RE (1998) Cardiovascular risk continuum: implications of insulin resistance and diabetes. *Am J Med* 105: 4S-14S.
344. Lusis AJ (2000) Atherosclerosis. *Nature* 407: 233-241.
345. Brahma MK, Pepin ME, Wende AR (2017) My Sweetheart Is Broken: Role of Glucose in Diabetic Cardiomyopathy. *Diabetes Metab J* 41: 1-9.
346. Fokkens BT, Mulder DJ, Schalkwijk CG, Scheijen JL, Smit AJ, et al. (2017) Vitreous advanced glycation endproducts and alpha-dicarbonyls in retinal detachment patients with type 2 diabetes mellitus and non-diabetic controls. *PLoS One* 12: e0173379.
347. Peng W, Zhang Y, Zhu R, Mechref Y (2017) Comparative Membrane Proteomics Analyses of Breast Cancer Cell Lines to Understand the Molecular Mechanism of Breast Cancer Brain Metastasis. *Electrophoresis*.
348. Garcia-Campos MA, Espinal-Enriquez J, Hernandez-Lemus E (2015) Pathway Analysis: State of the Art. *Front Physiol* 6: 383.
349. Takahashi E, Unoki-Kubota H, Shimizu Y, Okamura T, Iwata W, et al. (2017) Proteomic analysis of serum biomarkers for prediabetes using the Long-Evans Agouti rat, a spontaneous animal model of type 2 diabetes mellitus. *J Diabetes Investig*.
350. Voss JG, Shagal AG, Tsuji JM, MacDonald JW, Bammler TK, et al. (2017) Time Course of Inflammatory Gene Expression Following Crush Injury in Murine Skeletal Muscle. *Nurs Res* 66: 63-74.
351. Lu MY, Huang CI, Hsieh MY, Hsieh TJ, Hsi E, et al. (2016) Dynamics of PBMC gene expression in hepatitis C virus genotype 1-infected patients during combined peginterferon/ribavirin therapy. *Oncotarget* 7: 61325-61335.
352. Hatzirodos N, Glister C, Hummitzsch K, Irving-Rodgers HF, Knight PG, et al. (2017) Transcriptomal profiling of bovine ovarian granulosa and theca interna cells in primary culture in comparison with their in vivo counterparts. *PLoS One* 12: e0173391.
353. Lindsey ML, Mayr M, Gomes AV, Delles C, Arrell DK, et al. (2015) Transformative Impact of Proteomics on Cardiovascular Health and Disease: A Scientific Statement From the American Heart Association. *Circulation* 132: 852-872.
354. Geyer PE, Kulak NA, Pichler G, Holdt LM, Teupser D, et al. (2016) Plasma Proteome Profiling to Assess Human Health and Disease. *Cell Syst* 2: 185-195.
355. Diabetes C, Complications Trial /Epidemiology of Diabetes I, Complications Research G, Lachin JM, White NH, et al. (2015) Effect of intensive diabetes therapy on the progression of diabetic retinopathy in patients with type 1 diabetes: 18 years of follow-up in the DCCT/EDIC. *Diabetes* 64: 631-642.

356. Shao B, Tang C, Sinha A, Mayer PS, Davenport GD, et al. (2014) Humans with atherosclerosis have impaired ABCA1 cholesterol efflux and enhanced high-density lipoprotein oxidation by myeloperoxidase. *Circ Res* 114: 1733-1742.
357. Huang Y, DiDonato JA, Levison BS, Schmitt D, Li L, et al. (2014) An abundant dysfunctional apolipoprotein A1 in human atheroma. *Nat Med* 20: 193-203.
358. Voronova V, Zhudenkov K, Helmlinger G, Peskov K (2017) Interpretation of metabolic memory phenomenon using a physiological systems model: What drives oxidative stress following glucose normalization? *PLoS One* 12: e0171781.
359. Roberto T, Rita BA, Prattichizzo F, La Sala L, De Nigris V, et al. (2017) The "Metabolic Memory" Theory and the Early Treatment of Hyperglycemia in Prevention of Diabetic Complications. *Nutrients* 9.
360. Patel VB, Parajuli N, Oudit GY (2014) Role of angiotensin-converting enzyme 2 (ACE2) in diabetic cardiovascular complications. *Clin Sci (Lond)* 126: 471-482.
361. Nguyen Dinh Cat A, Touyz RM (2011) A new look at the renin-angiotensin system--focusing on the vascular system. *Peptides* 32: 2141-2150.
362. Khan SA, Dong H, Joyce J, Sasaki T, Chu ML, et al. (2016) Fibulin-2 is essential for angiotensin II-induced myocardial fibrosis mediated by transforming growth factor (TGF)-beta. *Lab Invest* 96: 773-783.
363. Dong WQ, Chao M, Lu QH, Chai WL, Zhang W, et al. (2016) Prohibitin overexpression improves myocardial function in diabetic cardiomyopathy. *Oncotarget* 7: 66-80.
364. Cai L, Li W, Wang G, Guo L, Jiang Y, et al. (2002) Hyperglycemia-induced apoptosis in mouse myocardium: mitochondrial cytochrome C-mediated caspase-3 activation pathway. *Diabetes* 51: 1938-1948.
365. Cai L, Kang YJ (2001) Oxidative stress and diabetic cardiomyopathy: a brief review. *Cardiovasc Toxicol* 1: 181-193.
366. Bavelloni A, Piazzini M, Raffini M, Faenza I, Blalock WL (2015) Prohibitin 2: At a communications crossroads. *IUBMB Life* 67: 239-254.
367. Merchant ML, Niewczas MA, Ficociello LH, Lukenbill JA, Wilkey DW, et al. (2013) Plasma kininogen and kininogen fragments are biomarkers of progressive renal decline in type 1 diabetes. *Kidney Int* 83: 1177-1184.
368. Jaffa MA, Luttrell D, Schmaier AH, Klein RL, Lopes-Virella M, et al. (2016) Plasma Prekallikrein Is Associated With Carotid Intima-Media Thickness in Type 1 Diabetes. *Diabetes* 65: 498-502.

369. Munoz J, Heck AJ (2014) From the human genome to the human proteome. *Angew Chem Int Ed Engl* 53: 10864-10866.
370. Schwammle V, Aspalter CM, Sidoli S, Jensen ON (2014) Large scale analysis of co-existing post-translational modifications in histone tails reveals global fine structure of cross-talk. *Mol Cell Proteomics* 13: 1855-1865.
371. Gajjala PR, Fliser D, Speer T, Jankowski V, Jankowski J (2015) Emerging role of post-translational modifications in chronic kidney disease and cardiovascular disease. *Nephrol Dial Transplant* 30: 1814-1824.
372. Smith LE, White MY (2014) The role of post-translational modifications in acute and chronic cardiovascular disease. *Proteomics Clin Appl* 8: 506-521.
373. Del Monte F, Agnetti G (2014) Protein post-translational modifications and misfolding: new concepts in heart failure. *Proteomics Clin Appl* 8: 534-542.
374. Fiorentino TV, Priolella A, Zuo P, Folli F (2013) Hyperglycemia-induced oxidative stress and its role in diabetes mellitus related cardiovascular diseases. *Curr Pharm Des* 19: 5695-5703.
375. Matsuyama Y, Terawaki H, Terada T, Era S (2009) Albumin thiol oxidation and serum protein carbonyl formation are progressively enhanced with advancing stages of chronic kidney disease. *Clin Exp Nephrol* 13: 308-315.
376. Caimi G, Carollo C, Hopps E, Montana M, Lo Presti R (2013) Protein oxidation in chronic kidney disease. *Clin Hemorheol Microcirc* 54: 409-413.
377. Stephen EA, Venkatasubramaniam A, Good TA, Topoleski LD (2014) The effect of oxidation on the mechanical response and microstructure of porcine aortas. *J Biomed Mater Res A* 102: 3255-3262.
378. Van JAD, Scholey JW, Konvalinka A (2017) Insights into Diabetic Kidney Disease Using Urinary Proteomics and Bioinformatics. *Journal of the American Society of Nephrology* 28: 1050-1061.
379. Jenkin KA, O'Keefe L, Simcocks AC, Briffa JF, Mathai ML, et al. (2016) Renal effects of chronic pharmacological manipulation of CB2 receptors in rats with diet-induced obesity. *Br J Pharmacol* 173: 1128-1142.
380. Thongboonkerd V, Zheng S, McLeish KR, Epstein PN, Klein JB (2005) Proteomic identification and immunolocalization of increased renal calbindin-D28k expression in OVE26 diabetic mice. *Rev Diabet Stud* 2: 19-26.

381. Wang Y, Zhou J, Minto AW, Hack BK, Alexander JJ, et al. (2006) Altered vitamin D metabolism in type II diabetic mouse glomeruli may provide protection from diabetic nephropathy. *Kidney Int* 70: 882-891.
382. Liu X, Yang G, Fan Q, Wang L (2014) Proteomic profile in glomeruli of type-2 diabetic KK^{Ay} mice using 2-dimensional differential gel electrophoresis. *Med Sci Monit* 20: 2705-2713.
383. Herrington W, Lacey B, Sherliker P, Armitage J, Lewington S (2016) Epidemiology of Atherosclerosis and the Potential to Reduce the Global Burden of Atherothrombotic Disease. *Circ Res* 118: 535-546.
384. Fonarow GC (2007) The global burden of atherosclerotic vascular disease. *Nat Clin Pract Cardiovasc Med* 4: 530-531.
385. Association AH (2016) Atherosclerosis. Cholesterol- Why Cholesterol Matters. October 10, 2016 ed. AHA website: www.heart.org; American Heart Association (AHA).
386. Singh RB, Mengi SA, Xu YJ, Arneja AS, Dhalla NS (2002) Pathogenesis of atherosclerosis: A multifactorial process. *Exp Clin Cardiol* 7: 40-53.
387. Moore KJ, Tabas I (2011) Macrophages in the pathogenesis of atherosclerosis. *Cell* 145: 341-355.
388. Bennett MR, Sinha S, Owens GK (2016) Vascular Smooth Muscle Cells in Atherosclerosis. *Circ Res* 118: 692-702.
389. Yang SW, Lim L, Ju S, Choi DH, Song H (2014) Effects of matrix metalloproteinase 13 on vascular smooth muscle cells migration via Akt-ERK dependent pathway. *Tissue Cell*.
390. Takabe K, Kim RH, Allegood JC, Mitra P, Ramachandran S, et al. (2010) Estradiol induces export of sphingosine 1-phosphate from breast cancer cells via ABCC1 and ABCG2. *J Biol Chem* 285: 10477-10486.
391. Spiegel S, Milstien S (2007) Functions of the multifaceted family of sphingosine kinases and some close relatives. *J Biol Chem* 282: 2125-2129.
392. Bryan L, Kordula T, Spiegel S, Milstien S (2008) Regulation and functions of sphingosine kinases in the brain. *Biochim Biophys Acta* 1781: 459-466.
393. Spiegel S, Milstien S (2003) Sphingosine-1-phosphate: an enigmatic signalling lipid. *Nat Rev Mol Cell Biol* 4: 397-407.
394. Herr DR, Chun J (2007) Effects of LPA and S1P on the nervous system and implications for their involvement in disease. *Curr Drug Targets* 8: 155-167.

395. Pyne S, Pyne N (2000) Sphingosine 1-phosphate signalling via the endothelial differentiation gene family of G-protein-coupled receptors. *Pharmacol Ther* 88: 115-131.
396. Hobson JP, Rosenfeldt HM, Barak LS, Olivera A, Poulton S, et al. (2001) Role of the sphingosine-1-phosphate receptor EDG-1 in PDGF-induced cell motility. *Science* 291: 1800-1803.
397. Duchene J, Ahluwalia A (2009) The kinin B1 receptor and inflammation: new therapeutic target for cardiovascular disease. *Current Opinion in Pharmacology* 9: 125-131.
398. Groves P, Kurz S, Just H, Drexler H (1995) Role of endogenous bradykinin in human coronary vasomotor control. *Circulation* 92: 3424-3430.
399. Prasad A, Husain S, Quyyumi AA (1999) Abnormal flow-mediated epicardial vasomotion in human coronary arteries is improved by angiotensin-converting enzyme inhibition: a potential role of bradykinin. *J Am Coll Cardiol* 33: 796-804.
400. Hall JM (1997) Bradykinin receptors. *Gen Pharmacol* 28: 1-6.
401. McLean PG, Perretti M, Ahluwalia A (2000) Kinin B(1) receptors and the cardiovascular system: regulation of expression and function. *Cardiovasc Res* 48: 194-210.
402. Raidoo DM, Ramsaroop R, Naidoo S, Muller-Esterl W, Bhoola KD (1997) Kinin receptors in human vascular tissue: their role in atheromatous disease. *Immunopharmacology* 36: 153-160.
403. Naidu PS, Velarde V, Kappler CS, Young RC, Mayfield RK, et al. (1999) Calcium-calmodulin mediates bradykinin-induced MAPK phosphorylation and c-fos induction in vascular cells. *Am J Physiol* 277: H1061-1068.
404. Wilson PC, Lee MH, Appleton KM, El-Shewy HM, Morinelli TA, et al. (2013) The arrestin-selective angiotensin AT1 receptor agonist [Sar1,Ile4,Ile8]-AngII negatively regulates bradykinin B2 receptor signaling via AT1-B2 receptor heterodimers. *J Biol Chem* 288: 18872-18884.
405. Majack RA, Clowes AW (1984) Inhibition of vascular smooth muscle cell migration by heparin-like glycosaminoglycans. *J Cell Physiol* 118: 253-256.
406. El-Shewy HM, Johnson KR, Lee MH, Jaffa AA, Obeid LM, et al. (2006) Insulin-like growth factors mediate heterotrimeric G protein-dependent ERK1/2 activation by transactivating sphingosine 1-phosphate receptors. *J Biol Chem* 281: 31399-31407.
407. Christopher J, Velarde V, Jaffa AA (2001) Induction of B(1)-kinin receptors in vascular smooth muscle cells: cellular mechanisms of map kinase activation. *Hypertension* 38: 602-605.

408. Wunsche C, Koch A, Goldschmeding R, Schwalm S, Meyer Zu Heringdorf D, et al. (2015) Transforming growth factor beta2 (TGF-beta2)-induced connective tissue growth factor (CTGF) expression requires sphingosine 1-phosphate receptor 5 (S1P5) in human mesangial cells. *Biochim Biophys Acta* 1851: 519-526.
409. Abdallah RT, Keum JS, El-Shewy HM, Lee MH, Wang B, et al. (2010) Plasma kallikrein promotes epidermal growth factor receptor transactivation and signaling in vascular smooth muscle through direct activation of protease-activated receptors. *J Biol Chem* 285: 35206-35215.
410. Douillet CD, Velarde V, Christopher JT, Mayfield RK, Trojanowska ME, et al. (2000) Mechanisms by which bradykinin promotes fibrosis in vascular smooth muscle cells: role of TGF-beta and MAPK. *Am J Physiol Heart Circ Physiol* 279: H2829-2837.
411. Greene EL, Velarde V, Jaffa AA (2000) Role of reactive oxygen species in bradykinin-induced mitogen-activated protein kinase and c-fos induction in vascular cells. *Hypertension* 35: 942-947.
412. Velarde V, Ullian ME, Morinelli TA, Mayfield RK, Jaffa AA (1999) Mechanisms of MAPK activation by bradykinin in vascular smooth muscle cells. *Am J Physiol* 277: C253-261.
413. Blaukat A, Dikic I (2001) Activation of sphingosine kinase by the bradykinin B2 receptor and its implication in regulation of the ERK/MAP kinase pathway. *Biol Chem* 382: 135-139.
414. Game BA, He L, Jarido V, Nareika A, Jaffa AA, et al. (2007) Pioglitazone inhibits connective tissue growth factor expression in advanced atherosclerotic plaques in low-density lipoprotein receptor-deficient mice. *Atherosclerosis* 192: 85-91.
415. Jaffa AA, Usinger WR, McHenry MB, Jaffa MA, Lipstiz SR, et al. (2008) Connective tissue growth factor and susceptibility to renal and vascular disease risk in type 1 diabetes. *J Clin Endocrinol Metab* 93: 1893-1900.
416. Mochari-Greenberger H, Mosca L (2015) Differential Outcomes by Race and Ethnicity in Patients with Coronary Heart Disease: A Contemporary Review. *Curr Cardiovasc Risk Rep* 9.
417. Go AS, Mozaffarian D, Roger VL, Benjamin EJ, Berry JD, et al. (2013) Executive summary: heart disease and stroke statistics--2013 update: a report from the American Heart Association. *Circulation* 127: 143-152.
418. Ross R (1999) Atherosclerosis--an inflammatory disease. *N Engl J Med* 340: 115-126.

419. Tavori H, Su YR, Yancey PG, Giunzioni I, Wilhelm AJ, et al. (2015) Macrophage apoAI protects against dyslipidemia-induced dermatitis and atherosclerosis without affecting HDL. *J Lipid Res*.
420. Webb RC (2003) Smooth muscle contraction and relaxation. *Adv Physiol Educ* 27: 201-206.
421. Salabei JK, Hill BG (2013) Implications of autophagy for vascular smooth muscle cell function and plasticity. *Free Radic Biol Med* 65: 693-703.
422. Frigolet ME, Thomas G, Beard K, Lu H, Liu L, et al. (2017) The bradykinin(BK)-cGMP-PKG pathway augments insulin sensitivity via upregulation of MAPK phosphatase-5 and inhibition of Jun kinase (JNK). *Am J Physiol Endocrinol Metab*: ajpgendo.00298.02016.
423. Leo MD, Zhai X, Muralidharan P, Kuruvilla KP, Bulley S (2017) Membrane depolarization activates BK channels through ROCK-mediated beta1 subunit surface trafficking to limit vasoconstriction. 10.
424. (2015) 2015 ASCB Annual Meeting abstracts. *Mol Biol Cell* 26: 4523.
425. Lim SM, Kreipe BA, Trzeciakowski J, Dangott L, Trache A (2010) Extracellular matrix effect on RhoA signaling modulation in vascular smooth muscle cells. *Exp Cell Res* 316: 2833-2848.
426. Nevelsteen I, Van den Bergh A, Van der Mieren G, Vanderper A, Mubagwa K, et al. (2013) NO-dependent endothelial dysfunction in type II diabetes is aggravated by dyslipidemia and hypertension, but can be restored by angiotensin-converting enzyme inhibition and weight loss. *J Vasc Res* 50: 486-497.
427. Ramirez-Sanchez I, Maya L, Ceballos G, Villarreal F (2011) (-)-Epicatechin induces calcium and translocation independent eNOS activation in arterial endothelial cells. *Am J Physiol Cell Physiol* 300: C880-887.
428. Valles J, Lago A, Moscardo A, Tembl J, Parkhutik V, et al. (2013) TXA2 synthesis and COX1-independent platelet reactivity in aspirin-treated patients soon after acute cerebral stroke or transient ischaemic attack. *Thromb Res* 132: 211-216.
429. del Campo M, Sagredo A, del Campo L, Villalobo A, Ferrer M (2014) Time-dependent effect of orchidectomy on vascular nitric oxide and thromboxane A2 release. Functional implications to control cell proliferation through activation of the epidermal growth factor receptor. *PLoS One* 9: e102523.
430. Feng X, Liu P, Zhou X, Li MT, Li FL, et al. (2016) Thromboxane A2 Activates YAP/TAZ Protein to Induce Vascular Smooth Muscle Cell Proliferation and Migration. *J Biol Chem* 291: 18947-18958.

431. Sun Z, Li Z, Meininger GA (2012) Mechanotransduction through fibronectin-integrin focal adhesion in microvascular smooth muscle cells: is calcium essential? *Am J Physiol Heart Circ Physiol* 302: H1965-1973.
432. Maciver SK, Hussey PJ (2002) The ADF/cofilin family: actin-remodeling proteins. *Genome Biol* 3: reviews3007.
433. Galkin VE, Orlova A, Kudryashov DS, Solodukhin A, Reisler E, et al. (2011) Remodeling of actin filaments by ADF/cofilin proteins. *Proceedings of the National Academy of Sciences of the United States of America* 108: 20568-20572.
434. Rhee SG, Chae HZ, Kim K (2005) Peroxiredoxins: a historical overview and speculative preview of novel mechanisms and emerging concepts in cell signaling. *Free Radic Biol Med* 38: 1543-1552.
435. King-Briggs KE, Shanahan CM (2000) TGF-beta superfamily members do not promote smooth muscle-specific alternative splicing, a late marker of vascular smooth muscle cell differentiation. *Differentiation* 66: 43-48.
436. Abe KC, Mori MA, Pesquero JB (2007) Leptin deficiency leads to the regulation of kinin receptors expression in mice. *Regul Pept* 138: 56-58.
437. Chiu CZ, Wang BW, Shyu KG (2014) Angiotensin II and the ERK pathway mediate the induction of leptin by mechanical cyclic stretch in cultured rat neonatal cardiomyocytes. *Clin Sci (Lond)* 126: 483-495.
438. Yu YM, Tsai CC, Tzeng YW, Chang WC, Chiang SY, et al. (2017) Ursolic acid suppresses leptin-induced cell proliferation in rat vascular smooth muscle cells. *Can J Physiol Pharmacol* 95: 811-818.
439. Martinez-Martinez E, Rodriguez C, Galan M, Miana M, Jurado-Lopez R, et al. (2016) The lysyl oxidase inhibitor (beta-aminopropionitrile) reduces leptin profibrotic effects and ameliorates cardiovascular remodeling in diet-induced obesity in rats. *J Mol Cell Cardiol* 92: 96-104.
440. Martinez-Martinez E, Jurado-Lopez R, Valero-Munoz M, Bartolome MV, Ballesteros S, et al. (2014) Leptin induces cardiac fibrosis through galectin-3, mTOR and oxidative stress: potential role in obesity. *J Hypertens* 32: 1104-1114; discussion 1114.
441. Muir LA, Neeley CK, Meyer KA, Baker NA, Brosius AM, et al. (2016) Adipose tissue fibrosis, hypertrophy, and hyperplasia: Correlations with diabetes in human obesity. *Obesity (Silver Spring)* 24: 597-605.
442. Bielig H, Lautz K, Braun PR, Menning M, Machuy N, et al. (2014) The Cofilin Phosphatase Slingshot Homolog 1 (SSH1) Links NOD1 Signaling to Actin Remodeling. *PLOS Pathogens* 10: e1004351.

443. Komers R, Schutzer WE, Reed JF, Lindsley JN, Oyama TT, et al. (2006) Altered endothelial nitric oxide synthase targeting and conformation and caveolin-1 expression in the diabetic kidney. *Diabetes* 55: 1651-1659.
444. Patel HH, Murray F, Insel PA (2008) Caveolae as organizers of pharmacologically relevant signal transduction molecules. *Annu Rev Pharmacol Toxicol* 48: 359-391.
445. Frye RA (1999) Characterization of five human cDNAs with homology to the yeast SIR2 gene: Sir2-like proteins (sirtuins) metabolize NAD and may have protein ADP-ribosyltransferase activity. *Biochem Biophys Res Commun* 260: 273-279.
446. Charles S, Raj V, Arokiaraj J, Mala K (2017) Caveolin1/protein arginine methyltransferase1/sirtuin1 axis as a potential target against endothelial dysfunction. *Pharmacol Res* 119: 1-11.
447. Feresin RG, Huang J, Klarich DS, Zhao Y, Pourafshar S, et al. (2016) Blackberry, raspberry and black raspberry polyphenol extracts attenuate angiotensin II-induced senescence in vascular smooth muscle cells. *Food Funct* 7: 4175-4187.
448. Al Hariri M, Zibara K, Farhat W, Hashem Y, Soudani N, et al. (2016) Cigarette Smoking-Induced Cardiac Hypertrophy, Vascular Inflammation and Injury Are Attenuated by Antioxidant Supplementation in an Animal Model. *Front Pharmacol* 7: 397.
449. Regoli D, Gobeil F (2017) Kallikrein-kinin system as the dominant mechanism to counteract hyperactive renin-angiotensin system. *Can J Physiol Pharmacol*: 1-8.
450. Regoli D, Gobeil F (2016) Kinins and peptide receptors. *Biol Chem* 397: 297-304.
451. Zhang G, Teggatz EG, Zhang AY, Koeberl MJ, Yi F, et al. (2006) Cyclic ADP ribose-mediated Ca²⁺ signaling in mediating endothelial nitric oxide production in bovine coronary arteries. *Am J Physiol Heart Circ Physiol* 290: H1172-1181.
452. Sharma JN, Narayanan P (2014) The kallikrein-kinin pathways in hypertension and diabetes. *Prog Drug Res* 69: 15-36.
453. Lynch M, Ahern T, Sweeney CM, Malara A, Tobin AM, et al. (2017) Adipokines, psoriasis, systemic inflammation, and endothelial dysfunction. *Int J Dermatol*.
454. Pierce RW, Giuliano JS, Jr., Pober JS (2017) Endothelial Cell Function and Dysfunction in Critically Ill Children. *Pediatrics* 140.
455. Cetindagli I, Kara M, Tanoglu A, Ozalper V, Aribal S, et al. (2017) Evaluation of endothelial dysfunction in patients with nonalcoholic fatty liver disease: Association of selenoprotein P with carotid intima-media thickness and endothelium-dependent vasodilation. *Clin Res Hepatol Gastroenterol*.

456. Krankel N, Katare RG, Siragusa M, Barcelos LS, Campagnolo P, et al. (2008) Role of kinin B2 receptor signaling in the recruitment of circulating progenitor cells with neovascularization potential. *Circ Res* 103: 1335-1343.
457. Ha YM, Lee DH, Kim M, Kang YJ (2013) High glucose induces connective tissue growth factor expression and extracellular matrix accumulation in rat aorta vascular smooth muscle cells via extracellular signal-regulated kinase 1/2. *Korean J Physiol Pharmacol* 17: 307-314.
458. O'Sullivan S, Dev KK (2017) Sphingosine-1-phosphate receptor therapies: Advances in clinical trials for CNS-related diseases. *Neuropharmacology* 113: 597-607.
459. Kunkel GT, Maceyka M, Milstien S, Spiegel S (2013) Targeting the sphingosine-1-phosphate axis in cancer, inflammation and beyond. *Nat Rev Drug Discov* 12: 688-702.